



HAL
open science

Studying ecosystem stability to global change across spatial and trophic scales

Ceres Barros

► **To cite this version:**

Ceres Barros. Studying ecosystem stability to global change across spatial and trophic scales. Earth Sciences. Université Grenoble Alpes, 2017. English. NNT : 2017GREAV013 . tel-01685584

HAL Id: tel-01685584

<https://theses.hal.science/tel-01685584v1>

Submitted on 16 Jan 2018

HAL is a multi-disciplinary open access archive for the deposit and dissemination of scientific research documents, whether they are published or not. The documents may come from teaching and research institutions in France or abroad, or from public or private research centers.

L'archive ouverte pluridisciplinaire **HAL**, est destinée au dépôt et à la diffusion de documents scientifiques de niveau recherche, publiés ou non, émanant des établissements d'enseignement et de recherche français ou étrangers, des laboratoires publics ou privés.

THÈSE

Pour obtenir le grade de

DOCTEUR DE LA COMMUNAUTE UNIVERSITE GRENOBLE ALPES

Spécialité : **Biodiversité Ecologie Environnement**

Arrêté ministériel : 25 mai 2016

Présentée par

Ceres BARROS

Thèse dirigée par **Wilfried THULLER**, Directeur de Recherche,
Laboratoire d'Écologie Alpine, Grenoble, et
codirigée par **Tamara Münkemüller**, Chargée de Recherche,
Laboratoire d'Écologie Alpine, Grenoble

préparée au sein du **Laboratoire d'Écologie Alpine**
dans l'**École Doctorale de Chimie Sciences du Vivant**

Étude de la stabilité des écosystèmes aux changements globaux, à plusieurs échelles spatiales et trophiques

Thèse soutenue publiquement le **23 juin 2017**,
devant le jury composé de :

Dr Sandra LAVOREL

Directrice de recherche au Laboratoire d'Écologie Alpine, Grenoble
Présidente

Prof. Jonathan LEVINE

Professeur à ETH Zürich, Rapporteur

Dr Franck JABOT

Chargé de recherche au Laboratoire d'Ingénierie pour les Systèmes
Complexes, Clermont-Ferrand, Rapporteur

Dr Xavier MORIN

Chargé de recherche au Centre d'Écologie Fonctionnelle et Evolutive,
Montpellier, Membre

Dr Wilfried THULLER

Directeur de recherche au Laboratoire d'Écologie Alpine, Membre



*À minha Mãe que me ensinou a nunca desistir
ao meu Pai, o principal culpado pelo meu amor por tudo o que é vivo
à Ireth, que me faz acreditar em fadas
ao Gale, cujo amor e carinho não deixam de me surpreender*

CONTENTS

Summary	v
Résumé	vi
Acknowledgements	vii
Preface	viii
INTRODUCTION	10
CHAPTER I	23
CHAPTER II	44
CHAPTER III	70
CHAPTER IV	78
DISCUSSION AND PERSPECTIVES	89
REFERENCES	99
APPENDICES	120
Appendix 1	121
Appendix 2: Supplementary materials to Chapter I	128
Appendix 3: Supplementary materials to Chapter II	149
Appendix 4: Supplementary materials to Chapter III	188
Appendix 5: Supplementary materials to Chapter IV	213
Appendix 6: Simulating plant invasion dynamics in mountain ecosystems under global change scenarios	233
Curriculum Vitae	256
Publications	257
Glossary	258

stability /stə'biləti/ noun. The quality or state of being steady and not changing or being disturbed in any way (= the quality of being stable)¹

¹ From the *Oxford Advanced Learner's Dictionary* (Turnbull *et al.* 2010)

SUMMARY

As global change threatens ecosystems worldwide with biodiversity loss, studying ecosystem stability has never been so important. Most ecosystem stability studies have heretofore focused on single ecosystems and disturbances, usually following the behaviour of particular ecosystem properties, such as productivity and diversity indices. However, ecosystems are subjected to multiple disturbances simultaneously and at large spatial scales different ecosystems co-occur, each responding specifically to any given disturbance. Hence, the study of ecosystem stability needs to move towards approaches that can be informative at broad scales that are relevant for ecosystem management. This thesis is a step forward in this direction. Here, I used several approaches to assess how multiple global change drivers, such as climate change, extreme weather events, and land-use changes, affect ecosystem stability at landscape and larger spatial scales, and from single to multi-trophic level perspectives.

I begin by highlighting the importance of considering the interactions between gradual and extreme climate changes, in conjunction with land-use changes, for the management of highly diverse landscapes, such as the European Alps. Using a spatially explicit dynamic vegetation model, I show that increasing drought frequency and intensity will likely change the trends of treeline movement expected under future gradual climate warming scenarios. I then investigated whether drought and gradual climate warming caused plant communities to shift in different ways, using n -dimensional hypervolumes to describe community states in multidimensional space. Drought effects on forest and grassland structure did not greatly change the long-term trajectories caused by gradual climate warming alone, but showed that forest communities became more unstable than grasslands in the future. However, focusing on vegetation dynamics remains limited to a single trophic level. Because trophic networks represent energy flows in an ecosystem, studying their stability to disturbances should provide more accurate information on overall ecosystem stability. Hence, I also investigated trophic network stability in European protected areas to future scenarios of land-use and climate changes. My results show that these trophic networks may be highly sensitive to climate changes, even if no land-use changes occur. Importantly, I show that considering different dispersal limitations will greatly impact network robustness, and stress the importance of accounting for these processes in future studies of trophic network robustness and when planning ecosystem management and conservation.

In my thesis, I demonstrate that ecosystem stability concepts can and should be applied at scales that are relevant for management, while embracing the multidimensional nature of ecosystems.

RESUME

Dans un contexte de changement global qui continue de menacer les espèces et l'intégrité des écosystèmes à travers le monde, l'étude de la stabilité des écosystèmes n'a jamais été aussi importante. Jusqu'à aujourd'hui, la plupart des études sur la stabilité des écosystèmes se sont centrées sur des écosystèmes simples et des perturbations individuelles, en focalisant généralement sur le comportement de propriétés écosystémiques particulières, comme les indices de productivité et de diversité. Cependant, les écosystèmes sont soumis simultanément à de multiples perturbations. De plus, à grande échelle spatiale, différents écosystèmes se succèdent, chacun répondant différemment à une perturbation donnée. L'étude de la stabilité des écosystèmes doit donc progresser vers des approches plus intégratives qui seront informatives à des échelles pertinentes pour la gestion des écosystèmes. Cette thèse est un pas en avant dans cette direction. Ici, j'ai utilisé plusieurs approches pour évaluer la façon dont de multiples facteurs de changement global, tels que les changements climatiques graduels et extrêmes et les changements d'usage du sol, affectent la stabilité des écosystèmes à grande échelle spatiale, du point de vue d'un seul niveau trophique à un point de vue multitrophique.

Je commence par souligner l'importance de considérer les interactions entre les changements climatiques graduels et extrêmes, en conjonction avec les changements de l'usage du sol, pour la gestion de paysages hétérogènes, comme les Alpes européennes. En utilisant un modèle de végétation dynamique et spatialement explicite, je montre qu'une augmentation de la fréquence et de l'intensité de la sécheresse pourrait drastiquement changer les tendances d'embroussaillage des habitats ouverts alpins et subalpins qui sont généralement prévues par les projections ne prenant pas en compte ces événements extrêmes dans le futur. J'ai ensuite étudié si la sécheresse et le réchauffement climatique progressif amenaient les communautés végétales à souffrir des transitions différentes, en utilisant une approche innovatrice dans laquelle les états des communautés sont décrits d'une façon multidimensionnelle. Je montre que bien que les effets de la sécheresse sur la structure des forêts et des pâturages ne devraient pas trop affecter les trajectoires à long terme causées seulement par le réchauffement climatique graduel, ils devraient rendre les communautés forestières plus instables que les prairies dans le futur. Cependant, l'analyse des réponses de la végétation reste limitée à un seul niveau trophique. Vu que les réseaux trophiques représentent les flux d'énergie dans un écosystème, l'étude de leur stabilité aux perturbations devrait fournir des informations plus précises sur la stabilité globale de l'écosystème. Donc, j'ai aussi étudié la stabilité des réseaux trophiques dans les aires protégées européennes face à des scénarios futurs d'usage du sol et de climat. Mes résultats montrent que ces réseaux trophiques peuvent être très sensibles aux changements climatiques, même s'ils ne sont soumis à aucun changement d'usage du sol. Notamment, je montre que la prise en compte des phénomènes de dispersion des espèces aura un impact important sur la robustesse des réseaux, et je souligne l'importance de leur prise en compte dans futures études sur la robustesse des réseaux et pour la gestion des écosystèmes.

Dans ma thèse, je démontre que les concepts de stabilité de l'écosystème peuvent et doivent être appliqués à des échelles pertinentes pour la gestion des écosystèmes, tout en adoptant la nature multidimensionnelle des écosystèmes.

ACKNOWLEDGEMENTS

A first BIG thank you obviously goes to my two advisors, Wilfried Thuiller and Tamara Münkemüller. It is almost 4 years ago now that they took a leap of faith and accepted a complete stranger to start a PhD on a theme that she happened to be fascinated about. Wil and Tami, I can't thank you enough for the wonderful opportunity that you have given me, and I just hope that I have been up to your expectations! Also, I must say, Tami, I don't think I would've managed to write this without your guidance! Thanks!

Secondly, I will always feel grateful to Justin Travis who was incredibly supportive of me starting a research career. Equally, a big thanks to Steve Palmer and Greta Bocedi for the exciting discussions and the help they provided me in Aberdeen. I should also thank Cristina Branquinho, who has been a mentor since 2009. She has always provided good advice and instigated me to go further and fly higher. Thank you.

I also feel thankful for the wonderful teachers and professors that, throughout the years, have stimulated by brain and kept my eagerness to learn alive. In particular, I thank two great maths teachers Vasco Morais and Henrique “Monalisa”, my dear biology and life sciences teachers Antónia Ruas, Madalena Barros – I hope you are in a better place now... – and Guilherme, professores “Ruas” and Francisco Rocha for teaching me to think critically, and Vera Carnall for believing that high school “kids” can also do serious research! From the Faculdade de Ciências da Universidade de Lisboa, I thank the two Professors that walked us through biostatistics and numerical ecology, Profs. Dinis Pestana and Henrique Cabral, but also Susana Varela for her support in my departure to Scotland.

Two teachers from the University of Aberdeen also deserve my acknowledgment: David Lusseau, for embarking with me in my first stability and resilience adventure and for showing me France in Scotland, and Alex Douglas for the amazing statistics courses!

Of course, I also thank all my co-authors for their support and inestimable help in writing the manuscripts that are presented here, but also others that have not been included in this thesis: Isabelle, Damien, Maya, Rolland, Marta, Wilfried and Tamara, of course, Nick Zimmermann, João, José Montoya, Núria, Dominique Gravel, Luigi Maiorano, Francesco Ficetola, Justin, Greta and Steve, David, Rita, Cristina, Sofia, Pedro, Prof. Máguas e Prof. Maria João, a big thank you to you all!

I would also like to thank Nicolas Mouquet for being present during my first thesis committee, as well as Sonia Kéfi whose work has been most inspiring to me and who I sincerely admire.

Finally, my life in Grenoble would have been sad and boring if I hadn't made wonderful friends here: Marta, Coline, Hannah, Marco, Baptiste, Luca and Iolanda. Thank you for the *soirées*, for the laughs, for listening to my complaints and sometimes silliness, and for taking care of Miso when we couldn't be here! You are wonderful people that have brightened my days! Also, a special thanks to Marta and Baptiste for dedicating their time to reading parts of this thesis!

Last but not least, a huge thank you to all my family and friends in Portugal. Knowing that you supported me has kept me going this far! Mom, seriously, what would I do without you? Dad, you are responsible for putting me on this path. Johnny, seu, adoro-te pah! And my little soul sister, I wouldn't ever be complete without you!

My last thanks go to my wonderful partner João, with whom I can be my whole self, the good and the bad. Thank you for supporting me throughout this journey and wanting to continue to do so. I love you.

PREFACE

A Google Search on the term “stability” generates around 364 000 000 results that span a wide array of subjects, from the definition of the term, to its employment on mathematics, physics, chemistry, ecology and political and social sciences. Clearly, the concept of stability is a concept that most, if not all, disciplines use in some form or another. Although definitions of stability can vary depending on the field of research (and even within a particular field), in general terms a system is considered stable if it returns to its equilibrium point after being perturbed. Hence, understanding the stability of complex systems implies an understanding of what causes them to be unstable and what governs their dynamics. What makes A remain A? What happens to A if X or Y occur? How did A become B? Can we revert it? How? Quite likely, humans started asking themselves these questions ever since they began to consciously observe natural phenomena and, as scientific knowledge progressed and grew, we quickly realised that nature and the universe seem to be governed by an imperfect balance that reflects itself as an apparent stability. Two obvious examples are homeostasis, which allows the maintenance of an individual’s physiological balance – or low entropy at the expense of the environment – and dynamical geochemical equilibria observed in atmospheric, oceanic and geological complex chemistry. The reader will notice, however, the use of the terms “apparent stability”. Although thermodynamics teaches us that all systems converge to a state of lowest possible entropy, the fact that "closed systems" do not exist in reality means that absolute stability is ultimately impossible. That is, as low entropy is achieved at the expense of energy transformation low entropy states are temporary and, thus, unstable. Perceiving stability therefore depends on the scale (temporal and spatial) of analysis. For instance, planetary orbits can be considered stable at the millennial scale, but are certainly not if we consider time lengths spanning a star's lifetime. Nonetheless, the importance of studying the stability, instability and transient dynamics of complex systems has long been recognised in numerous fields, from chemistry to electrical engineering, from astrophysics to ecology (Hirsch *et al.* 2012). In many cases this came from the desire for pure knowledge, but often it came from the desire or need to maintain particular states, as is the case for ecosystem and land-use management and conservation.

The study of ecological and ecosystem stability has been thus gained significant attention from researchers in the last two decades (Fig. 1). As we realise that ecosystems are being driven into undesired states by global change forcing, understanding how ecosystems will respond to environmental change has become essential. However, studying the consequences

of environmental change for the stability of complex ecosystems or their realistic representations is not straightforward. Partly because ecosystems, like many other complex systems, often present non-linear dynamics, and partly because the “rules” governing ecosystems remain largely unknown. Even if there is a growing body of literature aiming to describe equilibrium dynamics of the biosphere (e.g. Rockström *et al.* 2009; Hughes *et al.* 2013), the usefulness of these studies for management is not clear, especially at regional scales (Steffen *et al.* 2015). On the other hand, studies on ecosystem stability at smaller scales remain largely univariate (i.e. they follow the stability of isolated ecosystem components) and have usually focused on very few examples of ecosystems and, or, their simplified models.

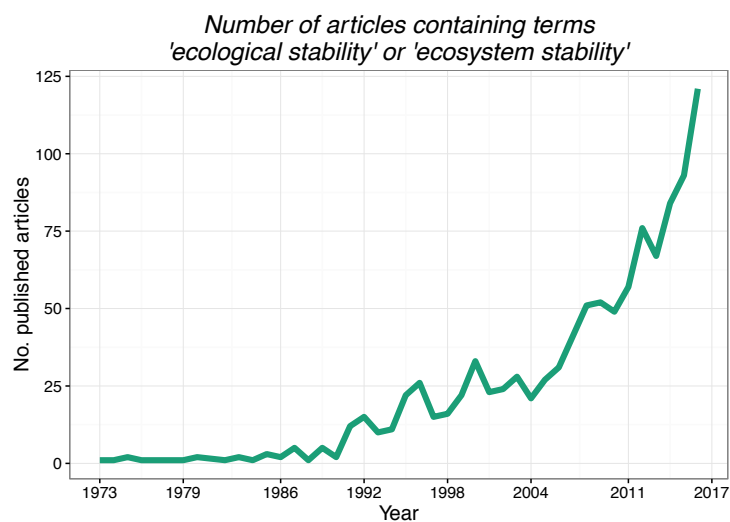


Figure 1. Number of articles published containing the terms "ecological stability" or "ecosystem stability" since the 1970s. Search query done in ISI Web of Knowledge (<http://apps.isiknowledge.com>), on the Science Citation Index Expanded (1900 to present) and Social Sciences Citation Index (1956 to present) databases.

As global change drivers continue to menace ecosystems worldwide, coupling the notions of stability with realistic representations of complex ecosystems at large spatial scales is crucial to adequately predict the consequences of environmental change and inform management and policy making. The work presented here intends to be a step forward in this direction. Essentially, I aimed to show that studying ecosystem stability can be done from an applied perspective and at regional spatial scales, while encompassing the multivariate nature of ecosystems. Far from offering complete solutions, I propose that achieving adequate ecosystem management in face of global change will not only require considering the stability dynamics of ecosystems, but to do so while looking at ecosystems as multidimensional entities, whose stability depends on the dynamics of their multiple components.

INTRODUCTION

Society is now more than ever concerned about how ecosystems respond to disturbances. As ecosystems around the globe are subjected climate change and direct anthropogenic action, large scale changes in ecological cycles, shifts in species ranges and increased rates of extinction are believed to be causing a sixth mass extinction (Barnosky *et al.* 2011, 2012). Hence, studying how ecosystems respond to drivers of environmental change is of utmost importance if we are to predict “what will happen to ecosystems” and “what we can do about it”. Importantly, different global change drivers will not only impact ecosystems differently, but they are also very likely to interact and aggravate, or compensate, each other (Brook *et al.* 2008). Moreover, environmental disturbances will certainly have distinct impacts on different facets of biodiversity. Take for instance two communities of equal taxonomic diversity (i.e. species richness) that differ in their functional and phylogenetic diversity². An equal loss of species richness will cause larger decreases in functional and phylogenetic diversity in the community with lower functional and phylogenetic redundancy (i.e. low proportion of species sharing similar functional traits or phylogenetic lineages). On the other hand, even if species loss does not result in the loss of functionally or phylogenetically distinct species, it may degrade redundancy and render communities more susceptible to further extinctions (Sundstrom *et al.* 2012). It is, therefore, important that the impact of disturbances is considered across different facets of diversity, especially because their role for maintaining ecosystem functioning can differ, as we will see later.

² Functional diversity refers to the variety of species’ ecological strategies, which are determined by their functional trait values. Phylogenetic diversity refers to the average evolutionary divergence between species and has been often used as a proxy for functional diversity, assuming that closely related species are functionally more similar than distantly related ones (Cadotte *et al.* 2009). Several indices are used to measure different facets of both functional and phylogenetic diversity and I recommend the work by Mouchet *et al.* (2010) and Tucker *et al.* (2016) for their respective overview.

It was this need for a multidimensional assessment of ecosystem responses to different global change drivers and their interactions that drove the research presented in this thesis. The work I have developed during the past 3 years or so can be organised in a gradient of increasing complexity, through which I investigate three major questions:

1. How do ecosystems respond to the interaction of multiple drivers of climate change and land-use changes at large spatial scales, and more specifically in the European Alps?
2. Can we describe and study ecosystem stability without focusing on particular biodiversity facets, species, or ecosystem functions?
3. What is the stability of ecosystems to land-use and climate changes from a multitrophic perspective at the continent landscape scale?

In the next three sections, I will briefly review our current knowledge on each of these problems and define the working hypotheses that guided my work towards answering some of the research gaps identified.

Interactions between different components of global change cannot be ignored

Different human-induced drivers of global change not only impact ecosystems in distinct ways, but are also likely to interact (Sala *et al.* 2000; Brook *et al.* 2008; Murphy & Romanuk 2014). For instance, forest logging and fragmentation can cause local, as well as regional, shifts in precipitation regimes that then feedback on vegetation (Brook *et al.* 2008), and alien species introduced outside of their native ranges may benefit from climate changes and invade mountain environments (Carboni *et al.* in prep. – see Appendix 6). Since plant communities are the basis of most, if not all, terrestrial ecosystems, understanding how global changes alone or in interaction will impact vegetation at landscape scales is highly relevant for the management of ecosystems and the services they provide.

Mountain ecosystems are particularly prone to suffer changes in vegetation patterns as a result of environmental changes. As species inhabiting these environments are often at the lower limits of their temperature niches, their ranges are highly sensitive to climate warming (Pauli *et al.* 2012; Lenoir & Svenning 2015). In addition, millennia of human intervention have shaped ecosystems and species distributions in many mountain ranges (Delcourt & Delcourt 1988; Sarmiento & Frolich 2002; Carrión *et al.* 2007; Cunill *et al.* 2013; Walsh *et al.* 2014), and changes in land-use management are leading to important vegetation shifts, as is the case in the European Alps (Gehrig-Fasel *et al.* 2007; Tasser *et al.* 2007). Although several studies have explored the responses of alpine plants and vegetation to environmental change,

at both local (e.g. Lenoir *et al.* 2010b; Spasojevic *et al.* 2013) and continental scales (Dullinger *et al.* 2012), few have investigated the interplay between climatic drivers and land-use changes at spatial scales that are relevant for ecosystem management, e.g. national parks (but see Boulangeat *et al.* 2014a). Additionally, many of these studies focus on a specific type of vegetation or community, like forests (Palombo *et al.* 2013) or grasslands (Alatalo *et al.* 2016), or on proxies for vegetation condition, such as remote sensing vegetation indices (Ivits *et al.* 2016), that may reflect some plant communities' responses better than others'. For instance, measuring changes the fraction of photosynthetically active radiation (FAPAR) relies on detecting the start and end of the vegetation growing season, which may not be detected in highly productive communities with low seasonal variation in productivity (Ivits *et al.* 2016). Also, correlations between the normalised difference vegetation index (NDVI)³ and land surface temperature depend not only on geographic location and season, but also on the type of vegetation. Hence, we lack approaches that allow us to capture the effects and interactions of multiple drivers of global change, while encompassing community dynamics across different types of vegetation. Such approaches will be important to adapt ecosystem management and conservation in regions like the European Alps, where different ecosystems exist within a few kilometres, and are subjected to distinct land-use regimes, but also to changes in climate and land use.

Climate change in Alpine communities is not only predicted to occur through gradual changes of average climate values, but also through changes in the patterns of extreme weather events, such as drought, flooding regimes, extreme winds and storms (IPCC 2012, 2013). Drought regimes, in particular, have already been aggravated in the past decades (Spinoni *et al.* 2014) and caused forest diebacks across the globe (Allen *et al.* 2010) and changes in forest composition in the European Alps (Rigling *et al.* 2013). Worryingly, drought frequency and intensity are very likely to further increase during the 21st century, due to decreases in precipitation and, or, increases in evapotranspiration (IPCC 2012, 2013). This will have important repercussions for vegetation worldwide, as temperature extremes and water limitation directly impact plant photosynthesis and respiration (Frank *et al.* 2015). In fact, drought effects on plant growth and survival have been widely studied and are well understood, particularly in trees and forest systems (McDowell *et al.* 2008; Hartmann *et al.*

³ Vegetation indices like NDVI and FAPAR have been commonly used to assess vegetation conditions at landscape, continental and even global scales. They rely on satellite observations in multispectral bands reflecting surface “greenness”, reflecting vegetation health. I recommend Gu *et al.* (2007) who succinctly and clearly introduce the use of vegetation indices, with particular focus on NDVI-derived indices.

2013; Nardini *et al.* 2013). For instance, increases in temperature alone, i.e. without precipitation deficits, can trigger drought-responses in trees, increasing foliar transpiration due to higher vapour pressure deficits and water evaporation. In consequence, the individual tree can respond by closing its stomata and avoid further transpiration, in the case of isohydric species (species that maintain a constant leaf water potential), but increasing the risk of carbon starvation. Alternatively, anisohydric species (species that allow their leaf water potential to vary) maintain their stomata open and prevent carbon starvation, but risk hydraulic failure (see the review by McDowell *et al.* 2008 for a thorough explanation of plant physiological responses to drought). In either case, prolonged and severe drought can ultimately result in mortality increases across biomes, from monsoonal savannahs, to temperate and tropical ecosystems (Allen *et al.* 2010).

Despite evidence indicating that drought regimes will have important consequences for the management of mountain ecosystems, their combined effects with gradual climate warming and changing land use are not clear. In the case of drought and climate warming, we can expect them to operate at different timescales, but also to have different consequences for vegetation at high elevations. While drought can halt plant growth and induce plant mortality at relatively short time scales (Bigler *et al.* 2006; Worrall *et al.* 2008), the effects of gradual temperature increases will operate at longer time scales and may counterbalance drought effects by benefiting plant growth (Lloyd & Fastie 2002) and facilitate the establishment of new species in previously colder environments (Gottfried *et al.* 2012). For instance, in European subalpine forests climate warming and drought have led to upslope colonisations of thermophilous species, which eventually outcompete the native species that suffer habitat reductions with climate warming (Rigling *et al.* 2013). On the other hand, very severe drought events may impede or delay species upward migrations, hindering species as they track climate change. The combined effects of these two drivers will largely depend on their relative strengths, on the position of species relatively to their environmental niche optima, and on interactions with other species. These dynamics are then further complicated by interactions with land-use and its changing trends. The long history of forest and grassland management in the European Alps for timber, fodder production and agriculture led to the establishment of artificial treelines and open habitats (Motta & Nola 2001; Giguet-Covex *et al.* 2014; Walsh *et al.* 2014). However, as a consequence of the European industrial movement, the mid-1800s saw the beginning of the abandonment of traditional agro-pastoral activities, which has been on-going until present days (Tasser *et al.* 2017). Land-use abandonment of subalpine and alpine grasslands favours their re-colonisation by woody

species – woody encroachment – with detrimental effects on biodiversity and on the provisioning of several ecosystem services (Lavorel *et al.* 2011; Ratajczak *et al.* 2012). Moreover, climate warming is likely to facilitate woody encroachment by shifting the environmental niche optima of woody species towards higher elevations (Sanz-Elorza *et al.* 2003). Interactions with drought, however, are yet to be explored (but see Cáceres *et al.* 2015).

Land managers are thus facing significant challenges when it comes to land-use planning in mountain ecosystems facing climate and land-use changes. While setting-up experimental and field-based studies to investigate these synergies and capture their effects across large spatial scales is temporally and practically very ambitious, modelling approaches provide a complementary way to explore these issues. There is a wide range of models aiming at simulating drought effects, from fine-detail modelling of individual physiological drought responses, to models of long-term ecosystem dynamics with direct simulation of tree mortality (see review by Seidl *et al.* 2011). In parallel, time series of remote sensing vegetation indices have also been used to estimate water budgets and assess drought-prone conditions (Chakroun *et al.* 2012) and plant community responses to environmental conditions at the landscape scale (Dedieu *et al.* 2016). However, these approaches lack the integration of different vegetation strata, their spatial and temporal dynamics. As such they do not allow comparing the responses of different facets of biodiversity to the combined effects of drought, gradual climate warming and land-use changes.

Simulating the effects of these three components of global change across different species and/or plant groups can be extremely complex from a physiological point of view, especially at large spatial scales. Not only because drought-response strategies differ across woody species, but also because we lack information regarding drought response strategies and drought response traits for most non-woody plants. Instead, hybrid mechanistic models allow combining trait-based and statistically derived relationships with models of population dynamics to simulate how vegetation responds to environmental change at large landscape scales (Vincenot *et al.* 2016). Albeit coarser than physiological models, hybrid models provide an excellent tool for landscape scale assessments of multiple disturbance effects on species population dynamics and arising ecosystem-level responses (Seidl *et al.* 2011). In Chapter I, I used and further developed a hybrid dynamic vegetation model, FATE-HD (Boulangeat *et al.* 2014b), to assess the synergies and effects of gradual climate change, different drought regimes and different land-use trajectories for treeline advancement in a national park in the French Alps. More specifically, I hypothesised that frequent and intense

drought would counteract treeline advancement towards higher elevations that is expected under land-use abandonment and climate warming. I also expected severe drought regimes to result in distinct trends of taxonomic and functional turnover in communities situated in the forest-grassland ecotone belt.

Beyond a one-dimensional assessment of ecosystem responses to global change

In the study presented in Chapter I, I chose three single ecosystem properties to summarise and assess ecosystem responses to global change drivers. Following the response of particular ecosystem properties⁴ to environmental change has been of common practice amongst ecosystem stability studies. For instance, biodiversity and ecosystem functioning (BEF) studies have mostly focused on the relationship between species richness and productivity (but see Hector & Bagchi 2007), while many other studies focused on how different facets of biodiversity respond to disturbances (perturbation-biodiversity studies; see Appendix 1 for examples). These studies have largely contributed to our understanding of the mechanisms through which biodiversity stabilises ecosystem functioning and, in turn, how biodiversity itself is affected by disturbances (these findings have been summarised in Appendix 1). Despite it being largely accepted that higher levels of biodiversity allow greater ecosystems stability to a wide array of disturbances (Hooper *et al.* 2005), the mechanisms through which this happens may not be consistent across ecosystems and disturbances (see Appendix 1). Not only that, but some facets of biodiversity are likely to contribute more to ecosystem stability than others (de Bello *et al.* 2008; Pillar *et al.* 2013), and relationships between them can also change across ecosystems and disturbance gradients (Mayfield *et al.* 2010; Biswas & Mallik 2011). Moreover, the large majority of these studies has not provided cross-ecosystem, cross-disturbance or cross-ecosystem-function comparisons (but see Gamfeldt *et al.* 2008, Mayfield *et al.* 2010 and Hautier *et al.* 2015). Most remained largely focused on grassland plant productivity responses to controlled diversity treatments and disturbances such as grazing and nitrogen addition, since their easy manipulation and relatively fast dynamics make them excellent systems to test hypotheses. Thus, so far, the study of ecosystem stability has failed to provide an assessment of stability at large landscape scales where mosaics of different habitats co-exist, despite the utility of applying stability concepts for ecosystem management (Mori 2016).

⁴ Here I use the term “properties” to refer to set metrics and variables that can be used to describe and summarise an ecosystem or community. As such, they include both indices used to measure different facets of biodiversity (i.e. taxonomic, functional and phylogenetic diversity indices), and variables related to ecosystem functions, like productivity, nutrient cycling, litter decomposition, etc.

Landscape-scale and comparative analyses of ecosystem stability will require steering away from using isolated summary metrics of biodiversity, as these are likely to be related differently across ecosystems and have unequal contributions for stability. Likewise, even if plant productivity is the basis of most terrestrial systems, tracking changes in productivity alone may lead to ignoring other essential ecosystem functions (Hector & Bagchi 2007), and to ignoring the dynamics of less productive and, or, rare species whose role as providers of functional diversity and redundancy can be crucial to sustain ecosystem functioning (Mouillot *et al.* 2013). However, finding response variables that are ecosystem- and disturbance-independent and, at the same time, comparable across systems is not an easy task (Reiss *et al.* 2009). It has been recently proposed that response diversity⁵ should be used to summarise the contributions of different components of ecosystems (namely, their species) for the stabilisation of ecosystem function (Mori *et al.* 2013; Baskett *et al.* 2014). Because it integrates both taxonomic and functional diversity, as well as functional redundancy and compensation, response diversity provides a holistic perspective on the contribution of biodiversity for ecosystem stability and resilience (i.e. the capacity of a system to remain in the same state; but see Appendix 1 for a clarification of the terms ‘stability’ and ‘resilience’). However, because it depends on identifying key functional traits that reflect species’ contributions to ecosystem functioning and species’ responses to disturbances (‘effect traits’ and ‘response traits’, respectively; Lavorel & Garnier 2002) most studies have considered particular communities, and the use of response diversity to study stability and resilience across different ecosystems and disturbances remains complex.

The second chapter of my thesis is based on the hypothesis that a multidimensional approach that encompasses the contribution of the multiple components of an ecosystem for its stabilisation, should provide a better reflection of stability, without being tied to particular ecosystem functions and particular conditions (Chapter II). To demonstrate this, I make use of n -dimensional hypervolumes to represent ecosystems in their different states (i.e. before and after disturbances) and compare them in order to assess departures from stability (i.e. the pre-disturbance state). I then apply this framework to evaluate whether drought and gradual climate change have different consequences for the stability of grassland and forest communities in the forest-grassland ecotone (Chapter III).

⁵ Although used in other disciplines, ‘response diversity’ was initially defined in ecology by Elmqvist *et al.* (2003) as “the diversity of responses to environmental change among species that contribute to the same ecosystem function”.

Scaling up: ecosystem stability from a multi-trophic perspective at large spatial scales

Until now, we have discussed ecosystem stability from a single-trophic-level perspective, considering only ecosystem producers – namely, plant communities. This stems in part from plant communities being the basis of most terrestrial ecosystems and assuming that the stability of plant productivity will reflect the stability of the overall ecosystem. But also, because plant communities (such as grasslands) are more easily manipulated to provide an experimental basis for hypothesis testing. However, ecosystem producers are but one of the many levels of complexity in ecosystems, which are composed by several other trophic levels and groups of organisms, linked by trophic and non-trophic interactions, like parasitism, pollination and decomposition to name a few. By summarising both species (or groups of species) as well as their interactions in an ecosystem, ecological networks bring together the contributions of both taxonomical and functional facets of diversity for ecosystem functioning (Thompson *et al.* 2012). As such, they are powerful tools to explore how ecosystem stability is affected by top-down and, or, bottom-up propagation of perturbations (Schleuning *et al.* 2016), and even study how disturbances can impact the provisioning of ecosystem services (Dee *et al.* 2016).

Ecological networks have been used to represent species interdependencies at least since the 1700s (Egerton 2007), but they were not used specifically until Pearce *et al.* (1912) described “*the boll weevil complex*”, the network of parasitic and trophic interactions associated with the cotton boll weevil (Fig. 2). From thereon, the number of published studies of particular trophic networks kept increasing and, in 1955, MacArthur was the first to my knowledge to relate trophic network diversity to ecosystem stability (MacArthur 1955). Since trophic networks represent species (nodes or vertices) interconnected by predator-prey links (or edges), they reflect the flow of energy and biomass in ecosystems and mediate species’ responses to perturbations (Pascual & Dunne 2006). Although the majority of ecological networks have classically represented single types of relationships between species – mainly trophic interactions – increasing work is being developed to integrate and compare different types of networks, and understand how their properties and structure differ (see for instance Thebault & Fontaine 2010; Kéfi *et al.* 2015).

After MacArthur’s seminal piece on the relationship between network species diversity and stability, several studies have investigated the capacity of trophic networks to withstand perturbations, both in theoretical and empirical networks (Namba 2015). In many cases, network stability has been defined as network robustness, this is, a network’s propensity to lose nodes secondarily after the removal of another node (e.g. Dunne *et al.* 2002; Gilbert

2009; Kaiser-Bunbury *et al.* 2010; Evans *et al.* 2013). Importantly, several network properties seem to be related to higher, or lower, network robustness (Saint-Béat *et al.* 2015; Table 1).

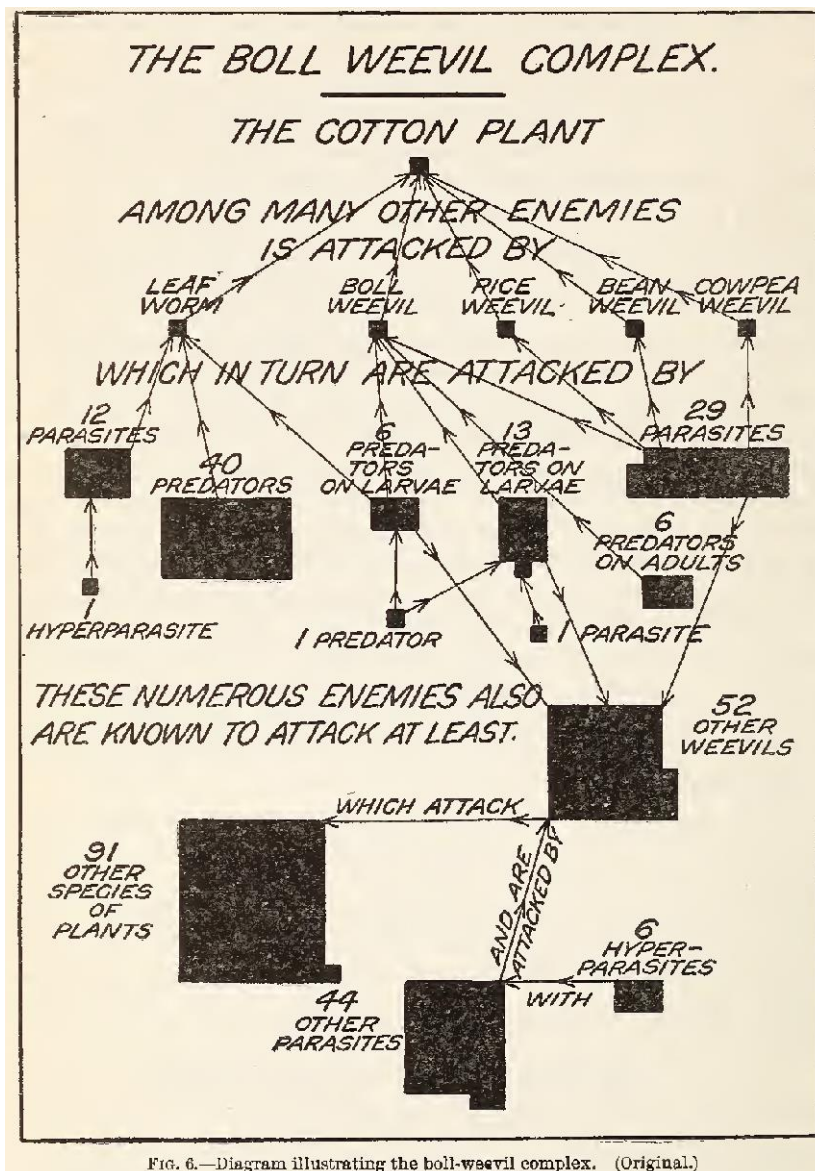


Figure 2. Possibly the first formal representation of a specific ecological network, by Pearce *et al.* (1912), depicting the parasitic and trophic interactions associated with the cotton boll weevil and its host, the cotton plant.

In general, networks with higher link redundancy (which may be delivered by higher species diversity and omnivory) and higher connectance (proportion of realized links relatively to all potential links in a network) are more robust to disturbances. It is important to highlight that although higher connectance allows for higher robustness, this relationship will vary depending on how species are removed from the network. Ecological networks are known to be quite robust to random species removal, but not to targeted species removal (Dunne *et al.* 2002; Memmott *et al.* 2004; Gilbert 2009; Kaiser-Bunbury *et al.* 2010; Cai *et al.* 2016). While

random species removal is less likely to affect a network's connectance and disrupt it, the targeted removal of highly connected species decreases connectance, creating cascading extinctions. On the other hand, the removal of poorly connected species increases overall network connectance and, like random removal, has lower probability of disrupting the network. Since the relationship between connectance and robustness can vary according to species removal scenarios, Gilbert (2009) suggests considering changes in connectance (rather than network connectance values) as indicative of ecosystem robustness. After simulating several scenarios of species removal in 16 real food webs, Gilbert concluded that the larger the declines in connectance were associated with larger losses of robustness (i.e. networks became more susceptible to fragment or lose nodes secondarily). Moreover, although the removal of less connected species led to increases in overall network connectance, this still caused a decrease in robustness (Gilbert 2009).

Given the tight relationships between trophic network properties (here included species richness) and network stability, trophic networks have been increasingly used to study overall ecosystem stability to biodiversity changes (Saint-Béat *et al.* 2015). Most of these studies have focussed on direct species removal in theoretical (e.g. Thebault & Fontaine 2010), as well as empirical networks (or networks modelled based on empirical data; e.g. Dunne *et al.* 2002; Cai *et al.* 2016), and a few studies have simulated species removal via realistic disturbances, such as habitat loss (Evans *et al.* 2013), climate change (Albouy *et al.* 2014; Schleuning *et al.* 2016), or different ecosystem management practices (Condie *et al.* 2014). Except for those regarding marine environments (such as Albouy *et al.* 2014 or Condie *et al.* 2014), these studies have been limited to geographically and temporally punctual or discontinuous, networks. Given the importance of considering the consequences of global change drivers for ecosystem stability at large landscape scales, the lack of spatially continuous information on how terrestrial trophic networks respond these disturbances is a clear impairment to their integration in ecosystem management and conservation, such as prioritisation of protected areas based on trophic network sensitivity to habitat conversion.

Table 1. Ecological networks' properties and analyses indices, their meaning and calculation, and their relationship with ecological stability and resilience (please refer to Appendix 1 for their working definition). Partially summarised from Saint-Béat *et al.* (2015), although not all formulas correspond to those presented in their review.

Category	Property		Link with resilience
Structure complexity	Species diversity	Number of nodes S	Increases resilience
	Connectance*	Amount of connections in the network, measured as the proportion of realized links	Increases stability and resilience*

		($T_{o,o}$) in terms of potential links	
		$C = \frac{T_{o,o}}{S^2}$	
Functioning of ecosystem	Link strength	Measured as i) the effect of an individual of species A on an individual of species B (<i>per capita</i> effect), or ii) the impact of link changes on the dynamics of other species or on ecosystem functioning	Weak interactions, or a mix of weak and strong interactions increase stability and resilience
Ecological network analysis indices	Cycling	Series of links between components of an ecosystem that begin and end in the same component, without going through the same component twice. Can be measured by several indices, e.g. Comprehensive Cycling Index is the difference between the sum of flows and all simple paths (paths without repeated compartments; Allesina & Ulanowicz 2004)	Increases resilience (but not always)
	Omnivory	Number, or proportion, of parallel pathways between two compartments (i.e. trophic level)	Increases stability and resilience
	Ascendency	Measures the activity and organisation within the system (Ulanowicz 2000) and can be calculated as: $A = \sum_{i,j} T_{i,j} \log \left(\frac{T_{i,j} T_{o,o}}{T_{i,o} T_{o,j}} \right)$ with i and j representing prey and predator species, T representing trophic links, $T_{i,o}$ being the links from one prey to all its predators and $T_{o,j}$ the links from a predator to all its prey (Arreguín-Sánchez 2014)	Decreases resilience

*Changes in connectance (rather than their absolute values) seem to be more appropriate measures of robustness (Gilbert 2009).

As large datasets become easier to compile and analyse, the construction of metawebs opens the possibility to study ecological networks at large spatial scales. Metawebs summarise the potential interactions among all species of a given species pool (at any given spatial scale) and, when combined with appropriate species distribution data, allow building local or ‘realised’ networks whose properties and stability can be analysed in spatially contiguous manner. For the last chapter of this thesis, I used a metaweb of trophic interactions across all pan-European terrestrial vertebrates to investigate the consequences of land-use and climate changes for trophic networks across European protected areas (Chapter IV). My main working hypothesis was that trophic networks with higher species diversity and higher link redundancy (offered by higher connectance and larger proportions of omnivorous species) would be more robust across all scenarios of disturbance. A large component of this work also consisted in highlighting regions of particularly lower, or higher, network robustness, thus paving the way for landscape scale analyses of network robustness that can be used to inform

management and conservation.

Towards a large-scale assessment of ecosystem stability to multiple global change drivers

As we have seen above, many of the approaches used to study ecosystem stability do not allow for an overall perspective of stability at landscape scales where different ecosystems exist. Moving the study of ecosystem stability towards a multi-ecosystem and multi-disturbance direction requires using i) spatially explicit models and simulating different scenarios of change, ii) measures of stability that are ecosystem- and disturbance-independent, and whenever possible iii) investigating the stability of ecological networks to realistic disturbances. In addition, if ecosystem stability studies aim to be relevant for ecosystem management and conservation, they should aim to focus on spatial scales that correspond to those typically addressed by managers. The research presented in this thesis was driven by the need to answer these issues and is outlined in Figure 3.

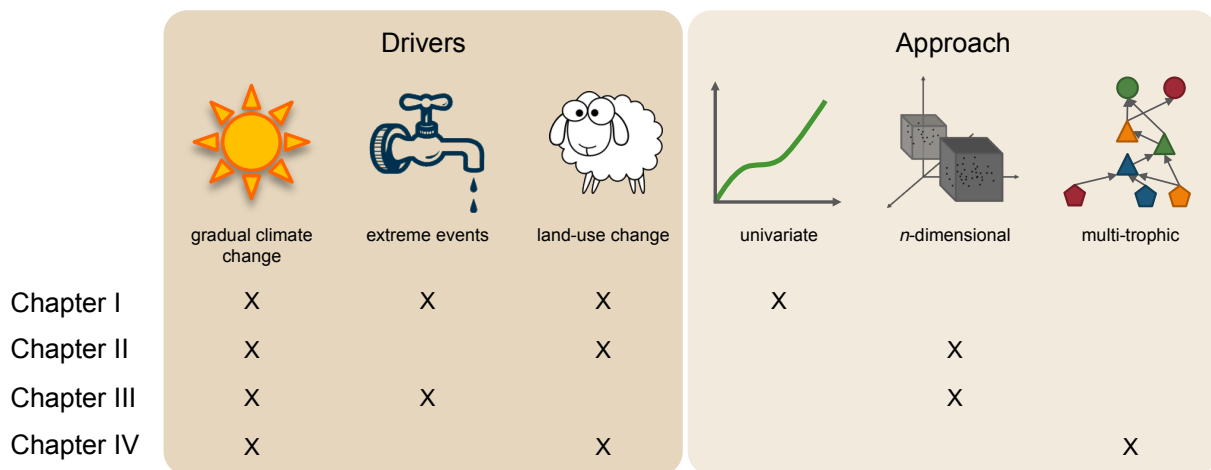


Figure 3. Schematic representation of the analysed combinations of global change drivers and the approaches used to investigate their effects on ecosystem stability.

I began by investigating the synergies between multiple drivers of global change and their consequences for ecosystems in the European Alps at the landscape scale (Chapter I). To do so, I used a hybrid mechanistic model to simulate plant community under scenarios of gradual climate changes, drought regimes and land-use changes, and explored their consequences for treeline movement and spatio-temporal dynamics of taxonomic and functional diversity in forest-grassland ecotone communities.

I then extended my analysis to a multidimensional perspective of how distinct plant communities are destabilised in their whole by different global change drivers (Chapter II and Chapter III). Using n -dimensional hypervolumes, I described and compared community stable

Introduction

states before and after perturbations, to assess how much communities depart from their pre-perturbed states in terms of taxonomic and functional structure and composition.

Finally, I then increased the scale of my analysis once more and investigated the robustness of multitrophic systems to changes in climate and land use, at the continental scale (Chapter IV). Thanks to an impressive data collection effort, I build spatially continuous trophic networks across all European Union (EU) protected areas – except for Croatia – and analysed their robustness to realistic scenarios of land-use and climate change, considering different dispersal limitations.

I bring all the results of this thesis together in the Discussion and Perspectives section, where I discuss future study directions and comment on the applicability of my findings for ecosystem management and conservation.

CHAPTER I

EXTREME CLIMATE EVENTS COUNTERACT THE EFFECTS OF CLIMATE AND LAND-USE CHANGES IN ALPINE TREE LINES

Ceres Barros^{1,2}, Maya Guéguen^{1,2}, Rolland Douzet³, Marta Carboni^{1,2}, Isabelle Boulangeat⁴,
Niklaus E. Zimmermann^{5,6}, Tamara Münkemüller^{1,2} and Wilfried Thuiller^{1,2} (2017).
J. Appl. Ecol., 54, 39–50

¹ Laboratoire d'Écologie Alpine (LECA), Université Grenoble Alpes, F-38000 Grenoble, France

² Laboratoire d'Écologie Alpine (LECA), CNRS, F-38000 Grenoble, France

³ Station Alpine Joseph Fourier - UMS 3370, Université Grenoble Alpes, SAJF, F-38000 Grenoble, France

⁴ Département de Biologie, Chimie et Géographie, Université du Québec à Rimouski, 300 Allée des Ursulines, Québec G5L 3A1, Canada

⁵ Landscape Dynamics Unit, Swiss Federal Research Institute WSL, CH-8903 Birmensdorf, Switzerland

⁶ Department of Environmental Systems Science, Swiss Federal Institute of Technology ETH, CH-8092 Zürich, Switzerland

Abstract

1. Climate change and extreme events, such as drought, threaten ecosystems world-wide and in particular mountain ecosystems, where species often live at their environmental tolerance limits. In the European Alps, plant communities are also influenced by land-use abandonment leading to woody encroachment of subalpine and alpine grasslands.
2. In this study, we explored how the forest–grassland ecotone of Alpine tree lines will respond to gradual climate warming, drought events and land-use change in terms of forest expansion rates, taxonomic diversity and functional composition. We used a previously validated dynamic vegetation model, FATE-HD, parameterized for plant communities in the Ecrins National Park in the French Alps.
3. Our results showed that intense drought counteracted the forest expansion at higher elevations driven by land-use abandonment and climate change, especially when combined with high drought frequency (occurring every 2 or less than 2 years).
4. Furthermore, intense and frequent drought accelerated the rates of taxonomic change and resulted in overall higher taxonomic spatial heterogeneity of the ecotone than would be expected under gradual climate and land-use changes only.
5. *Synthesis and applications.* The results from our model show that intense and frequent drought counteracts forest expansion driven by climate and land-use changes in the forest– grassland ecotone of Alpine tree lines. We argue that land-use planning must consider the effects of extreme events, such as drought, as well as climate and land-use changes, since extreme events might interfere with trends predicted under gradual climate warming and agricultural abandonment.

Keywords: agricultural abandonment, climate change, drought, dynamic vegetation model, forest–grassland ecotone, global change, land-use changes, mountain ecosystems, synergistic effects of disturbances, woody encroachment

Introduction

Many ecosystems around the globe are threatened by changes in climate and land use, which impact biodiversity at different levels. Mountain ecosystems, in particular, are especially vulnerable to the effects of climate change, as they harbour many species that are near their environmental tolerance limits. Changes in climate drive species range shifts and impact physiological processes, and might also impact the provisioning of ecosystem services (Bellard *et al.* 2012). Land-use changes, be it by conversion of natural habitats into agricultural or urban lands, or by abandonment of managed areas, could aggravate the effects of climate change, as well as contribute to large and sudden changes of available habitats and ecosystem services (Asner *et al.* 2004). Climate, however, is not only predicted to change in its long-term average, but also with regard to extreme events (e.g. drought), expected to intensify in many regions (IPCC 2012).

Drought affects plant reproduction, growth and survival and can ultimately lead to changes in forest (Park Williams *et al.* 2012) and grassland (Gu *et al.* 2007) productivity, to changes in vegetation composition of landscapes (Clark *et al.* 2016), and result in significant forest dieback at the global scale (Allen *et al.* 2010). Forest dieback can have cascading effects on biodiversity, carbon, water and nutrient cycling, and ultimately on the provisioning of ecosystem services, such as carbon uptake and storage (Anderegg *et al.* 2013). Such effects are likely very important in forest–grassland ecotones of mountain environments, where many tree species live close to their lower temperature limits and may reach their soil moisture limits in dry valleys (Goldblum & Rigg 2010). This is the case even in regions like the European Alps, where tree lines are further constrained by land use for farmlands, grazing and mowing (Carlson *et al.* 2014). In recent years, drought events have caused Swiss forests to suffer significant diebacks of Scots pine (*Pinus sylvestris* L.), favouring replacement colonization by pubescent oak (*Quercus pubescens* L.) and a turnover of forest composition (Rigling *et al.* 2013). Moreover, plant communities in mountainous areas are threatened by changes in land use that affect plant community structure and composition (Tasser & Tappeiner 2002). For example, simulations of vegetation dynamics in the European Alps predict that land-use abandonment and climate warming will interact and increase forest expansion towards higher elevations (Dirnböck *et al.* 2003; Boulangeat *et al.* 2014a).

Although forest–grassland ecotones in the European Alps are facing environmental changes originating from three fronts (i.e. gradual and extreme climate change, and land-use

Chapter I - Extreme climate events counteract the effects of climate and land-use changes in alpine tree lines

abandonment), so far no study has investigated their joint effects, especially from a forecasting perspective (Seidl *et al.* 2011). While climate change and land abandonment should lead to forest expansion and woody encroachment of subalpine and alpine pastures (Asner *et al.* 2004), drought stress increases tree mortality, causing forest dieback. Consequently, we can expect that drought might counter the effects of gradual climate change and land-use abandonment, but this is likely to depend on drought frequency and intensity, as well as on the identity of species within communities. Milder droughts may contribute to faster woody encroachment of subalpine and alpine pastures by favouring species adapted to drier environments. On the other hand, very severe and, or frequent droughts are likely to slow forest progression. Such effects may not be homogeneous in space, especially if certain areas are prone to more intense or more frequent drought (Dobbertin *et al.* 2005; Worrall *et al.* 2013).

Here, we study, in a spatially explicit manner, how drought frequency and intensity interact with climate and land-use practices and affect forest–grassland ecotones in the European Alps using the landscape dynamic vegetation model FATE-HD (Boulangeat *et al.* 2014b). Although FATE-HD does not simulate drought effects at the individual and physiological level, it can capture drought at the community level providing useful insights for management and conservation planning of complex ecosystems. For example, ecosystem management and conservation in the European Alps focuses on maintaining a bundle of ecosystem services (Grêt-Regamey *et al.* 2008; EC 2015), managing for a high diversity of habitats and on protecting biodiversity per se. Although this includes maintaining forest cover, there is also an important focus on avoiding woody encroachment of open habitats. FATE-HD provides information on these different conservation goals.

Specifically, we explored i) under which conditions drought reversed the trend of forest expansion that is observed under climate change and land-use abandonment; ii) whether forest–grassland ecotones suffered important changes in taxonomic and functional diversity when exposed to extreme events; and iii) the possible spatio-temporal dynamics of these changes. Finally, iv) we evaluated the consequences of drought regimes in the context of current land-use management and the provisioning of ecosystem services in the European Alps.

Materials and methods

Study area

We focused our study on the forest–grassland ecotone habitats of the Ecrins National Park (ENP), situated in south-east France in the French Alps. The park covers an area of 178 400 ha (elevation ranging from 669 to 4102 m a.s.l.), with a rich diversity of plant species (ca. 2000) and ecosystems, from mountainous to alpine habitats – the majority being open habitats (60% of the park surface). Land use consists mainly of agricultural activities (grazing, 48%; crop fields and mown grasslands, 9.8%; and forest management, 14%), which are accurately mapped (Esterni *et al.* 2006).

The base model: FATE-HD

FATE-HD has already been parameterized to explore the synergistic effects of land-use (LU) and climate changes (CC) on the vegetation of the ENP (Boulangeat *et al.* 2014a), and we have now extended it to incorporate drought effects. We first give a brief description of the base model (further details in the section *FATE-HD ‘base model’ description* in Appendix 2 and in Boulangeat *et al.* 2014b) and then follow with a more detailed description of the new drought module.

FATE-HD models the spatio-temporal dynamics of plant functional groups (PFGs) by explicitly simulating their population dynamics and dispersal, interactions for light resources, and their responses to climate and different LU regimes. FATE-HD has been parameterized for 24 PFGs representative of both the taxonomic and functional diversity of the rich flora in the ENP (Boulangeat *et al.* 2012). They consist of six chamaephyte groups (C1-6), 10 herbaceous groups (H1-10) and eight phanerophyte groups (P1-8), each occupying up to five height strata and passing through four ages (1–4) that have different responses to disturbances (see Table S1 in Appendix 2). The abundance of a given stratum in a pixel determines the amount of light that reaches lower strata. Interactions for light resources are simulated by accounting for the amount of light reaching each PFG cohort in a stand and the PFG’s light preferences. Responses to climate are simulated through habitat suitability (HS) maps (constructed a priori based on observed occurrences) for each PFG, and climate change is simulated by changing HS maps at regular intervals (see *FATE-HD ‘base model’ description* in Appendix 2). Land-use disturbances are modelled in a spatially explicit manner, by assigning mowing, grazing (with intensities low, medium or high) or no disturbance to each

pixel (see *FATE-HD 'base model' description* in Appendix 2). Model output consists of yearly strata and PFG abundances per pixel.

Simulating drought events

Whether or not a PFG was affected by drought depended on the comparison of the PFG's past drought exposure to simulated yearly drought intensity values. To calculate each PFG's past drought exposure, we combined PFG occurrences (from the vegetation data base of the Conservatoire Botanique National Alpin; see Boulangeat *et al.* 2012 and CBNA 2015) with monthly values of a moisture index (MI; Thornthwaite 1948) across the entire French Alps for 1961–1990 (see *Parameterising and simulating drought effects* in Appendix 2). MI was calculated as the difference between precipitation and potential evapotranspiration (negative MI indicating drought; see *Parameterising and simulating drought effects* in Appendix 2). For each PFG, we extracted the distribution of monthly MI values from each plot where it occurred (hereafter $MI_{1961-1990}$). We then defined drought intensity (*Din*) as the lowest MI value in a year for each occurrence plot. Finally, a PFG's past drought exposure was defined as the distribution of these experienced *Din* values (hereafter $Din_{1961-1990}$).

At each year, the PFGs' past drought exposure calculated above was compared with values of *Din* within each pixel (*Din* maps; Fig. 4). The comparison triggered, or not, consequences of drought events through two sequential modelling steps: i) 'identifying drought effects' and ii) 'modelling drought response'.

1. Identifying drought effects under past and future conditions

In the simulations, yearly *Din* values per pixel were obtained from past observations of MI values in the French Alps (validation runs) or from calculations of MI values using future climate predictions (future drought scenario runs). Drought was detected for a PFG in a given pixel, for a given simulation year, when the pixel *Din* was 'abnormally' low relative to the PFGs past drought exposure ($Din_{1961-1990}$ distribution, Fig. S1 in Appendix 2). The drought status was classified as 'no drought', 'moderate drought' or 'severe drought', depending on two 'drought detection thresholds', which were defined as deviations from mean values of PFGs' past drought exposure ($Din_{1961-1990}$ distribution). No drought was detected if the pixel *Din* value was greater than $\bar{x} - 1.5 \times SD$ of $Din_{1961-1990}$ (\bar{x} and SD being the mean and standard deviation, respectively; step 2.1 in Fig. 4). Moderate and severe drought occurred if the pixel *Din* was less than $\bar{x} - 1.5 \times SD$ of $Din_{1961-1990}$ (step 2.2) and less than $\bar{x} - 2.0 \times SD$ of $Din_{1961-1990}$, respectively (step 2.3; see PFG drought detection thresholds in Table S3 in Appendix 2).

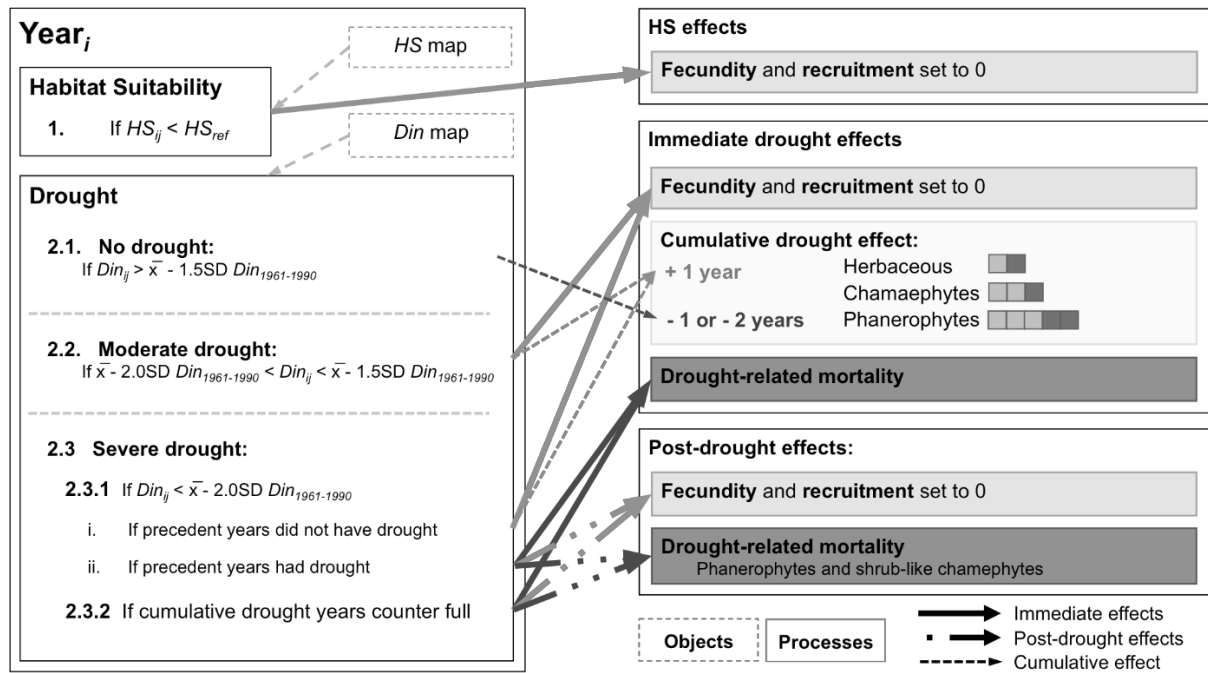


Figure 4. Drought simulation scheme. For each year i , a PFG's habitat suitability (HS ; step 1) and drought effects (step 2) are evaluated within a pixel j . If HS_{ij} or Din_{ij} are below reference values (HS_{ref} and $\bar{x} - 1.5SD$ of $Din_{1961-1990}$, respectively) PFG fecundity and recruitment are set to 0 (medium-grey arrows and boxes). Additionally, if Din_{ij} crosses the reference value, one drought year is added to the PFG's cumulative drought effects counter (thin dashed arrows and light grey box). Severe drought effects occur if conditions 2.3.1.i or 2.3.2 are met (dark grey arrows and boxes), consisting in immediate and post-drought effects (full and dash-dot arrows, respectively). Otherwise, only moderate drought effects are caused (2.1 and 2.3.1.i; medium grey full arrows). Drought recovery is simulated by subtracting one (phanerophytes and shrub chamaephytes, C4) or two drought events from the cumulative drought effects counter (thin, dark grey and dashed arrow). Small light grey squares indicate the 'drought sensitivity' parameter and the total number of squares indicates the size of the counter ('cumulative drought response' parameter). See Table S3 in Appendix 2 for full parameter list and refer to main text for further details.

Effects of severe drought depended on the accumulation of past drought events ('cumulative effect of drought'; steps 2.3.1 ii and 2.3.2). This cumulative effect of drought was meant to simulate the fact that after long periods of water stress, less intense droughts may also have severe effects on tree mortality (McDowell *et al.* 2008; Allen *et al.* 2010). Cumulative effects of drought were twofold and are regulated by two PFG-specific parameters: the PFG's sensitivity to a severe drought ('drought sensitivity'; Table S3 in Appendix 2) and the PFG's response to successive droughts ('cumulative drought response'; Table S3 in Appendix 2). Drought sensitivity expressed the number of droughts a PFG must experience before suffering severe effects due to a severe drought (step 2.3; see 'Modelling drought responses' below). For herbaceous groups, severe drought effects occurred during the first severe drought they experienced (drought sensitivity = 1). In contrast, chamaephytes and phanerophytes were less sensitive: chamaephytes only suffered severe effects during the second drought they experienced, while phanerophytes and shrubs (C4) were only affected severely during the third drought event (step 2.3.1 ii; years represented as light grey squares

in Fig. 4). After a certain number of droughts experienced, the PFG's tolerance is weakened and all drought events (moderate or severe) have severe consequences. The cumulative drought response parameter expressed how many successive drought events were tolerated by a PFG before any subsequent drought events started having severe effects (step 2.3.2). Again, chamaephytes and phanerophytes (together with group C4) were more tolerant and only suffered severe effects from subsequent droughts after three and five drought events, respectively (total number of squares in Fig. 4). Herbaceous groups only needed two drought years to be severely affected by any subsequent drought.

Finally, to simulate drought recovery (and avoid accumulating drought years indefinitely), we removed one drought year (phanerophytes and shrub chamaephytes) or 2 years (herbaceous groups and most chamaephytes) from the PFGs' cumulative effect counters during each non-drought year (dark grey dashed arrow in Fig. 4).

2. Modelling drought responses

Drought effects were twofold, immediate and/or post-drought (occurring the year after drought), in order to simulate demographic responses during and after drought occurs (Allen *et al.* 2010). Drought immediately affected a PFG's recruitment and fecundity, which were set to 0 during the present drought year (moderate and severe droughts). A severe drought also increased PFGs mortality (0–60% depending on the PFG type, soil moisture preference and age) and caused PFGs to resprout (0–80% depending on PFG type, soil moisture preference and age). Post-drought effects were only modelled after a severe drought. To this end, PFG recruitment and fecundity were set to 0, PFG mortality was increased, and resprouting of PFGs was activated (although less than for immediate drought effects: 0–20% for mortality and 0–50% for resprouting). We calculated each PFG's soil moisture preference class (0 = drought tolerant to 3 = drought intolerant; see details in *Parameterising and simulating drought effects* in Appendix 2) considering both PFGs' past drought exposure (via their $MI_{1961-1990}$ distributions) and expert knowledge on the soil moisture requirements of the PFGs. Drought-intolerant PFGs responded with higher mortality rates, and, across PFGs, younger and older PFGs (extremes of the size gradient) also suffered higher mortality rates (McDowell *et al.* 2008). Herbaceous and most chamaephyte PFGs never resprouted during drought, did not suffer post-drought mortality, but always resprouted after a severe drought. Younger individuals (age 1) were never capable of resprouting (see *Parameterising and simulating drought effects* in Appendix 2 for further details, and Table S3 for the full list of drought-related parameters).

Finally, we also simulated the protective effect of canopy cover as a buffer against drought effects. Canopy cover has been shown to increase seedling survival, by an amelioration of local microclimate conditions in terms of air and soil temperature, radiation and humidity (Gómez-Aparicio *et al.* 2005; Kane *et al.* 2011). Hence, in simulations, pixel *Din* values were increased by 25% in pixels where tree cover (strata > 1.5 m) was at least 40% (Esterni *et al.* 2006) – recall that less negative *Din* values correspond to less severe drought.

Simulation experiments

Simulations started with an initialization phase of 850 years during which current climate and land-use regimes were modelled (Fig. 5). This phase allowed a stabilization of PFGs and achieving the current vegetation state before any future scenarios of climate, land-use or drought regime changes were applied (Boulangeat *et al.* 2014b). All scenario simulations started from the last year of the initialization phase, which will be referred to as year 0 hereafter.

We simulated one scenario of gradual CC, five scenarios of increasing drought frequency that were combined with three scenarios of increasing drought intensity (see below) and with two scenarios of LU change, totalling to 30 scenarios runs (Fig. 5). Since changes in drought regimes are thought to be a consequence of CC, we always changed background climate through its impact on habitat suitability for PFGs. Additionally, we ran two baseline simulations with only gradual CC (i.e. no drought), each with a scenario of LU.

Drought was implemented similarly to CC, by feeding maps of drought intensity (*Din*) values. Like maps of ‘current’ HS, ‘current’ *Din* maps were calculated by averaging past MI values across years 1961–1990. Since drought events are caused by extreme values of temperature and/or precipitation (IPCC 2012), we used the predicted temperature and precipitation maps for 2080 (following the A1B scenario described in *FATE-HD ‘base model’ description* in Appendix 2) to calculate future maps of *Din* values. Current IPCC predictions indicate that drought frequency and intensity are to increase in the future (IPCC 2012); hence, we simulated three different drought intensities with linearly increasing drought frequencies and fixed periods without drought events to test our hypotheses. This allowed the vegetation to recover by avoiding long periods of continuous drought if frequency was high. Drought was then set to occur either every year or every 2, 4, 8 or 16 years (five drought frequency scenarios), with a 10-year no-drought period after each sequence of five drought events.

Future and current *Din* maps were alternated to create drought and no-drought years, respectively. As for drought intensity, we calculated three levels of intensity ('low', 'medium' and 'high') that would not greatly deviate from climate predictions. Medium intensity corresponded to forecasted *Din* values for the year 2080, and low/high intensity corresponded to an increase/decrease of these values by 20%, respectively (three intensity scenarios; see Fig. S1 in Appendix 2).

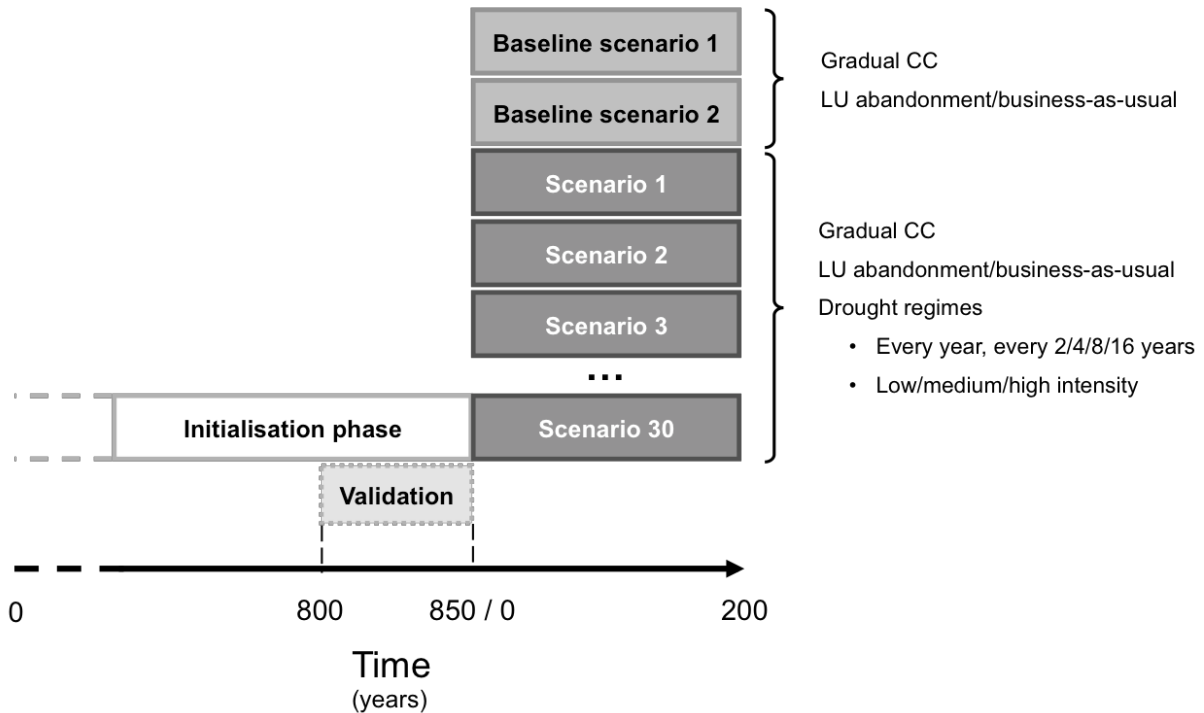


Figure 5. Simulation experiment workflow. An initialisation phase (0-850 years) allowed reproducing the current vegetation state of the Ecrins National Park. The last 50 years of the initialisation phase (800-850 years) were used to validate the drought module, while the last year (year 850) was the starting point of scenario simulations, which lasted 200 years. Climate change was implemented from years 15 to 90. Land-use changes were implemented at year 4, remaining unchanged until the end of the simulations. Drought regimes were initiated at year 15, lasting at least as long as climate change, up to year 105.

Land-use scenarios consisted of removing all grazing and mowing activities to simulate LU abandonment, or to continue current LU practices to simulate a 'business-as-usual' scenario (two LU scenarios). Land-use abandonment was applied at year 4 until the end of the simulation, whereas gradual CC was applied by changing PFG habitat suitability at regular 15-year intervals, starting at year 15 until year 90 (see *FATE-HD 'base model' description* in Appendix 2 and Boulangeat *et al.* 2014a). The duration of drought regimes depended on the scenario of drought frequency, but covered at least the period of gradual CC (years 15–90) and finished before year 105. For all scenarios, simulations were run for a total of 200 years and replicated three times (Fig. 4).

We validated the drought module by running a simulation using observed data of drought events that occurred between 1961 and 1990 (Fig. 4). Model output was compared to vegetation plots from the ENP database and the previous validation of FATE-HD (Boulangéat *et al.* 2014b). We found that the simulated vegetation represented the observed vegetation of the park well and concluded that the inclusion of drought effects led to good model performance (see *Validation of drought module* in Appendix 2).

Analysis of results

To answer our first question regarding the effects of drought and LU on forest expansion, we analysed how different combinations of drought intensity, drought frequency and LU regimes influenced the speed at which forest and shrubland migrated towards higher elevations. Forest and shrubland pixels were identified based on the percentage of tree cover (strata > 1.5 m), which was larger than 60% for forest and between 10% and 60% for shrubland (Esterni *et al.* 2006). Rates of forest and shrubland expansion (RFE and RSE, respectively) were estimated independently for three different time frames. The first reflected the initial impacts of gradual CC, LU and drought disturbances (years 0–49). The second reflected responses to on-going CC and drought events and medium-term responses after they ended (years 50–149). The last time frame reflected long-term responses to gradual climate and LU changes, as well as recovery from drought events and the eventual establishment of new equilibria (years 150–200). Hence, for each time frame (and each scenario), we regressed yearly maximum elevation obtained for forest and for shrubland pixels against time to obtain the rates of expansion (regression slopes). Responses of RFE and of RSE to drought and LU regimes, and their interactions, were analysed separately for each time frame using analyses of variance (ANOVAs). Four levels of drought intensity ('no drought', 'low', 'medium' and 'high') and six of drought frequency ('no drought', every year and every 2, 4, 8 and 16 years) were used as independent factors. Land use was used as a factor with two levels ('abandonment' and 'business-as-usual'). Model selection was based on Akaike Information Criterion (AIC) values, model parsimony and analyses of residuals.

Taxonomic response of the forest–grassland ecotone to simulated drought, CC and LU, was assessed by quantifying PFG turnover both spatially and temporally, using a measure of β -diversity. The ecotone was spatially delimited for each scenario at year 0, using a buffer distance around the upper tree line (1000 m above and 500 m below), tree line being defined at the third quartile of elevation values of forest pixels. Mean β -diversity was calculated using

a multiplicative decomposition of γ - and α -diversity, calculated as the inverse Simpson concentration (Whittaker 1972):

$$\alpha / \gamma = \frac{1}{\sum p_{(i)}} \quad (\text{Eq. 1})$$

$$\beta = \gamma \times \sum \left(\frac{1}{n} \times \frac{1}{\alpha_i} \right) \quad (\text{Eq. 2})$$

where p is the relative abundance of each PFG across pixels (for γ -diversity), or in each pixel i (for α -diversity), and n the total number of communities. Alpha and γ -diversity are bounded between unity and the maximum number of PFGs; β -diversity is bounded between unity and the maximum number of communities (Tuomisto 2010). For temporal turnover, β -diversity was calculated per pixel (i.e. communities) with reference to year 0 at subsequent 5-year intervals (year five against year zero, year 10 against year zero, etc.), then averaged across all ecotone pixels to obtain a value per pair of years. Spatial turnover was calculated across all ecotone pixels (for a given year) every 5 years.

We also explored how community-averaged soil moisture preference changed spatially under different drought regimes and different LU practices. Focusing again on the ecotone, we calculated community-weighted mean values of soil moisture preference classes (CWM_{SM}) every 5 years, by weighing PFG soil moisture preference values (SM_j) by PFG relative abundances ($abund_j$, j being a PFG) for each pixel (Garnier *et al.* 2004; Violle *et al.* 2007):

$$CWM_{SM} = \sum SM_j \times abund_j \quad (\text{Eq. 3})$$

Since we were interested in mapping increases or decreases of CWM_{SM} , rather than following its temporal evolution, we calculated changes in CWM_{SM} per pixel, as the difference between CWM_{SM} values of a given year and year 0. Negative values indicated shifts towards communities with preference for drier soils, while positive values indicated shifts to communities with higher moisture requirements. Resulting CWM_{SM} changes were mapped for different scenarios of drought intensity/frequency and LU management to obtain a spatial image of functional community shifts. In addition, we assessed whether changes towards communities with higher or lower soil moisture preference were linked to elevation, by calculating Pearson product-moment correlation coefficients between values of change and elevation across ecotone pixels.

Results

When considering all scenarios of drought and land-use regimes, rates of forest expansion (RFE) towards higher elevations were not significantly different from the rates of shrubland expansion (RSE; Fig. S4 in Appendix 2). While RSE was always significantly affected by drought intensity and frequency, RFE only responded significantly to these factors during the early phases of the simulations (years 0–49 and 50–149 in Fig. 6a and Tables S5 and S6). Both RSE and RFE were more affected by different drought intensities, rather than frequencies (Table S6 in Appendix 2). Also, RSE and RFE responded differently to the interaction between drought intensity and frequency, which significantly affected RFE between years 0 and 149, but only had a significant effect on RSE during the last 50 years.

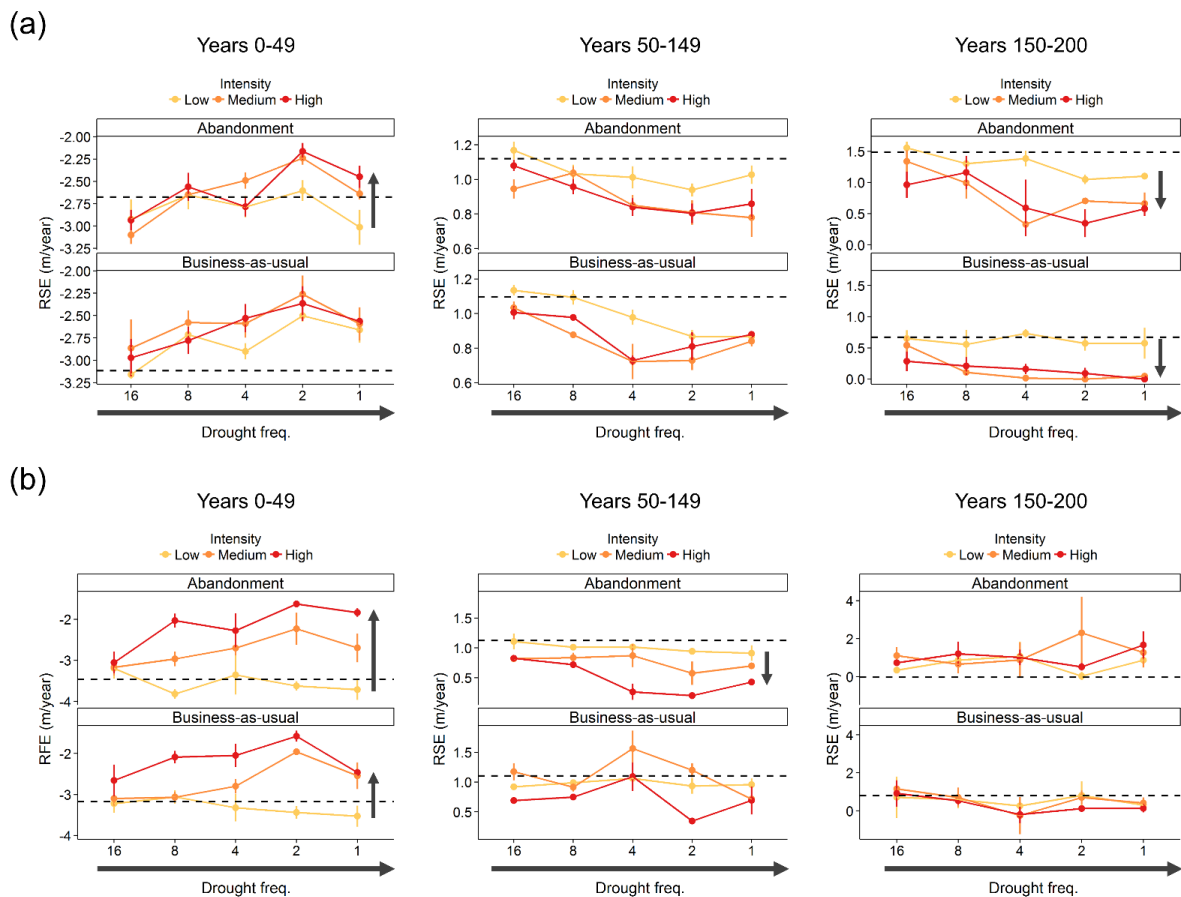


Figure 6. Effects of drought intensity, drought frequency and land-use practices on a) rates of shrubland expansion (RSE) and on b) rates of forest expansion (RFE) for the three simulation time frames. Plots show the rates of expansion of all forest and shrubland pixels averaged across the three simulation repetitions. Dashed lines show baseline levels. Vertical arrows indicate increasing drought intensities (colour coded from low to high), while horizontal arrows along the x-axis indicate increasing frequency (from every 16 years, “16”, to every year, “1”). Climate change and drought were implemented between years 15-90 (drought regimes up to year 105) and land-use abandonment started at year 4 onward.

Between years 0 and 49, high drought intensity generally increased RSE and RFE, especially when associated with higher drought frequencies (RSE ~ 2.5 m year⁻¹ and RFE between approximately 2.5 and 2 m year⁻¹; left panels in Fig. 6a,b). This pattern was then reversed between years 50–149, where medium and high drought intensities caused RSE to decrease (RSE almost always <1 m year⁻¹; middle panel in Fig. 6a), a pattern that could also be seen for forest expansion under land-use abandonment (middle panel in Fig. 6b) and for shrubland expansion during the last time frame (right panel in Fig. 6a). The effect of drought frequency on RSE was more evident during the first two time frames, where increasing frequencies led to larger departures from baseline expansion rates (left and middle panels in Fig. 6a). On the other hand, the effect of drought frequency on RFE (and on RSE during the last 50 years) was largely dependent on drought intensity. While increasing the frequency of low intensity drought events did not seem to impact forest expansion more than climate and land-use changes alone, it clearly aggravated the effects of high intensity drought events (left and middle panels in Fig. 6b, but see also right panel in Fig. 6a for a similar pattern). The effect of LU gained importance during the two last time frames, where land-use abandonment generally increased RSE and RFE across the different drought intensity and frequency levels (middle and right panels in Fig. 6a,b). In fact, during the last 50 years, the response of RFE was only significantly affected by LU, despite that there seems to be a negative effect of high drought intensity when current land-use practices were kept (see right panel in Fig. 6b).

Given that higher drought frequencies generally increased the effects of high intensity drought events, enhancing the differences between drought intensity levels, we analysed ecotone community responses by contrasting the two most extreme drought frequency scenarios (in terms of RSE and RFE) across LUs: i) infrequent droughts (occurring every 16 years) and ii) frequent droughts (occurring every 2 years). Drought regimes only seemed to affect PFG turnover (measured by β -diversity) when drought was frequent and their impact differed between LU scenarios (Fig. 7). In general, the ecotone became increasingly different from its initial state during the period of gradual CC, especially under a LU abandonment scenario (Fig. 7; see also Fig. S5 in Appendix 2). However, frequent drought events affected the rates at which these changes occurred. Temporal taxonomic turnover accelerated during periods of drought, but stabilized at lower levels towards the end of the simulations, especially if drought intensity was high (Fig. 7b). Similarly, more frequent drought events increased spatial taxonomic heterogeneity, especially in combination with high drought intensity (Fig. S5 in Appendix 2).

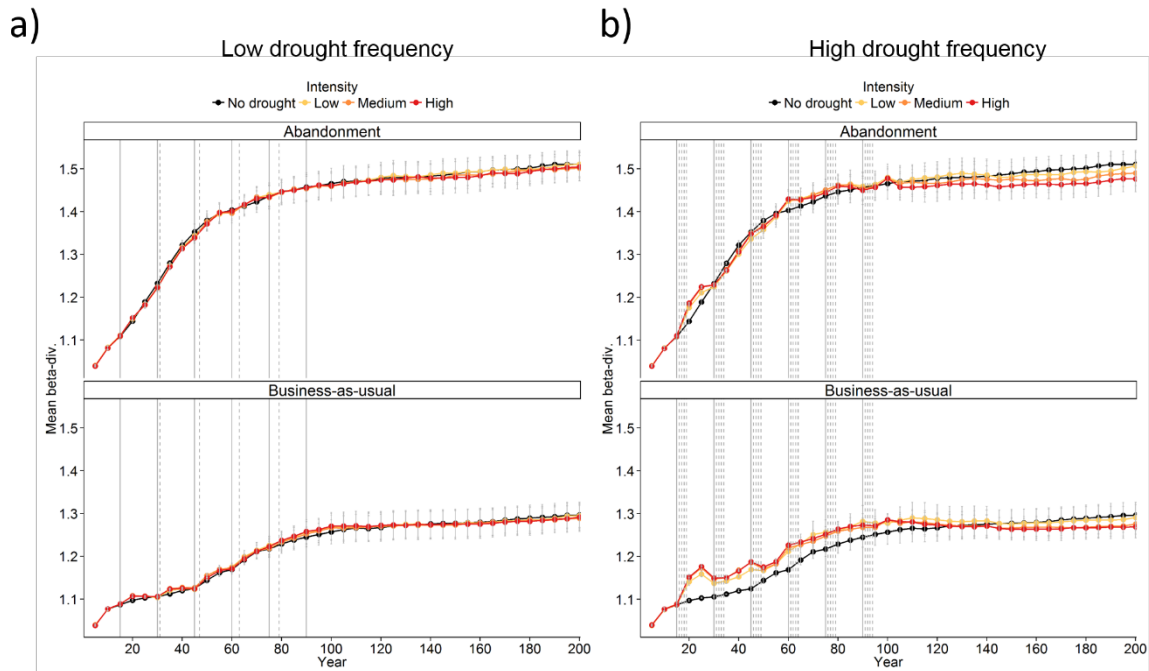


Figure 7. Effects of drought intensity (colour coded) and land-use practices on temporal β -diversity are shown for scenarios of a) low drought frequency (every 16 years) and b) high frequency (every two years). Temporal β -diversity was calculated every 5 years with respect to year 0, within forest–grassland ecotone boundaries defined at year 0 in each scenario, and averaged across simulation repetitions. Vertical lines indicate climate changes (full line) and drought events (dashed lines); land-use abandonment started at year 4 onward. Standard error bars are shown in grey for each point.

Since drought effects on forest and shrubland expansion were stronger during the first two simulation phases (years 0–149), we analysed functional changes in forest–grassland ecotone communities during this period. In general, soil moisture preference showed important changes across this time period (differences between years 145 and year 0 ranged from 2.17 to 1.55 CWM_{SM} units; Fig. 8). These changes were significantly correlated with elevation, although correlation values were relatively low due to higher variance at lower elevations (Fig. S6 in Appendix 2). Mapping the difference in soil moisture preference values between year 145 and year 0 revealed a tendency for communities to become more drought tolerant across the landscape, especially at higher elevations (see sign of correlations with elevation in Fig. 8). Although visual patterns are very similar with or without drought effects, the correlation between CWM_{SM} and elevation is weaker under highly intense and frequent drought. Land-use abandonment contributed to larger changes towards lower values of CWM_{SM} than did current LU activities and also decreased the strength of the correlation between CWM_{SM} and elevation (compare upper and lower panels in Fig. 8a–c).

Discussion

Despite the likelihood that drought frequency and intensity will increase in European mountainous areas (Calanca 2007), their impact has been largely understudied. Our simulations revealed that drought can have significant impacts on the dynamics of forest–grassland ecotones in the European Alps and that these impacts can partially change under different land-use scenarios.

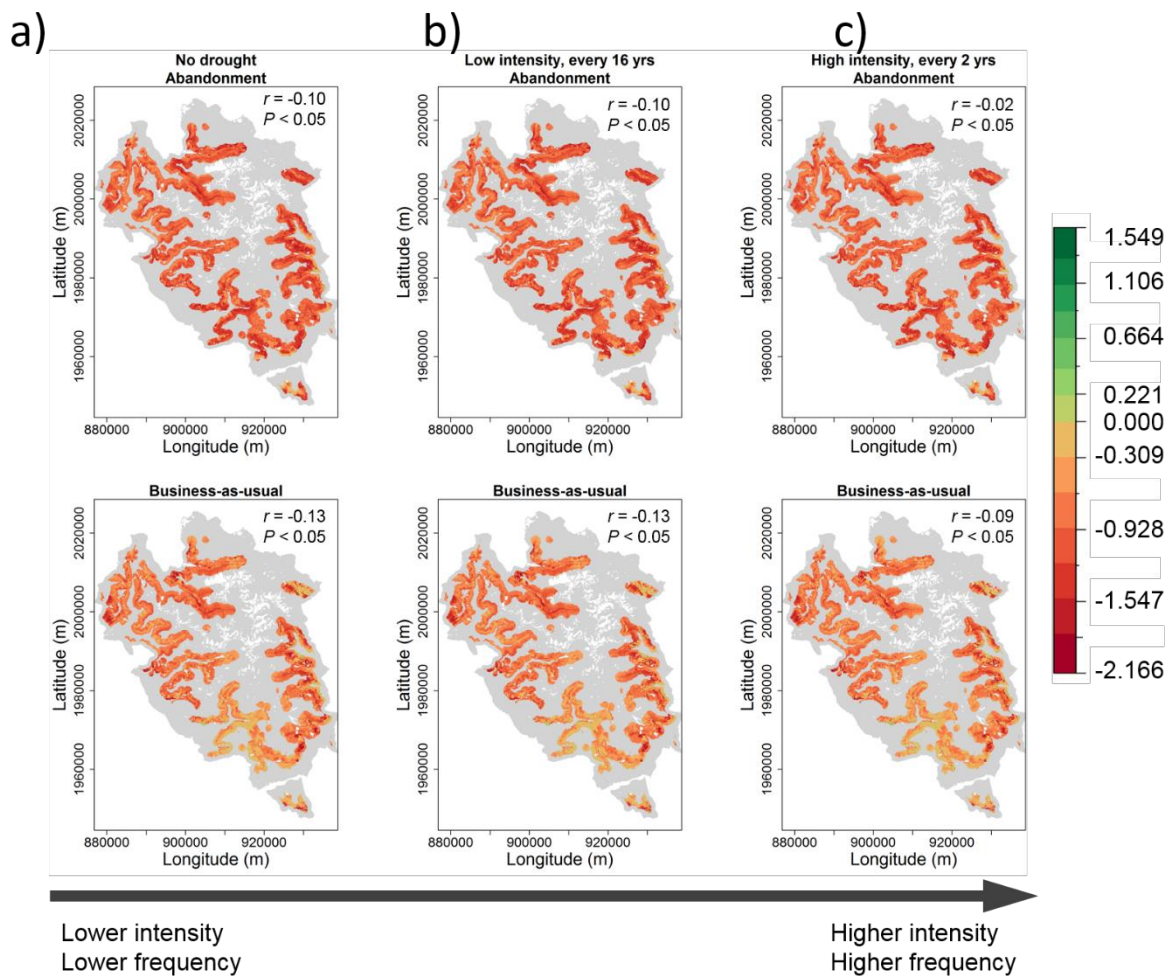


Figure 8. Functional responses of the forest–grassland ecotone across land-use scenarios for a) baseline simulations and for two extreme scenarios of drought: b) low intensity drought events occurring every 16 years and c) high intensity drought events occurring every two years. Maps show differences in community-weighted mean (CWM) soil moisture preference values calculated between year 145 and year 0 of the scenario simulations, averaged across simulation repetitions. Negative values indicate communities that became more drought-tolerant. Pearson moment correlation values between CWM differences and elevation are shown in the top right corners. Also, see Fig. S6 in Appendix 2 for temporal evolution of CWM values.

We used a dynamic vegetation model to simulate drought effects on vegetation. Unlike physiological approaches that provide prediction of drought effects at the individual level, FATE-HD provides an overview at the landscape level bypassing the issues associated with

simulating physiological processes. The validation of FATE-HD suggests that the model gives a realistic picture of the mechanisms driving vegetation dynamics in the park. Using a particular period (here 1961–1990) for parameterization may have biased our estimates of drought sensitivity and severity, since two important drought events have affected the ENP in the early 2000s (Bonet *et al.* 2016). Yet, this bias is equal among scenarios and should not affect their relative differences. Our approach might also suffer from the fact that it does not include other important factors that may interact with drought, such as pests, insect outbreaks or atmospheric CO₂, which may influence vegetative growth. However, this would require a complex physiological model difficult to parameterize for such a rich and diverse region. Therefore, our aim was not to provide quantitative estimates of vegetation changes, but instead provide a qualitative comparison of the possible effects of different drought regimes on landscape succession.

Drought effects on woody encroachment

Drought events showed opposing effects compared to land-use abandonment and gradual climate change, by accelerating forest and shrubland expansion during the first years of drought and decelerating it in subsequent years, especially when drought frequency and intensity were high. While effects of infrequent drought (occurring every 16 years) or of low intensity drought were not easily distinguishable from simply ignoring extreme events, an increase of drought frequency to every 1–2 years, or of drought intensity, changed forest and shrubland expansion rates (Fig. 6). Indeed, high drought frequencies have been shown to aggravate the effects of short drought events, causing similar levels of tree mortality as those observed during prolonged droughts (Adams *et al.* 2009). Similarly, our results showed that, when drought was frequent, low and medium drought intensities resulted in rates of shrubland expansion almost as low as those of high drought intensities (years 50–149 in Fig. 6a). On the other hand, mild drought events may increase forest expansion if they remain below species-specific tolerance thresholds (Bachelet *et al.* 2001), which could explain the higher forest and shrubland expansion rates during the first 50 years (Fig. 6a,b). In fact, in our simulations, herbaceous and most chamaephyte PFGs were more sensitive to drought than phanerophytes, meaning that these groups were more negatively affected by successive moderate droughts and competed less for light resources, eventually reducing forest retraction.

Obviously, quantitative expansion rates are related to the way drought effects were parameterized. We used a conservative approach when simulating drought-related mortality, which only occurred in response to severe drought. In addition, severe drought effects were

only triggered if a minimum number of drought events were accumulated, with phanerophyte groups being the least affected by drought. Although this led to smaller effects of drought at low frequencies, our parameterization reflects the observed resistance of these groups to drought in the study area, relatively to the climate period of reference. Furthermore, decisions on cumulative effects for different PFG life forms were based on expert knowledge from botanists working within the ENP, which we believe is highly valuable. While our parameterization of drought effects might not reflect true quantitative estimates, it allows exploring how different drought frequencies affect the progression of tree line towards higher elevations in the Alps and how these effects are modulated by land uses.

Drought effects on ecotone biodiversity

Unlike woody encroachment, changes in tree line biodiversity were mainly impacted by gradual climate change and land-use regimes. Climate-induced changes in community composition invariably increased with time (Fig. 7). Land-use abandonment led to more homogeneous landscapes due to grassland conversion to forest, while current land-use practices led to higher heterogeneity, as grasslands were artificially kept open and forests colonized unmanaged areas (Fig. S5 in Appendix 2). However, drought regimes had important effects on the rate at which these changes occurred. Turnover rates increased during periods of frequent drought (Fig. 7b) and the ecotone became spatially more heterogeneous than under the effect of gradual climate change (Fig. S5 in Appendix 2). Under land-use abandonment, this was due to the fact that despite the conversion of large open areas to forest, which increased overall spatial homogeneity (upper panels in Figs. 4b and 5b), higher PFG mortality caused by drought negatively affected the colonization of certain warm-adapted and/or drought-adapted PFGs, reducing the effects of gradual climate change (such as C1, C4, C5 and P7; see Tables S2 and S3 in Appendix 2). Oppositely, the business-as-usual scenario prevented forest colonization in managed areas but allowed it in other areas, maintaining a higher spatial β -diversity (Boulangeat *et al.* 2014a); however, frequent drought selected against PFGs with lower drought resistance (such as H6, H7 and P2; Tables S2 and S3 in Appendix 2) and in favour of less sensitive herbaceous and chamaephyte groups (such as C5 and H5; Tables S2 and S3 in Appendix 2) increasing the speed at which the ecotone changed (see lower panel in Fig. 7b) and the heterogeneity between managed areas and those that became invaded (lower panel in Fig. S5b in Appendix 2).

As with taxonomic turnover, changes in community soil moisture preference were also mainly driven by gradual climate change and land-use practices (Fig. 8). Community soil

moisture preference generally decreased during, and sometime after, the period of simulated drought and climate change (years 0–145); yet, this varied not only between scenarios of land-use change, but also with elevation (see steeper curves at lower elevations in Fig. S6 in Appendix 2). This functional homogenization following gradual climate change, especially in combination with land-use abandonment, was due to the replacement of drought-intolerant ecotone communities by more drought-tolerant ones across the entire landscape. Furthermore, our results suggest that frequent and intense drought may cause functional shifts in communities that are not necessarily similar to those observed under gradual climate warming (Fig. 5 and Fig. S6 in Appendix 2).

Changes in understory communities may be the direct result of drought-related mortality, but also the indirect result of change in forest cover. Not only did we simulate changes in light interception at the canopy level, but also its buffering effect against drought stress, two factors that are at the origin of negative feedbacks of forest cover reduction on understory communities (McDowell *et al.* 2008; Allen *et al.* 2010; Anderegg *et al.* 2013). Therefore, the simulated loss of tree cover exposed understory communities to stronger drought effects and changed their exposure to light, most likely leading to changes in community composition and structure that may be similar to what has been reported in previous studies (Anderegg *et al.* 2012). Future studies will be needed to evaluate these changes, whether community composition can revert back to pre-drought conditions and how long this takes to happen.

Consequences for land-use management and ecosystem services

Land-use abandonment did not significantly reduce the effects of high drought intensity and frequency on forest expansion, suggesting that it affected forest expansion less than drought or gradual climate change, at least at the analysed time scale (Fig. 6b and Table S6 in Appendix 2). Land-use abandonment increased forest expansion for high drought frequencies and intensities mostly during the first 50 years of simulations (Fig. 6b) and baseline rates of forest expansion were always similar between the two land-use scenarios. The effect of land-use practices seemed to gain importance in later years, with land-use practices being the only factor significantly affecting forest expansion during the last 50 years of the simulation (years 150–200 in Fig. 6b and Table S6 in Appendix 2). Although land use had impacts on the short term, changes to PFG colonization that greatly impact vegetation structure were more visible on the long term, since in FATE-HD there is a lagged response of PFG demography, dispersal and biotic conditions necessary to establish canopy cover (Boulangeat *et al.* 2014a). On the other hand, the effects of land-use abandonment on the spatial and temporal turnover of

taxonomic and functional composition were evident on the short term, but partially affected under frequent and intense drought.

These results have important implications for the way land-use planning should consider drought effects on vegetation. Current ecosystem management in the European Alps responds to recent trends of land-use abandonment and climate change, as both promote the loss of open habitats by woody encroachment (MacDonald *et al.* 2000; Gehrig-Fasel *et al.* 2007). In the ENP, management focuses on maintaining biodiversity at different levels, from protecting diversity and ecosystems *per se*, to preserving multiple ecosystem services (Parc National des Ecrins 2015). Sustainable grazing and mowing practices prevent forest expansion, help protect subalpine and alpine grasslands and species of conservation concern (Andrello *et al.* 2012) and ensure the provision of fodder for cattle and the maintenance of open habitats for cultural and leisure activities (Parc National des Ecrins 2015). Our predictions indicate that frequent and intense drought will counteract the effects of gradual climate change, leading to lower forest expansion rates even under land-use abandonment (see also Lenoir *et al.* 2010a). Projections under the IPCC SRES A2 scenario by Calanca (2007) predicted a 50% probability of drought occurrence between 2071 and 2100 in the European Alps, in comparison with 18% calculated for the period 1901–2004. Recent drought events have been reported to cause important forest dieback in the Swiss Alps (Rebetez & Dobbertin 2004; Rigling *et al.* 2013), and drought sensitivity has increased in the last century even for forest stands on mesic sites (Weber *et al.* 2013). If drought frequency and intensity increase and forests retract, we may not only expect losses of forest cover and biodiversity, but also habitat shifts and important changes in ecosystem service provisioning. Forests in the European Alps are important carbon sinks, but also exert control on avalanches, rock fall (Berger & Chauvin 1996; Weber *et al.* 2013) and flood regimes at lower elevations (Descroix & Gautier 2002; Marston *et al.* 2003). If ecosystem management continues to prioritize the conservation of multiple ecosystems services and, thus, a mosaic of habitats (as is current practice in the ENP), land-use planning in the Alps needs to prevent woody encroachment (and the loss of open habitats), as well as to incorporate accurate and spatially explicit drought predictions to avoid loss of forest cover in areas where drought effects are expected to be very severe. This is not only valid in the European Alps, but also in other mountain ecosystems where tree line is actively managed and where land-use and climate changes will likely interact with changes in drought regimes. Besides delaying forest progression, drought might also compromise grassland communities by driving phenological, taxonomic and functional shifts (De Boeck *et al.* 2015), which could

be different from those observed under gradual climate changes (Figs. 4, 5, S5 and S6). These shifts can alter the ratios between more and less productive species, having repercussions on nutrient cycling and other ecosystem services, such as fodder production (Nandintsetseg & Shinoda 2013). Hence, conserving the taxonomic and functional biodiversity of forest–grassland ecotones in mountain areas is of great importance to ensure the provisioning of multiple ecosystem services. In a European context, management of these ecosystems must not only focus on tree line advancement driven by land-use abandonment and facilitated by warming, but also on eventual forest retraction and changes to grassland diversity caused by drought, which might impact the provisioning of ecosystem services.

Data accessibility

Rates of shrubland and forest expansion, taxonomic temporal and spatial turnover, changes in community-weighted mean soil moisture preferences at ecotone level and R scripts for analysis of results are available from Dryad Digital Repository <http://dx.doi.org/10.5061/dryad.s3015> (Barros *et al.* 2016a).

CHAPTER II

N-DIMENSIONAL HYPERVOLUMES TO STUDY STABILITY OF COMPLEX ECOSYSTEMS

Ceres Barros^{1,2}, Wilfried Thuiller^{1,2}, Damien Georges^{1,2}, Isabelle Boulangeat³, and Tamara Münkemüller^{1,2} (2016). *Ecol. Lett.*, 19, 729–742

¹ Laboratoire d'Écologie Alpine (LECA), Université Grenoble Alpes, F-38000 Grenoble, France

² Laboratoire d'Écologie Alpine (LECA), CNRS, F-38000 Grenoble, France

³ Département de Biologie, Chimie et Géographie, Université du Québec à Rimouski, 300 Allée des Ursulines, Québec G5L 3A1, Canada

Abstract

Although our knowledge on the stabilising role of biodiversity and on how it is affected by perturbations has greatly improved, we still lack a comprehensive view on ecosystem stability that is transversal to different habitats and perturbations. Hence, we propose a framework that takes advantage of the multiplicity of components of an ecosystem and their contribution to stability. Ecosystem components can range from species or functional groups, to different functional traits, or even the cover of different habitats in a landscape mosaic. We make use of n -dimensional hypervolumes to define ecosystem states and assess how much they shift after environmental changes have occurred. We demonstrate the value of this framework with a study case on the effects of environmental change on Alpine ecosystems. Our results highlight the importance of a multidimensional approach when studying ecosystem stability and show that our framework is flexible enough to be applied to different types of ecosystem components, which can have important implications for the study of ecosystem stability and transient dynamics.

Keywords: climate change, ecosystem stability, land-use changes, n -dimensional hypervolumes, perturbations

Introduction

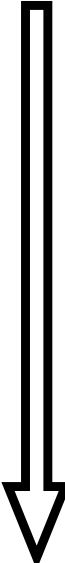
Across the globe, ever-increasing changes to ecosystems such as regional intensification or land-use abandonment, and climate change, threaten taxonomic and functional composition and associated ecosystem functions and services (Diaz *et al.* 2006; Weiner *et al.* 2014; Kortsch *et al.* 2015; Oliver *et al.* 2015). These changes may compromise the ability of ecosystems to recover from future perturbations and lead to departures from stability, which may ultimately result in shifts to other ecosystem states (Standish *et al.* 2014).

Therefore, studying stability is important to understand the response of ecosystems to afore mentioned land-use and climate changes. Stability is a multifaceted concept that can be studied in different ways (Ives 1995; de Mazancourt *et al.* 2013). However, most empirical studies on ecosystem stability have been focused on the role of biodiversity for the stabilisation of a particular ecosystem function – biodiversity-ecosystem functioning (BEF) studies (e.g. Tilman & Downing 1994; Jousset *et al.* 2011; Pillar *et al.* 2013). The majority of these studies have aimed at understanding how biodiversity maintains and promotes productivity (e.g. Cadotte *et al.* 2012; Roscher *et al.* 2012; but see Hautier *et al.* 2015) and have shown that the processes through which this occurs can differ between communities (Morin *et al.* 2014). Fewer studies investigated the stability of biodiversity itself to perturbations – perturbation-biodiversity studies. These have shown that relationships between taxonomic and functional diversity can change across environmental and disturbance gradients (Flynn *et al.* 2009; Biswas & Mallik 2011), affecting the relationship between ecosystem function and biodiversity (shown for steppe communities by Zhou *et al.* 2006). However, studies rarely investigated the impact of disturbances on the stability of ecosystem function and of biodiversity together (but see Steudel *et al.* 2012). This is an important drawback, since both the stability of ecosystem functions and of ecosystem structure and composition can be important aspects in terms of management planning and policy making for complex ecosystems, especially if several types of habitats exist and ecotone dynamics can change (MacDonald *et al.* 2015).

Considering how different components of an ecosystem – e.g. species abundances, their functional and phylogenetic composition, and resulting ecosystem functions and services (cf. Table 2 for a non-exhaustive list of components relevant for different facets of ecosystem stability) – contribute to its stabilisation can be important in complex ecosystems, where summarising stability into a single metric might be a challenge and likely inaccurate. For

instance, diverse habitat mosaics can be composed of communities that are very different in terms of productivity levels and their seasonality, but all equally stable in terms of species richness. In such cases, ecosystem stability is not easily summarised by a single metric, such as productivity, and considering multiple taxonomic and functional community components is likely to provide better information about overall ecosystem stability.

Table 2. Examples of components that can be considered for assessing ecosystem stability using the hypervolumes framework. In this non-exhaustive list, types of ecosystem components are sorted by increasing level of organisation, although some can be considered across different organisational scales (e.g. diversity metrics). We distinguished between ecosystem functioning components and ecosystem services components following Lavorel & Grigulis (2012).

Ecosystem components	
increasing level of organisation 	<ul style="list-style-type: none"> - Organisms (usually raw/relative abundances, cover) E.g. species, guilds, functional groups, MOTUS (molecular operational taxonomical units) - Community trait values (generally averaged and weighted by species abundance, but variances in trait values can also be used) - Diversity metrics E.g. taxonomic richness and evenness, functional richness, evenness, divergence and dispersion, mean phylogenetic distance - Properties of ecological networks E.g. species diversity, connectance, modularity - Habitat/vegetation cover - Ecosystem functioning (often productivity, but other functions like nutrient cycling can also be considered) E.g. biomass, nitrogen, carbon and water availability - Ecosystem services E.g. quantity and quality of fodder, nutrient cycling, carbon storage, water quality

Defining the state of a complex ecosystem can be challenging, since ecosystems and their multiple components often have temporal fluctuations. In a two-dimensional case, these oscillations are usually well represented in phase portraits, where the two response variables are plotted against each other at several points in time (Fig. 9). If the system reaches equilibrium, its trajectory will converge to an equilibrium point, or a limit cycle in an oscillatory equilibrium (Fig. 9b). In complex systems involving more than two response variables (Fig. 9c), the trajectory becomes a path in n -dimensional space. In this case, the ecosystem state can be described as an n -dimensional cloud of points or an n -dimensional hypervolume (Fig. 9d). An ecosystem state is then determined by both the intrinsic dynamics of its components and environmental conditions. If changes in these conditions occur and the

ecosystem is disturbed, ecosystem components and their trajectories may be affected, leading to another n -dimensional hypervolume (Fig. 9d). Comparing the two hypervolumes will provide an assessment of the magnitude of changes the ecosystem suffered, i.e. its shift from the initial state. Although in this study we were not interested in detecting shifts between alternative stable states, *sensu* Scheffer *et al.* (2001), the ball-and-cup analogy of resilience (Holling 1996; Folke *et al.* 2004) provides an intuitive visual representation of how n -dimensional hypervolumes relate to ecosystem stability. If we consider that n -dimensional hypervolumes represent the states of a system under different environmental conditions, comparing hypervolumes before and after perturbations will reflect how far the system has moved from its initial basin of attraction (i.e. state; Figs. 9e, f, g). Our focus is not on how fast a community returns to its pre-perturbation state (engineering resilience, or the basin's slope), nor to assess whether the community has undergone a permanent state shift. Although these can be investigated, here, we focus on the departures from an ecosystem state (stable or transient), i.e. the magnitude of changes that the ecosystem suffered.

We, thus, propose using hypervolumes built from several components of an ecosystem as a means to reflect their integrated variability. The choice of the type of components will depend on what the analysis of stability falls unto. We believe that ecosystem stability should be investigated across different components; the approach we propose here is sufficiently flexible to be applied to different sets of data and can be used for this integrative approach (Table 2). For example, if the research focus is on the stability of biodiversity at the community scale, time series of species abundances or community-weighted means (CWMs) or variances (CWV) of functional traits (i.e. trait values of all species in the community weighted by species abundances) can be used. At a larger scale, the stability of biodiversity can also be assessed using taxonomic, functional and phylogenetic diversity metrics that can constitute the hypervolumes. At the landscape scale, in mosaic ecosystems, it may be interesting to analyse stability in terms of proportions of different habitat patches, building hypervolumes from coverage values of each habitat type.

We present this novel approach using simulated plant communities of different habitats in the European Alps. In Alpine mountain ecosystems, sharp gradients drive both abiotic and biotic constraints that result in the presence of distinct plant communities within relatively small spatial extents. These systems are especially vulnerable to climate and land-use changes (LUC; Serreze *et al.* 2000; Tappeiner & Bayfield 2009; Dullinger *et al.* 2012; Thuiller *et al.* 2014), since they harbour species that are frequently at their niche limits and are likely to respond faster to environmental change (Wookey *et al.* 2009; Rigling *et al.* 2013). For

example, land-use abandonment and climate warming can cause shifts in grassland composition and structure, leading to woody encroachment (Tasser & Tappeiner 2002; Asner *et al.* 2004) and changes in forest-grassland ecotones (Boulangeat *et al.* 2014a; Carlson *et al.* 2014). Hence, these ecosystems provide a rich study case for our proposed framework. Our results show that the framework successfully distinguishes what types of perturbations most affect Alpine communities and can provide indication of how different community components respond to the same perturbation. More importantly, this framework is a successful first step into integrating the multiplicity of ecosystem components for the analysis of ecosystem stability in a global change context.

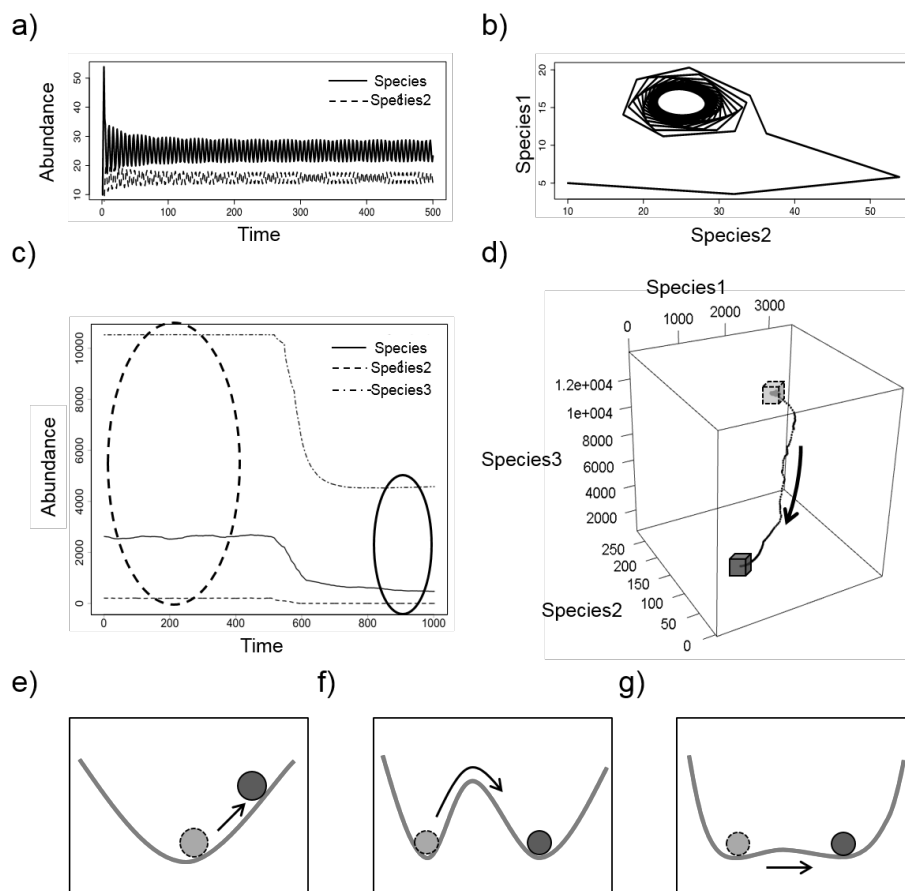


Figure 9. The utility of phase portraits for studying stability. A system of a) two species can be represented by b) a classical two-dimensional phase portrait. The system's state at equilibrium is represented by a circling behaviour in b) that corresponds to oscillations of species abundances in a). This concept can be extended to higher dimensions, where the c) dynamics of a three-species community are represented by a d) three-dimensional phase portrait. In multidimensional space, states at equilibrium become clouds of points in d), which can be represented by n -dimensional hypervolumes (schematic cubes). Comparisons between hypervolumes can be related to the ball-and-cup analogy of resilience, as they indicate departures from the first that can happen e) within the same basin of attraction, f) when the system shifts to an alternative stable state, or g) when the equilibrium is displaced (Beisner *et al.* 2003; Horan *et al.* 2011).

A general framework for comparing community states

Our framework to study ecosystem stability in face of environmental changes using n -dimensional hypervolumes is presented in two sections. In the present section, we explain the workflow and its four steps in general terms (Fig. 10). In the second section, we present its application to a case study, aiming to assess the departures of distinct plant communities from their initial states in a national park, in the French Alps.

Step 1. Choice of components

To detect changes in ecosystem states, we propose building n -dimensional hypervolumes using time series of n -ecosystem components at equilibrium (Fig. 10, Step 1). A wide range of different components can be used (Table 2). Ultimately, the choice of components depends on what properties and changes are under focus. For instance, if the user wishes to focus on changes in community structure and evenness patterns, relative species abundances should be considered, while changes in overall species abundances should be followed using raw abundances if the rareness of species is important for the research question. On the other hand, if the focus is on a community's functional characteristics and structure, then functional traits should constitute the hypervolumes. Also, depending on the chosen components, stability can be assessed at different spatial scales. For simplicity, we henceforth speak about community stability, but the same approach can be applied at the habitat and landscape scales.

Finally, hypervolumes can be used to follow community changes in time, by building separate hypervolumes for different time slices and comparing between them, or against a reference period. Alternatively, 'space-for-time' comparisons can also be used if hypervolumes are built from replicates of communities under different disturbance treatments.

Step 2. Data treatment and hypervolume calculation

Components that will constitute the axes for hypervolume calculation must follow certain criteria (Fig. 10, Step 2). To start with, the number of dimensions will influence hypervolume metrics and should be fixed to ensure comparability between hypervolumes (Blonder *et al.* 2014). Components entering the analysis should be in comparable units (e.g. centred and scaled) and uncorrelated (Blonder *et al.* 2014). When the different components one wants to include are correlated, we suggest the use of multivariate analyses, such as principal components analyses (PCAs), or Hill and Smith analyses (Hill & Smith 1976) if a mix of continuous, categorical and ordinal variables are used (e.g. Heiser *et al.* 2014). Alternatively,

principal coordinates analyses (PCoAs) based on distance matrices and designed to represent differences between objects as faithfully as possible (i.e. distances based on traits values), are also a suitable option (Maire *et al.* 2015). These approaches will reduce dimensionality and extract a number of centred and scaled orthogonal axes from the data. Hypervolumes are then built using the factor scores on the chosen principal components (PCs), or the pre-selected uncorrelated (and eventually scaled) variables. Since the interest is to assess differences between pre- and post-perturbation states of a given community (comparing pre- and post-perturbation hypervolumes), the PCA is calculated on the pre- and post-perturbation datasets together; separate hypervolumes should then be calculated from the factor scores corresponding to each dataset. The final number of variables, or PCs, to be used should be decided based on knowledge of key components for community stability, the percentage of explained variance, or expert knowledge. When using a PCoA, Maire *et al.* (2015) proposed to assess the quality of the reduced space using the mean squared deviation between the initial distances between objects (e.g. trait values) and the standardised distances in the new space. In any case, the number of variables/PCs should not exceed 5–8, to avoid having highly disjunct hypervolumes (Blonder *et al.* 2014).

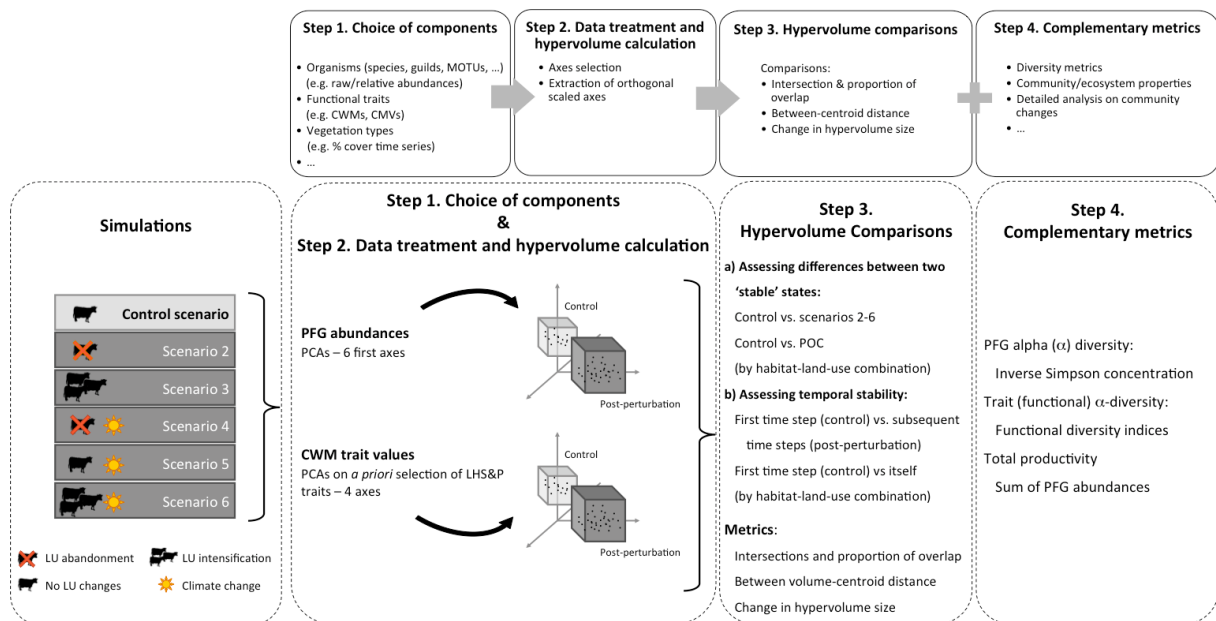


Figure 10. Framework scheme. Several types of time series data can be used (Step 1). In our study case, we used simulated plant functional groups' (PFG) abundances and community weighted mean (CWM) trait values per habitat-land-use combination, under a given scenario of land-use and/or climate changes. Variables used for hypervolume calculations should be scaled and uncorrelated (Step 2), which was ensured by selecting axes extracted from Principal Components Analyses (PCAs) on scaled time series of PFG abundances and of CWM trait values. Pre- and post-perturbation hypervolumes are then calculated using, in this example, the PCAs factor scores referring to control (scenario 1) and post-perturbation data (remaining scenarios), and then compared (Step 3). Comparisons between hypervolumes can be complemented using other metrics (Step 4) for a further analysis of community changes. In Step 3, 'POC' stands for 'proof-of-concept' hypervolumes (see methods section 'Step 3. Comparing hypervolumes to analyse community changes').

The calculation of hypervolumes follows a multidimensional kernel density estimation procedure. Briefly, this consists in the estimation of overlapped hyperbox kernels from which a uniform point density is extracted using random sampling, importance-sampling and range-testing techniques (Blonder *et al.* 2014). The values of kernel bandwidths can be chosen by the user and should avoid having disjoint observations (Blonder *et al.* 2014). Although there is no minimum number of data points needed to compute the hypervolumes, analyses with few observations (roughly < 10 times the number of dimensions) are more influenced by the choice of bandwidth (Blonder *et al.* 2014). In the scope of our approach, we suggest a standardised method to choose the bandwidth value see *Bandwidth selection for hypervolume calculation* in Appendix 3, guaranteeing comparability between different hypervolumes even with low sample size.

Step 3. Comparing hypervolumes to analyse community changes

Sufficiently large changes in environmental conditions are expected to produce shifts in community structure and composition that will cause the hypervolume to shift. We propose three metrics to assess differences in pre- and post-perturbation states (Fig. 10, Step 3) that focus on: (1) the overall similarity/ dissimilarity between two states, (2) changes in mean values of the chosen components and (3) changes in their variance.

First, the proportion of overlap between pre- and post-perturbation hypervolumes (Fig. 9d) will reflect overall differences between the two corresponding states. Overlap is calculated as the ratio between the intersection volume and the total volume occupied by the two hypervolumes, being expected to decrease as a community changes. For instance, if a plant community has suffered significant changes in structure and composition and became another vegetation type, hypervolumes will be farther away and may not intersect (overlap = 0). Whether or not this indicates a permanent state-shift (i.e. irreversible even if environmental conditions are returned to pre-shift values) will depend on the community in question and the type of disturbance. Conversely, if hypervolumes intersect, their overlap will be indicative of similarities between them.

Second, the distance between the centroids of the pre- and post-perturbation hypervolumes will reflect how much mean values of the ecosystem components have departed from their pre-perturbation levels (changes in mean values).

Third, changes in hypervolume size may indicate changes in the amplitude of variation of the selected components (changes in variance).

It is also important to consider that in certain cases, the number of observations used to calculate the hypervolumes may differ. Blonder *et al.* (2014) did not discuss this issue and seemed to compare hypervolumes calculated using data with different sizes (see their example of morphological comparisons of species of Darwin's finches); however, we suggest that in these cases, the user can perform randomised permutation testing with data subsets (see e.g. Brandl & Bellwood 2014) to avoid influencing comparisons between hypervolumes.

Step 4. Complementary metrics for more detailed analyses

Hypervolume comparisons *per se* do not provide information about what type of changes the community went through. Hence, we suggest analysing complementary metrics that reflect changes in community composition or structure (Fig. 10, Step 4). The choice of these metrics depends on the focus of the analysis and on the ecosystem components being analysed. For instance, when studying the stability of taxonomic and functional composition, we recommend using indices that reflect changes in taxonomic, functional or phylogenetic diversity (or their combination), both in average terms and in terms of dispersion (see Pavoine & Bonsall 2011 for a detailed review).

Illustration: a mosaic alpine landscape under land-use and climate changes

Our general framework has the ability of deciphering the consequences of environmental changes for ecosystems over large spatial scales and heterogeneous landscapes, while analysing multiple ecosystem components at the same time. This is illustrated by the following analysis of a mosaic alpine landscape within a national park subject to abrupt land-use and climate changes.

Case study and simulated vegetation dynamics

The Ecrins National Park (ENP) is situated in southeast France in the French Alps, covering a surface area of 178 400 ha. It is composed of a mosaic of mountainous to alpine ecosystems, harbouring a rich flora (~ 2000 species) and present land-use practices are accurately mapped (extensive grazing, 50%, crop fields and mown grasslands, 15%, and forest management, 10%). The ENP presents an interesting case where highly diverse Alpine landscapes face current threats of changing land-use practices and climate warming, which are likely to have synergistic effects.

To simulate the vegetation dynamics and associated community shifts resulting from climate and LUCs, we used FATE-HD, a recently developed dynamic landscape vegetation model that has been previously parameterised for the ENP (Boulangeat *et al.* 2014b). The model simulated the spatiotemporal dynamics of 24 plant functional groups (Boulangeat *et al.* 2012) at 100 m resolution. Competition for light between PFGs, their population dynamics, dispersal and responses to land-use regimes and climate are all explicitly modelled. Land-use regimes were modelled spatially and included grazed areas with three levels of intensity (low, medium and high) and mown areas. Yearly outputs used here were the abundance of each PFG in each pixel. A more detailed description of the study area and of FATE-HD can be found in *FATE-HD model description and simulation workflow* in Appendix 3; we refer the reader to Boulangeat *et al.* (2014b) for model details and parameterisation, and to Boulangeat *et al.* (2014a) for details on chosen climate and LUC scenarios.

Scenario building

FATE-HD is an equilibrium model, having the capacity of internal regulation and feedback mechanisms that contribute to a directional response of equilibrium system behaviour. Therefore, it successfully simulated the equilibrium vegetation dynamics of the ENP subject to present land-use (Boulangeat *et al.* 2014b). Based on those validated simulations, we analysed six different scenarios (Boulangeat *et al.* 2014a): no change at all (control scenario), abandonment of all grazing and mowing activities (scenario 2), intensification of grazing (to high levels) in all grazed areas and creation of new grazing and mowing areas (scenario 3) and the previous three scenarios combined with climate change (scenarios 4–6; Fig. 10).

An initialisation phase was run for 1650 years to reach present equilibrium vegetation dynamics (see *FATE-HD model description and simulation workflow* in Appendix 3 for details). Scenarios were then applied to the equilibrium state. LUCs were applied 4 years after the equilibrium was reached and changes were kept until the end of the simulation; climate change (CC) was applied continuously from the 15th to the 90th year after equilibrium was reached and remained constant afterwards until the end of the simulation. Scenario simulations were run for a total of 500 years after the initialisation phase to allow the establishment of new equilibria. Both the initialisation phase and scenario simulations were replicated three times.

Given the high heterogeneity of the ENP and to avoid mixing together ecosystems with contrasted vegetation dynamics, we decided to analyse community stability through the lens of habitat type (see *FATE-HD model description and simulation workflow* in Appendix 3 for

the list of habitat types and their map in Fig. S1a in Appendix 3) and current land uses (grazing intensities low, medium and high, mowing and non-disturbed habitats, as well as potentially grazed, mown and non-disturbed habitats under intensification scenarios; see Fig. S1b in Appendix 3 for land-use maps), taking advantage of the very detailed habitat and land-use characterisation of the ENP (Esterni *et al.* 2006). For example, all woodland mosaics under present grazing pressure were considered together (the pixel-based abundances of PFGs being summed across the same habitat type). This resulted in temporal information on the 24 PFG abundances in 56 pairs of habitat and land-use types.

We applied our framework to explore the differences between pre-perturbation and post-perturbation community states in two ways: (1) an analysis focusing on differences between pre- and post-perturbation states and (2) an example focused on analysing temporal stability. Where appropriate, we distinguish the methodology and results referring to these two approaches.

Step 1. Choice of components

As we were interested in the stability of taxonomic and functional diversity at the community level, we chose to use the time series of PFG abundances (24 components) and the time series of CWM trait values (4 components), which we analysed independently from each other. We calculated yearly raw and relative PFG abundances for each habitat and land-use combination by summing them across the ENP.

To estimate changes in the overall trait combination of each habitat type for a given land use, we calculated CWM trait values based on the simulated abundances of each PFG and their respective trait values (Table S1 in Appendix 3). We selected three traits reflecting the leaf-height-seed (LHS) plant ecology strategy by Westoby (1998) – mean specific leaf area (SLA), log-height, log-seed mass – plus one reflecting PFG responses to grazing – palatability. Palatability was treated as a continuous trait to allow a better representation of the variability in its CWM values (hence, we followed the assumption that palatability classes are evenly spaced; Jouglet 1999).

Step 2. Data treatment and hypervolume calculation

To ensure orthogonality and a feasible number of dimensions for hypervolume calculations, we used PCAs on the abundances (raw or relative) of the 24 PFGs and on the CWM trait values. Data scaling was done prior to the PCA, using root mean squares on both the control and scenario of change datasets together. We then selected the first six orthogonal PCs to be

used as dimensions for the ‘PFG hypervolumes’, which still retained a cumulative explained variance $> 95\%$ (obtained using raw PFG abundances; Fig. S2 in Appendix 3). The same number of axes was used to build hypervolumes from relative PFG abundances. As for ‘trait hypervolumes’, we used the totality of the four PCs, since only four traits were selected, the PCA only ensuring orthogonality. Hypervolumes were then built using the factor scores on the selected axes. Although we treated all traits as continuous variables, in other situations, a mix of continuous, categorical and ordinal traits may be wanted. In these cases, the PCA can be substituted by a generalisation of the Hill and Smith analysis available in the ‘ade4’ R package, *dudi.mix* (Dray & Dufour 2007).

Comparing two states.

To assess differences between pre-perturbation and post-perturbation states, we compared PFG and trait hypervolumes of the control scenario (no LUC, no CC) to the five scenarios of LUC and/or CC (post-perturbation hypervolumes), for each habitat land-use combination and each of the three repetitions. Control hypervolumes were calculated from the 500 years of the control scenario (no climate and no LUCs, equivalent to a pre-perturbation state), while the last 100 years of the five scenarios of LUC/CC were used to calculate post-perturbation hypervolumes, since vegetation had stabilised by then.

Assessing temporal stability.

In addition, we analysed the potential of our framework to investigate temporal stability using a demonstrative example. We selected two habitats (grasslands and thickets and scrublands) subjected to current land-use practices (three intensities of grazing, mowing and no-disturbance) and CC (scenario 5). We focused on community responses during and shortly after climate changes, analysing the first 150 years of the scenario simulation. Time series of raw and relative PFG abundances were broken into time steps of 15 years length, from which hypervolumes were built. The calculation of hypervolumes followed the description above, with control datasets spanning the 15 years prior to the first climate change (control hypervolume) and subsequent time steps of 15 years considered as post-perturbation data (post-perturbation hypervolumes).

Step 3. Comparing hypervolumes

As a proof-of-concept (POC) of our method, we first tested our framework on the control scenario where nothing should be detected in theory. We did this by (1) comparing control hypervolumes to ‘POC’ hypervolumes calculated from an additional 100 years ran from the

end of the initialisation phase (for both PFG abundances and CWM traits) and (2) comparing the first time step hypervolume to itself (i.e. control hypervolume, built from the first 15 years of the scenario simulation). These comparisons provided a ‘no change’ baseline that was used as reference for statistical analyses and to interpret results.

Comparing two states

Hypervolume comparisons (proportion of overlap, centroid distances and changes in size) were made for pairs of control and post-perturbation hypervolumes (control vs. scenario hypervolumes; control vs. POC hypervolumes) for each habitat-land-use combination and each repetition, resulting in 1008 comparisons (five scenarios against the control and POC against the control \times 56 habitat-land-use combinations \times 3 repetitions). Changes in control vs. post-perturbation hypervolume sizes (Δ size) were calculated as the difference between post-perturbation and control hypervolume sizes, after scaling them relatively to the largest hypervolume obtained across communities (enabling a comparison between PFG and trait hypervolumes).

Repetitions were analysed together as samples of a same treatment. Effects of CC, LUC and habitat-land-use combinations (explanatory variables) on overlap, centroid distances and Δ size (response variables) were assessed using analyses of variance (ANOVAs). In all model analyses, control vs. POC hypervolume comparisons were used as ‘no change’ observations that corresponded to no climate and no LUCs. Linear model assumptions (normality and homoscedasticity of residuals) were ensured by doing a square-root transformation on overlap values from raw PFG abundance and from trait hypervolumes, and a variant of the *logit* transformation on overlap values from relative PFG abundances (see *Results obtained using relative PFG abundances* in Appendix 3 for details). Centroid distances and Δ size values did not require any transformation; however, extreme outliers were removed from the analyses of Δ size values of relative PFG abundances and trait hypervolumes (two and three outliers respectively); best models were selected on the basis of AICc scores, starting with full models (one response variable in function of all explanatory variables and all their possible interactions) that were gradually simplified (final models are listed in Table S2 and in *Results obtained using relative PFG abundances* in Appendix 3). Model outputs were analysed in terms of the importance of main effects and interaction effects, while differences between factor levels were analysed graphically (fitted values were back-transformed where appropriate), due to the high number of level combinations.

Assessing temporal stability

To assess changes in hypervolumes through time, the first time step [control] hypervolume was compared against each hypervolume from subsequent time steps. This was done for 270 pairs of hypervolumes (first time step against \times subsequent time steps \times 1 scenario \times 10 habitat-land-use combinations \times 3 repetitions). We focused on the temporal evolution of overlap and analysed its response to CC under different habitat-land-use combinations using generalised additive models (GAMs), with a Gaussian smoother fitted for each habitat land-use combination. Overlap values of relative PFG abundances were analysed after a square-root transformation, which improved the residual distribution of the models.

Step 4. Complementary metrics for more detailed analyses

For a deeper analysis on how pre- and post-perturbation states differed, we calculated yearly complementary metrics for each habitat-land-use combination and each scenario. Yearly PFG α -diversity was calculated as the inverse Simpson concentration to reflect changes in taxonomic richness and evenness (Leinster & Cobbold 2012). Two functional diversity indices, functional dispersion (FDis; Laliberté & Legendre 2010) and functional evenness (FEve; Villéger *et al.* 2008) were used to assess changes in average functional distances in the community and their variance among PFGs respectively (Pavoine & Bonsall 2011). Analogously to hypervolume comparisons, these indices indicated changes in the mean and variance of functional α -diversity. Finally, we also calculated total productivity, in the form of total PFG abundance, since it has been used to study ecosystem responses to perturbations (e.g. Kerkhoff & Enquist 2007; Polley *et al.* 2013; Keersmaecker *et al.* 2014).

The responses of diversity indices and productivity to CC, LUC and habitat-land-use combinations were also analysed statistically (detailed in *Choice and analysis of complementary metrics* in Appendix 3). Since the analysis of temporal stability was merely demonstrative, complementary metrics were not used in this situation.

Hypervolumes were calculated using the recently made available *R* package ‘hypervolume’ (Blonder *et al.* 2014). Selection of optimal bandwidth sizes for each set of components is detailed in *Bandwidth selection for hypervolume calculation* in Appendix 3 (along with a sensitivity analysis of bandwidth effects on overlap). All hypervolumes were built using a quantile threshold of 0% (Blonder *et al.* 2014). Functional diversity indices were calculated within the *R* package ‘FD’ (Laliberté & Legendre 2010). Source code for calculating and comparing hypervolumes, together with nine example datasets are available in electronic supplementary materials published in Barros *et al.* (2016c).

Results

Comparing two states

We assessed differences between pre- and post-perturbation states by comparing hypervolumes built from the control scenario with hypervolumes built from each scenario of change (but see examples of full system trajectories in Fig. 11). Concerning PFG hypervolumes, here, we present results obtained using raw abundances, instead of relative abundances, because we were interested in accounting for changes in the abundances of all PFGs, rather than focusing on structural and dominance changes. In general, comparisons between hypervolumes built from relative abundances resulted in more frequent intersections and larger overlaps, smaller distances between hypervolumes and smaller size changes (full results are available in *Results obtained using relative PFG abundances* in Appendix 3).

Testing the framework: confronting POC and control hypervolumes

When comparing ‘POC’ and control hypervolumes, 100% of all pairs of hypervolumes intersected and the proportion of overlap between them was much larger than that obtained between control and post-perturbation hypervolumes (Fig. 12). Also, centroid distances (Fig. 13a,b) were always small, despite combinations for hypervolume overlaps for the different components is presented as Supporting Information (see Fig. S3, Table S2 and *Supplementary results and discussion* in Appendix 3).

Finally, hypervolume overlaps were mostly independent from hypervolume size, with an exception for POC comparisons for which the two were negatively correlated (Fig. S4 in Appendix 3). This indicates that, all else remaining equal (under no perturbations), larger sizes did not drive larger overlaps.

Distances between hypervolumes and changes in size

In all situations, models explaining the response of centroid distances and changes in size (Δ size) included all three main factors (CC, LUC and habitat-land-use combinations) and possible interactions between them; all model terms were significant, but again their relative importance changed depending on the type of components used and the response variable (Table S2 in Appendix 3). While mean PFG abundances were most affected by CC, LUC and their interaction, the variance in PFG abundances was most affected by habitat-land-use combinations and their interaction with LUC, followed by CC and remaining terms. On the other hand, mean trait values were most affected by LUC, CC and their interaction, while trait

variances were most affected by CC and its interactions with LUC and with habitat-land-use combinations (Table S2 in Appendix 3).

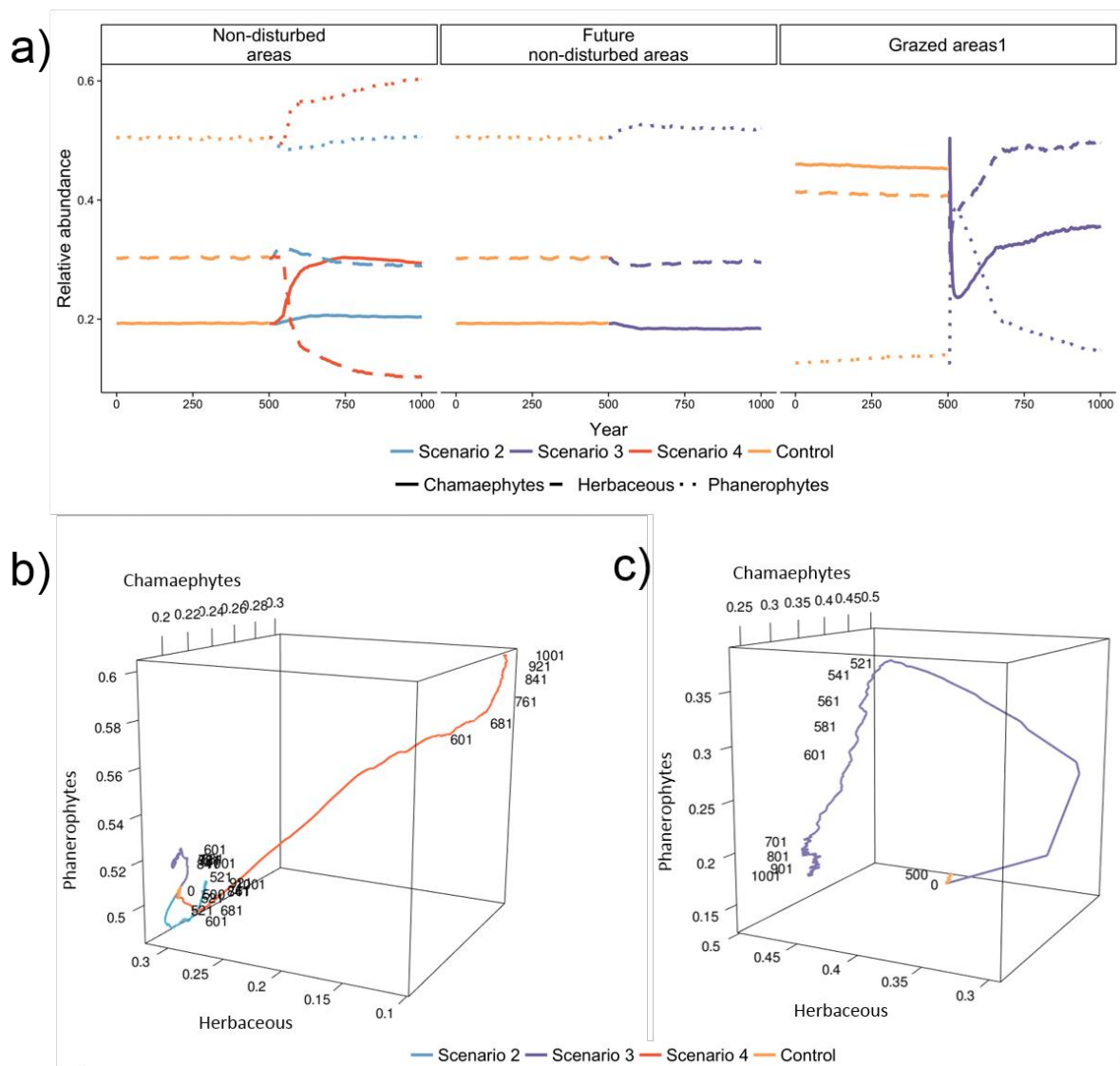


Figure 11. Full system trajectories under different scenarios and land-use practices. The full trajectories of thickets and scrubland vegetation are shown for three scenarios of climate and/or land-use changes, under three types of land-use practices. The first 500 years correspond to the control scenario (in orange), followed by another 500 years of climate and/or land-use changes: land-use abandonment without and with climate change in blue and red (scenarios 2 and 4, respectively) and land-use intensification in purple (scenario 3). Since we are graphically constrained to three dimensions, we plotted the trajectories using relative abundances of chamaephyte (full lines), herbaceous (dashed lines) and phanerophyte (dotted lines) plant functional groups (by adding up separate group's abundances per life form type). The three-dimensional plot in b) corresponds to trajectories in non-disturbed areas – first two panels in a) – whereas in c) it corresponds to trajectories in intensified grazed areas – last panel in a).

Plotting the observed mean centroid distances has shown that, considering the same LUC, CC almost always increased the distance between hypervolume centroids, driving changes in mean PFG abundances and CWM traits (Figs. 13a, b). However, observed Δ size values show a different pattern. Changes in variance of PFG abundances seemed to be mostly associated

with habitats being disturbed or not (disturbed habitats showing decreases in variance in post-perturbation hypervolumes; Fig. 13c), while changes in variance of trait values are associated with the presence of CC (CC driving increases of variance; Fig. 13d). Finally, it is also interesting to note that trait hypervolumes had generally much smaller sizes (data not shown) and Δ size values than PFG hypervolumes. We provide further results of the effects of CC, LUC and habitat-land-use combinations on centroid distances and Δ size in the appendices (see Figs. S5 and S6, Table S2 and *Supplementary results and discussion* in Appendix 3).

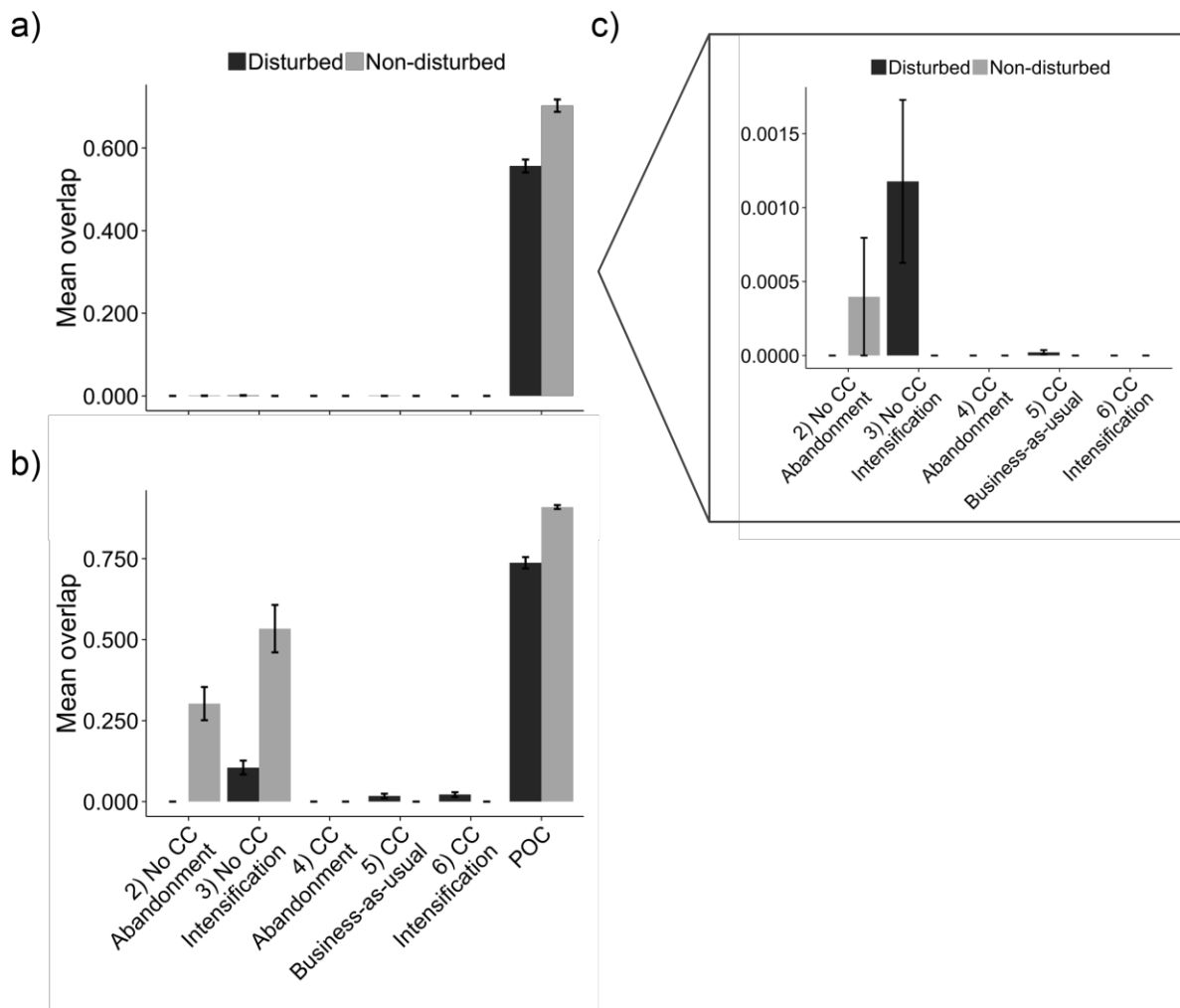


Figure 12. Overlap in disturbed and non-disturbed areas. Proportion overlap between control and post-perturbation hypervolumes of a,c) PFG raw abundances – a) and c) only differ in the y-axis scale – and b) CWM trait values. The proportion of overlap (overlap) was calculated as the ratio between the intersection volume and the total volume occupied by the two hypervolumes (standard errors shown as error bars). Observed mean overlaps are shown by scenario, across all habitat types and grouped by disturbed areas (areas under present grazing or mowing regimes and areas that will become grazed on mown under scenarios of land-use intensification) and non-disturbed areas (all areas that are not currently grazed or mown and those that will remain so, under land-use intensification scenarios). Standard errors are shown as error bars. Comparisons between proof-of-concept ('POC') and control scenario hypervolumes are shown in a) and b), but not in c), so that overlap values obtained in other scenario comparisons can be seen.

Exploring temporal stability

We exemplify the use of our framework to explore the temporal stability of two different communities that showed opposite results in terms of overlap, when only subjected to CC (scenario 5, considering PFG hypervolumes): grasslands and thickets and scrublands. For this analysis, only the first 150 years of the scenario simulation were considered, as we were interested in following community responses during and shortly after CC. Again, results presented here were obtained using raw PFG abundances (see *Results obtained using relative PFG abundances* Appendix 3).

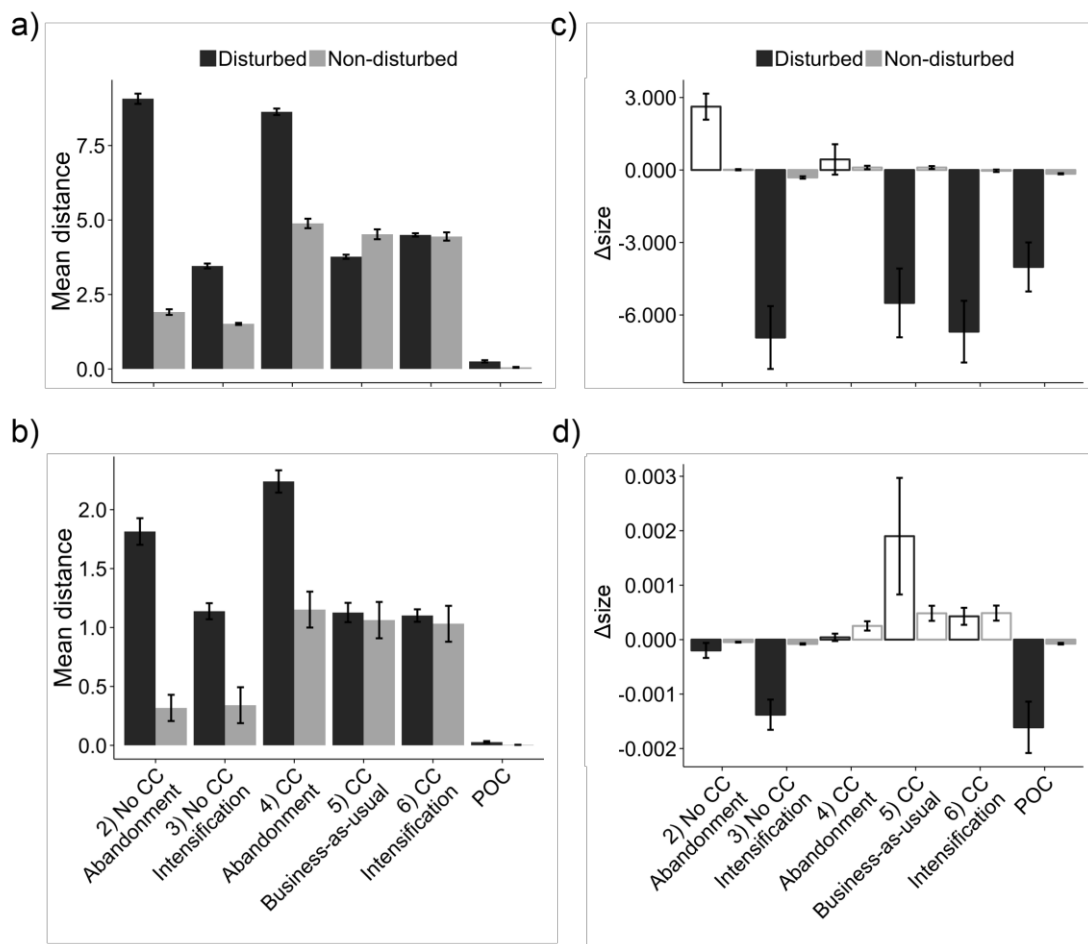


Figure 13. Mean distances and changes in size, in disturbed and non-disturbed areas. Mean centroid distances between control and post-perturbation hypervolumes and differences in their sizes (post-perturbation minus pre-perturbation; $\Delta size$) are shown for a,c) PFG raw abundances and b,d) CWM trait values. Negative $\Delta size$ values indicate that the post-perturbation hypervolume was smaller than the pre-perturbation hypervolume, and vice-versa for positive $\Delta size$ values. Both metrics are shown by scenario, across all habitat types and grouped by disturbed areas (areas under present grazing or mowing regimes and areas that will become grazed on mown under scenarios of land-use intensification) and non-disturbed areas (all areas that are not currently grazed or mown and those that will remain so, under land-use intensification scenarios). Standard errors are shown as error bars. Comparisons between proof-of-concept ('POC') and control scenario hypervolumes are also shown.

Testing the framework: comparing first time step hypervolume with itself

Confronting the first time step hypervolume to itself provided an estimate of the variability associated with the calculation of hypervolumes and their overlap, as well as a baseline values for the temporal analysis of changes in hypervolumes. Overlap was always positive and generally similar between habitat land-use combinations (Fig. 14). It was also always larger than the overlap measured between the first time step and subsequent time steps (Fig. 14).

Hypervolume overlap in time

Overlap decreased in time as communities changed, reaching 0 before the CC period ended; yet, the rate at which it decreased depended on the habitat-land-use combination (Fig. 14). Mown grasslands were less stable, showing larger and faster decreases of overlap, while grasslands grazed at low intensity ('grazed areas1') were more stable, showing slower decreases of overlap (Fig. 14). Thickets and scrublands were generally less stable, with overlap values reaching 0 before they did so in grassland habitats. Mown thickets and scrublands had smaller overlaps even before CC started.

Complementary metrics

Models of PFG α -diversity showed that this metric was not significantly affected by any of the model terms included (Table S3 in Appendix 3). However, a graphical analysis of mean PFG α -diversity across the last 100 years of the simulations showed that when compared with control levels, the abandonment of disturbed areas increased PFG diversity, while CC and land use intensification generally decreased it (Fig. S7 in Appendix 3).

Metrics of functional α -diversity responded significantly to all effects, with the exception of FEve, which was not differently affected by CC when land-use was intensified (see 'set 2' models in Table S3 and *Choice and analysis of complementary metrics* in Appendix 3). Yet, the importance of CC, LUC and habitat-land-use combinations depended on the metric used (Table S3 in Appendix 3). For instance, like hypervolume metrics, FEve was most affected by LUC, CC and their combination; yet, FDis was more affected by the interaction between CC and LUC, followed by habitat-land-use combinations, while CC alone had a comparatively weaker effect. As with PFG α -diversity, FEve generally increased after land-use abandonment and decreased after CC and land-use intensification (when compared to control levels; Fig. S8b in Appendix 3). FDis had similar responses to FEve, but differences between disturbed and non-disturbed areas in terms of mean FDis were usually smaller (Fig. S8c in Appendix 3).

Finally, productivity was also significantly affected by all model terms included, with habitat-land-use combinations having the strongest effect on its variation (sets 1 and 2; Table S3 in Appendix 3). Mean productivity in non-disturbed areas was much higher than in disturbed areas, even after abandonment. As with metrics of taxonomic and functional diversity, mean productivity increased after land-use abandonment and decreased after CC and land-use intensification (Fig. S10 in Appendix 3).

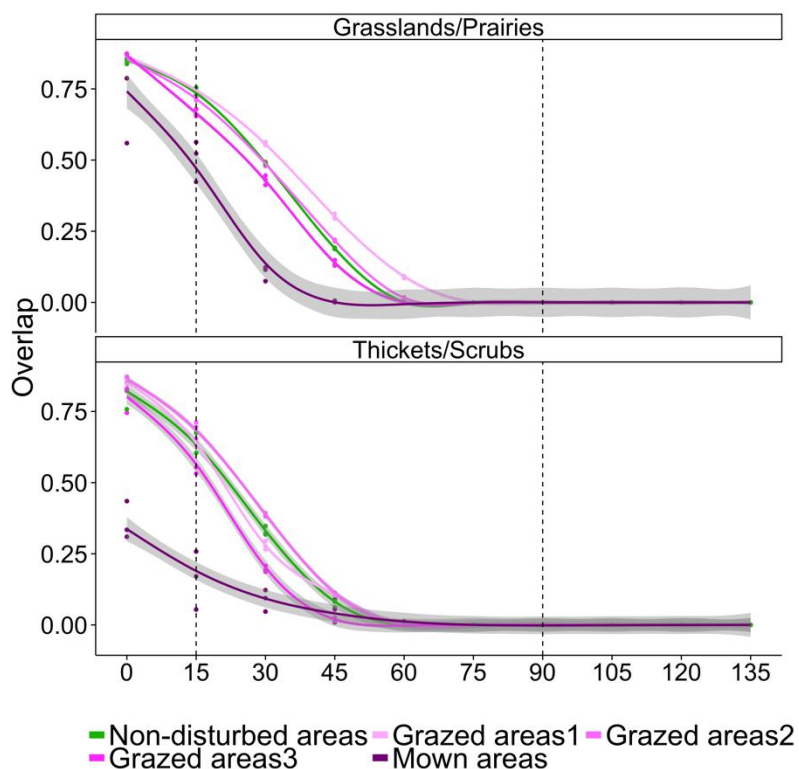


Figure 14. Temporal stability measured by hypervolume overlap. Temporal stability was analysed by modelling the temporal response of the proportion of overlap (overlap) under different habitat-land-use combinations, using generalised additive models (GAMs) with a Gaussian smoother fitted for each habitat-land-use combination. Each coloured point corresponds to the comparison between a hypervolume at a given time slice and the first hypervolume, with colours referring to land-use (the first year of each 15-year time slice is indicated in the x-axis). Dashed vertical lines indicate the start and end of simulated climate changes.

Discussion

Environmental changes impact biodiversity at different levels and may lead to changes in community and ecosystem structure and functioning. Instead of studying ecosystem stability through the lens of single diversity or ecosystem functioning metrics, we propose that the contribution of different taxonomic, functional or landscape entities should be considered. Our framework makes use of n -dimensional hypervolumes to assess changes in ecosystem states that are driven by the responses of different ecosystem components to environmental

changes. It provides a flexible way to quantitatively assess ecosystem changes and the relative impact of different disturbances on ecosystem stability. Most importantly, it allows analysing ecosystem responses at different levels of biodiversity and/or ecosystem functioning, enabling an integrative analysis of stability. Moreover, our framework can be combined with other metrics for a detailed analysis of the type of changes the system suffered.

Assessing the magnitude of change

Comparing hypervolumes in terms of their intersection and overlap, the distance between their centroids and their changes in size, provides a measure of the magnitude of changes an ecosystem has suffered. If different types of components are used, these hypervolume metrics are also informative about their relative stability. In our example, we have shown that both taxonomic and functional diversity are destabilised by climate and LUCs; yet, functional traits changed less than PFG abundances, suggesting higher functional stability. Also, hypervolume metrics allow analysing changes in ecosystem states both in terms of mean values of the chosen components (centroid distances) and in terms of changes in their variance. For instance, climate and LUCs affected mean PFG abundances and mean trait values similarly, but differed in their effect on PFG and trait variances. Moreover, since hypervolumes do not summarise different components into a single metric, but instead describe them as a multidimensional cloud, changes in volume may not only indicate changes in oscillatory patterns of the considered components, but also changes in synergies and trade-offs between them.

Furthermore, since the approach can be applied across different types of perturbations, their relative effects on ecosystem stability can be directly compared. This can be achieved by modelling the response of hypervolume metrics to the combinations of perturbations under focus, as we have done here. In our simulated plant communities, the interaction between climate and LUCs had a larger impact on hypervolume overlap and centroid distances than the effect of habitat and land use regime types, indicating that the synergy between these two global change threats has an overall large effect that may be generalised across the different Alpine ecosystems.

Additionally, because our framework can be applied to different types of habitats, it allows comparing their responses to similar perturbations; although we did not present the full extent of the results from our case study application, we were able to detect cases where particular habitats did not follow the general pattern of responses to the simulated perturbations (see *Supplementary and discussion* in Appendix 3).

Assessing the type of change

Using n -dimensional hypervolumes is not only useful to detect overall changes in ecosystems but can also be informative about what facets of an ecosystem were most affected by perturbations. For instance, in our case study, hypervolume comparisons indicated that PFG abundances were more affected by land-use and climate changes than trait values. In case we had been interested in investigating how perturbations impacted the communities under focus, this information would have directed our attention towards changes in taxonomic structure and composition, and in population dynamics, perhaps saving a broader exploratory analysis.

Complementing the analysis of the global variation of the ecosystem with diversity metrics, productivity measurements, or even a more detailed analysis on changes that occurred to particular ecosystem components (not shown here, but see, for example, Lenoir *et al.* 2010a) adds a finer understanding of changes that occurred in the system. Complementary metrics must be carefully chosen with regard to the focal research question. How to do this has been discussed elsewhere (see Pavoine & Bonsall 2011) and we recommend that users select metrics that add complementary information to hypervolume metrics, reflecting changes in both community structure and composition.

However, using these metrics independently may provide a false notion of stability. For instance, if we had followed classical ways of analysing stability and focused only on productivity, we would have concluded that land-use abandonment and climate change do not cause major changes to Alpine communities; similarly, had we only investigated perturbation effects on taxonomic and functional diversity, we would have not detected large changes in mean trait values of undisturbed rocky and scree vegetation in result of land-use abandonment in adjacent areas (see *Supplementary results and discussion* in Appendix 3).

Following changes in time

The approach we propose here also enables tracking transient dynamics when communities have lagged responses to perturbations. To do so, the user should have several observations per time period and we remind them to fix bandwidths across time periods for hypervolume calculations. As we have demonstrated, this can be done across various communities and perturbations to analyse which communities are more sensitive and which perturbations cause the fastest changes. In our case study, both grasslands and thickets and scrublands suffered large changes in PFG composition and/or structure in result of climate change, regardless of land-use management type, due to the expected species turnover caused by climate warming (Asner *et al.* 2004; Gottfried *et al.* 2012). Alternatively, it is possible to do ‘space-for-time’

comparisons, where communities are subjected to treatments of different perturbation intensities; in this case, hypervolumes built from different replica can be compared within community types and across perturbation treatments, or across community types for a given perturbation treatment, to allow investigating the effect of perturbations and how different communities respond.

In either case, we believe that the overall measure of ecosystem state that this framework provides may allow applying the concepts of ecosystem resilience while accounting for the multivariate and stochastic nature of complex ecosystems. Since hypervolumes measure and define different states of an ecosystem and enable their comparison, they may be used to estimate ecosystem resilience, i.e. measuring rates of return to equilibria – engineering resilience – or the magnitude of perturbation a community can withstand before shifting states – ecological resilience (*sensu* Holling 1996; Gunderson 2000). Although we have not directly applied our framework to quantify ecosystem resilience *per se*, we provide a short discussion on these aspects under *Supplementary results and discussion* in Appendix 3. In future work, it would be interesting to investigate whether communities are able to return to their pre-perturbation states (or hypervolumes) if environmental changes are reversed and assess whether irreversible state-shifts are associated with particular thresholds of hypervolume metrics, such as the distance between centroids. This can have important implications for the provisioning of ecosystem services if we consider that large changes in a community state will also imply large changes in the ecosystem services it provides (Folke *et al.* 2004; Nagendra *et al.* 2013). Also, investigating under which conditions communities revert to their original states would enable finding a criterion to define a ‘new’ hypervolume after a disturbance (new stable state). Although hypervolumes can be said to be ‘different’ if they do not intersect (overlap = 0), very small overlaps can already be indicative of large changes in a community. Although this is not an issue in our simulation data because sufficient time was allowed for communities to reach new equilibria after perturbations, it can be if real data are used. In this case, we suggest that users report to changes in overlap to assess the magnitude of the effect and describe transient dynamics.

Advantages of using hypervolumes to assess community stability

Accounting for the multiplicity of components within an ecosystem, may reveal changes that cannot be detected if only one dimension is accounted for (e.g. productivity, diversity). The reason for this is that measures of diversity and productivity are community properties, which indicate ecosystem stability from a particular perspective. Diversity metrics will often be

weighted differently according to species/PFG abundances. The choice of abundance currency has been shown to affect predictive models of biodiversity (Certain *et al.* 2014) and it is likely that it can impact results obtained when following stability of diversity in time. In addition, productivity will usually represent variations of the most productive species (Doak *et al.* 1998; Polley *et al.* 2007), which may not allow detecting finer changes in less productive species that may be important for other ecosystem functions. One strong advantage of our proposed method is that all community components chosen can have equal contributions to the analysis of stability of biodiversity. This allows detecting changes in the variability of community components without the need to weight components differently, or to summarise them into a one-dimensional measure, while still providing an overall measure of community stability. Furthermore, in complex situations where habitat mosaics exist and ecotone dynamics are observed, or when different types of communities are considered, relationships between community stability and metrics such as productivity and diversity indices are likely to change between communities, as well as across different disturbance regimes, hampering integrated analyses of community stability. When analysing ecosystem stability by directly integrating ecosystem components, this ceases to be an issue: changes occurring in different communities become comparable and analysing community stability at the landscape scale or across different organisational levels becomes possible.

Also, the approach we propose is flexible enough to be applied to different types of components, from real or simulated data. The choice of components depends on the focus of the analysis, but several components can be used separately to provide comparative analyses of stability, as we demonstrated here by comparing PFG abundances and CWM trait values. With the increasing popularity of environmental DNA approaches (Taberlet *et al.* 2012) and the continuously growing remote sensing datasets, temporal data on community and ecosystem composition, at taxonomical, functional, phylogenetic and landscape levels are more and more available. As these different datasets open new avenues for the study of ecosystem stability, integrative tools like the one presented here will be needed to assess stability across different types of communities, ecosystems and environmental and disturbance gradients in a consistent and robust way. They also become increasingly important to assess ecosystem stability under future environmental conditions. With evidence pointing to increases in frequency and intensity of extreme climatic events, such as drought (Allen *et al.* 2010; IPCC 2012), it is crucial that models incorporate these events for future biodiversity predictions. We have shown that our framework can be coupled with a dynamic landscape vegetation model to study community stability under realistic scenarios of future

land-use and climate changes. It can certainly be applied to other ecological models – like forest gap models (Lischke *et al.* 2006), dynamic global vegetation models, DGVMs (Krisner *et al.* 2005), or dynamic network models (see e.g. Steenbeek *et al.* 2016) – to study community stability under diverse scenarios (e.g. climate warming, extreme events, management).

In conclusion, integrating the variability of multiple ecosystem components can provide indication on general ecosystem stability. It is also informative about what types of perturbations cause the largest changes in ecosystems and which ecosystem facets are most affected by a given perturbation, which is useful for assessing community and ecosystem stability under forecasts of global change. Although here applied to Alpine ecosystems, our approach can be extended to any type of ecosystem and different ecosystem components, having the potential to be used for different purposes and at different landscape scales. Finally, this framework is a first step into the study of stability from a multidimensional perspective in complex ecosystems composed of habitat mosaics.

CHAPTER III

DROUGHT CHANGES THE EFFECTS OF CLIMATE WARMING ON FOREST-GRASSLAND ECOTONE STABILITY

Ceres Barros^{1,2}, Wilfried Thuiller^{1,2} and Tamara Münkemüller^{1,2}.
In prep.

¹ Laboratoire d'Écologie Alpine (LECA), Université Grenoble Alpes, F-38000 Grenoble, France

² Laboratoire d'Écologie Alpine (LECA), CNRS, F-38000 Grenoble, France

Abstract

Plant communities in forest-grassland ecotones of the European Alps suffer from gradual climate warming. While the intensity and frequency of drought events are predicted to increase even at high elevations, their consequences on plant community stability are largely unknown. Here, we investigate how drought and climate warming destabilise plant community structure in forest-grassland ecotones in the French Alps. We simulated the interactive effects of gradual climate warming and three drought scenarios on 24 plant functional groups. Using n -dimensional hypervolumes, we assessed how the different drought scenarios affected community stability depending on the type of vegetation and land-use management. Drought effects on forest and grassland structure did not greatly change the long-term trajectories caused by gradual climate warming alone, but determined final community structure and functional diversity. These effects differed between grasslands and forests, as well as management, with community structure being most stable in managed grasslands, and least stable in forests. Our results have implications for ecosystem management, but also highlight that effects of drought are most evident when stability is analysed using multidimensional approaches.

Keywords: FATE-HD, n -dimensional hypervolumes; ecological modelling

Introduction

Across the globe, ever-increasing changes to ecosystems such as regional intensification or land-use abandonment, and climate change, threaten taxonomic and functional composition and associated ecosystem functions and services (Díaz *et al.* 2006; Weiner *et al.* 2014; Kortsch *et al.* 2015; Oliver *et al.* 2015). These changes may compromise the ability of ecosystems to recover from future perturbations and lead to departures from stability, which may ultimately result in shifts to other ecosystem states (see, for instance, the review by Standsch *et al.* 2014).

Climate change is expected to not only affect average temperature and precipitation values, but also extreme climate events (IPCC 2013). While droughts already caused significant forest diebacks around the globe (Allen *et al.* 2010) and plant productivity decline in Europe (Ciais *et al.* 2005), they are predicted to become more frequent and intense in the future, even in areas such as the European Alps (IPCC 2013; Gobiet *et al.* 2014). Since drought can have negative effects on plant growth and survival (Bottero *et al.* 2016), changes in drought regimes have implications for plant community structure and composition (Rigling *et al.* 2013), ultimately affecting ecosystem functioning and services (Anderegg *et al.* 2013).

In the European Alps, forests and grasslands along the forest-grassland ecotone are sources of important ecosystem services (Tappeiner & Bayfield 2009). Yet, they are threatened by climate and land-use changes, whose effects on community composition and structure may degrade taxonomic and functional diversity (Tappeiner & Bayfield 2009; Alatalo *et al.* 2016). For instance, land-use abandonment and temperature increases facilitate the upward movement of the treeline, leading to woody encroachment in subalpine and alpine grasslands and loss of grazing pastures (Theurillat & Guisan 2001; Tasser *et al.* 2017). Depending on their frequency and intensity, drought events may either revert these trends by increasing tree mortality, or facilitate the upward movement of species adapted to warmer and drier climates (Theurillat & Guisan 2001; Rigling *et al.* 2013). Intense and frequent drought can accelerate shifts in species composition, but slow down forest expansion when compared to climate and land-use changes alone (Barros *et al.* 2017). However, guaranteeing the provision of ecosystem services (ESs) requires going beyond studying single aspects of stability (e.g. treeline advancement) and taking a multidimensional view that includes multiple aspects of communities (Barros *et al.* 2016c). Moreover, as ecosystems respond

differently to global change (Frank *et al.* 2015), adequate ecosystem management requires knowledge on their relative stability to different interacting drivers. Hence, here we sought to understand how climate warming and drought jointly affect the stability of grasslands and forest communities in function of land-use practices.

An ecosystem is considered stable if, when disturbed, it shows small departures from its initial values and has low temporal variance (Tilman *et al.* 2012; Gross *et al.* 2014). While most stability studies focused on single ecosystem properties (e.g. productivity; Isbell *et al.* 2015), here we explore the stability of community structure by looking at the relative abundances of all community components (i.e. functional groups). The hypervolumes framework allows comparing a community's pre- and post-disturbance states built from the time series of functional group' abundances (Barros *et al.* 2016c). Departures from an initial state can be measured as the distance between the centroids of pre- and post-disturbance hypervolumes. Changes in temporal variability can be measured as differences in hypervolumes' sizes, and the overlap between pre- and post-disturbance hypervolumes summarises the destabilisation of communities. Importantly, this framework enables cross-ecosystem and cross-disturbance comparisons.

Methods

Simulation experiment

We used the dynamic vegetation model FATE-HD (Boulangéat *et al.* 2014b) to simulate the effects of gradual climate warming and drought events on the vegetation of the Ecrins National Park (French Alps) under current land use. The model simulates the population dynamics, dispersal, biotic interactions and responses to disturbances of 24 plant functional groups (PFGs), in a spatio-temporal manner. PFGs grouped the dominant species of the park, based on their functional traits and tolerance to biotic and abiotic conditions (Boulangéat *et al.* 2012). Their responses to drought and land-use practices (grazing and mowing) depended on their functional traits and historic climatic exposure, while responses to climate changes were simulated as changes in habitat suitability (for details see *The FATE-HD simulation platform and drought simulation experiment* in Appendix 4 and Barros *et al.* 2017).

Simulations had three phases: an initialisation phase of 850 years to achieve the 'pre-disturbance state' (Boulangéat *et al.* 2014b), a scenario phase of 150 years during which one

Chapter III - Drought changes the effects of climate warming on forest-grassland ecotone stability

of three scenarios was simulated, and a stabilisation phase of 50 years during which PFGs reached a quasi-equilibrium post-disturbance state (Fig. S2 in Appendix 4). The scenarios varied only in drought regime: *no drought*, *sporadic/moderate drought* and *frequent/severe drought*. Gradual climate warming was based on the IPCC A1B scenario and droughts events consisted in anomalies of a moisture index calculated based on the last year of the A1B scenario prediction (see *The FATE-HD simulation platform and drought simulation experiment* in Appendix 4 and Barros *et al.* 2017 for further details).

Hypervolume calculation

We focused on forests (unmanaged) and grasslands (managed or unmanaged) from the ecotone belt and analysed changes in the 24 simulated PFGs using yearly relative abundances (see *Treatment of model outputs* in Appendix 4 and Barros *et al.* 2016c). For each pair of pre- and post-disturbance states (9 pairs = 3 drought scenarios x 3 plant community and management combinations), hypervolumes were calculated from the first three PCA axes calculated on relative PFG abundances (see *Applying the hypervolumes framework and statistical analysis* in Appendix 4). Stability was assessed in three ways. Average changes in PFG abundances were measured as the distance between pre- and post-disturbance hypervolumes' centroids (mean distance), changes in the temporal variance of PFG abundances were measured as the ratio of post- and pre-disturbance hypervolumes' sizes (size changes), and overall changes in community structure were measured as the amount of overlap between the two hypervolumes (overlap). Since uncertainty in the calculation of the hypervolumes can arise from small sample sizes such as ours (Blonder *et al.* 2014), each pair of hypervolumes was calculated and compared 100 times. Also, results were compared to a set of 'null comparisons', built from comparing the pre-disturbance hypervolume with additional hypervolumes from 50-year-long simulations, replicated 100 times, where neither climate warming nor drought were implemented (see *Applying the hypervolumes framework and statistical analysis* in Appendix 4).

Statistical analyses

We analysed changes in hypervolumes in response to drought scenarios, type of plant community and management regime separately for each variable (mean distance, size changes and overlap) using ANOVAs. Additionally, we calculated the standardised effect sizes (SES)

of the different drought scenarios with respect to the null comparisons for each plant community and management combination. To complement the SES, we ran ANOVAs that included the null comparisons as a control treatment (see *Applying the hypervolumes framework and statistical analysis* in Appendix 4 for details).

Results

Climate warming and drought clearly caused forest and grassland communities to depart from their initial community structure, leading to significant changes in the mean and variance of relative PFG abundances (i.e. mean distance and size changes), as well as significant overall changes in community structure (i.e. overlap; Figs. 15 and 16, Table S3 in Appendix 4). Although different drought regimes had qualitatively similar effects (Fig. 16), they had quantitatively different effects when null comparisons were excluded (Table S4 in Appendix 4). Also, drought regimes had strong short-term effects on community structure, especially if drought was frequent/severe (Fig. 15).

Notably, the effect of drought regimes depended on the community and management type considered (Table S4 in Appendix 4). Grasslands appeared to be more stable than forests, showing smaller departures from initial mean PFG abundances and varying less after disturbances, especially when drought was frequent/severe and grasslands were managed (Fig. 16). In contrast, forest structure became particularly more variable under frequent/severe drought (Fig. 16). Importantly, community structure changes were driven by different PFGs depending on the type of community/management; yet, for a given plant community and management combination, PFGs driving community changes were consistent across drought scenarios and could be translated in shifts in functional composition. For instance, in managed grasslands drought scenarios led to a general increase of woody PFGs and reductions in average specific leaf area (SLA; Fig. 15), while forest communities became dominated by drought-tolerant PFGs (see *Additional results and discussion* in Appendix 4).

Discussion

Climate warming and drought affect the stability of forest-grassland ecotone communities, even if management remains unchanged. In accordance to previous results (Barros *et al.* 2017), climate warming was the main driver of long-term destabilisation of grassland and

Chapter III - Drought changes the effects of climate warming on forest-grassland ecotone stability

forest communities. Although drought did not offset this overall destabilisation effect in the long-term, it had strong short-term effects on community structure and less pronounced long-term effects. For instance, frequent/severe drought caused managed grasslands to be less encroached in the long-term, but offered a short-term advantage to woody PFGs (Fig. 15).

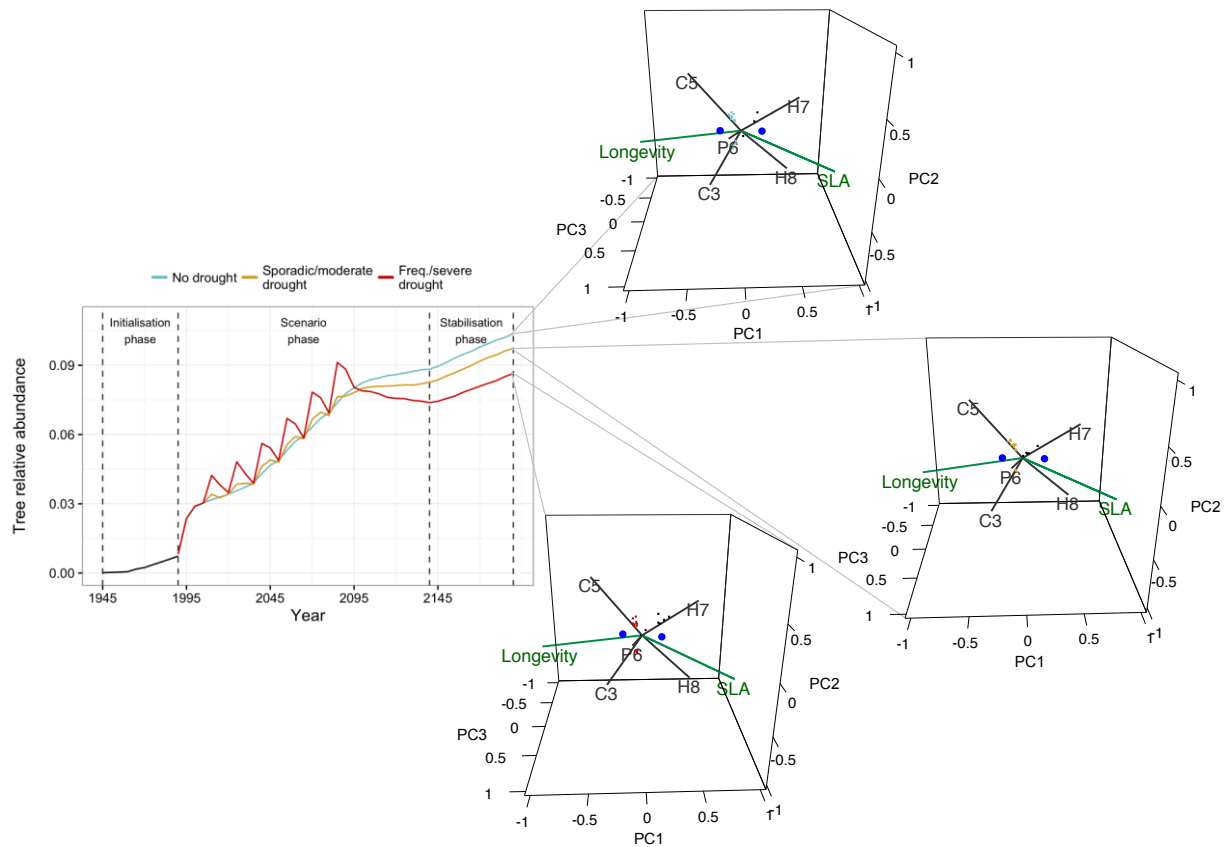


Figure 15. Tree transient dynamics in managed grasslands under different scenarios of drought, and corresponding pre-disturbance (in black) and post-disturbance (blue, yellow and red) hypervolumes shown with their centroids (in dark blue). Five PFGs with the largest absolute factor loadings on the first three principal components are shown in grey. Functional traits most correlated with PC1 are shown in green (see Applying the hypervolumes framework and statistical analysis in Appendix 4 for further details). For visual clarity, only 300 random sampled points are shown per hypervolume (Blonder *et al.* 2014).

We detected different sensitivities of grasslands and forests to drought. For instance, forest community structure was overall less stable than grassland's, probably due to relatively slower forest dynamics and longer periods of recovery from drought-related mortality. Conversely, the continued management of grasslands partly counterbalanced changes driven by drought and climate warming.

Changes in community structure induced changes in functional diversity that may impact ecosystem functioning. For instance, the decreases in SLA observed in managed grasslands can impact fodder production (Lavorel & Grigulis 2012), while changes in forest composition can affect carbon and water cycles (Wang *et al.* 2012). These results are highly relevant for ecosystem management in this region. At present, traditional pastoral activities are subsidised

to prevent the loss of open habitats and associated biodiversity and ESs (Tasser *et al.* 2017). Yet, forest die-backs and changes in forest composition and structure can negatively affect other ESs, like avalanche and soil protection, flood regulation and carbon nutrient cycles (Marston *et al.* 2003; Anderegg *et al.* 2013). Managing for high ESs diversity will, thus, require assessing the relative stability of grasslands and forests to global change drivers and understand its consequences for functional diversity.

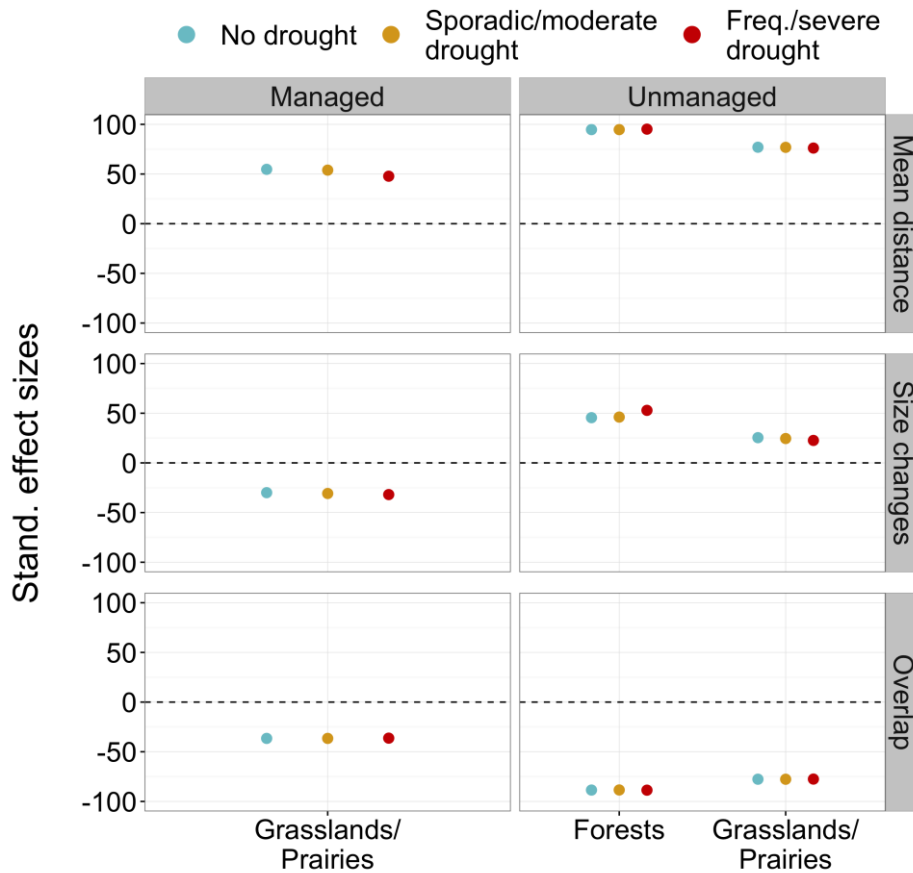


Figure 16. Standardised effect sizes of drought scenarios by community and management types on hypervolume metrics, relatively to null comparisons. Dashed lines indicate a zero or no effect.

CHAPTER IV

ARE TROPHIC NETWORKS IN EUROPEAN PROTECTED AREAS ROBUST TO GLOBAL CHANGE? A SPATIALLY EXPLICIT ANALYSIS.

Ceres Barros^{1,2}, João Braga^{1,2}, Núria Galiana³, Luigi Maiorano⁴, Francesco Ficetola^{1,2,5},
Alessandro Montemaggiore⁴, Dominique Gravel⁶, Tamara Münkemüller^{1,2}, José M. Montoya³
and Wilfried Thuiller^{1,2}. *In prep.*⁶

¹ Laboratoire d'Écologie Alpine (LECA), Université Grenoble Alpes, F-38000 Grenoble, France

² Laboratoire d'Écologie Alpine (LECA), CNRS, F-38000 Grenoble, France

³ Centre for Biodiversity Theory and Modelling, Station d'Écologie Théorique et Expérimentale du CNRS,
09200 Moulis, France

⁴ Dipartimento di Biologia e Biotechnologie 'Charles Darwin', Università di Roma 'La Sapienza', Roma 00185,
Italy

⁵ Department of Biosciences, Università degli Studi di Milano, Via Celoria 26, 20133 Milano, Italy

⁶ Département de Biologie, Faculté des Sciences, Université de Sherbrooke, 2500 Boulevard Université
Sherbrooke, Qc., J1K 2R, Canada

⁶ This chapter is composed of a manuscript under preparation to be submitted to *Nature* as a *Letter*-type piece, which is why the text structure does not follow a conventional organisation.

Abstract

As global change drivers continue to cause important biodiversity losses, the Intergovernmental Platform on Biodiversity and Ecosystem Services (IPBES) stresses the importance of protecting biodiversity holistically. In European Union (EU) countries, an extensive network of protected areas (PAs) exists, yet it mostly focuses on preserving key species or particular habitats. Despite it being increasingly defended that ecosystem management should consider the multi-trophic nature of ecosystems (Fraser *et al.* 2015), so far we ignore how trophic networks will respond to climate and land-use changes, especially at regional scales. Here, we analysed the robustness of vertebrate trophic networks to global change in PAs across EU countries, in a spatially explicit manner. To do so, we submitted these trophic networks to climate and land-use changes projected for the next 20-30 years, and assessed their robustness in terms of secondary extinctions. We show that trophic networks are possibly not robust to climate change, even under optimal habitat protection. Yet, network robustness to climate changes was highly dependent on species abilities to migrate and colonise new habitats. We also identify that regions with particularly lower robustness across scenarios of global change suffered larger taxonomic turnover and larger changes in connectance (i.e. ratio of realised to potential interactions). Network properties also influenced robustness to climate and land-use changes. Although larger and better-connected networks were generally more robust, this relationship was lost when more than ten species went extinct secondarily. Our work shows that considering trophic interactions and species' dispersal limitations affects predictions of biodiversity under global change. We highlight the need for large-scale and spatially explicit studies of ecological network stability under environmental change.

Keywords: land-use changes; climate changes; extinctions; vertebrates

Chapter IV - Are trophic networks in European protected areas robust to global change? A spatially explicit analysis.

Direct and indirect anthropogenic actions are causing important massive biodiversity loss, both via habitat destruction and conversion, and via climate change (Barnosky *et al.* 2011). As a result, habitat protection usually aims at protecting charismatic, endangered and rare species, or particularly rare habitats. Conversely, consequences of global change are also often studied for single species and, or, single trophic levels. For instance, changes in species distributions under future habitat and climate conditions have often been assessed by considering species as separate entities. Similarly, responses of vegetation to future scenarios of global change have also rarely considered feedbacks with higher trophic levels, pollinators or pests and parasites (but see Schleuning *et al.* 2016). Yet, despite that biotic interactions are likely going to influence the outcomes of global change for biodiversity (Grassein *et al.* 2014; Mod *et al.* 2015), the stability of ecological networks to global change drivers has seldom been investigated (but see Evans *et al.* 2013; Albouy *et al.* 2014; Valiente-Banuet *et al.* 2015; Schleuning *et al.* 2016), especially at scales relevant for management. In particular, the stability of terrestrial trophic networks has mostly been studied in a spatially implicit manner, covering relatively small areas and providing a very localised picture of overall ecosystem stability to species extinctions (Dunne *et al.* 2002; Evans *et al.* 2013; Cai *et al.* 2016). Yet, increasing data availability provides the opportunity to study trophic network robustness to global change drivers. Here, we use a metaweb of trophic interactions amongst all pan-European terrestrial tetrapods (narrowed down to the 840 vertebrate species present in all EU countries, excluding Croatia: 83 amphibians, 435 birds, 201 mammals and 121 squamata and freshwater testudinae, hereafter ‘reptiles’) to assess the robustness of vertebrate trophic networks in European protected areas (PAs) to climate and land-use changes. By combining this metaweb with information on species’ geographical ranges and habitat preferences, we built spatially continuous trophic networks across all EU countries (excluding Croatia) and analysed their robustness to species primary and secondary extinctions caused by different global change scenarios. These scenarios combined land-use projection for 2040, with climate changes projected for 2030-2050. Climate changes determined species ranges, which were extracted from consensus projections of species distributions models that were filtered according to species habitat preferences. Scenarios including climate change were crossed with two extreme species dispersal scenarios (global dispersal or no dispersal). More specifically, we aimed at 1) assessing trophic network robustness in PAs to different scenarios of global change and 2) identifying particularly sensitive areas, as well as 3) understanding what network properties drive trophic network robustness to global change in European PAs.

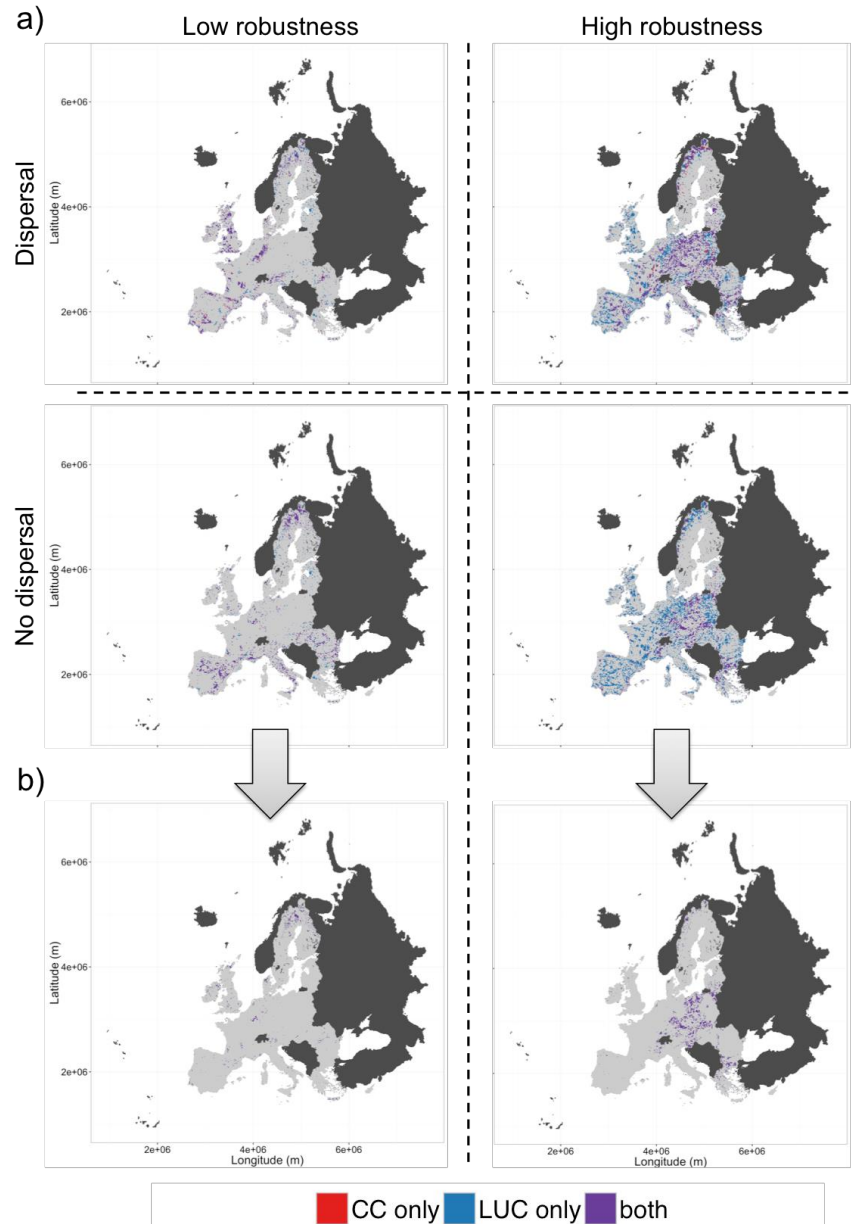


Figure 17. Protected areas with low and high robustness to global change scenarios. Protected areas' (PAs) pixels were classified as having low/high robustness to a given scenario, if their network robustness was in the first/third quartile of robustness values across all PAs pixels for that scenario. Panels in b) show overlapping purple pixels across each dispersal scenario (i.e. pixels with low/high robustness to both scenarios of LUC + CC). Note that because climate change was the major cause of secondary extinctions, red and purple pixels of panels in a) almost always overlap.

Trophic networks across European PAs had generally high robustness to land-use changes alone (right panels in Fig. 17). This scenario assumed no habitat conservation, whereby land use changed according to a nationally-oriented European governance, with overall cropland intensification and low expansion of wild areas (Nakicenovic *et al.* 2000; Stürck *et al.* 2015). Conversely, PAs were largely affected by climate changes predicted for the next 20-30 years, which resulted in large changes in species composition even under maximal habitat conservation (i.e. no land-use changes in PAs; Fig. 17 and Fig. S1 in

Chapter IV - Are trophic networks in European protected areas robust to global change? A spatially explicit analysis.

Appendix 5). Protected areas with consistently low robustness to combinations of land-use and climate changes, regardless of whether species were allowed to disperse or not, were mostly situated N-NE Sweden, Ireland and the British Isles, and some near the Franco-German border (Fig. 17b). On the other hand, PAs with high robustness to land-use and climate changes across dispersal scenarios were mostly situated in central European countries and the western Balkans. These differences in robustness were related to dissimilarities in how much networks changed in terms of species richness and connectance. Networks with low robustness suffered larger changes in species richness and connectance across scenarios, than networks with high robustness (Fig. 18).

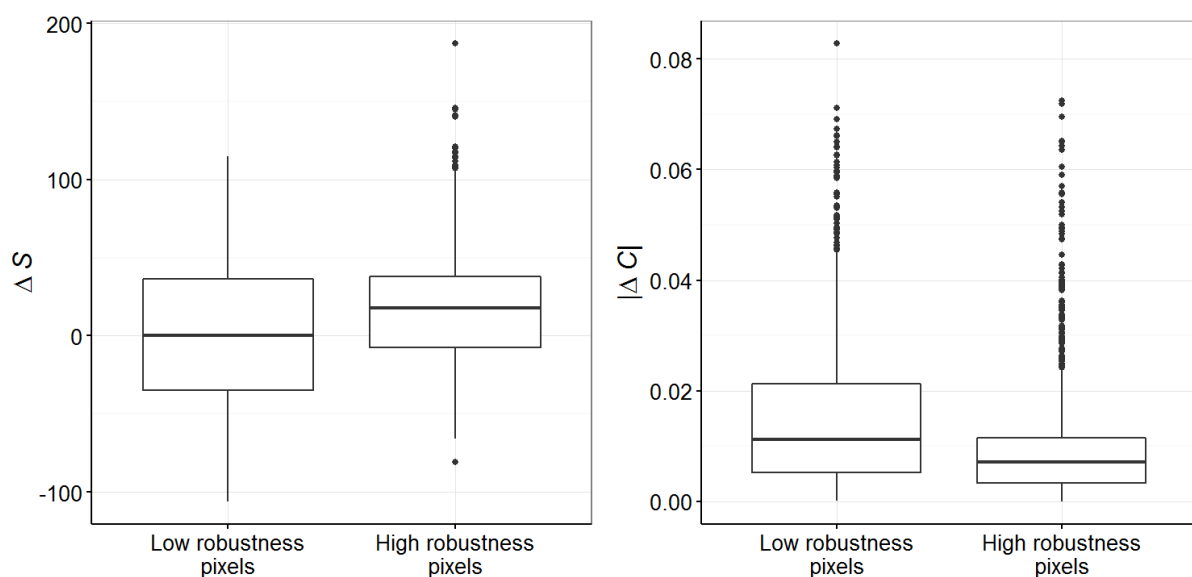


Figure 18. Changes in species richness (ΔS) and connectance ($|\Delta C|$) in networks with consistently low and high robustness. In both cases, changes were calculated by subtracting baseline network values to future network values, but are shown in absolute values for connectance (as suggested by Gilbert 2009). Only the pixels that had low/high robustness to the two scenarios of LUC + CC (with and without dispersal) are shown here (see Fig. 17b).

Notably, a large proportion of networks that were highly robust to the combination of land-use and climate changes when dispersal was allowed, were not robust to these disturbances if species were not allowed to disperse and colonise new pixels (compare top and bottom right panels in Fig. 17). We are aware that range shifts do not depend solely on abiotic factors (Urban *et al.* 2013), being significantly affected by synergies between species' life-history, dispersal traits and landscape configuration (Barros *et al.* 2016b), but also by species interactions (HilleRisLambers *et al.* 2013). Yet, we currently lack data to explicitly simulate population and dispersal dynamics across the range of species included in our analysis, and models allowing to project species distributions conditioned by biotic interactions are still in their infancy (Urban *et al.* 2013). Nonetheless we accounted for the possible impacts of

different dispersal limitations in our simulations, with two scenarios that illustrate two opposite sides of a dispersal gradient. Under the full-dispersal scenario all vertebrates are equally capable to disperse to wherever climate is suitable. The no-dispersal scenario accounts for climate-driven extinctions, but species are not able to colonise new climatically suitable areas. Many amphibian, reptile and mammal species in our metaweb have small body sizes (data not shown), which usually indicates poor dispersal capabilities and the inability to track climate change (at least for mammals; Santini *et al.*, 2016). Considering the spatial resolution of our simulations (10 Km² pixels), for these species no-dispersal scenario maybe more realistic than global-dispersal ones. Additionally, even under a full dispersal scenario, we see that including trophic interactions led to lower species richness than what would be expected by stacking species SDMs (Fig. S8 in Appendix 5)

Robustness is generally thought to be positively related with the number of species in a network and the redundancy of links, given by higher connectance and omnivory values (Dunne *et al.* 2002; Gilbert 2009; Saint-Béat *et al.* 2015). In addition, networks that suffer smaller changes in connectance after species extinctions are also more robust (Gilbert 2009). Our results partly followed these expectations and networks with higher initial species richness (S) and higher initial connectance (C) – i.e. before land-use and climate changes - tended to be more robust (Fig. 19). However, we were surprised to see that beyond a certain number of secondary extinctions ($Sext$) larger and better-connected networks did not have an advantage relatively to smaller and poorly connected ones, regarding their robustness to global change scenarios (Fig. 19 and Fig. S2a in Appendix 5). In fact, higher trophic network diversity and complexity did not provide higher robustness when habitat and climate-driven extinctions caused approximately more than ten $Sext$ (Fig. 19). Benefits of S and C were also highly dependent on the scenario of extinction (Fig. S2b and Table S1 in Appendix 5). While no-dispersal climate change scenarios largely weakened the effects of S , the opposite was true for C whose effects on robustness were weaker when dispersal was allowed. Hence, network complexity, measured as C , seemed to play an important role in providing network robustness when species diversity was strongly decreased by climate-driven extinctions. Indeed, the effect of C slightly increased for large numbers of $Sext$ (Fig. S2a in Appendix 5). Although network species richness and connectance have been shown to promote trophic network robustness before (Dunne *et al.* 2002; Gilbert 2009), to our knowledge, these relationships have never been shown across spatially continuous networks submitted to realistic disturbances. Most importantly, our results highlight that communities and ecosystems should not be assumed to sustain higher levels of biodiversity in face of global change based solely

Chapter IV - Are trophic networks in European protected areas robust to global change? A spatially explicit analysis.

on their current biodiversity levels. In the case of European vertebrate trophic networks, the effects of network diversity and connectance were already quite low for networks that loss ca. 10 species secondarily, even though S in these networks was high (varying from 70 to 289 species).

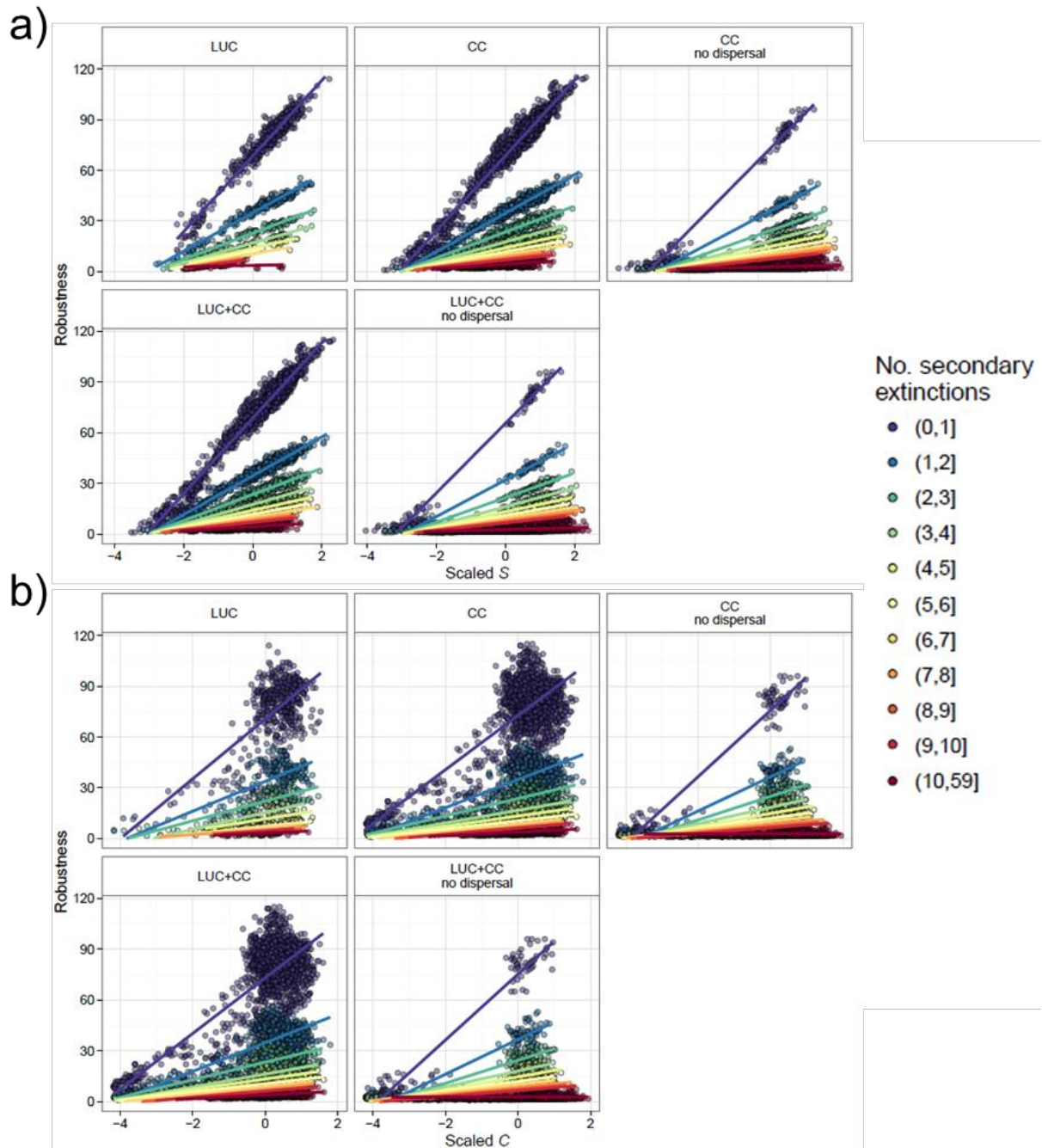


Figure 19. Relationships between robustness and a) initial species richness (S), and between robustness and b) initial connectance (C). Both S and C were centred and scaled to avoid model convergence issues. Points are coloured by the number of secondary extinctions, which was binned in 10 classes for visual clarity (unit increments between 1 and 9 secondary extinctions, and ≥ 10 secondary extinctions). Points shown correspond to pixels inside protected areas (PAs), which had at least one secondary extinction and initial modularity values ≥ 0 .

Our results suggest that trophic networks across European PAs may be seriously affected by climate changes predicted for the next 20-30 years, and that species dispersal limitations will play a major role in determining their robustness to these changes. This low trophic network robustness may reflect that European ecosystems are at risk from global change, even if we assume that habitats can be fully protected, which should not be possible as vegetation will also shift in response to CC. Moreover, we join others in highlighting the importance of ensuring species motility within and across PAs, but also of considering the role of dispersal processes in predictive models of biodiversity, as they can drastically change predictions.

Methods

Trophic data, species distributions and land-use maps

Metawebs represent all potential interactions between species of a given species-pool and, when combined with species distribution data, allow reconstructing ecological networks at local scales. After an important compilation of available data and expert knowledge, we constructed a trophic metaweb of all pan-European vertebrates (comprising 92 species of amphibians, 229 species of reptiles, 283 species of mammals and 503 species of birds; see *Extended methods* in Appendix 5 further details), which was used to construct local trophic networks at 10 Km scale, when combined with species' geographic distributions and habitat preferences, as well as habitat maps. The metaweb also included 11 diet categories that were treated as basal nodes that were ubiquitous across Europe and scenarios of change. Species distributions were obtained from species distribution models projections based in climate values for year 2000 and IPCC climate projections for years 2030-2050 following the A2 emissions scenario. Species habitat preferences were obtained from Maiorano *et al.* (2013), but land-use classes were converted to match those used in the land-use change projections (see Table S2 in Appendix 5). Habitat maps were obtained from land-use projections from the model Dyna-CLUE for years 2000 and 2040 (see Fig. S3 in Appendix 5). Land-use projections for 2040 also followed an A2 IPCC-equivalent scenario, and were only available for EU countries, thus restricting our study area to these territories. Please see *Extended methods* in Appendix 5 for details on species distribution models, and land-use and climate projections used.

Building local networks

Local networks were built per 10 Km² pixel, by conditioning species presences to the presences of their prey and preferred habitats (see Fig. S4 in Appendix 5 for network calculation workflow). A first set of baseline webs was calculated based on present species distributions and habitat maps for year 2000, assuming that species only required one prey item to colonise a given pixel ('no threshold of extinction'). Given that networks were restricted to EU countries and their available habitats, the total number of species present across these baseline networks was narrowed down to 840 species, of which there were 83 amphibians, 435 birds, 201 mammals and 121 reptiles. Since assuming that species only require one prey item is quite unrealistic, we constrained species presences by a minimum number prey defined on a species by species basis, i.e. species-specific extinction thresholds. These extinction thresholds were obtained per species from the distribution of their number of prey across all baseline networks built without a threshold of extinction ('species prey distributions'). We then extracted the 10% quantile values of each species' prey distribution and recalculated all baseline networks using these values as the minimum number of prey each species required to survive in any given pixel. We tested the sensitivity of baseline networks properties to changes in quantile values. Larger quantile percentages caused large disruptions of baseline networks across Europe, resulting in a large loss of analysable networks. On the other hand, lower percentages did not greatly differ much from not using a threshold (see *Sensitivity analysis* in Appendix 5). We thus chose to use the 10% quantile threshold for further simulations. By using the same quantile percentage across species, we assumed all species required the same proportion of their dietary niche to survive. Although it can be argued that specialist species should require larger proportions of their dietary niche than generalist species, a constant threshold ensured that we did not select against specialist species when building our baseline webs.

To explore the robustness of the baseline networks, we simulated local species extinctions/colonisations in response to LUC and CC across all pixels inside protected areas (PAs) in EU countries. Our list of PAs included both terrestrial and wetland PAs, designated and inscribed at the national and international levels (the later including all IUCN PA categories) at year 2015, offering a maximum coverage of protected sites across EU countries that was well distributed across the study area (obtained from <https://www.protectedplanet.net/c/world-database-on-protected-areas>). Scenarios of LUC and CC were based on the future land-cover and climate projections mentioned above and combined with two possible dispersal scenarios: full dispersal or no dispersal. Scenarios of

LUC assumed that EU countries would abandon habitat conservation actions and PAs would suffer land-use changes predicted for year 2040 under the A2 IPCC scenario (see *Extended methods* in Appendix 5 for further details); on the other hand, scenarios without LUC assumed maximal and optimal habitat conservation, with habitats inside PAs remaining unchanged relatively to year 2000.

We simulated a total of 5 global change scenarios - LUC only, CC only, CC only without dispersal, LUC + CC, and LUC + CC without dispersal – for which we recalculated all trophic networks using the same species-specific minimum prey thresholds used for calculating baseline networks. This way, we guaranteed that changes in species composition were only due to land-use and climate effects, rather than changes in species minimum dietary requirements. Species were then considered primarily extinct if they were predicted to be absent from a pixel under future climatic conditions, or had lost suitable habitat, and secondarily extinct when they could be present in terms of climate and habitat suitability, but had too few prey items. Note that basal species could not go secondarily extinct. Network robustness to species extinctions was then measured as:

$$Robustness = \left(\frac{Sext}{S - B} \right)^{-1} \quad (\text{Eq. 1})$$

where *Sext* is the number of secondary extinctions and *S* and *B* are, respectively, species richness and the number of basal species in the baseline network. Higher values indicated more robust networks and tended to infinity as *Sext* tended to 0.

Assessing drivers of robustness

After building baseline and future scenario networks, we calculated a set of network properties known to be related with network robustness (species richness, connectance, omnivory; Dunne *et al.* 2002; Gilbert 2009; Saint-Béat *et al.* 2015), as well as additional properties that reflect both network topology and complexity and could be potential predictors of robustness (see full list in Table S3 in Appendix 5). All properties, except for those related with species trophic levels (mean and standard deviation of trophic level, proportion of basal, intermediate and top predators, and omnivory), were calculated on vertebrate species only, given that diet categories have a different taxonomic resolution from species nodes. After a preliminary analysis of pairwise correlations between robustness and network properties (Table S4 in Appendix 5), we selected species richness, *S*, and connectance, *C*, as predictors of robustness and modelled their effect using linear mixed effects models, whereby we included the fixed effects of *S* and *C* and their interactions with scenarios, and the random

Chapter IV - Are trophic networks in European protected areas robust to global change? A spatially explicit analysis.

effect of *Sext* (see *Extended methods* in Appendix 5 for detailed description of the statistical analyses). Additionally, we assessed the temporal turnover in species composition (temporal β -diversity) per group of species (amphibians, birds, mammals and reptiles). Temporal β -diversity was calculated on a pixel basis for each future scenario network, with reference to the baseline network, using a multiplicative decomposition of α - and γ -diversity, which were in turn calculated as the inverse Simpson concentration (Whittaker 1972):

$$\alpha / \gamma = \frac{1}{\sum p_{(i)}} \quad (\text{Eq. 2})$$

$$\beta = \gamma \times \sum \left(\frac{1}{n} \times \frac{1}{\alpha_i} \right) \quad (\text{Eq. 3})$$

where p is the presence/absence of each species across the baseline and scenario network (for γ -diversity), or in each network i (for α -diversity), and n the total number of networks being compared (two in this case, corresponding to pairwise comparisons between baseline and scenario networks).

DISCUSSION AND PERSPECTIVES

Studying ecosystem stability in face of global change is crucial to adapt ecosystem management and avoid further loss of biodiversity, as well as the disruption of ecosystems and the services they provide. Doing so will require accounting for synergies between different global change drivers, but also integrating several levels of ecosystem complexity in our analyses and projections.

Synergies between climatic drivers and land-use changes & consequences for management

Notably, evaluations of global change consequences for vegetation dynamics need to consider more than trends of mean temperature and precipitation values. Land-use changes and other climatic drivers, like changes in drought regimes, need also to be considered, especially because they are likely to impact vegetation (and consequently ecosystems) at different time scales (see Kulakowski *et al.* 2011 and Boulangeat *et al.* 2014b). To my knowledge, I have been the first to simulate the synergies between gradual climate change, drought regimes and changes in land-use management using a landscape dynamic vegetation model, and to assess their consequences for different ecosystems in the European Alps.

Interestingly, long-term vegetation dynamics were mostly driven by gradual climate changes, yet drought determined the final composition and structure of Alpine communities in ways that are extremely relevant for ecosystem management. In Alpine ecosystems, strong abiotic gradients and historical land-use have constrained species distributions and plant community assemblages, whose structure and composition are menaced by climate warming and the abandonment of traditional agro-pastoral activities. Increasing drought severity (i.e. more intense and frequent drought) may on the short-term accelerate the woody encroachment of alpine open habitats – which is already being observed with land-use abandonment – by

benefiting drought-tolerant groups like woody species, but on the long run decelerate this trend (Chapter I). Alpine open habitats host important levels of biodiversity, including endemic and protected species (Andrello *et al.* 2012), and provide several ecosystem services (like fodder production for cattle, pollination and hydrological regulation Crouzat *et al.* 2015). Grazing and mowing in subalpine and alpine grasslands not only maintain woody species at bay, but also promote higher biodiversity by creating a variety of ecological niches thanks to increased spatial heterogeneity in nutrient distribution and seed input (Maurer *et al.* 2006). Hence, continuing traditional grazing and mowing activities will be important to maintain higher levels of taxonomic β -diversity (see Chapter I and Appendix 2) and to stabilise grassland communities under climate change (Chapter III). On the other hand, the combination of drought and climate warming may prove more destabilising for forest communities, whose slow dynamics take longer to recover from drought-related mortality and to find a new equilibrium state with new climate conditions (Chapter III). Forests, like open habitats, also provide important ecosystem services, namely wood production, vertebrate diversity and carbon storage (Crouzat *et al.* 2015). Yet, their supply may be jeopardized if climate warming and drought cause large changes in forest structure and composition. Finally, these changes will impact functional diversity, with further implications for ecosystem functioning and ecosystem services. For instance, turnover towards more drought-adapted Alpine grasslands and forests may be accompanied by decreases in community-level specific leaf area (SLA), which can result in lower overall grassland and forest productivity and negatively affect fodder and wood production (Chapter I and Chapter III; Jung *et al.* 2014). Thus, managing for the provisioning of the bundles of ecosystem services now available in the European Alps will require considering the interplay between global change drivers and maintaining a degree of landscape heterogeneity.

Perspectives

Spatially explicit modelling of drought effects at landscape scales and across different plant groups can be a challenge. There are still large knowledge gaps concerning the physiological responses of different plant species and even plant life forms to drought, which hinder the use of physiological models across different types of vegetation, or a more accurate parameterisation of drought effects in mechanistic models. To overcome these data limitations, I have used a statistical approach to parameterise drought effects across different plant functional groups (PFGs) present in the Ecrins National Park. I assumed that PFG presences recorded in the past years reflected that PFGs survived past drought events, and

thus large departures from their experienced past drought values would cause negative effects on PFG dynamics. Together with expert knowledge that allowed fine tuning the parameterisation, I was able to recreate the present vegetation state of the park while accounting for past drought events (Appendix 2). But uncertainty remains regarding the quantitative effects of drought across the variety of PFGs that we simulated. Only with further empirical data will next studies be able to correctly estimate the impacts of changing drought regimes on vegetation dynamics. Namely, how drought affects seed production, germination and juvenile recruitment across plant life forms, how repeated drought events affect the capacity for resprouting, growth and fertility, and how this depends on life form and life history traits, are some of the very pertinent questions that future studies should investigate.

I have also analysed which types of plant communities – forests or grasslands – were more stable to drought and climate warming effects. In a next step, I believe that it will be interesting to investigate whether, within these communities, there are particular taxonomic and functional compositions that allow for greater, or lower, stability via higher, or lower, drought resilience (*sensu lato*). It is known that different forest types have different resistances to drought due to differences in species composition (Frank *et al.* 2015), and the same is likely to be true for grasslands (Craine *et al.* 2012). FATE-HD could potentially be used to study these differences by comparing how drought and climate warming affect forests along an altitudinal gradient, across which there exists spatial turnover in species composition before simulating drought and climate warming. However, species-specific drought strategies are likely to be very important for overall community resilience to drought events (Craine *et al.* 2012; Liu *et al.* 2015). Therefore, I believe that modelling drought physiological responses will be more appropriate to assess which taxonomic and functional combinations increase community stability to drought. Again, more data on drought response mechanisms across PFGs will be necessary to progress in this direction and, eventually, couple mechanistic models like FATE-HD with a physiological drought model. Alternatively, PFGs could also be rebuilt to take into account species' drought sensitivities. Since PFGs are built according to species' similarity in climatic niche and trait values (Boulangeat *et al.* 2012), past moisture index values could be included as an additional climatic variable and species' soil moisture preference trait values could be added as an extra trait. It would be extremely interesting to compare the results we obtained in Chapters I and III against results obtained with a new set of PFGs. Although I believe that results would be qualitatively similar, if PFGs differed more in terms of their drought sensitivities, taxonomic and functional changes under drought would likely depart more from those expected under gradual climate warming alone.

Additionally, drought is known to have interactions with other factors that have relevant implications for ecosystem functioning in Alpine ecosystems. Other climate change drivers such as carbon dioxide (CO₂) and nitrogen (N) deposition increases are thought to facilitate plant growth (Theurillat & Guisan 2001), but also suffer feedbacks from drought effects (see reviews by Wang *et al.* 2012 and Frank *et al.* 2015 and references therein). For instance, tree mortality from drought decreases leaf area index and results in lower productivity levels on the short term (Brando *et al.* 2008), but can also increase relative N and light availability for surviving trees, and increase soil N cycling rates (Bloor & Bardgett 2012). Also, tree mortality results in lower carbon storage capacity and increased litterfall, the latter leading to higher carbon release from decomposition processes (Brando *et al.* 2008). Biotic interactions with pests and parasites are also an extremely important factor to consider, as drought can render trees more vulnerable to pest and parasite attacks, increasing the likelihood for pest outbreaks (Allen *et al.* 2010; Wang *et al.* 2012; Frank *et al.* 2015). Likewise, interactions between climate and land-use changes and wildfires are important to consider. Although the Ecrins National Park does not suffer from extensive fire events on a regular basis, higher drought frequency and severity, together with globally warmer temperatures and land-use abandonment, will likely increase the propensity for wildfires across the European Alps (Cane *et al.* 2013; Bebi *et al.* 2017; Dupire *et al.* 2017). Should fires become recurrent in the Ecrins, not only could we expect important changes in vegetation structure and composition, but also that reductions in forest cover would impact the provisioning of forest services, like avalanche and rock fall protection (Elkin *et al.* 2013; Dupire *et al.* 2017).

Finally, the impacts of drought on intraspecific variability also need to be further explored and considered in future studies. Intraspecific trait variance can largely contribute to overall community-level trait variance (relatively to interspecific trait variance) and strongly determine changes in community-averaged trait values in response to drought, even when no significant specie turnover occurs (Jung *et al.* 2014). Declines in intraspecific variability may also degrade species' and, consequently, ecosystems' abilities to cope with disturbances (Lepš *et al.* 2011; Barabás & D'Andrea 2016). Therefore, intraspecific variability will have an important role on species' adaptability to drought and for the stability ecosystem functioning, which needs to be accounted for in future modelling of drought consequences for vegetation. Despite current data limitations, FATE-HD and similar hybrid models still provide the opportunity to investigate drought consequences for vegetation at landscape scales, and its interactions with other important drivers of global change such as land-use. Not only that, but FATE-HD also allowed exploring these effects dynamically and across different vegetation

strata and plant groups, which are aspects that have been poorly addressed in the literature so far.

Multivariate and multitrophic perspectives on ecosystem stability

In addition to highlighting the importance of considering multiple drivers of environmental change, I have shown that multidimensional and multi-trophic approaches can change how we perceive and conclude about ecosystem stability.

It is worthwhile mentioning that my view on stability differs from classical mathematical stability concepts, whereby one focuses on the local stability of a system (or asymptotic stability), i.e. its behaviour close to equilibrium after a perturbation (Connell & Sousa 1983; Pimm 1984; Ives 1995). Instead, my view on ecological stability is closer to that of resilience (Holling 1973), since I have focused on a community's, or an ecosystem's, capacity of to withstand perturbations and maintain a similar composition and structure. Analysing local stability requires considering temporary perturbations – pulse perturbations (Connell & Sousa 1983) – in order to measure how fast the system returns to its initial state, or the equilibrium point. Yet, if perturbations are continuous and, or, permanent – press perturbations (Connell & Sousa 1983) – the system may not return to its initial state. Hence, as stated by Connell & Sousa, the study of mathematical stability is hard to achieve in ecological systems, especially when changes in environmental conditions occur. However, I do not think that this renders the study of ecological stability impossible, or futile. By focusing on the stability of community structure and composition (from a taxonomical or functional perspective, or both) I was able to consider the effects of both pulse- (e.g. drought events) and press- type perturbations (e.g. land-use changes and gradual climate warming) together, even if this meant that communities would not return to their initial states. Instead of focusing on return rates after pulse perturbations, I focused on community transient dynamics after and during realistic perturbation regimes simulated as environmental changes, and on the differences between their initial and final states once environmental conditions were stabilised. Thus, my work has mostly concerned the global stability (Holling 1973) of ecosystems in face of environmental change.

The hypervolumes approach allowed me to detect departures from stability in Alpine communities in terms of their composition and structure, which otherwise remained unnoticed when using diversity indices or productivity measures. For instance, hypervolume comparisons revealed important functional changes in undisturbed rocky and scree vegetation

after land-use abandonment. Yet, no particular effect was noticed when using metrics of functional diversity (Chapter II and Appendix 3). Moreover, multivariate approaches like n -dimensional hypervolumes can be used to integrate the responses of all community/ecosystem components to a disturbance. This provides information on changes in both structure and composition, which are usually obtained by measuring several different indicators of diversity (Chapter II). Importantly, the hypervolumes framework can quantitatively measure and compare an ecosystem's responses to distinct types of disturbances, but also the responses of different ecosystems (Chapter II and Chapter III). As mentioned above, drought and gradual climate warming caused higher instability in forests than in grasslands, and grasslands were even more stable when continuously managed (Chapter III). A similar trend was observed for temporal changes in hypervolume overlap calculated in grassland and thicket/scrubland communities under climate warming only (Chapter II). As already discussed above, these changes in composition and structure of Alpine communities can have important implications for ecosystem management in European Alps.

The effects of global change were also different when trophic interactions were taken into account. Stacking the predictions of species distribution model (SDM) projections under future climate conditions resulted in overestimates for vertebrate diversity, when compared to final richness in trophic networks (Chapter IV). This result highlights the importance of considering trophic interactions to predict the consequences of global change drivers for biodiversity. It is known that disturbances such as climate change and habitat loss can affect species interactions before they cause extinctions (Valiente-Banuet *et al.* 2015). Yet, responses of ecological networks to realistic disturbances have been rarely considered in previous studies (but see Evans *et al.* 2013; Valiente-Banuet *et al.* 2015; Schleuning *et al.* 2016), which have investigated network robustness by testing species removal scenarios. In Chapter IV I have gone further and tested the effects of global on vertebrate trophic networks, both in terms of species diversity and species interactions. Since shifting conservation plans from protecting single to multispecies will require assessing how well current management actions will protect ecological networks from global change, I have focused my analyses on protected areas. Worryingly, vertebrate trophic networks in protected areas of European Union (EU) countries seem to be highly sensitive to future climate changes, despite their robustness to future land-use changes (Chapter IV). Importantly, the robustness of trophic networks to climate changes depended on whether species were able to migrate and colonise new habitats or not (Chapter IV). Species' spread rates are known to not only depend on their capacity to disperse, but also on habitat quality and the quantity of habitat available (Barros *et*

al. 2016b). Therefore, effects of climate change on trophic networks will depend on how much habitat remains available, the degree of habitat fragmentation, and species' abilities to disperse across a matrix of unsuitable habitat. This means that climate change mitigation will require the protection of currently available habitat, but also that protected areas include areas that will become suitable for species to disperse to in the future.

Perspectives

So far, ecosystem stability and resilience have often been investigated using one-dimensional approaches (but see Vasilakopoulos & Marshall 2015). However, hypervolume metrics can also be related to ecosystem stability and resilience notions, particularly if high-resolution time-series are available to build and compare hypervolumes from different time slices. Changes in overlap and in the distance between centroids are related with ecosystem resistance (i.e. the extent of changes caused by a perturbation; Table 3 in Appendix 1) and reductions in overlap quantify the changes the ecosystem suffered. Hypervolume size provides a measure of the overall variability of the components used. Therefore, it is inversely related with stability, just as the coefficient of variation measuring the temporal or spatial variability of a given variable is inversely related to its stability (e.g. Loreau & de Mazancourt 2013; Table 3 in Appendix 1). Also, state shifts may be detected when hypervolumes cease to overlap and become very distant in multivariate space, and continue to do so even if they are re-exposed to pre-shift environmental conditions (see notions of irreversibility in Folke *et al.* 2004).

Even if long time series of ecosystem dynamics are not available, as is often the case, the hypervolumes framework can still be applied. Issues related to small sample sizes can be resolved using randomised permutation testing with data subsets, repetitions of hypervolume calculations and comparisons, and null-model-type comparisons. All of these solutions provide a measure of the variability in the calculation of hypervolume metrics and comparisons, guaranteeing the robustness of qualitative results (see Chapter III for the demonstration of the last two solutions). There is also the possibility to use space-for-time data substitutions when time series are not available. This means that geographically different points exposed to the same conditions, are assumed to reflect a state in a particular environment or under a particular disturbance, and compared to another set of points exposed to distinct conditions or disturbances (each set of points being used to build a hypervolume). Alternatively, large fossil and eDNA datasets with high temporal resolution are increasingly available. These data can be used to explore very interesting questions regarding the stability

of community structure and composition to past climate and land-use changes. For example, changes in hypervolume overlap and mean centroid distances could theoretically be used as response variables to explore past ecosystem shifts under gradual climate change, using early warning signals to detect approaching tipping points (Dakos 2008). This is certainly something that I would personally be very excited to explore in my future work.

The fact that many ecosystems are not at equilibrium could be regarded as an issue when assuming that hypervolumes reflect ‘stable states’. However, this issue is pervasive across many other types of analyses that aim to describe community stable states, with or without disturbances. In community ecology, for instance, species assemblages are typically assumed to be at equilibrium with the environment, and the relative importance of assembly mechanisms is also assumed to be stable. Both assumptions are increasingly questioned in the literature (Gerhold *et al.* 2015), but so far no obvious solutions exist. Clearly, more studies are needed to assess community and ecosystem dynamics under different conditions, but also to gather time-series data in the field (Münkemüller *et al.* in prep.). In my view, we must remember and accept that ecosystems and communities are not static entities and nothing in nature is ultimately stable at large time scales. This does not mean, however, that analysing stability is not a valid objective, especially since many environmental policies aim to maintain a certain degree of stability. In any case, hypervolumes can be used to track community transient dynamics without the need to assume stability, as I have shown in Chapter II.

Future studies aiming to explore the consequences of global change for ecosystems will also need to incorporate more complex dynamics, alongside with biotic interactions. In particular, modelling dynamic networks while integrating dispersal dynamics, top-down effects and feedbacks with primary producers, will be important to more accurately predict the effects of global change drivers. In order to account for the effect of different dispersal limitations under climate change, I have simulated two opposite extremes of a dispersal limitation gradient (full dispersal and no dispersal), affecting all species equally (Chapter IV). A next step will be to account for interspecific variability in dispersal capabilities, based on available trait data (Santini *et al.* 2016). For instance, body size and dispersal capabilities are known to be positively related in mammals (Santini *et al.* 2016) and birds (Sutherland *et al.* 2000). In amphibians and reptiles these allometric relationships are less known, but no dispersal scenario may be realistic for these animals at spatial scale that we considered (10km²). For now, we lack trait data across the range of species that I included in my study to enable fine tuning the dispersal scenarios, but this could be done on a smaller region with

fewer, well-studied species. Using dynamic trophic networks will also allow reproducing top-down control effects and the consequences of losing top predators. Predators exert top-down regulation of lower trophic levels, releasing producers from herbivory, *sensu lato* (see Leroux & Loreau 2015 for a review on bottom-up and top-down effects in trophic networks). Extinctions of secondary consumers can therefore lead to the overexploitation of resources by lower trophic levels, causing the extinction of primary producers (Leroux & Loreau 2015; Donohue *et al.* 2017) and, potentially, of other species that depended on them. In addition, incorporating different types of interactions is also essential to accurately predict the consequences of species extinctions. Donohue *et al.* (2017) have demonstrated that only by including two types of non-trophic interactions in their model (competition for space and predator avoidance behaviour) could they reproduce the extinctions observed after a predator removal experiment in a marine rocky shore community. On the other hand, Poggiato *et al.* (submitted) show that future projections for the distribution of *Rupicabra rupicabra* L. in the Bauges Natural Park (French Alps) change dramatically when interactions with vegetation are considered together with climate projections. In their simulations, the lagged response of vegetation to climate warming meant that this herbivore's populations were able to persist, rather than meet extinction in face of climate change projections. I expect that a similar effect may occur at the EU scale with our trophic networks. Using Poggiato and colleagues' approach to couple species distribution models (SDMs) with vegetation projections from a global dynamic vegetation model will be an interesting follow-up work if data regarding species-vegetation associations are available. These more realistic species distribution projections could then be combined with the metaweb information to build local trophic networks, as I have done in Chapter IV.

Finally, my analysis suggested that turnover might promote trophic network robustness to climate changes in EU countries. It will now be important to assess whether this turnover will have negative consequences for ecosystem functioning and stability. To my knowledge, how the redundancy in species and links of a particular type of interaction relates to this same redundancy in another type of interaction is still understudied. Similarly, little is known regarding the relationship between redundancy in species and links, and different ecosystem functions. For instance, I can imagine that high redundancy in trophic interactions may not be related to the redundancy in interactions between pollinators and host plants. As such, the loss of predators may, for instance, negatively impact rodent pest control but not pollination, whereas the loss of insect pollinators will affect pollination more immediately than rodent populations. Thus, future studies need to consider the relationships between species and link

Discussion and Perspectives

redundancy across and within different interaction types, and its role for ecosystem functioning and stability to disturbances.

All in all, research on ecosystem stability needs to adopt large scale and multidimensional perspectives of ecosystems, their dynamics and their responses to disturbances. This is possible by using approaches that encompass multiple components and levels of complexity of ecosystems, integrating several facets of biodiversity. The n -dimensional hypervolumes framework and trophic networks are two approaches that allow for this. On the other hand, using these approaches to assess the effects of different global change drivers on ecosystems will be extremely relevant for ecosystem management and conservation.

REFERENCES

1. Adams, H.D., Guardiola-Claramonte, M., Barron-Gafford, G. a, Villegas, J.C., Breshears, D.D., Zou, C.B., *et al.* (2009). Temperature sensitivity of drought-induced tree mortality portends increased regional die-off under global-change-type drought. *Proc. Natl. Acad. Sci. U. S. A.*, 106, 7063–7066
2. Alatalo, J.M., Jägerbrand, A.K. & Molau, U. (2016). Impacts of different climate change regimes and extreme climatic events on an alpine meadow community. *Sci. Rep.*, 6, 21720
3. Albouy, C., Velez, L., Coll, M., Colloca, F., Le Loc'h, F., Mouillot, D., *et al.* (2014). From projected species distribution to food-web structure under climate change. *Glob. Chang. Biol.*, 20, 730–741
4. Allen, C.D., Macalady, A.K., Chenchouni, H., Bachelet, D., McDowell, N., Vennetier, M., *et al.* (2010). A global overview of drought and heat-induced tree mortality reveals emerging climate change risks for forests. *For. Ecol. Manage.*, 259, 660–684
5. Allesina, S. & Ulanowicz, R.E. (2004). Cycling in ecological networks: Finn's index revisited. *Comput. Biol. Chem.*, 28, 227–233
6. Anderegg, W.R.L., Anderegg, L.D.L., Sherman, C. & Karp, D.S. (2012). Effects of Widespread Drought- Induced Aspen Mortality on Understory Plants. *Conserv. Biol.*, 26, 1082–1090
7. Anderegg, W.R.L., Kane, J.M. & Anderegg, L.D.L. (2013). Consequences of widespread tree mortality triggered by drought and temperature stress. *Nat. Clim. Chang.*, 3, 30–36
8. Andrello, M., Bizoux, J.P., Barbet-Massin, M., Gaudeul, M., Nicolè, F. & Till-Bottraud, I. (2012). Effects of management regimes and extreme climatic events on plant population viability in *Eryngium alpinum*. *Biol. Conserv.*, 147, 99–106
9. Araújo, M.B. & New, M. (2007). Ensemble forecasting of species distributions. *Trends Ecol. Evol.*, 22, 42–47
10. Arreguín-Sánchez, F. (2014). Measuring resilience in aquatic trophic networks from supply–demand-of-energy relationships. *Ecol. Modell.*, 272, 271–276

References

11. Asner, G.P., Elmore, A.J., Olander, L.P., Martin, R.E. & Harris, A.T. (2004). Grazing systems, ecosystem responses, and global change. *Annu. Rev. Environ. Resour.*, 29, 261–299
12. Bachelet, D., Neilson, R.P., Lenihan, J.M. & Drapek, R.J. (2001). Climate change effects on vegetation distribution and carbon budget in the United States. *Ecosystems*, 4, 164–185
13. Baiser, B., Gotelli, N.J., Buckley, H.L., Miller, T.E. & Ellison, A.M. (2012). *Geographic variation in network structure of a nearctic aquatic food web. Glob. Ecol. Biogeogr.*
14. Barabás, G. & D’Andrea, R. (2016). The effect of intraspecific variation and heritability on community pattern and robustness. *Ecol. Lett.*, 19, 977–986
15. Barnosky, A.D., Hadly, E.A., Bascompte, J., Berlow, E.L., Brown, J.H., Fortelius, M., *et al.* (2012). Approaching a state shift in Earth’s biosphere. *Nature*, 486, 52–58
16. Barnosky, A.D., Matzke, N., Tomiya, S., Wogan, G.O.U., Swartz, B., Quental, T.B., *et al.* (2011). Has the Earth’s sixth mass extinction already arrived? *Nature*, 471, 51–57
17. Barros, C., Guéguen, M., Douzet, R., Carboni, M., Boulangeat, I., Zimmermann, N.E., *et al.* (2016a). Data from: Extreme climate events counteract the effects of climate and land-use changes in Alpine treelines. *Dryad Digit. Repos.*
18. Barros, C., Guéguen, M., Douzet, R., Carboni, M., Boulangeat, I., Zimmermann, N.E., *et al.* (2017). Extreme climate events counteract the effects of climate and land-use changes in Alpine tree lines. *J. Appl. Ecol.*, 54, 39–50
19. Barros, C., Palmer, S.C.F., Bocedi, G. & Travis, J.M.J. (2016b). Spread rates on fragmented landscapes: the interacting roles of demography, dispersal and habitat availability. *Divers. Distrib.*, 22, 1266–1275
20. Barros, C., Thuiller, W., Georges, D., Boulangeat, I. & Münkemüller, T. (2016c). N-dimensional hypervolumes to study stability of complex ecosystems. *Ecol. Lett.*, 19, 729–742
21. Baskett, M.L., Fabina, N.S. & Gross, K. (2014). Response Diversity Can Increase Ecological Resilience to Disturbance in Coral Reefs. *Am. Nat.*, 184, E16–E31
22. Bates, D., Mächler, M., Bolker, B.M. & Walker, S.C. (2015). Fitting linear mixed-effects models using lme4. *J. Stat. Softw.*, 67, 1–48
23. Bebi, P., Seidl, R., Motta, R., Fuhr, M., Firm, D., Krumm, F., *et al.* (2017). Changes of forest cover and disturbance regimes in the mountain forests of the Alps. *For. Ecol. Manage.*, 388, 43–56
24. Beisner, B.E., Haydon, D.T. & Cuddington, K. (2003). Alternative stable states in ecology. *Front. Ecol. Environ.*, 1, 376–382
25. Bellard, C., Bertelsmeier, C., Leadley, P., Thuiller, W. & Courchamp, F. (2012). Impacts of climate change on the future of biodiversity. *Ecol. Lett.*, 15, 365–377

26. de Bello, F., Lavorel, S., Lavergne, S., Albert, C.H., Boulangéat, I., Mazel, F., *et al.* (2013). Hierarchical effects of environmental filters on the functional structure of plant communities: A case study in the French Alps. *Ecography*, 36, 393–402
27. de Bello, F., Lepš, J., Lavorel, S. & Moretti, M. (2008). Importance of species abundance for assessment of trait composition: an example based on pollinator communities. *Community Ecol.*, 8, 163–170
28. Benichou, P. & Le Breton, O. (1987). Prise en compte de la topographie pour la cartographie des champs pluviométriques statistiques. Une application de la méthode Aurelhy: la cartographie nationale de champs de normales pluviométriques. *Météorologie*
29. Berger, F. & Chauvin, C. (1996). Cartographie des fonctions de protection de la forêt de montagne: appréciation des potentialités d'avalanche sous couvert forestier. *Rev. géographie Lyon*, 71, 137–145
30. Bestelmeyer, B., Havstad, K., Damindsuren, B., Han, G., Brown, J.R., Herrick, J., *et al.* (2009). Resilience theory in models of rangeland ecology and restoration: the evolution and application of a paradigm. *New Model. Ecosyst. Dyn. Restor.*, 78–96
31. Bigler, C., Bräker, O.U., Bugmann, H., Dobbertin, M., Rigling, A., Ulrich, O., *et al.* (2006). Drought as an inciting mortality factor in Scots Pine stands of the Valais, Switzerland. *Ecosystems*, 9, 330–343
32. Biswas, S.R. & Mallik, A.U. (2011). Species diversity and functional diversity relationship varies with disturbance intensity. *Ecosphere*, 2, art52
33. Blonder, B., Lamanna, C., Violle, C. & Enquist, B.J. (2014). The n-dimensional hypervolume. *Glob. Ecol. Biogeogr.*, 23, 595–609
34. Bloor, J.M.G. & Bardgett, R.D. (2012). Stability of above-ground and below-ground processes to extreme drought in model grassland ecosystems: Interactions with plant species diversity and soil nitrogen availability. *Perspect. Plant Ecol. Evol. Syst.*, 14, 193–204
35. De Boeck, H.J., Bassin, S., Verlinden, M., Zeiter, M. & Hiltbrunner, E. (2015). Simulated heat waves affected alpine grassland only in combination with drought. *New Phytol.*, n/a-n/a
36. Bonet, R., Arnaud, F., Bodin, X., Bouche, M., Boulangéat, I., Bourdeau, P., *et al.* (2016). Indicators of climate: Ecrins National Park participates in long-term monitoring to help determine the effects of climate change. *Eco.mont*, 8, 44–52
37. Bottero, A., D'Amato, A.W., Palik, B.J., Bradford, J.B., Fraver, S., Battaglia, M.A., *et al.* (2016). Density-dependent vulnerability of forest ecosystems to drought. *J. Appl. Ecol.*
38. Boulangéat, I., Georges, D., Dentant, C., Bonet, R., Van Es, J., Abdulhak, S., *et al.* (2014a). Anticipating the spatio-temporal response of plant diversity and vegetation structure to climate and land use change in a protected area. *Ecography*, 37, 1230–1239
39. Boulangéat, I., Georges, D. & Thuiller, W. (2014b). FATE-HD: a spatially and temporally explicit integrated model for predicting vegetation structure and diversity at regional scale.

References

Glob. Chang. Biol., 20, 2368–2378

40. Boulangéat, I., Philippe, P., Abdulhak, S., Douzet, R., Garraud, L., Lavergne, S.S.S., *et al.* (2012). Improving plant functional groups for dynamic models of biodiversity: at the crossroads between functional and community ecology. *Glob. Chang. Biol.*, 18, 3464–3475

41. Brandl, S.J. & Bellwood, D.R. (2014). Individual-based analyses reveal limited functional overlap in a coral reef fish community. *J. Anim. Ecol.*, 83, 661–70

42. Brando, P.M., Nepstad, D.C., Davidson, E.A., Trumbore, S.E., Ray, D. & Camargo, P. (2008). Drought effects on litterfall, wood production and belowground carbon cycling in an Amazon forest: results of a throughfall reduction experiment. *Philos. Trans. R. Soc. B Biol. Sci.*, 363, 1839–1848

43. Brook, B.W., Sodhi, N.S. & Bradshaw, C.J.A. (2008). Synergies among extinction drivers under global change. *Trends Ecol. Evol.*, 23, 453–460

44. Cáceres, M. De, Martínez-Vilalta, J., Coll, L., Llorens, P., Casals, P., Poyatos, R., *et al.* (2015). Coupling a water balance model with forest inventory data to predict drought stress: the role of forest structural changes vs. climate changes. *Agric. For. Meteorol.*, 213, 77–90

45. Cadotte, M., Dinnage, R. & Tilman, D. (2012). Phylogenetic diversity promotes ecosystem stability. *Ecology*, 93, S223–S233

46. Cadotte, M.W., Cavender-Bares, J., Tilman, D. & Oakley, T.H. (2009). Using phylogenetic, functional and trait diversity to understand patterns of plant community productivity. *PLoS One*, 4, 1–9

47. Cai, Q., Liu, J., Boyd, I.L., Jørgensen, S.E., Nielsen, S.N., Fath, B.D., *et al.* (2016). The robustness of ecosystems to the species loss of community. *Sci. Rep.*, 6, 35904

48. Cairns, J. & Dickson, K.L. (1977). Recovery of streams from spills of hazardous materials. *Recover. Restor. damaged Ecosyst. Univ. Virginia Press. Charlottesville.*, 24–42

49. Calanca, P. (2007). Climate change and drought occurrence in the Alpine region: How severe are becoming the extremes? *Glob. Planet. Change*, 57, 151–160

50. Cane, D., Wastl, C., Barbarino, S., Renier, L.A., Schunk, C. & Menzel, A. (2013). Projection of fire potential to future climate scenarios in the Alpine area: some methodological considerations. *Clim. Change*, 119, 733–746

51. Carlson, B.Z., Renaud, J., Biron, P.E. & Choler, P. (2014). Long-term modeling of the forest-grassland ecotone in the French Alps: implications for land management and conservation. *Ecol. Appl.*, 24, 1213–1225

52. Carmona, C.P., Azcárate, F.M., de Bello, F., Ollero, H.S., Lepš, J. & Peco, B. (2012). Taxonomical and functional diversity turnover in Mediterranean grasslands: Interactions between grazing, habitat type and rainfall. *J. Appl. Ecol.*, 49, 1084–1093

53. Carpenter, S.R. & Brock, W.A. (2006). Rising variance: a leading indicator of ecological

transition. *Ecol. Lett.*, 9, 311–318

54.Carpenter, S.R., Brock, W.A., Cole, J.J., Kitchell, J.F. & Pace, M.L. (2008). Leading indicators of trophic cascades. *Ecol. Lett.*, 11, 128–138

55.Carpenter, S.R., Ludwig, D. & Brock, W.A. (1999). Management of eutrophication for lakes subject to potentially irreversible change. *Ecol. Appl.*, 9, 751–771

56.Carrión, J.S., Fuentes, N., González-Sampériz, P., Sánchez Quirante, L., Finlayson, J.C., Fernández, S., *et al.* (2007). Holocene environmental change in a montane region of southern Europe with a long history of human settlement. *Quat. Sci. Rev.*, 26, 1455–1475

57.CBNA. (2015). *Conservatoire Botanique Nationale Alpin*. Available at: <http://www.cbn-alpin.fr>. Last accessed 1 September 2015

58.Certain, G., Dormann, C.F. & Planque, B. (2014). Choices of abundance currency, community definition and diversity metric control the predictive power of macroecological models of biodiversity. *Glob. Ecol. Biogeogr.*, 23, 468–478

59.Chakroun, H., Mouillot, F., Nouri, M. & Nasr, Z. (2012). Integrating MODIS images in a water budget model for dynamic functioning and drought simulation of a Mediterranean forest in Tunisia. *Hydrol. Earth Syst. Sci. Discuss.*, 9, 6251–6284

60.Ciais, P., Reichstein, M., Viovy, N., Granier, A., Ogee, J., Allard, V., *et al.* (2005). Europe-wide reduction in primary productivity caused by the heat and drought in 2003. *Nature*, 437, 529–533

61.Condie, S. a., Johnson, P., Fulton, E. a. & Bulman, C.M. (2014). Relating food web structure to resilience, keystone status and uncertainty in ecological responses. *Ecosphere*, 5, art81

62.Connell, J.H. & Sousa, W.P. (1983). On the Evidence Needed to Judge Ecological Stability or Persistence. *Am. Nat.*, 121, 789–824

63.Craigne, J.M., Ocheltree, T.W., Nippert, J.B., Towne, E.G., Skibbe, A.M., Kembel, S.W., *et al.* (2012). Global diversity of drought tolerance and grassland climate-change resilience. *Nat. Clim. Chang.*, 3, 63–67

64.Crouzat, E., Mouchet, M., Turkelboom, F., Byczek, C., Meersmans, J., Berger, F., *et al.* (2015). Assessing bundles of ecosystem services from regional to landscape scale: insights from the French Alps. *J. Appl. Ecol.*, 52, 1145–1155

65.Cunill, R., Soriano, J.M., Bal, M.C., Pèlachs, A., Rodriguez, J.M. & Pérez-Obiol, R. (2013). Holocene high-altitude vegetation dynamics in the Pyrenees: A pedoanthracology contribution to an interdisciplinary approach. *Quat. Int.*, 289, 60–70

66.Curtin, C.G. & Parker, J.P. (2014). Foundations of resilience thinking. *Conserv. Biol.*, 28, 912–923

67.Dakos, V. (2008). Slowing down as an early warning signal for abrupt climate change.

References

Proc. Natl Acad. Sci. USA, 105, 14308–14312

68. Dakos, V., Carpenter, S.R., Brock, W.A., Ellison, A.M., Guttal, V., Ives, A.R., *et al.* (2012). Methods for detecting early warnings of critical transitions in time series illustrated using simulated ecological data. *PLoS One*, 7, e41010

69. Dakos, V., Carpenter, S.R., van Nes, E.H. & Scheffer, M. (2015). Resilience indicators: prospects and limitations for early warnings of regime shifts. *Philos. Trans. R. Soc. B Biol. Sci.*, 370, 20130263–20130263

70. Dakos, V., Kéfi, S., Rietkerk, M., van Nes, E.H. & Scheffer, M. (2011). Slowing down in spatially patterned ecosystems at the brink of collapse. *Am. Nat.*, 177, E153–E166

71. Dedieu, J.P., Carlson, B.Z., Bigot, S., Sirguey, P., Vionnet, V. & Choler, P. (2016). On the importance of high-resolution time series of optical imagery for quantifying the effects of snow cover duration on alpine plant habitat. *Remote Sens.*, 8

72. Dee, L.E., Allesina, S., Bonn, A., Eklöf, A., Gaines, S.D., Hines, J., *et al.* (2016). Operationalizing Network Theory for Ecosystem Service Assessments. *Trends Ecol. Evol.*, xx, 1–13

73. Delcourt, H.R. & Delcourt, P.A. (1988). Quaternary landscape ecology: Relevant scales in space and time. *Landsc. Ecol.*, 2, 23–44

74. Descroix, L. & Gautier, E. (2002). Water erosion in the southern French Alps: Climatic and human mechanisms. *Catena*, 50, 53–85

75. Diaz-Nieto, J. & Wilby, R.L. (2005). A comparison of statistical downscaling and climate change factor methods: impacts on low flows in the River Thames, United Kingdom. *Clim. Change*, 69, 245–268

76. Díaz, S., Fargione, J., Chapin, F.S. & Tilman, D. (2006). Biodiversity loss threatens human well-being. *PLoS Biol.*, 4, 1300–1305

77. Dirnböck, T., Dullinger, S. & Grabherr, G. (2003). A regional impact assessment of climate and land- use change on alpine vegetation. *J. Biogeogr.*, 30, 401–417

78. Doak, D.F., Bigger, D., Harding, E.K., Marvier, M.A., O'Malley, R.E. & Thomson, D. (1998). The statistical inevitability of stability-diversity relationships in community ecology. *Am. Nat.*, 151, 264–276

79. Dobbertin, M., Mayer, P., Wohlgemuth, T., Feldmeyer-Christe, E., Graf, U., Zimmermann, N.E., *et al.* (2005). The decline of *Pinus sylvestris* L. forests in the Swiss Rhone valley - A result of drought stress? *Phyt.*, 45, 153

80. Donohue, I., Petchey, O.L., Kéfi, S., Génin, A., Jackson, A.L., Yang, Q., *et al.* (2017). Loss of predator species, not intermediate consumers, triggers rapid and dramatic extinction cascades. *Glob. Chang. Biol.*

81. Donohue, I., Petchey, O.L., Montoya, J.M., Jackson, A.L., McNally, L., Viana, M., *et al.*

- (2013). On the dimensionality of ecological stability. *Ecol. Lett.*, 16, 421–429
82. Dray, S. & Dufour, A.-B. (2007). The ade4 package: implementing the duality diagram for ecologists. *J. Stat. Softw.*, 22, 1–20
83. Dullinger, S., Gatttringer, A., Thuiller, W., Moser, D., Zimmermann, N.E., Guisan, A., *et al.* (2012). Extinction debt of high-mountain plants under twenty-first-century climate change. *Nat. Clim. Chang.*, 2, 619–622
84. Dunne, J.A., Williams, R.J. & Martinez, N.D. (2002). Network structure and biodiversity loss in food webs: Robustness increases with connectance. *Ecol. Lett.*, 5, 558–567
85. Dupire, S., Curt, T. & Bigot, S. (2017). Spatio-temporal trends in fire weather in the French Alps. *Sci. Total Environ.*, 595, 801–817
86. EC. (2015). *European Commission - Environment: Biodiversity strategy*. Available at: http://ec.europa.eu/environment/nature/biodiversity/strategy/index_en.htm. Last accessed 1 August 2015
87. Egerton, F.N. (2007). Understanding Food Chains and Food Webs, 1700–1970. *Bull. Ecol. Soc. Am.*, 88, 50–69
88. Elkin, C., Gutiérrez, A.G., Leuzinger, S., Manusch, C., Temperli, C., Rasche, L., *et al.* (2013). A 2 °C warmer world is not safe for ecosystem services in the European Alps. *Glob. Chang. Biol.*, 19, 1827–1840
89. Elmqvist, T., Folke, C., Nystrom, M., Peterson, G., Bengtsson, J., Walker, B., *et al.* (2003). Response diversity, ecosystem change, and resilience. *Front. Ecol. Environ.*, 1, 488–494
90. ESRI. (2011). ArcGIS Desktop: Release 10
91. Esterni, M., Rovera, G., Bonet, R., Salomez, P., Cortot, H. & Guilloux, J. (2006). *DELPHINE - Découpage de l'Espace en Liaison avec les Potentialités Humaines et en Interrelation avec la Nature*
92. Evans, D.M., Pockock, M.J.O. & Memmott, J. (2013). The robustness of a network of ecological networks to habitat loss. *Ecol. Lett.*, 16, 844–852
93. Flynn, D.F.B., Gogol-Prokurat, M., Nogeire, T., Molinari, N., Richers, B.T.B.T., Lin, B.B., *et al.* (2009). Loss of functional diversity under land use intensification across multiple taxa. *Ecol. Lett.*, 12, 22–33
94. Folke, C., Carpenter, S., Walker, B., Scheffer, M., Elmqvist, T., Gunderson, L., *et al.* (2004). Regime shifts, resilience, and biodiversity in ecosystem management. *Annu. Rev. Ecol. Evol. Syst.*, 35, 557–581
95. Frank, D., Reichstein, M., Bahn, M., Thonicke, K., Frank, D., Mahecha, M.D., *et al.* (2015). Effects of climate extremes on the terrestrial carbon cycle: Concepts, processes and potential future impacts. *Glob. Chang. Biol.*, 21, 2861–2880

References

96. Fraser, L.H., Harrower, W.L., Garris, H.W., Davidson, S., Hebert, P.D.N., Howie, R., *et al.* (2015). A call for applying trophic structure in ecological restoration. *Restor. Ecol.*, 23, 503–507
97. Gamfeldt, L., Hillebrand, H. & Jonsson, P.R. (2008). Multiple functions increase the importance of biodiversity for overall ecosystem functioning. *Ecology*, 89, 1223–1231
98. Gardner, M.R. & Ashby, W.R. (1970). Connectance of large dynamic (cybernetic) systems: critical values for stability. *Nature*
99. Garnier, E., Cortez, J., Billès, G., Navas, M.L., Roumet, C., Debussche, M., *et al.* (2004). Plant functional markers capture ecosystem properties during secondary succession. *Ecology*, 85, 2630–2637
100. Gehrig-Fasel, J., Guisan, A. & Zimmermann, N.E. (2007). Tree line shifts in the Swiss Alps: Climate change or land abandonment? *J. Veg. Sci.*, 18, 571
101. Gerhold, P., Cahill, J.F., Winter, M., Bartish, I. V. & Prinzing, A. (2015). Phylogenetic patterns are not proxies of community assembly mechanisms (they are far better). *Funct. Ecol.*, 29, 600–614
102. Giguet-Covex, C., Pansu, J., Arnaud, F., Rey, P.-J., Griggo, C., Gielly, L., *et al.* (2014). Long livestock farming history and human landscape shaping revealed by lake sediment DNA. *Nat. Commun.*, 5, 1951–1965
103. Gilbert, A.J. (2009). Connectance indicates the robustness of food webs when subjected to species loss. *Ecol. Indic.*, 9, 72–80
104. Gobiet, A., Kotlarski, S., Beniston, M., Heinrich, G., Rajczak, J. & Stoffel, M. (2014). 21st century climate change in the European Alps-A review. *Sci. Total Environ.*, 493, 1138–1151
105. Goldblum, D. & Rigg, L.S. (2010). The deciduous forest–boreal forest ecotone. *Geogr. Compass*, 4, 701–717
106. Gómez-Aparicio, L., Gómez, J.M., Zamora, R., Boettinger, J.L. & Ezcurra, E. (2005). Canopy vs. soil effects of shrubs facilitating tree seedlings in Mediterranean montane ecosystems. *J. Veg. Sci.*, 16, 191–198
107. Gottfried, M., Pauli, H., Futschik, A., Akhalkatsi, M., Barančok, P., Alonso, B., *et al.* (2012). Continent-wide response of mountain vegetation to climate change. *Nat. Clim. Chang.*, 2, 111–115
108. Grassein, F., Lavorel, S. & Till-Bottraud, I. (2014). The importance of biotic interactions and local adaptation for plant response to environmental changes: field evidence along an elevational gradient. *Glob. Chang. Biol.*, 20, 1452–1460
109. Grêt-Regamey, A., Walz, A. & Bebi, P. (2008). Valuing Ecosystem Services for Sustainable Landscape Planning in Alpine Regions. *Mt. Res. Dev.*, 28, 156–165

110. Gross, K., Cardinale, B.J., Fox, J.W., Gonzalez, A., Loreau, M., Wayne Polley, H., *et al.* (2014). Species Richness and the Temporal Stability of Biomass Production: A New Analysis of Recent Biodiversity Experiments. *Am. Nat.*, 183, 1–12
111. Gu, Y., Brown, J.F., Verdin, J.P. & Wardlow, B. (2007). A five- year analysis of MODIS NDVI and NDWI for grassland drought assessment over the central Great Plains of the United States. *Geophys. Res. Lett.*, 34, 1–6
112. Gunderson, L.H. (2000). Ecological resilience - in theory and application. *Annu. Rev. Ecol. Syst.*, 35, 425–439
113. Gustafson, E.J., Lietz, S.M. & Wright, J.L. (2003). Predicting the spatial distribution of aspen growth potential in the upper Great Lakes region. *For. Sci.*, 49, 499–508
114. Hartmann, H., Ziegler, W., Kolle, O. & Trumbore, S. (2013). Thirst beats hunger - declining hydration during drought prevents carbon starvation in Norway spruce saplings. *New Phytol.*, 200, 340–349
115. Hastings, A. & Wysham, D.B. (2010). Regime shifts in ecological systems can occur with no warning. *Ecol. Lett.*, 13, 464–472
116. Hautier, Y., Tilman, D., Isbell, F., Seabloom, E.W., Borer, E.T. & Reich, P.B. (2015). Anthropogenic environmental changes affect ecosystem stability via biodiversity. *Science*, 348, 336–340
117. Hector, A. & Bagchi, R. (2007). Biodiversity and ecosystem multifunctionality. *Nature*, 448, 188–190
118. Heiser, M., Dapporto, L. & Schmitt, T. (2014). Coupling impoverishment analysis and partitioning of beta diversity allows a comprehensive description of Odonata biogeography in the Western Mediterranean. *Org. Divers. Evol.*, 14, 203–214
119. Hill, M.O. & Smith, A.J.E. (1976). Principal Component Analysis of Taxonomic Data with Multi-State Discrete Characters. *Taxon*, 25, 249
120. HilleRisLambers, J., Harsch, M.A., Ettinger, A.K., Ford, K.R. & Theobald, E.J. (2013). How will biotic interactions influence climate change-induced range shifts? *Ann. N. Y. Acad. Sci.*, 1297, n/a-n/a
121. Hirsch, M.W., Smale, S. & Devaney, R.L. (2012). *Differential equations, dynamical systems, and an introduction to chaos*. Academic press
122. Hodgson, D., McDonald, J.L. & Hosken, D.J. (2015). What do you mean, “resilient”? *Trends Ecol. Evol.*, 30, 503–506
123. Holling, C.S. (1973). Resilience and stability of ecological systems. *Annu. Rev. Ecol. Syst.*, 4, 1–23
124. Holling, C.S. (1996). Engineering resilience vs. ecological resilience. In: *Engineering*

References

within ecological constraints (ed. Schulze, P.C.). National Academy Press, Washington, D.C., pp. 31–43

125. Hooper, D.U., Chapin, F.S., Ewel, J.J., Hector, A., Inchausti, P., Lavorel, S., *et al.* (2005). Effects of biodiversity on ecosystem functioning: a consensus of current knowledge. *Ecol. Monogr.*, 75, 3–35

126. Horan, R.D., Fenichel, E.P., Drury, K.L.S. & Lodge, D.M. (2011). Managing ecological thresholds in coupled environmental-human systems. *Proc. Natl. Acad. Sci. U. S. A.*, 108, 7333–8

127. Hughes, T.P., Carpenter, S., Rockström, J., Scheffer, M. & Walker, B. (2013). Multiscale regime shifts and planetary boundaries. *Trends Ecol. Evol.*, 28, 389–395

128. IPCC. (2012). *Managing the Risks of Extreme Events and Disasters to Advance Climate Change Adaptation - SREX Summary for Policymakers. A Spec. Rep. Work. Groups I II Intergov. Panel Clim. Chang.*

129. IPCC. (2013). *Climate Change 2013: The Physical Science Basis. Contribution of Working Group I to the Fifth Assessment Report of the Intergovernmental Panel on Climate Change. Fifth Assess. Rep.* Cambridge, United Kingdom and New York, NY, USA

130. Isbell, F., Craven, D., Connolly, J., Loreau, M., Schmid, B., Beierkuhnlein, C., *et al.* (2015). Biodiversity increases the resistance of ecosystem productivity to climate extremes. *Nature*, 526, 574–577

131. Isbell, F.I., Polley, H.W. & Wilsey, B.J. (2009). Biodiversity, productivity and the temporal stability of productivity: Patterns and processes. *Ecol. Lett.*, 12, 443–451

132. Ives, A.R. (1995). Measuring resilience in stochastic systems. *Ecol. Monogr.*, 65, 217–233

133. Ivits, E., Horion, S., Erhard, M., Fensholt, R. & Penuelas, J. (2016). Assessing European ecosystem stability to drought in the vegetation growing season. *Glob. Ecol. Biogeogr.*, 25, 1131–1143

134. Jouget, J.-P. (1999). *Les végétations des alpages des Alpes françaises du Sud: guide technique pour la reconnaissance et la gestion des milieux pâturés d'altitude.* Editions Quae

135. Jousset, A., Schmid, B., Scheu, S. & Eisenhauer, N. (2011). Genotypic richness and dissimilarity opposingly affect ecosystem functioning. *Ecol. Lett.*, 14, 537–545

136. Jung, V., Albert, C.H., Violle, C., Kunstler, G., Loucougaray, G. & Spiegelberger, T. (2014). Intraspecific trait variability mediates the response of subalpine grassland communities to extreme drought events. *J. Ecol.*, 102, 45–53

137. Kaiser-Bunbury, C.N., Muff, S., Memmott, J., Müller, C.B. & Caflisch, A. (2010). The robustness of pollination networks to the loss of species and interactions: A quantitative approach incorporating pollinator behaviour. *Ecol. Lett.*, 13, 442–452

- 138.Kane, J.M., Meinhardt, K.A., Chang, T., Cardall, B.L., Michalet, R. & Whitham, T.G. (2011). Drought-induced mortality of a foundation species (*Juniperus monosperma*) promotes positive afterlife effects in understory vegetation. *Plant Ecol.*, 212, 733–741
- 139.Kattge, J., Díaz, S., Lavorel, S., Prentice, I.C., Leadley, P., Bönsch, G., *et al.* (2011). TRY - a global database of plant traits. *Glob. Chang. Biol.*, 17, 2905–2935
- 140.Keersmaecker, W., Lhermitte, S., Honnay, O., Farifteh, J., Somers, B. & Coppin, P. (2014). How to measure ecosystem stability? An evaluation of the reliability of stability metrics based on remote sensing time series across the major global ecosystems. *Glob. Chang. Biol.*, 20, 2149–2161
- 141.Kéfi, S., Berlow, E.L., Wieters, E.A., Joppa, L.N., Wood, S.A., Brose, U., *et al.* (2015). Network structure beyond food webs: mapping non- trophic and trophic interactions on Chilean rocky shores. *Ecology*, 96, 291–303
- 142.Kéfi, S., Dakos, V., Scheffer, M., Van Nes, E.H. & Rietkerk, M. (2013). Early warning signals also precede non-catastrophic transitions. *Oikos*, 122, 641–648
- 143.Kéfi, S., Rietkerk, M., van Baalen, M. & Loreau, M. (2007). Local facilitation, bistability and transitions in arid ecosystems. *Theor. Popul. Biol.*, 71, 367–379
- 144.Kennedy, T. a, Naeem, S., Howe, K.M., Knops, J.M.H., Tilman, D. & Reich, P. (2002). Biodiversity as a barrier to ecological invasion. *Nature*, 417, 636–638
- 145.Kerkhoff, A.J. & Enquist, B.J. (2007). The implications of scaling approaches for understanding resilience and reorganization in ecosystems. *Bioscience*, 57, 489–499
- 146.Kortsch, S., Primicerio, R., Fossheim, M., Dolgov, A. V. & Aschan, M. (2015). Climate change alters the structure of arctic marine food webs due to poleward shifts of boreal generalists. *Proc. R. Soc. B Biol. Sci.*, 282, 20151546
- 147.Krinner, G., Viovy, N., de Noblet-Ducoudré, N., Ogée, J., Polcher, J., Friedlingstein, P., *et al.* (2005). A dynamic global vegetation model for studies of the coupled atmosphere-biosphere system. *Global Biogeochem. Cycles*, 19, 1–33
- 148.Kulakowski, D., Bebi, P. & Rixen, C. (2011). The interacting effects of land use change, climate change and suppression of natural disturbances on landscape forest structure in the Swiss Alps. *Oikos*, 120, 216–225
- 149.Laliberté, E. & Legendre, P. (2010). A distance-based framework for measuring functional diversity from multiple traits. *Ecology*, 91, 299–305
- 150.Lavorel, S. & Garnier, E. (2002). Predicting changes in community composition and ecosystem functioning from plant traits: revisiting the Holy Grail. *Funct. Ecol.*, 16, 545–556
- 151.Lavorel, S. & Grigulis, K. (2012). How fundamental plant functional trait relationships scale-up to trade-offs and synergies in ecosystem services. *J. Ecol.*, 100, 128–140
- 152.Lavorel, S., Grigulis, K., Lamarque, P.P., Colace, M.P., Garden, D., Girel, J., *et al.*

References

- (2011). Using plant functional traits to understand the landscape distribution of multiple ecosystem services. *J. Ecol.*, 99, 135–147
153. Leinster, T. & Cobbold, C.A. (2012). Measuring diversity: the importance of species similarity. *Ecology*, 93, 477–489
154. Lenoir, J., Gégout, J., Guisan, A., Vittoz, P., Wohlgemuth, T., Zimmermann, N.E., *et al.* (2010a). Going against the flow: potential mechanisms for unexpected downslope range shifts in a warming climate. *Ecography*, 33, 295–303
155. Lenoir, J., Gégout, J.C., Dupouey, J.L., Bert, D. & Svenning, J.C. (2010b). Forest plant community changes during 1989–2007 in response to climate warming in the Jura Mountains (France and Switzerland). *J. Veg. Sci.*, 21, 949–964
156. Lenoir, J. & Svenning, J.-C. (2015). Climate-related range shifts - a global multidimensional synthesis and new research directions. *Ecography*, 38, 15–28
157. Lepš, J., de Bello, F., Šmilauer, P. & Doležal, J. (2011). Community trait response to environment: disentangling species turnover vs intraspecific trait variability effects. *Ecography*, 34, 856–863
158. Leroux, S.J. & Loreau, M. (2015). Theoretical perspectives on bottom-up and top-down interactions across ecosystems. *Trophic Ecol.*, 3–28
159. Levine, J.M. (2000). Species diversity and biological invasions: relating local process to community pattern. *Science*, 288, 852–854
160. Lewontin, R.C. (1969). The meaning of stability. *Brookhaven Symp. Biol.*, 22, 13–24
161. Lischke, H., Zimmermann, N.E., Bolliger, J., Rickebusch, S. & Löffler, T.J. (2006). TreeMig: a forest-landscape model for simulating spatio-temporal patterns from stand to landscape scale. *Ecol. Modell.*, 199, 409–420
162. Liu, D., Ogaya, R., Barbeta, A., Yang, X. & Peñuelas, J. (2015). Contrasting impacts of continuous moderate drought and episodic severe droughts on the aboveground-biomass increment and litterfall of three coexisting Mediterranean woody species. *Glob. Chang. Biol.*, 21, 4196–4209
163. Lloyd, A.H. & Fastie, C.L. (2002). Spatial and temporal variability in the growth and climate response of treeline trees in Alaska. *Clim. Change*, 52, 481–509
164. Loreau, M. (2001). Biodiversity and Ecosystem Functioning: Current Knowledge and Future Challenges. *Science*, 294, 804–808
165. Loreau, M. & de Mazancourt, C. (2013). Biodiversity and ecosystem stability: A synthesis of underlying mechanisms. *Ecol. Lett.*, 16, 106–115
166. MacArthur, R. (1955). Fluctuations of Animal Populations and a Measure of Community Stability. *Ecology*, 36, 533–536

167. MacDonald, D., Crabtree, J. R., Wiesinger, G., Dax, T., Stamou, N., Fleury, P., *et al.* (2000). Agricultural abandonment in mountain areas of Europe: environmental consequences and policy response. *J. Environ. Manage.*, 59, 47–69
168. MacDonald, R.L., Chen, H.Y.H., Bartels, S.F., Palik, B.J. & Prepas, E.E. (2015). Compositional stability of boreal understorey vegetation after overstorey harvesting across a riparian ecotone. *J. Veg. Sci.*, 26, 733–741
169. MacDougall, A.S., McCann, K.S., Gellner, G. & Turkington, R. (2013). Diversity loss with persistent human disturbance increases vulnerability to ecosystem collapse. *Nature*, 494, 86–9
170. Maiorano, L., Amori, G., Capula, M., Falcucci, A., Masi, M., Montemaggiore, A., *et al.* (2013). Threats from Climate Change to Terrestrial Vertebrate Hotspots in Europe. *PLoS One*, 8, e74989
171. Maire, E., Grenouillet, G., Brosse, S. & Villiger, S. (2015). How many dimensions are needed to accurately assess functional diversity? A pragmatic approach for assessing the quality of functional spaces. *Glob. Ecol. Biogeogr.*, 24, 728–740
172. Marston, R.A., Bravard, J.P. & Green, T. (2003). Impacts of reforestation and gravel mining on the Malnant River, Haute-Savoie, French Alps. *Geomorphology*, 55, 65–74
173. Maurer, K., Weyand, A., Fischer, M. & Stöcklin, J. (2006). Old cultural traditions, in addition to land use and topography, are shaping plant diversity of grasslands in the Alps. *Biol. Conserv.*, 130, 438–446
174. Mayfield, M.M., Bonser, S.P., Morgan, J.W., Aubin, I., McNamara, S. & Vesik, P.A. (2010). What does species richness tell us about functional trait diversity? Predictions and evidence for responses of species and functional trait diversity to land-use change. *Glob. Ecol. Biogeogr.*, 19, 423–431
175. de Mazancourt, C., Isbell, F., Larocque, A., Berendse, F., De Luca, E., Grace, J.B., *et al.* (2013). Predicting ecosystem stability from community composition and biodiversity. *Ecol. Lett.*, 16, 617–625
176. McDowell, N., Pockman, W.T., Allen, C.D., Breshears, D.D., Cobb, N., Kolb, T., *et al.* (2008). Mechanisms of plant survival and mortality during drought: why do some plants survive while others succumb to drought? *New Phytol.*, 178, 719–739
177. Mchich, R., Auger, P. & Poggiale, J.C. (2007). Effect of predator density dependent dispersal of prey on stability of a predator-prey system. *Math. Biosci.*, 206, 343–356
178. McNaughton, S.J. (1977). Diversity and Stability of Ecological Communities: A Comment on the Role of Empiricism in Ecology. *Am. Nat.*, 111, 515–525
179. Memmott, J., Waser, N.M. & Price, M. V. (2004). Tolerance of pollination networks to species extinctions. *Proc. R. Soc. London. Ser. B Biol. Sci.*, 271, 2605–2611
180. Mod, H.K., le Roux, P.C., Guisan, A. & Luoto, M. (2015). Biotic interactions boost

References

spatial models of species richness. *Ecography*, 38, 913–921

181.Mori, A.S. (2016). Resilience in the Studies of Biodiversity-Ecosystem Functioning. *Trends Ecol. Evol.*, 31, 87–89

182.Mori, A.S., Furukawa, T. & Sasaki, T. (2013). Response diversity determines the resilience of ecosystems to environmental change. *Biol. Rev.*, 88, 349–364

183.Morin, X., Fahse, L., de Mazancourt, C., Scherer-Lorenzen, M. & Bugmann, H. (2014). Temporal stability in forest productivity increases with tree diversity due to asynchrony in species dynamics. *Ecol. Lett.*, 17, 1526–1535

184.Morin, X., Fahse, L., Scherer-Lorenzen, M. & Bugmann, H. (2011). Tree species richness promotes productivity in temperate forests through strong complementarity between species. *Ecol. Lett.*, 14, 1211–1219

185.Motta, R. & Nola, P. (2001). Growth trends and dynamics in sub-alpine forest stands in the Varaita Valley (Piedmont, Italy) and their relationships with human activities and global change. *J. Veg. Sci.*, 12, 219–230

186.Mouchet, M.A., Villéger, S., Mason, N.W.H. & Mouillot, D. (2010). Functional diversity measures: An overview of their redundancy and their ability to discriminate community assembly rules. *Funct. Ecol.*, 24, 867–876

187.Mouillot, D., Bellwood, D.R., Baraloto, C., Chave, J., Galzin, R., Harmelin-Vivien, M., *et al.* (2013). Rare Species Support Vulnerable Functions in High-Diversity Ecosystems. *PLoS Biol.*, 11

188.Murphy, G.E.P. & Romanuk, T.N. (2014). A meta-analysis of declines in local species richness from human disturbances. *Ecol. Evol.*, 4, 91–103

189.Nagendra, H., Reyers, B. & Lavorel, S. (2013). Impacts of land change on biodiversity: making the link to ecosystem services. *Curr. Opin. Environ. Sustain.*, 5, 503–508

190.Nakicenovic, N., Alcamo, J., Davis, G., Vries, B. de, Fenhann, J., Gaffin, S., *et al.* (2000). *Special report on emissions scenarios*

191.Namba, T. (2015). Multi-faceted approaches toward unravelling complex ecological networks. *Popul. Ecol.*, 57, 3–19

192.Nandintsetseg, B. & Shinoda, M. (2013). Assessment of drought frequency, duration, and severity and its impact on pasture production in Mongolia. *Nat. hazards*, 66, 995–1008

193.Nardini, A., Battistuzzo, M. & Savi, T. (2013). Shoot desiccation and hydraulic failure in temperate woody angiosperms during an extreme summer drought. *New Phytol.*, 200, 322–329

194.NCAR community. (2004). Community Climate System Model, version 3.0.

195.van Nes, E.H. & Scheffer, M. (2007). Slow recovery from perturbations as a generic

indicator of a nearby catastrophic shift. *Am. Nat.*, 169, 738–747

196. Neubert, M.G. & Caswell, H. (1997). Alternatives to resilience for measuring the responses of ecological systems to perturbations. *Ecology*, 78, 653–665

197. Norberg, J. (2004). Biodiversity and ecosystem functioning: a complex adaptive systems approach. *Limnol. Oceanogr.*, 49, 1177–1269

198. Oliver, T.H., Isaac, N.J.B., August, T.A., Woodcock, B.A., Roy, D.B. & Bullock, J.M. (2015). Declining resilience of ecosystem functions under biodiversity loss. *Nat. Commun.*, 6, 10122

199. Palombo, C., Chirici, G., Marchetti, M. & Tognetti, R. (2013). Is land abandonment affecting forest dynamics at high elevation in Mediterranean mountains more than climate change? *Plant Biosyst. - An Int. J. Deal. with all Asp. Plant Biol.*, 147, 1–11

200. Parc National des Ecrins. (2015). *La charte en actions: programme 2014-2016*. Available at: <http://www.ecrins-parcnational.fr/document/la-charte-en-actions-programme-2014-2016-0>. Last accessed

201. Park Williams, A., Allen, C.D., Macalady, A.K., Griffin, D., Woodhouse, C.A., Meko, D.M., *et al.* (2012). Temperature as a potent driver of regional forest drought stress and tree mortality. *Nat. Clim. Chang.*, 3, 292–297

202. Pascual, M. & Dunne, J.A. (2006). From small to large ecological networks in a dynamic world. In: *Ecological networks: linking structure to dynamics in food webs* (eds. Pascual, M. & Dunne, J.A.). Oxford University Press, New York, pp. 3–24

203. Pauli, H., Gottfried, M., Dullinger, S., Abdaladze, O., Akhalkatsi, M., Alonso, J.L.B., *et al.* (2012). Recent Plant Diversity Changes on Europe's Mountain Summits. *Science*, 336, 353–355

204. Pauli, H., Gottfried, M., Reiter, K., Klettner, C. & Grabherr, G. (2007). Signals of range expansions and contractions of vascular plants in the high Alps: observations (1994–2004) at the GLORIA* master site Schrankogel, Tyrol, Austria. *Glob. Chang. Biol.*, 13, 147–156

205. Pavoine, S. & Bonsall, M.B. (2009). Biological diversity: Distinct distributions can lead to the maximization of Rao's quadratic entropy. *Theor. Popul. Biol.*, 75, 153–163

206. Pavoine, S. & Bonsall, M.B. (2011). Measuring biodiversity to explain community assembly: A unified approach. *Biol. Rev.*, 86, 792–812

207. Pierce, W.D., Cushman, R.A. & Hood, C.E. (1912). The insect enemies of the cotton boll weevil. *U.S. Dept. Agric. Bur. Entomol. Bull.*, 100, 1–99

208. Pillar, V.D., Blanco, C.C., Müller, S.C., Sosinski, E.E., Joner, F. & Duarte, L.D.S. (2013). Functional redundancy and stability in plant communities. *J. Veg. Sci.*, 24, 963–974

209. Pimm, S.L. (1984). The complexity and stability of ecosystems. *Nature*, 307, 321–326

References

- 210.Pimm, S.L. (1991). *The balance of nature? : ecological issues in the conservation of species and communities*. University of Chicago Press
- 211.Polley, H.W., Isbell, F.I. & Wilsey, B.J. (2013). Plant functional traits improve diversity-based predictions of temporal stability of grassland productivity. *Oikos*, 122, 1275–1282
- 212.Polley, H.W., Wilsey, B.J. & Derner, J.D. (2007). Dominant species constrain effects of species diversity on temporal variability in biomass production of tallgrass prairie. *Oikos*, 116, 2044–2052
- 213.R Core Team. (2016). R: A language and environment for statistical computing
- 214.Ratajczak, Z., Nippert, J.B. & Collins, S.L. (2012). Woody encroachment decreases diversity across North American grasslands and savannas. *Ecology*, 93, 697–703
- 215.Rebetez, M. & Dobbertin, M. (2004). Climate change may already threaten Scots pine stands in the Swiss Alps. *Theor. Appl. Climatol.*, 79, 1–9
- 216.Reichstein, M., Bahn, M., Ciais, P., Frank, D.C.D., Mahecha, M.D., Seneviratne, S.I., *et al.* (2013). Climate extremes and the carbon cycle. *Nature*, 500, 287–295
- 217.Reiss, J., Bridle, J.R., Montoya, J.M. & Woodward, G. (2009). Emerging horizons in biodiversity and ecosystem functioning research. *Trends Ecol. Evol.*, 24, 505–514
- 218.Rigling, A., Bigler, C., Eilmann, B., Feldmeyer-Christe, E., Gimmi, U., Ginzler, C., *et al.* (2013). Driving factors of a vegetation shift from Scots pine to pubescent oak in dry Alpine forests. *Glob. Chang. Biol.*, 19, 229–240
- 219.Rockström, J., Steffen, W., Noone, K., Persson, Å., Chapin, F.S., Lambin, E.F., *et al.* (2009). Planetary Boundaries: Exploring the Safe Operating Space for Humanity Johan. *Ecol. Soc.*, 14, [online]
- 220.Roscher, C., Schumacher, J., Gubsch, M., Lipowsky, A., Weigelt, A., Buchmann, N., *et al.* (2012). Using plant functional traits to explain diversity-productivity relationships. *PLoS One*, 7
- 221.Roscher, C., Weigelt, A., Proulx, R., Marquard, E., Schumacher, J., Weisser, W.W., *et al.* (2011). Identifying population- and community-level mechanisms of diversity-stability relationships in experimental grasslands. *J. Ecol.*, 99, 1460–1469
- 222.Saint-Béat, B., Baird, D., Asmus, H., Asmus, R., Bacher, C., Pacella, S.R., *et al.* (2015). Trophic networks: How do theories link ecosystem structure and functioning to stability properties? A review. *Ecol. Indic.*, 52, 458–471
- 223.Sala, O.E., Stuart Chapin, F., III, Armesto, J.J., Berlow, E., Bloomfield, J., *et al.* (2000). Global Biodiversity Scenarios for the Year 2100. *Science*, 287, 1770–1774
- 224.Samuelsson, P., Jones, C.G., Willén, U., Ullerstig, A., Gollvik, S., Hansson, U., *et al.* (2011). The Rossby Centre Regional Climate model RCA3: model description and performance. *Tellus A*, 63, 4–23

- 225.Santini, L., Cornulier, T., Bullock, J.M., Palmer, S.C.F., White, S.M., Hodgson, J.A., *et al.* (2016). A trait-based approach for predicting species responses to environmental change from sparse data: How well might terrestrial mammals track climate change? *Glob. Chang. Biol.*, 22, 2415–2424
- 226.Sanz-Elorza, M., Dana, E.D.E.D., Gonzalez, A., Sobrino, E., González, A. & Sobrino, E. (2003). Changes in the high- mountain vegetation of the central Iberian Peninsula as a probable sign of global warming. *Ann. Bot.*, 92, 273–280
- 227.Sarmiento, F.O. & Frolich, L.M. (2002). Andean Cloud Forest Tree Lines. *Mt. Res. Dev.*, 22, 278–287
- 228.Scheffer, M., Bascompte, J., Brock, W.A., Brovkin, V., Carpenter, S.R., Dakos, V., *et al.* (2009). Early-warning signals for critical transitions. *Nature*, 461, 53–59
- 229.Scheffer, M. & Carpenter, S. (2003). Catastrophic regime shifts in ecosystems: linking theory to observation. *Trends Ecol. Evol.*, 18, 648–656
- 230.Scheffer, M., Carpenter, S., Foley, J.A., Folke, C. & Walker, B. (2001). Catastrophics shifts in ecosystems. *Nature*, 413, 591–596
- 231.Schleuning, M., Fründ, J., Schweiger, O., Welk, E., Albrecht, J., Albrecht, M., *et al.* (2016). Ecological networks are more sensitive to plant than to animal extinction under climate change. *Nat. Commun.*, 7, 13965
- 232.Seidl, R., Fernandes, P.M., Fonseca, T.F., Gillet, F., Jönsson, A.M., Merganičová, K., *et al.* (2011). Modelling natural disturbances in forest ecosystems: a review. *Ecol. Modell.*, 222, 903–924
- 233.Serreze, M.C., Walsh, J.E., Chapin, F.S.I., Osterkamp, T., Dyurgerov, M., Romanovsky, V., *et al.* (2000). Observational evidence of recent change in the northern high- latitude environment. *Clim. Change*, 46, 159–207
- 234.Sharma, Y., Abbott, K.C., Dutta, P.S. & Gupta, A.K. (2014). Stochasticity and bistability in insect outbreak dynamics. *Theor. Ecol.*, 8, 163–174
- 235.Shea, K. & Chesson, P. (2002). Community ecology theory as a framework for biological invasions. *Trens Ecol. Evol.*, 17, 170–176.
- 236.Spasojevic, M., Bowman, W.D., Humphries, H.C., Seastedt, T. & Suding, K.N. (2013). Changes in alpine vegetation over 21 years: Are patterns across a heterogeneous landscape consistent with predictions? *Ecosphere*, 4, 117
- 237.Spinoni, J., Naumann, G., Carrao, H., Barbosa, P. & Vogt, J. (2014). World drought frequency, duration, and severity for 1951–2010. *Int. J. Climatol.*, 34, 2792–2804
- 238.Standish, R.J., Hobbs, R.J., Mayfield, M.M., Bestelmeyer, B.T., Suding, K.N., Battaglia, L.L., *et al.* (2014). Resilience in ecology: Abstraction, distraction, or where the action is? *Biol. Conserv.*, 177, 43–51

References

239. Steenbeek, J., Buszowski, J., Christensen, V., Akoglu, E., Aydin, K., Ellis, N., *et al.* (2016). Ecopath with Ecosim as a model-building toolbox: Source code capabilities, extensions, and variations. *Ecol. Modell.*, 319, 178–189
240. Steffen, W., Richardson, K., Rockstrom, J., Cornell, S.E., Fetzer, I., Bennett, E.M., *et al.* (2015). Planetary boundaries: Guiding human development on a changing planet. *Science*, 347, 1259855–1259855
241. Steudel, B., Hector, A., Friedl, T., Löffke, C., Lorenz, M., Wesche, M., *et al.* (2012). Biodiversity effects on ecosystem functioning change along environmental stress gradients. *Ecol. Lett.*, 15, 1397–1405
242. Stürck, J., Levers, C., van der Zanden, E.H., Schulp, C.J.E., Verkerk, P.J., Kuemmerle, T., *et al.* (2015). Simulating and delineating future land change trajectories across Europe. *Reg. Environ. Chang.*, 1–17
243. Sundstrom, S.M., Allen, C.R. & Barichievy, C. (2012). Species, Functional Groups, and Thresholds in Ecological Resilience. *Conserv. Biol.*, 26, 305–314
244. Sutherland, G.D., Harestad, A.S., Price, K. & Lertzman, K.P. (2000). Scaling of Natal Dispersal Distances in Terrestrial Birds and Mammals. *Conserv. Ecol.*, 4, 16
245. Taberlet, P., Coissac, E., Hajibabaei, M. & Rieseberg, L.H. (2012). Environmental DNA. *Mol. Ecol.*, 21, 1789–1793
246. Tappeiner, U. & Bayfield, N. (2009). Management of mountaineous areas. In: *Land Use, Land Cover and Soil Sciences* (ed. Verheye, W.H.). Eolss Publishers/UNESCO, Oxford, UK
247. Tasser, E., Leitinger, G. & Tappeiner, U. (2017). Land Use Policy Climate change versus land-use change — What affects the mountain landscapes more ? *Land use policy*, 60, 60–72
248. Tasser, E. & Tappeiner, U. (2002). Impact of land use changes on mountain vegetation. *Appl. Veg. Sci.*, 5, 173–184
249. Tasser, E., Walde, J., Tappeiner, U., Teutsch, A. & Noggler, W. (2007). Land-use changes and natural reforestation in the Eastern Central Alps. *Agric. Ecosyst. Environ.*, 118, 115–129
250. Thebault, E. & Fontaine, C. (2010). Stability of Ecological Communities and the Architecture of Mutualistic and Trophic Networks. *Science*, 329, 853–856
251. Theurillat, J.J.-P.J.-P. & Guisan, A. (2001). Potential impact of climate change on vegetation in the European Alps: a review. *Clim. Change*, 50, 77–109
252. Thibaut, L.M., Connolly, S.R. & Sweatman, H.P.A. (2011). Diversity and stability of herbivorous fishes on coral reefs. *Ecology*, 93, 891–901
253. Thompson, R.M., Brose, U., Dunne, J.A., Hall, R.O., Hladysz, S., Kitching, R.L., *et al.* (2012). Food webs: Reconciling the structure and function of biodiversity. *Trends Ecol. Evol.*,

27, 689–697

254. Thornthwaite, C.W. (1948). An approach toward a rational classification of climate. *Geogr. Rev.*, 38, 55–94

255. Thuiller, W., Guéguen, M., Georges, D., Bonet, R., Chalmandrier, L., Garraud, L., *et al.* (2014). Are different facets of plant diversity well protected against climate and land cover changes? A test study in the French Alps. *Ecography*, 37, 1254–1266

256. Thuiller, W., Lafourcade, B., Engler, R. & Araujo, M.B. (2009). BIOMOD - a platform for ensemble forecasting of species distributions. *Ecography*, 32, 369–373

257. Tilman, D. & Downing, J. a. (1994). Biodiversity and stability in grasslands. *Nature*, 367, 363–365

258. Tilman, D., Reich, P.B. & Isbell, F. (2012). Biodiversity impacts ecosystem productivity as much as resources, disturbance, or herbivory. *Proc. Natl. Acad. Sci.*, 109, 10394–10397

259. Tilman, D., Reich, P.B. & Knops, J.M.H. (2006). Biodiversity and ecosystem stability in a decade-long grassland experiment. *Nature*, 441, 629–632

260. Tucker, C.M., Cadotte, M.W., Carvalho, S.B., Davies, T.J., Ferrier, S., Fritz, S.A., *et al.* (2016). A guide to phylogenetic metrics for conservation, community ecology and macroecology. *Biol. Rev.*

261. Tuomisto, H. (2010). A diversity of beta diversities: straightening up a concept gone awry. Part 1. Defining beta diversity as a function of alpha and gamma diversity. *Ecography*, 33, 2–22

262. Turc, L. (1961). Evaluation des besoins en eau d'irrigation, évapotranspiration potentielle. *Ann. Agron.*, 12, 13–49

263. Turnbull, J., Lea, D., Parkinson, D., Phillips, P., Francis, B., Webb, S., *et al.* (2010). *Oxford Advanced Learner's Dictionary, 8th Edition: Paperback*. Oxford Advanced Learner's Dictionary, 8th Edition. OUP Oxford

264. Ulanowicz, R.E. (2000). Ascendancy: A Measure of Ecosystem Performance. In: *Handbook of ecosystem theories and management* (eds. Jørgensen, S.E. & Müller, F.). Lewis Publishers, Boca Raton, pp. 303–315

265. Urban, M.C., Zarnetske, P.L. & Skelly, D.K. (2013). Moving forward: dispersal and species interactions determine biotic responses to climate change. *Ann. N. Y. Acad. Sci.*, 1297, 44–60

266. Valiente-Banuet, A., Aizen, M.A., Alcántara, J.M., Arroyo, J., Cocucci, A., Galetti, M., *et al.* (2015). Beyond species loss: The extinction of ecological interactions in a changing world. *Funct. Ecol.*, 29, 299–307

267. Vanschoenwinkel, B., Waterkeyn, A., Jocqué, M., Boven, L., Seaman, M. & Brendonck, L. (2010). Species sorting in space and time - the impact of disturbance regime on community

References

- assembly in a temporary pool metacommunity. *J. North Am. Benthol. Soc.*, 29, 1267–1278
268. Vasilakopoulos, P. & Marshall, C.T. (2015). Resilience and tipping points of an exploited fish population over six decades. *Glob. Chang. Biol.*, 21, 1834–1847
269. Vermaat, J.E., Dunne, J.A. & Gilbert, A.J. (2009). Major dimensions in food-web structure properties. *Ecology*, 90, 278–282
270. Villéger, S., Mason, N.W.H. & Mouillot, D. (2008). New multidimensional functional diversity indices for a multifaceted framework in functional ecology. *Ecology*, 89, 2290–2301
271. Vincenot, C.E., Mazzoleni, S. & Parrott, L. (2016). Editorial: Hybrid Solutions for the Modeling of Complex Environmental Systems. *Front. Environ. Sci.*, 4, 53
272. Violle, C., Navas, M.L., Vile, D., Kazakou, E., Fortunel, C., Hummel, I., *et al.* (2007). Let the concept of trait be functional! *Oikos*, 116, 882–892
273. Walsh, K., Court-Picon, M., de Beaulieu, J.-L., Guiter, F., Mocci, F., Richer, S., *et al.* (2014). A historical ecology of the Ecrins (Southern French Alps): Archaeology and palaeoecology of the Mesolithic to the Medieval period. *Quat. Int.*, 353, 52–73
274. Wang, W., Peng, C., Kneeshaw, D.D., Larocque, G.R. & Luo, Z. (2012). Drought-induced tree mortality: ecological consequences, causes, and modeling. *Environ. Rev.*, 20, 109–121
275. Wardle, D.A., Bonner, K.I. & Barker, G.M. (2000). Stability of ecosystem properties in response to above-ground functional group richness and composition. *Oikos*, 89, 11–23
276. Weber, P., Bugmann, H., Pluess, A.R., Walthert, L. & Rigling, A. (2013). Drought response and changing mean sensitivity of European beech close to the dry distribution limit. *Trees - Struct. Funct.*, 27, 171–181
277. Weiner, C.N., Werner, M., Linsenmair, K.E. & Blüthgen, N. (2014). Land-use impacts on plant-pollinator networks: interaction strength and specialization predict pollinator declines. *Ecology*, 95, 466–74
278. Westman, W.E. (1978). Measuring the inertia and resilience of ecosystems. *Bioscience*, 28, 705–710
279. Westoby, M. (1998). A leaf-height-seed (LHS) plant ecology strategy scheme. *Plant Soil*, 199, 213–227
280. Whittaker, R.H. (1972). Evolution and measurement of species diversity. *Taxon*, 213–251
281. Wilman, H., Belmaker, J., Simpson, J., de la Rosa, C., Rivadeneira, M.M. & Jetz, W. (2014). EltonTraits 1.0: Species-level foraging attributes of the world's birds and mammals. *Ecology*, 95, 2027–2027
282. Wookey, P.A., Aerts, R., Bardgett, R.D., Baptist, F., Bråthen, K.A., Cornelissen, J.H.C., *et al.* (2009). Ecosystem feedbacks and cascade processes: understanding their role in the

responses of Arctic and alpine ecosystems to environmental change. *Glob. Chang. Biol.*, 15, 1153–1172

283. Worrall, J.J., Egeland, L., Eager, T., Mask, R.A., Johnson, E.W., Kemp, P.A., *et al.* (2008). Rapid mortality of *Populus tremuloides* in southwestern Colorado, USA. *For. Ecol. Manage.*, 255, 686–696

284. Worrall, J.J., Rehfeldt, G.E., Hamann, A., Hogg, E.H., Marchetti, S.B., Michaelian, M., *et al.* (2013). Recent declines of *Populus tremuloides* in North America linked to climate. *For. Ecol. Manage.*, 299, 35–51

285. Zhou, Z., Sun, O.J., Huang, J., Gao, Y. & Han, X. (2006). Land use affects the relationship between species diversity and productivity at the local scale in a semi-arid steppe ecosystem. *Funct. Ecol.*, 20, 753–762

APPENDICES

APPENDIX 1

This first appendix is dedicated to an overview of the history of ecological stability studies, as well as some of the approaches used to investigate stability-related questions. More than providing additional and relevant information for the understanding of this thesis, this appendix is a summary of the work that fascinates and compels me for the study of ecosystem stability and resilience.

Ecologists and resource managers have been seeking to understand how ecosystems respond to change at least since the nineteenth century, but it was during the 1950s that the stability of ecological function gained attention from academia (Curtin & Parker 2014). Robert MacArthur's (MacArthur 1955) diversity-stability hypothesis linked ecosystem stability to the pattern of interconnectivity between species in food webs. Later, Richard Lewontin used "vector fields" models to describe the stability of community structure within basins of attraction, considering alternative stable states (Lewontin 1969), a conceptualisation that became the basis of resilience science.

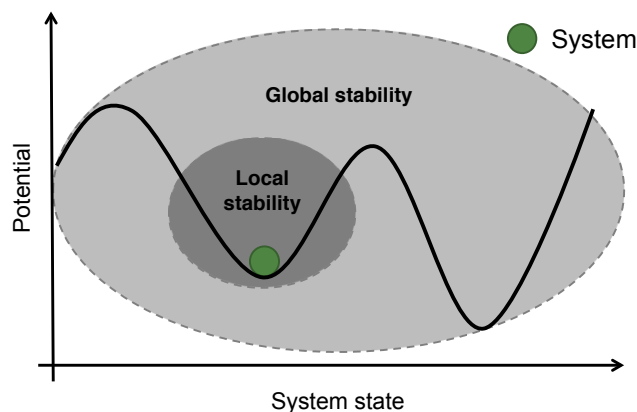


Figure 20. Global and local stability concepts – two facets of stability that refer to the behaviour of a system close and far from an equilibrium point, i.e. attractor.

Following Lewontin's footsteps, Crawford S. Holling (1973) defined the concepts of stability and resilience as reflecting two facets of the behaviour of ecological systems (Fig. 20). Stability is linked to the behaviour of the system in the proximity of the basin of attraction and reflects its local stability. It was defined as "*the ability of a system to return to an equilibrium state after a disturbance*", emphasizing "*equilibrium, the maintenance of a predictable world*" (Holling 1973). On the other hand, resilience is linked a system's ability to remain within a basin of attraction, its global stability. It "*determines the persistence of relationships within a system and is a measure of the ability of these systems to absorb changes of state variables, driving variables, and parameters, and still persist*" (Holling

1973). Resilience emphasizes the existence of several domains of attraction and the need for persistence. In the following years, the terminology used to reflect the concepts he discussed by Holling grew rapidly.

A mere five years after Holling's seminal paper, Walter Westman (1978) recognized that Holling's concepts of stability and resilience had already been renamed by several authors (for instance, Cairns & Dickson 1977 referred to Holling's definitions of stability and resilience as elasticity and inertia, respectively). Redefinitions continued as Stuart Pimm (1984) re-coined the term resilience as the behaviour of a system in the vicinity of an equilibrium point. Oppositely to Holling, Pimm's resilience refers to the local stability of a system, which can be measured as the speed of return to equilibrium. Despite efforts by Westman (1978), and later Holling (1996) amongst others, to clarify resilience terminology (see for instance Hodgson *et al.* 2015), resilience science is still crowded by a panoply of interchangeable terms, which has contributed to increasing confusion surrounding its applicability (Beisner *et al.* 2003; Standish *et al.* 2014; Hodgson *et al.* 2015; Mori 2016). To avoid further confusion, the terminology used during in the present thesis follows the concepts of stability and resilience initially proposed by Holling (1973). Their correspondence with properties identified by Westman (1978), Pimm (1984) and recently revisited by Donohue, *et al.* (2013) are presented in Table 3. Regardless of its rather confusing terminology, resilience theory provides a solid ground to formulate expectations regarding how systems respond to disturbances. Most importantly, it highlights that local and global stability are two complementary facets of ecosystem stability in its general sense.

Studying ecosystem stability: the role of biodiversity for stabilisation

After MacArthur's publication of his diversity-stability hypothesis, the number of studies trying to understand whether or not diversity promotes stability increased rapidly and controversy soon arose⁷. While mathematical evidence pointed that higher complexity and diversity rendered systems more unstable (e.g. Gardner & Ashby 1970), empirical studies indicated the opposite (McNaughton 1977). This discordance came from theoreticians and field ecologists using different definitions of stability, focusing on different components of complexity and working at different organisational scales (Pimm 1991). In fact, when theoretical and empirical studies looked at the same facets of diversity-stability relationships, their conclusions agreed with MacArthur's initial hypothesis.

⁷an excellent account of the history of ecological stability studies is available in Pimm's *The Balance of Nature? Ecological Issues in the Conservation of Species and Communities* (1991)

Studying ecosystem stability to global change across spatial and trophic scales

Table 3. Holling’s stability and resilience concepts with the definitions suggested by Holling (1996). Their corresponding properties suggested by Westman (1978), Pimm (1984) are presented together with examples of measurement.

Definitions (Holling 1996)	Properties (Westman 1978)	Properties (Pimm 1984; Donohue <i>et al.</i> 2013)	Measurement (example: lake eutrophication)
<p>stability “concentrates on stability near an equilibrium steady state”</p>	<p>inertia magnitude of a disturbance needed to cause a particular change in the system</p>	<p>resistance – the extent of changes caused by a perturbation</p>	<ul style="list-style-type: none"> – inertia: amount of nutrients that need to be accumulated to cause ecosystem damage (e.g. the local extinction of species A & B) – resistance: how much did the community change after an X amount of nutrients were added to the lake?
	<p>elasticity rate of return, or the time the system takes to return to equilibrium after being disturbed</p>	<p>resilience (= elasticity)</p>	<p>persistence – change in ecosystem properties over time. Includes robustness (number of extinctions) and number of invasions. Communities that lose less species and/or are harder to invade are more persistent</p>
<p>resilience “emphasizes conditions far from any equilibrium steady state, where instabilities can flip a system into another [...] stability domain”</p>	<p>amplitude magnitude of disturbance that can be absorbed before a state-shift</p>	<p>variability – temporal or spatial variability of the system, inversely related to stability.</p>	<ul style="list-style-type: none"> – coefficient of variation (CV) of an ecosystem property, such as biomass (Loreau & de Mazancourt 2013)
	<p>hysteresis degree to which the path of restoration is the reversal of the path to degradation</p>		
	<p>malleability degree of similarity between the new stable state and the former one</p>		

A large part of the literature addressing the role of diversity in stabilising ecosystem function can be broadly organised into three categories: 1) biodiversity and ecosystem functioning (BEF) studies, 2) perturbation-diversity studies and 3) perturbation-BEF-studies. The majority of these studies measured ecosystem stability as the degree of temporal variation of an ecosystem property, frequently productivity. However, perturbation-BEF-studies have also looked at ecosystem stability to changes in composition, such as invasions. These different measures of stability have been nicely summarised by Donohue *et al.* (2013) with their correspondence to the properties described by Westman (1978).

1) Biodiversity and ecosystem functioning (BEF) studies have mostly considered how biodiversity promotes the local stability and short-term stability of ecosystem function, by assessing how varying species richness affect and stabilise productivity levels. It has been shown that higher levels of biodiversity promote and stabilise ecosystem function (e.g. Cadotte *et al.* 2012; Polley *et al.* 2013; see also the review by Loreau *et al.* 2001) and that the mechanisms through which this occurs can be divided into two main classes: selection effects and complementarity effects (Loreau 2001). Selection effects are related with stochastic community assembly processes. If a regional species pool contains many productive species with low demographic variance, then higher levels of diversity will stabilise productivity by chance alone. On the other hand, complementarity effects are related to deterministic community assembly processes arising from differences in species' fundamental niches. According to Loreau & de Mazancourt (2013), taxonomic diversity can increase stability via to 1) differences in species fundamental niches that lead to asynchronous responses to changes in environmental conditions, 2) differences in species intrinsic growth rates that affect the speed at which they respond to these changes, and 3) differences in species fundamental niches that result in lower interspecific competition. The relative importance of these complementarity mechanisms for the stabilisation of ecosystem function has been shown to vary across ecosystems. Asynchrony in species responses to environmental conditions, also termed 'response diversity', seemed to be the main driver of stability in coral reef fish communities (Thibaut *et al.* 2011), while competitive interactions for light resources were suggested as the main stabilising mechanism in simulated forest communities (Morin *et al.* 2011). In grasslands, the stability of productivity was showed to be driven by temporal asynchrony in species dynamics, by negative, as well as positive species interactions that lead to compensatory dynamics (Tilman *et al.* 2006; Isbell *et al.* 2009; Roscher *et al.* 2011; Gross *et al.* 2014), and simple selection effects (Polley *et al.* 2007).

2) Perturbation-diversity studies have sought to understand how biodiversity *per se*

responds to changing environmental conditions and disturbances. They show that the relationship between different facets of biodiversity not only changes for different environmental conditions, but can also vary with disturbance intensity. For instance, Carmona *et al.* (2012) have shown that in Mediterranean grasslands the relationship between alpha taxonomic and functional diversities depended on habitat type and on yearly environmental conditions. During dry years, functional diversity had a saturating response to increasing taxonomic diversity; and during wet years they had a linear relationship in wet habitats, but a negative relationship in dry habitats. On the other hand, Biswas & Mallik (2011) have shown that the slope of the relationship between taxonomic and functional diversity can also change across land-use disturbance levels. Interestingly, these results may reflect that the relative importance of community assembly mechanisms, such as competition and environmental filtering, may change across environmental and disturbance gradients (Mayfield *et al.* 2010; Vanschoenwinkel *et al.* 2010; de Bello *et al.* 2013). Biodiversity responses to disturbance may also differ between communities of different groups, as shown by Flynn *et al.* (2009) who assessed how land-use affected the relationships between taxonomic and functional diversity in bird, mammal and plant communities. For birds and mammals, losses of functional diversity were stronger than would be expected if functional diversity was determined solely by species richness, yet no signal of land use was detected in plant taxonomic-functional diversity relationships.

Finally, 3) perturbation-BEF-studies are somewhere between the first two categories, as they focus on how biodiversity stabilises ecosystem functioning in face of external disturbances (i.e. abnormal environmental variation, invasions, habitat loss, ...). Higher species richness has been shown to provide higher community resistance to invasions at small spatial scales (Levine 2000; Kennedy *et al.* 2002; Shea & Chesson 2002) and faster recovery from fire disturbances (MacDougall *et al.* 2013). Also, functional redundancy (i.e. fraction of species diversity not explained by functional diversity) was found to be a better predictor of community functional stability, than species richness *per se* (de Bello *et al.* 2008).

Despite their large contribution to understanding biodiversity generally stabilises ecosystems, these studies have also put in evidence that mechanisms behind this relationship may vary across ecosystems and across disturbance gradients, and that different facets of biodiversity differ in their relative importance for stabilisation (Pillar *et al.* 2013). Also, the fact that most studies focused on single ecosystems, single disturbances and single ecosystem functions hinders the prospect of having a cross-ecosystem, cross-disturbance and cross-ecosystem function perspective. Since stabilising mechanisms change across ecosystems, or

even across disturbance gradients for a given ecosystem, BEF-related approaches may not be appropriate to study ecosystem stability at the landscape scale, especially in cases where ecosystems are subjected to multiple disturbances.

Studying ecosystem resilience: tipping points, early warning signals and mathematical approximations

The concept of ecological resilience highlights the possibility of an ecosystem to shift between states, which is ignored by BEF-type studies. Classical examples, such as lake eutrophication (Carpenter *et al.* 1999) and the desertification of arid ecosystems (Kéfi *et al.* 2007; Bestelmeyer *et al.* 2009), show that slow changes in external variables (slow changing variables) can erode ecosystem resilience and lead to catastrophic state-shifts that are hard to reverse (Scheffer & Carpenter 2003). In recent years, a growing body of studies have developed approaches to detect the approximation to tipping points, serving as early warning signals of impending state-shifts. They are based on phenomena that can occur as systems approach a tipping point in result to slow changing variables, such as critical slowing down and flickering (van Nes & Scheffer 2007; Scheffer *et al.* 2009; Dakos *et al.* 2011, 2012). As the system approaches a tipping point, it will take longer to recover to its original stable state – critical slowing down – and it may be seen to oscillate between alternative stable states – flickering; both phenomena will be reflected in statistical properties of the time series of the response variable (Carpenter & Brock 2006; Carpenter *et al.* 2008; Dakos *et al.* 2012). Finally, mathematical approximations have also been used to study ecosystem resilience. Many use linear representations of relatively simple ecological systems that are studied through eigendecomposition to explore both stability and resilience (e.g. Ives 1995; Neubert & Caswell 1997). For instance, leading eigenvalues denote the rate of return to equilibrium, thus reflecting stability. Yet, it is also possible to evaluate the global behaviour of the system and the presence of attractive, or repulsive nodes, depending on the behaviour of the system around them (the system tends to attractive nodes, but moves away from repulsive nodes; Mchich *et al.* 2007). This potentially allows the detection of alternative stable states.

The application of early warning signals to predict tipping points, however, is limited to particular systems, under particular types of disturbances (Dakos *et al.* 2015). For instance, critical slowing down and flickering are known to occur in the vicinity of catastrophic shifts caused by slow changes in external variables, i.e. press-perturbations (but see Kéfi *et al.* 2013), and are not adequate to identify shifts in result of push-perturbations, such as insect outbreaks (Sharma *et al.* 2014). Also, many ecological systems are likely to exhibit complex

non-linear dynamics with multiple possible outcomes. In these cases, shifts will not be preceded by critical slowing down or flickering and may occur without warning (Hastings & Wysham 2010). Similarly, the use of mathematical approximations to quantify engineering resilience is restricted to relatively simple representations of ecological systems.

As we can see, the study of ecosystem stability has taken different directions and approaches throughout the decades. Yet, most of them have been focused in one-dimensional analyses of particular ecosystem properties and variables. Many have also been unable to provide relevant information for ecosystem management and conservation, since they either remained very theoretical or concerned small scales and very specific ecosystems.

APPENDIX 2: SUPPLEMENTARY MATERIALS TO CHAPTER I

FATE-HD ‘base model’ description

FATE-HD has been validated for the different plant communities present in the Ecrins National Park (ENP) (Boulangeat *et al.* 2014b). Although large areas of the park are managed and used for different activities (around 68% of the total area), the park has a very diverse flora, with ca. 2000 plant species. Different types of vegetation are mostly maintained by current abiotic conditions or land-use activities and can thus be expected to shift under climate and land-use changes.

FATE-HD currently simulates 24 plant functional groups (PFGs; Table S1 in this appendix) and five different height strata (0-1.5m; 1.5-4m; 4-10m; 10-20m; taller than 20m). Each group represents species that are similar in terms of bioclimatic niche, competitive ability for light resources, demography and response to disturbances (Boulangeat *et al.* 2012). Chamaephyte groups, C1-6, are only present in the first height stratum, except for C4 which reaches the second stratum; herbaceous groups, H1-10, are mostly hemicryptophytes and are only present in the first height stratum; and phanerophyte groups, P1-8, reach at least the third height stratum, with six reaching the fourth stratum and two reaching the fifth (Table S1 in this appendix). Population dynamics, dispersal and competition for light resources are all explicitly simulated for each PFG, both spatially and temporally.

Population dynamics partially depend on habitat suitability (HS). Habitat suitability is calculated for each PFG from a set of bioclimatic variables and includes a stochastic component in order to simulate yearly oscillations of habitat quality resulting from interannual climate variability. Maps of ‘current’ HS were produced using PFG presence/absence information across the French Alps (see Boulangeat *et al.* 2014b) that was related to seven environmental variables using the *R* package *biomod2* (Thuiller *et al.* 2009). These variables were slope, percentage of calcareous soil and five ‘BIOCLIM’ variables (isothermality, temperature seasonality, temperature annual range, mean temperature of coldest quarter and annual precipitation), averaged across years 1961-1990 to obtain ‘current’ climate values (i.e. ‘current’ HS). Predictions of PFG distributions using the chosen environmental variables were obtained from a set of different modelling approaches and combined into a single output using a weighted sum of predictions (Thuiller *et al.* 2009; Boulangeat *et al.* 2014b).

Dispersal of PFGs is modelled for both long and short distances, depending on the PFG in question. Competition for light resources is also modelled according to PFG type and

stratum, as both differ in relation to their shade tolerance. The amount of shade is calculated per pixel in function of PFGs abundances per stratum. The more abundant a stratum is the more shade it casts on below strata, decreasing the amount of available light (see Boulangeat *et al.* 2014b for more information on simulated population dynamics, competition and dispersal mechanisms).

Two types of disturbances were included in the model: grazing and mowing, with grazing having three levels of intensity, low (1), medium (2) and high (3). They were implemented in a spatially explicit manner, by assigning a binary variable reflecting the presence/absence of a particular disturbance to each pixel. Grazing affected PFGs by causing mortality, or resprouting (preventing mature plants from producing seeds) in proportions that varied according to PFGs' palatability classes (Table S1 in this appendix) and age. Mowing removed all trees above 1.5m (in the second stratum or higher) by causing their death (see Boulangeat *et al.* 2014b for more information on land-use disturbances).

Traits were used as basis for the parameterisation of PFG population dynamics, light competition and dispersal mechanisms, as well as responses to grazing and mowing. For instance, PFGs with higher palatability values suffered stronger effects from grazing. The full list of trait values are shown in Table S1 in this appendix, and we refer the reader to Boulangeat, *et al.* (2014b) for a complete list of parameters used in the base model.

Land-use and gradual climate change scenarios

Gradual climate change (CC) was simulated according to IPCC previsions of the A1B scenario for years 2020, 2050 and 2080. Values of BIOCLIM variables were projected using the regional climate model (RCM) RCA3 (Samuelsson *et al.* 2011) fed by the global circulation model (GCM) CCSM3 (derived from the ENSEMBLES EU project outputs; NCAR community 2004). Outputs from the RCM were then downscaled to 100 x 100 m resolution using the change factor method (Diaz-Nieto & Wilby 2005) and used to calculate future HS maps. We then interpolated between current HS projections (referring to the 1961-1990 period) and time step 2020, and between time steps 2020, 2050 and 2080 to obtain a more gradual change at every 15 years for 90 years (Boulangeat *et al.* 2014a). Current HS projections were used during simulation years 0 to 14, before CC was implemented.

The chosen land-use change scenario, the abandonment of all grazing and mowing activities, represents a current trend of land-use change observed not only in the ENP (Esterni *et al.* 2006), but in other regions of the European Alps (Gehrig-Fasel *et al.* 2007), and is

associated with the eventual interruption of European subsidies for agriculture (Boulangeat *et al.* 2014a).

Parameterising and simulating drought effects

Drought effects on vegetation dynamics in the Ecrins National Park (ENP) were simulated mechanistically, rather than physiologically. Drought was simulated in two phases that consisted first in the 1) identification of drought effects and then 2) on modelling drought responses. Both phases depended on PFGs' past drought exposure, which was reconstructed from historical climate data.

Identifying drought effects followed the same approach as the implemented habitat suitability (HS). Drought intensity (*Din*) maps were fed into the model to compare *Din* pixel values against parameters reflecting the PFGs' adaptations and tolerance to drought (past drought exposure). PFG responses also depended on their adaptation and tolerance to drought. In this appendix we detail how PFG past drought exposure was calculated, how PFG drought-related responses were parameterised and, lastly, how *Din* maps were produced to simulate drought events.

PFGs past drought exposure

Parameters for detecting and applying drought effects were based on PFGs' past drought exposure, built from PFG occurrence information and climate data across most of the French Alps.

Occurrence data for each PFG were obtained from the Conservatoire Botanique National Alpin (CBNA) vegetation-plot database, covering the majority of the French Alps (Boulangeat *et al.* 2012; CBNA 2015). Only data from exhaustive *relevés* (identification of all plant species within a plot) from 1980 to present were used. A PFG was considered present in a plot if at least one of its representative species was recorded (Table S2 in this appendix), resulting in the selection of 101 122 plots.

PFG past drought exposure was based on historical values of the moisture index (MI), an indicator of climatic drought that has been used in previous studies relating forest mortality and drought (Gustafson *et al.* 2003; Bigler *et al.* 2006). We calculated MI values across the whole French Alps using climate data obtained from the meteorological model Aurelhy (Benichou & Le Breton 1987), spanning years 1961 to 1990 and interpolated at a 100 m resolution. Monthly MI values (in mm) were calculated as:

$$MI_i = \sum_{j=1}^n P_j - PET_j \times n + 0.5$$

with P_j being daily precipitation, PET_i being the average daily potential evapotranspiration of month i – calculated following Turc’s (1961) formula – and n the number of days in month i . Values were then subset by plot and crossed with PFG occurrence data to obtain a distribution of historical MI values for each PFG ($MI_{1961-1990}$). We also built distributions of drought intensity (Din) values for each PFG, by extracting the lowest value of MI in a year for each plot ($Din_{1961-1990}$).

Parameterisation of drought-related mortality and resprouting

Severe drought effects (immediate or post-drought) triggered drought-related mortality, with the possibility of resprouting, which depended on the soil moisture preference class of a given PFG. Soil moisture preference classes were built from the PFGs $MI_{1961-1990}$ distributions, assuming that they reflect their moisture preferences and, or, adaptations to drought. For each PFG, we calculated $\bar{x} - 2.5 \times SD$ of $MI_{1961-1990}$ (with \bar{x} and SD being the mean and standard deviation, respectively) and scaled the results into four classes from zero (very low moisture preference) to four (very high moisture preference). These classes were then adjusted according to expert-based knowledge of the soil moisture preferences of the species present in the PFGs, resulting into four final classes ranging from zero to three (Table S2 in this appendix).

Validation of drought module

The parameterisation of drought effects was validated following the procedure described in Boulangeat *et al.* (2014b), in respect to the simulated PFG distribution and strata abundances, as well as in respect to tree cover (strata > 1.5 m).

A validation simulation was run starting from the 800th year of the initialisation phase (instead of year 850 used for scenario simulations; see initialisation details in main text), after which we applied past drought intensity (Din) values for 30 years. Maps of past Din values corresponded to the yearly minimum moisture index (MI) values registered from 1961-1990 (see *Parameterising and simulating drought effects* above for details on MI calculation). Given that the parameterisation of PFG responses to drought followed the same climatic period, we expected that including past drought events would not majorly affect model accuracy in comparison to what has been demonstrated by Boulangeat *et al.* (2014b). Hence, we re-assessed model accuracy by comparing simulated PFG distributions against PFG

occurrences from the ‘DELPHINE’ database of vegetation composition and structure in the Ecrins National Park (ENP) (see full procedure in Boulangeat *et al.* 2014b). For each PFG we calculated model specificity (proportion of correctly predicted PFG presences – true positives), model sensitivity (proportion of correctly predicted PFG absences – true negatives) and error rate (overall proportion of false positives and false negatives). As in Boulangeat *et al.* (2014b), resulting statistics were compared against the specificity, sensitivity and error rate of habitat suitability models calculated for each PFG (see details on PFG habitat suitability maps in *FATE-HD ‘base model’ description* in this appendix Boulangeat *et al.* 2014b). In addition, we assessed whether including drought effects improved vegetation structure predictions. Simulated tree cover (> 1.5 m) in different habitats and overall strata abundances at three levels (< 1.5 m, $1.5 - 4$ m and > 4 m) were compared against observation data and previous results obtained with the base model (see Boulangeat *et al.* 2014b for details on observation data and base model results).

Including drought effects lowered PFG abundance in general (data not shown), which improved general estimates of tree cover (strata > 1.5 m) in rocky and alpine habitats, but led to underestimates in pasture fields, lowlands and mountainous forests. In subalpine and mountainous open habitats tree cover went from being overestimated to underestimated, but closer to the observed cover in absolute terms (Fig. S2 in this appendix). In general, simulated strata abundances remained consistent with observed presences and absences, with larger strata abundances being predicted where the strata were indeed observed present (Fig. S3 in this appendix). The predicted accuracy (error rate) of PFG distributions was very similar to that of the base model (Boulangeat *et al.* 2014b), with slight increases for seven PFGs and decreases for six PFGs (Table S4 in this appendix).

All in all, we are confident that the simulated drought effects and their parameterisation did not negatively affect model performance, since the simulation of past drought events allowed the representation of the current vegetation of the park.

Supplementary Tables

Table S1. Plant functional groups and their trait values. Life form classes are chamaephytes (C1-6), herbaceous (H1-10) and phanerophytes (P1-8). PFGs with larger values of 'light', 'dispersal' and 'palatability' are, respectively, light-loving, long-distance dispersers and preferred by grazers (thus more affected by grazing). 'No. strata' indicates the number of strata a PFG can occupy in the model. 'SLA' and 'LDMC' stand for average specific leaf area and average leaf dry matter content, respectively. SLA values for species of PFGs H10 and P8 were obtained from Kattge et al. (2011). Table partially adapted from Boulangeat et al. (2012) and Boulangeat, Georges and Thuiller (2014b).

PFG	No. Strata	Dispersal	Light	Height (cm)	Palatability	Longevity (years)	Maturity (years)	Seed mass (g)	SLA (mm ² mg ⁻¹)	LDMC (mg g ⁻¹)	Leaf area (mm ²)
C1	1	6	7	27	3	27	5	23.91	19.21	262.74	12.95
C2	1	4	8	13	3	19	4	0.38	18.02	196.03	1.05
C3	1	1	8	7	0	45	6	0.51	14.39	221.21	0.66
C4	2	6	6	209	2	158	10	192.99	16.83	330.52	16.97
C5	1	6	6	76	0	39	8	75.01	8.28	390.18	0.94
C6	1	7	6	18	2	92	8	39.50	13.40	354.97	0.86
H1	1	3	8	17	3	11	4	0.86	17.22	260.65	5.00
H2	1	6	7	42	3	10	3	4.04	22.11	250.74	18.76
H3	1	7	7	50	3	9	3	2.37	24.43	238.24	79.05
H4	1	3	5	76	0	7	4	0.36	29.76	228.53	541.13
H5	1	3	7	40	3	7	4	1.94	20.71	243.02	31.34
H6	1	3	6	73	3	8	4	2.31	28.21	227.85	76.68
H7	1	5	6	19	0	7	4	0.40	19.25	195.45	97.07
H8	1	3	8	19	0	8	4	0.89	23.11	274.24	0.18
H9	1	7	8	19	3	9	4	0.38	21.09	417.58	1.40
H10	1	7	6	100	3	9	4	6.20	21.14	0.22	353.31
P1	3	6	6	1175	2	193	15	177.93	12.03	346.77	34.01
P2	3	5	6	750	2	177	15	0.13	17.17	350.81	14.43
P3	4	4	5	1667	2	351	18	86.41	15.30	265.26	65.52
P4	5	6	7	2500	0	600	15	6.82	10.06	279.75	0.20
P5	5	6	4	2500	2	450	25	114.06	11.86	309.25	20.28
P6	4	4	8	1650	2	160	20	6.10	19.24	282.18	12.36

Appendices - Appendix 2: Supplementary materials to Chapter I

P7	3	4	5	600	2	310	15	78.27	15.65	360.50	47.42
P8	3	4	7	800	2	100	15	0.17	14.62	0.36	8.26

Studying ecosystem stability to global change across spatial and trophic scales

Table S2. Description of the simulated plant functional groups (PFG) and their representative species. PFG occurrences were based on presence/absence data of their representative species across the French Alps. The PFG description reflects the main characteristics of the species it encompasses. Table partially adapted from Boulangeat, Georges and Thuiller (2014b).

PFG	Species	PFG description
C1	<i>Achillea millefolium</i> , <i>Anthyllis montana</i> , <i>Cotoneaster integerrimus</i> , <i>Helianthemum grandiflorum</i> , <i>Helianthemum nummularium</i> , <i>Hippocrepis comosa</i> , <i>Lonicera caerulea</i> , <i>Origanum vulgare</i> , <i>Potentilla neumanniana</i> , <i>Rubus idaeus</i> , <i>Rubus saxatilis</i> , <i>Rumex acetosella</i> , <i>Stachys recta</i> , <i>Teucrium chamaedrys</i> , <i>Thymus pulegioides</i> , <i>Valeriana montana</i>	Thermophilous chamaephytes with long dispersal distance
C2	<i>Antennaria dioica</i> , <i>Artemisia umbelliformis</i> , <i>Cerastium alpinum</i> , <i>Cerastium cerastoides</i> , <i>Cerastium latifolium</i> , <i>Cerastium pedunculatum</i> , <i>Cerastium uniflorum</i> , <i>Helictotrichon sedenense</i> , <i>Leucanthemopsis alpina</i> , <i>Rumex scutatus</i> , <i>Salix glaucosericea</i> , <i>Salix hastata</i> , <i>Saxifraga aizoides</i> , <i>Saxifraga oppositifolia</i> , <i>Sempervivum arachnoideum</i> , <i>Thymus polytrichus</i> , <i>Vaccinium uliginosum microphyllum</i>	Alpine and subalpine chamaephyte species
C3	<i>Androsace pubescens</i> , <i>Androsace vitaliana</i> , <i>Dryas octopetala</i> , <i>Empetrum nigrum hermaphroditum</i> , <i>Eritrichium nanum</i> , <i>Globularia cordifolia</i> , <i>Gypsophila repens</i> , <i>Juniperus sibirica</i> , <i>Noccaea rotundifolia</i> , <i>Polygala chamaebuxus</i> , <i>Primula hirsuta</i> , <i>Primula pedemontana</i> , <i>Pritzelago alpina</i> , <i>Rhododendron ferrugineum</i> , <i>Sagina glabra</i> , <i>Sagina saginoides</i> , <i>Salix herbacea</i> , <i>Salix reticulata</i> , <i>Salix retusa</i> , <i>Saxifraga bryoides</i> , <i>Saxifraga exarata</i> , <i>Sedum album</i> , <i>Sedum alpestre</i> , <i>Sedum dasyphyllum</i> , <i>Silene acaulis</i> , <i>Silene acaulis bryoides</i>	Chamaephytes with short dispersal distance
C4	<i>Alnus alnobetula</i> , <i>Amelanchier ovalis</i> , <i>Cornus sanguinea</i> , <i>Corylus avellana</i> , <i>Crataegus monogyna</i> , <i>Juniperus communis</i> , <i>Lonicera xylosteum</i> , <i>Ribes petraeum</i> , <i>Rosa pendulina</i> , <i>Salix laggeri</i> , <i>Salix purpurea</i>	Tall shrubs
C5	<i>Arctostaphylos uva-ursi crassifolius</i> , <i>Calluna vulgaris</i> , <i>Hippocrepis emerus</i>	Mountainous to subalpine heath found in dry climates
C6	<i>Vaccinium myrtillus</i> , <i>Vaccinium vitis-idaea</i>	Mountainous to subalpine heath found in wet climates
H1	<i>Achillea nana</i> , <i>Agrostis alpina</i> , <i>Agrostis rupestris</i> , <i>Alchemilla pentaphyllea</i> , <i>Alopecurus alpinus</i> , <i>Astragalus alpinus</i> , <i>Athamanta cretensis</i> , <i>Avenula versicolor</i> , <i>Campanula cochleariifolia</i> , <i>Carex capillaris</i> , <i>Carex curvula</i> , <i>Carex echinata</i> , <i>Carex foetida</i> , <i>Carex frigida</i> , <i>Carex nigra</i> , <i>Carex panicea</i> , <i>Carex rupestris</i> , <i>Doronicum grandiflorum</i> , <i>Epilobium anagallidifolium</i> , <i>Eriophorum latifolium</i> , <i>Eriophorum polystachion</i> , <i>Eriophorum scheuchzeri</i> , <i>Festuca halleri</i> , <i>Festuca quadriflora</i> , <i>Gentiana punctata</i> , <i>Geum montanum</i> , <i>Geum reptans</i> , <i>Hieracium glaciale</i> , <i>Juncus trifidus</i> , <i>Kobresia myosuroides</i> , <i>Leontodon montanus</i> , <i>Leontodon pyrenaicus helveticus</i> , <i>Linaria alpina</i> , <i>Lotus alpinus</i> , <i>Luzula alpinopilosa</i> , <i>Oxyria digyna</i> , <i>Phleum alpinum</i> , <i>Plantago alpina</i> , <i>Poa alpina</i> , <i>Poa cenisia</i> , <i>Poa laxa</i> , <i>Polygonum viviparum</i> , <i>Potentilla aurea</i> , <i>Potentilla erecta</i> , <i>Potentilla grandiflora</i> , <i>Ranunculus glacialis</i> , <i>Ranunculus kuepferi</i> , <i>Ranunculus montanus</i> , <i>Saxifraga stellaris robusta</i> , <i>Taraxacum alpinum</i> , <i>Trichophorum cespitosum</i> , <i>Trifolium alpinum</i> , <i>Trifolium pallescens</i> , <i>Trifolium saxatile</i> , <i>Trifolium thalii</i>	Alpine species, which do not tolerate shade and have short dispersal distance

	<i>Trisetum distichophyllum</i>	
H2	<i>Agrostis capillaris, Agrostis stolonifera, Alchemilla vulgaris, Carex caryophyllea, Carex sempervirens, Carum carvi, Chenopodium bonus-henricus, Festuca nigrescens, Fragaria vesca, Galium aparine, Galium odoratum, Galium verum, Geranium sylvaticum, Lathyrus pratensis, Leucanthemum vulgare, Lotus corniculatus, Meum athamanticum, Onobrychis montana, Rumex acetosa, Rumex pseudalpinus, Sesleria caerulea, Trifolium montanum, Trifolium pratense</i>	Mountainous species, which tolerate nitrophilous soils and have long dispersal distance
H3	<i>Aegopodium podagraria, Anthoxanthum odoratum, Arrhenatherum elatius, Crepis pyrenaica, Dactylis glomerata, Deschampsia cespitosa, Festuca rubra, Heracleum sphondylium, Pimpinella major, Plantago lanceolata, Poa pratensis, Ranunculus acris, Rumex arifolius, Taraxacum officinale, Trifolium repens, Trollius europaeus, Vicia cracca</i>	Mountainous to lowland species found in wet niches and with long dispersal distance
H4	<i>Aconitum lycoctonum vulparia, Aruncus dioicus, Prenanthes purpurea</i>	Undergrowth and shadow species that do not tolerate full light
H5	<i>Achnatherum calamagrostis, Agrostis agrostiflora, Anthericum liliago, Aster bellidiasstrum, Briza media, Deschampsia flexuosa, Epilobium dodonaei fleischeri, Festuca acuminata, Festuca flavescens, Festuca laevigata, Festuca marginata gallica, Festuca melanopsis, Festuca paniculata, Helictotrichon parlatorei, Hugueninia tanacetifolia, Hypericum maculatum, Laserpitium halleri, Laserpitium siler, Leontodon autumnalis, Leontodon hispidus, Luzula sieberi, Phleum alpinum rhaeticum, Pulsatilla alpina, Ranunculus bulbosus, Salvia pratensis, Silene flos-jovis, Stipa eriocaulis, Tolpis staticifolia, Trisetum flavescens</i>	Mountainous to subalpine species with short dispersal distance and tolerant to dry soils
H6	<i>Arabis alpina, Avenula pubescens, Brachypodium rupestre, Cacalia alliariae, Calamagrostis varia, Cardamine pentaphyllos, Carex flacca, Chaerophyllum aureum, Chaerophyllum villarsii, Cicerbita alpina, Epilobium angustifolium, Festuca altissima, Gentiana lutea, Hieracium murorum, Hieracium prenanthoides, Knautia dipsacifolia, Laserpitium latifolium, Luzula nivea, Melica nutans, Mercurialis perennis, Milium effusum, Molinia caerulea arundinacea, Oxalis acetosella, Poa nemoralis, Ranunculus aduncus, Saxifraga rotundifolia, Serratula tinctoria, Valeriana officinalis, Viola biflora</i>	Tall plants typical of <i>megaphorbiaies</i> that can form undergrowth
H7	<i>Cacalia alpina, Hieracium pilosella, Homogyne alpina, Petasites albus, Tussilago farfara</i>	Plants species found in rocky habitats and undergrowth at all elevations
H8	<i>Cacalia leucophylla, Cirsium spinosissimum, Gentiana alpina, Murbeckiella pinnatifida, Omalotheca supina, Veratrum lobelianum</i>	Subalpine to alpine species not usually grazed, which have a short dispersal distance
H9	<i>Anthoxanthum odoratum nipponicum, Nardus stricta, Poa supina, Silene vulgaris prostrata</i>	Short subalpine to alpine species with long dispersal distance
H10	<i>Heracleum sphondylium elegans</i>	Mountainous species with long dispersal distance and shade tolerant
P1	<i>Pinus cembra, Pinus sylvestris, Prunus avium, Sorbus aria, Sorbus aucuparia, Sorbus mougeotii</i>	Thermophilous pioneer trees (deciduous trees and pines)
P2	<i>Populus tremula, Salix daphnoides</i>	Small deciduous pioneer trees (e.g. colonising riversides)
P3	<i>Abies alba, Acer pseudoplatanus, Fraxinus excelsior, Tilia platyphyllos</i>	Tall forest edge trees

Studying ecosystem stability to global change across spatial and trophic scales

P4	<i>Larix decidua</i>	Tall pioneer (larch)
P5	<i>Fagus sylvatica, Picea abies</i>	Late succession trees found in wet climates
P6	<i>Betula pendula, Pinus uncinata</i>	Intermediate succession trees found in dry climates
P7	<i>Acer campestre, Acer opalus</i>	Small forest edge trees
P8	<i>Betula pubescens</i>	Small pioneer found in cold climates

Appendices - Appendix 2: Supplementary materials to Chapter I

Table S3. Drought-related parameters used in FATE-HD. Drought detection thresholds are based on plant functional groups' (PFG) $D_{in1961-1990}$ distributions and were calculated as $\bar{x} - 1.5 \times SD$ and $\bar{x} - 2.0 \times SD$ for moderate and severe droughts, respectively (\bar{x} and SD standing for mean and standard deviation of $D_{in1961-1990}$, respectively). 'Drought sensitivity' determines the number of drought years that a PFG must experience before a severe drought produces severe effects (i.e. drought-related mortality). The 'cumulative drought response' determines the number of drought years needed before any type of drought produces severe effects. 'Recovery' is the number of years subtracted to the accumulated drought events during non-drought years and 'moist. pref.' (moisture preference) is the PFG soil moisture preference class. Drought mortality and resprouting proportions (for immediate or post-drought effects) depend on the PFG type, soil moisture class and age, being larger when the soil moisture preference is higher (but not necessarily different for all classes). Post-drought mortality is always lower than immediate drought mortality, and herbaceous and chamaephyte PFGs (except for C4) do not suffer post-drought mortality. As for resprouting proportions, herbaceous PFGs always resprout after severe drought events, but only phanerophytes and shrub chamaephyte (C4) PFGs are able to resprout during drought. Empty cells denote proportions of 0.

PFG	Drought detection thresholds (in mm)		Cumulative effect thresholds (no. drought events)		Recovery (years)	Moist. pref.	Drought mortality (immediate)				Resprouting (immediate)				Drought mortality (post-drought)				Resprouting (post-drought)			
	Moderate	Severe	Drought sensitivity	Cumulative drought response			Age 1	Age 2	Age 3	Age 4	Age 1	Age 2	Age 3	Age 4	Age 1	Age 2	Age 3	Age 4	Age 1	Age 2	Age 3	Age 4
C1	-1679	-1891	2	3	2	0	0.1													1.0	1.0	1.0
C2	-1416	-1621	2	3	2	2	0.2				0.1									1.0	1.0	1.0
C3	-1515	-1737	2	3	2	2	0.2				0.1									1.0	1.0	1.0
C4	-1724	-1927	3	5	1	1	0.1				0.1		0.4	0.4						0.1	0.4	0.4
C5	-1674	-1885	2	3	2	0	0.1													1.0	1.0	1.0
C6	-1360	-1563	2	3	2	2	0.2				0.1									1.0	1.0	1.0
H1	-1431	-1637	1	2	2	2	0.2				0.1									1.0	1.0	1.0
H2	-1626	-1836	1	2	2	2	0.2				0.1									1.0	1.0	1.0
H3	-1681	-1885	1	2	2	2	0.2				0.1									1.0	1.0	1.0
H4	-1487	-1695	1	2	2	2	0.2				0.1									1.0	1.0	1.0
H5	-1676	-1888	1	2	2	1	0.2				0.1									1.0	1.0	1.0
H6	-1630	-1842	1	2	2	2	0.1				0.1									1.0	1.0	1.0
H7	-1620	-1847	1	2	2	2	0.2				0.1									1.0	1.0	1.0
H8	-1264	-1464	1	2	2	3	0.2				0.1									1.0	1.0	1.0
H9	-1387	-1586	1	2	2	3	0.4	0.1	0.1	0.2										1.0	1.0	1.0
H10	-1458	-1664	1	2	2	2	0.4	0.1	0.1	0.2										1.0	1.0	1.0
P1	-1673	-1883	3	5	1	0	0.1						0.4	0.4						0.1	0.4	0.4

Studying ecosystem stability to global change across spatial and trophic scales

P2	-1630	-1810	3	5	1	2	0.2			0.1	0.1	0.5	0.5	0.1				0.4	0.4	0.4
P3	-1637	-1838	3	5	1	2	0.2			0.1	0.1	0.5	0.5	0.1				0.4	0.4	0.4
P4	-1451	-1632	3	5	1	3	0.4	0.1	0.1	0.2	0.4	0.8	0.8	0.2	0.1	0.1	0.1	0.4	0.5	0.5
P5	-1525	-1734	3	5	1	1	0.1			0.1		0.4	0.4					0.1	0.4	0.4
P6	-1562	-1775	3	5	1	1	0.1			0.1		0.4	0.4					0.1	0.4	0.4
P7	-1683	-1862	3	5	1	0	0.1					0.4	0.4					0.1	0.4	0.4
P8	-1550	-1769	3	5	1	2	0.2			0.1	0.1	0.5	0.5	0.1				0.4	0.4	0.4

Table S4. Model accuracy after implementing drought effects. Validation of the drought module was done by comparing simulated PFG distributions with PFG occurrences obtained from vegetation relevés. PFG occurrence data was obtained via a correspondence between vegetation types and the PFGs (presences corresponding to the presence of a vegetation type that the PFG is characteristic of; see Boulangéat et al. 2014b). Resulting values of model specificity (proportion of true positives), model sensitivity (proportion of true negatives) and error rate (proportion of false positives and false negatives) were compared with those obtained from habitat suitability models (HSM). Error rates in bold indicate higher predictive accuracy when compared to the previously validated version.

PFG	Sensitivity		Specificity		Error rate	
	FATE-HD w/ drought	HSM	FATE-HD w/ drought	HSM	FATE-HD w/ drought	HSM
C1	0.76	0.87	0.45	0.51	0.51	0.44
C2	0.84	0.00	0.57	1.00	0.38	0.19
C3	0.94	0.96	0.49	0.47	0.31	0.31
C4	0.42	0.75	0.88	0.64	0.21	0.34
C5	0.26	0.52	0.75	0.57	0.31	0.44
C6	0.60	0.64	0.57	0.60	0.43	0.40
H1	0.84	0.00	0.41	1.00	0.44	0.36
H2	0.91	0.93	0.12	0.20	0.67	0.60
H3	0.10	0.78	0.91	0.44	0.21	0.51
H4	0.17	0.57	0.87	0.62	0.21	0.38
H5	0.88	0.88	0.25	0.32	0.59	0.54
H6	0.64	0.61	0.55	0.59	0.43	0.40
H7	0.63	0.72	0.34	0.33	0.60	0.59
H8	0.52	0.52	0.67	0.71	0.34	0.30
H9	0.24	0.63	0.70	0.58	0.33	0.42
H10	0.47	0.52	0.59	0.61	0.42	0.40
P1	0.35	0.75	0.88	0.56	0.15	0.43
P2	0.31	0.56	0.84	0.64	0.17	0.36
P3	0.10	0.64	0.97	0.66	0.06	0.34
P4	0.35	0.62	0.77	0.66	0.28	0.34
P5	0.57	0.60	0.84	0.78	0.17	0.22
P6	0.42	0.63	0.74	0.47	0.27	0.53
P7	0.08	0.22	0.93	0.81	0.09	0.21
P8	0.15	0.06	0.90	0.98	0.12	0.04

Studying ecosystem stability to global change across spatial and trophic scales

Table S5. Models of the response of forest and shrubland expansion to drought and land-use factors. Effects of drought frequency (DRfreq), drought intensity (DRint) and land-use (LU) on the rates of forest and shrubland expansion (RFE and RSE, respectively) were assessed using Analysis of Variance (ANOVAs) run for three different time frames (0-49 years, 50-149 years and 150-200 years). Interactions between factors are denoted with a “:”, and significant F values ($P < 0.05$) are shown in bold. Forest models are models F1, F2 and F3 and shrubland models are S1, S2 and S3.

Time frame		F value
Years 0-49	Model F1 RFE ~ DRint + DRfreq + DRint:DRfreq	$F_{15,80} = 13.24$
	Model S1 RSE ~ DRint + DRfreq	$F_{7,88} = 10.98$
Years 50-149	Model F2 RFE ~ LU + DRint + DRfreq + LU:DRint + LU:DRfreq + DRint:DRfreq	$F_{23,72} = 6.813$
	Model S2 RFE ~ LU + DRint + DRfreq	$F_{8,87} = 19.48$
Years 150-200	Model F3 RFE ~ LU	$F_{1,94} = 4.141$
	Model S3 RSE ~ LU + DRint + DRfreq + DRint:DRfreq	$F_{16,79} = 15.92$

Appendices - Appendix 2: Supplementary materials to Chapter I

Table S6. Effects of drought and land-use factors on forest and shrubland rates of expansion. Effects of drought frequency (DRfreq), drought intensity (DRint) and land-use (LU) on the rates of forest and shrubland expansion (RFE and RSE, respectively) were assed using Analysis of Variance (ANOVAs) run for three different time frames (0-49 years, 50-149 years and 150-200 years). Forest models are models F1, F2 and F3 and shrubland models are S1, S2 and S3. Interactions between factors are denoted with a “:”, and significant main effects or interactions (F values for which $P < 0.05$) are shown in bold. ‘Df’, ‘sum sq.’ and ‘mean sq.’ stand for degrees of freedom, sum of squares and mean squares, respectively. Factors are order by decreasing F value. See Table S5 in this appendix for model formulas.

			Df	Sum Sq	Mean Sq	F value
Years 0-49	Model F1	DRint	3	25.62	8.54	48.38
		DRfreq	4	4.03	1.01	5.71
		DRint:DRfreq	8	5.39	0.67	3.82
		Residuals	80	14.12	0.18	
	Model S1	DRfreq	4	3.66	0.91	15.12
		DRint	3	0.99	0.33	5.46
		Residuals	88	5.32	0.06	
Years 50-149	Model F2	DRint	3	3.07	1.02	22.67
		LU	1	0.72	0.72	15.94
		DRfreq	4	1.04	0.26	5.78
		LU:DRint	3	0.62	0.21	4.57
		LU:DRfreq	4	0.81	0.20	4.48
		DRint:DRfreq	8	0.81	0.10	2.25
		Residuals	72	3.24	0.05	
	Model S2	DRint	3	0.57	0.19	22.05
		DRfreq	4	0.73	0.18	21.40
		LU	1	0.03	0.03	4.10
		Residuals	87	0.74	0.01	
Years 150-200	Model F3	LU	1	4.24	4.24	4.14
		Residuals	94	96.22	1.02	
	Model S3	LU	1	10.02	10.02	130.74
		DRint	3	6.02	2.01	26.19
		DRfreq	4	2.36	0.59	7.68
		DRint:DRfreq	8	1.12	0.14	1.83
		Residuals	79	6.06	0.08	

Supplementary Figures

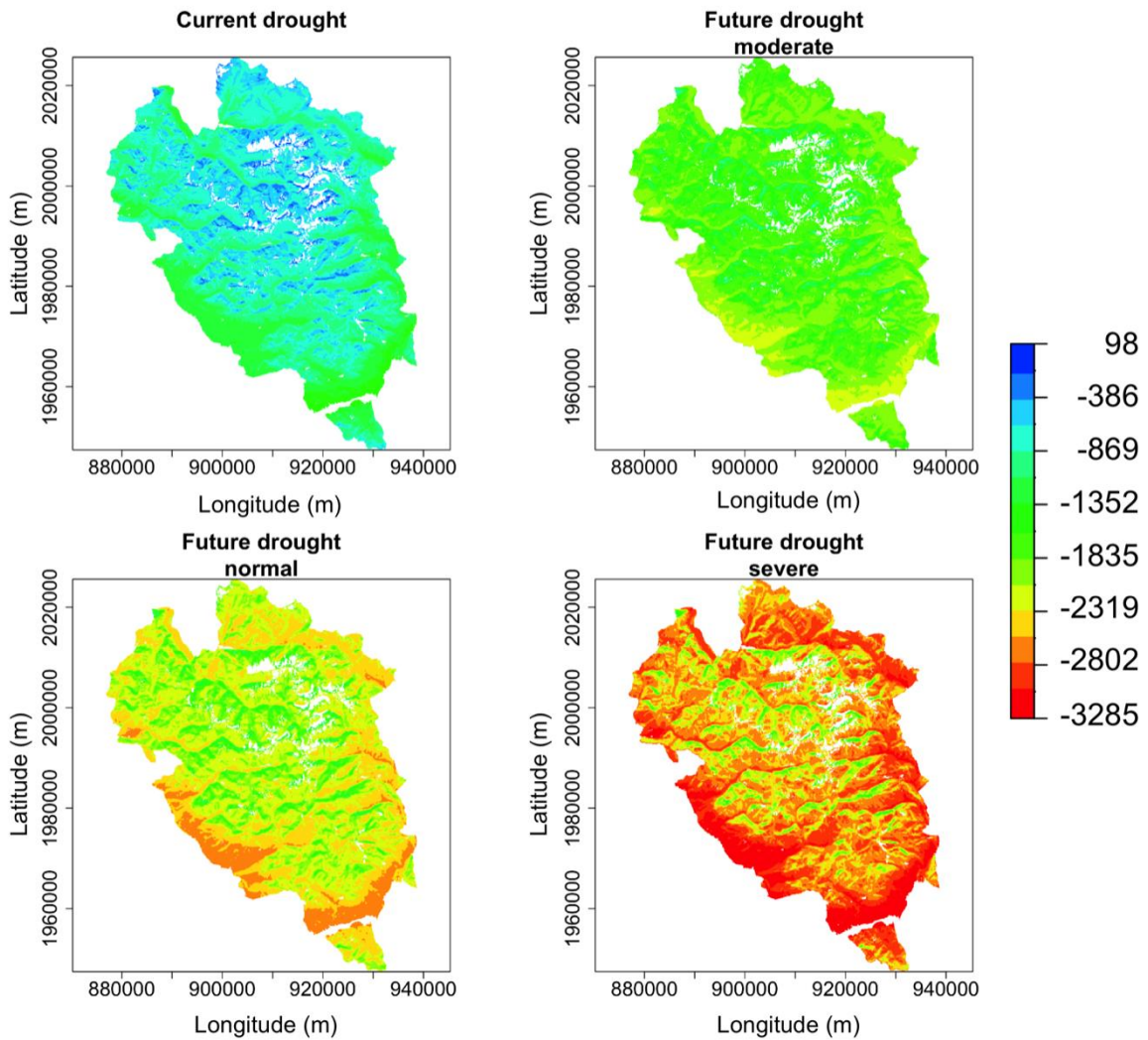


Figure S1. Current and future drought intensity (Din) maps. Drought events were simulated using Din (minimum yearly moisture index) maps that were fed into FATE-HD on a yearly basis. Current Din values were calculated as the average Din per pixel across years 1961-1990. Future 'normal' Din values were calculated from climate predictions for 2080 (following the A1B scenario; see FATE-HD 'base model' description in this appendix for further details), which were increased by 20% to calculate future 'moderate' Din values, or decreased by the same amount to calculate future 'severe' Din values (note that lower Din values cause more severe droughts).

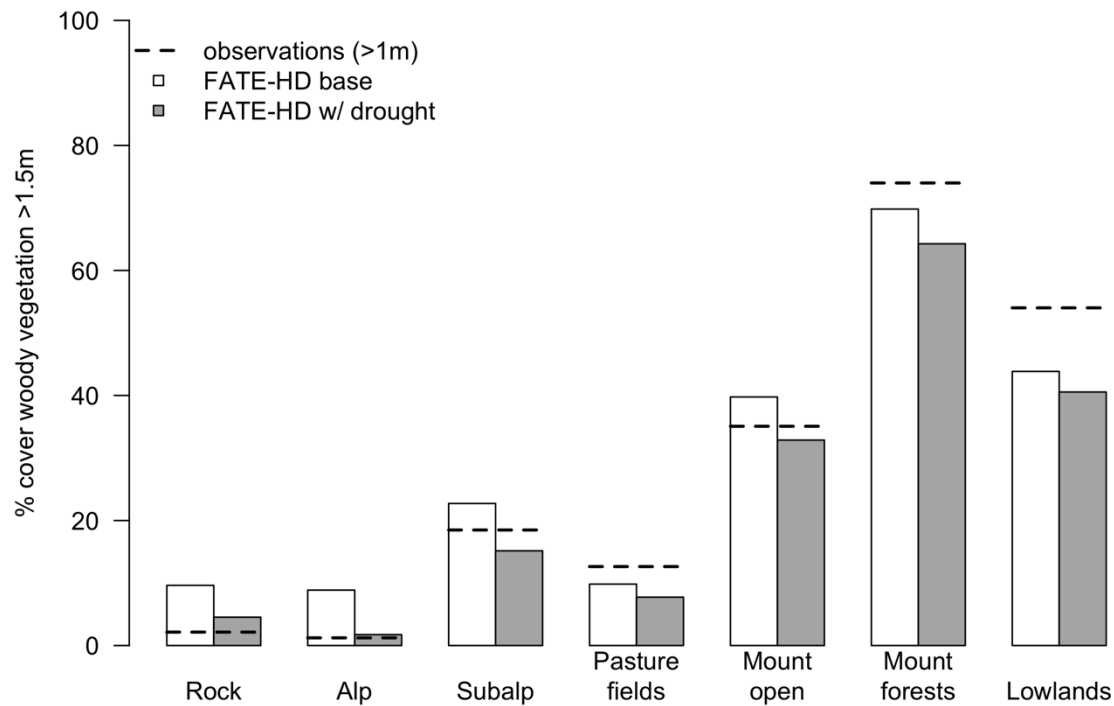


Figure S2. Observed vs. simulated tree cover in different habitats with and without drought effects. Percentages of observed and simulated tree cover were compared for seven broad habitat categories: rocky habitats (Rock, 29 791 pixels), alpine non-managed habitats (Alp, 2 154), subalpine non-managed habitats (Subalp, 5 544), managed habitats for grazing and mowing at all elevations (Pasture fields, 3 053), mountainous open habitats (Mount open, 779), young and mature mountainous forests (Mount forests, 8 881) and habitats of Mediterranean and colline (hill) vegetation (Lowlands, 390). Dashed lines indicate observed tree cover percentages, white bars are the predicted percentages of woody vegetation using the FATE-HD base model and grey bars the predicted percentages using the model with implemented drought effects.

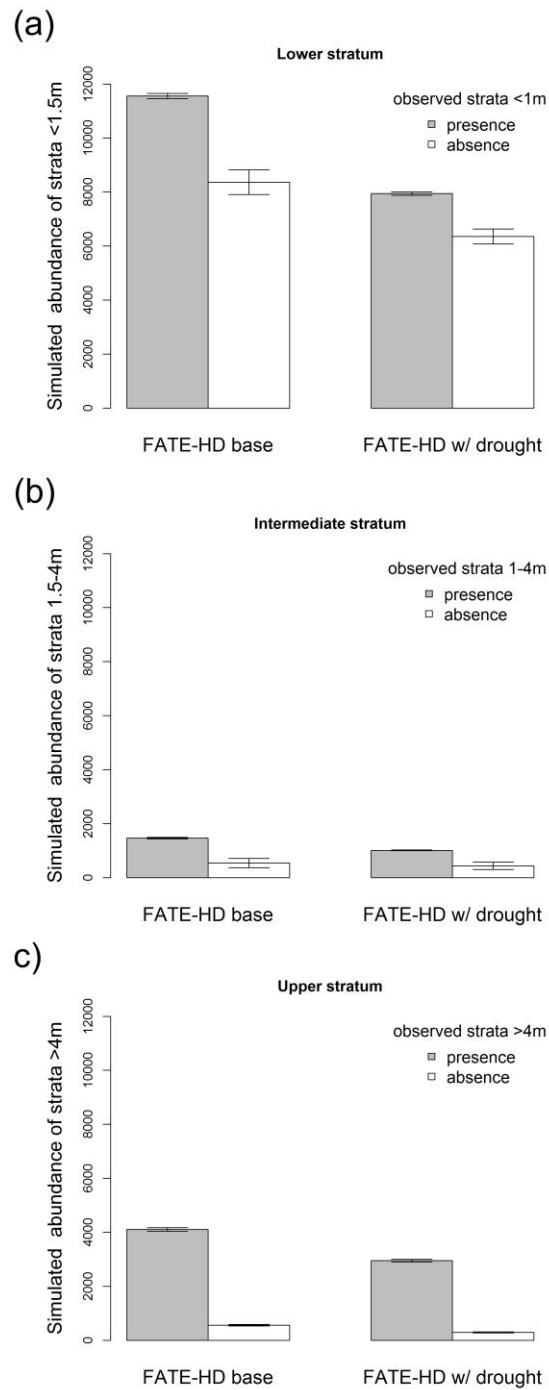


Figure S3. Observed vs. simulated strata abundances with and without drought effects. Observed presences and absences of three levels of vegetation strata (grey and white bars, respectively) are shown in relation to the predicted abundances (in y-axis) of the base model and the model with implemented drought effects. Note that lower strata observations correspond to vegetation up to 1 m tall, whereas the simulated first stratum represents vegetation up to 1.5 m.

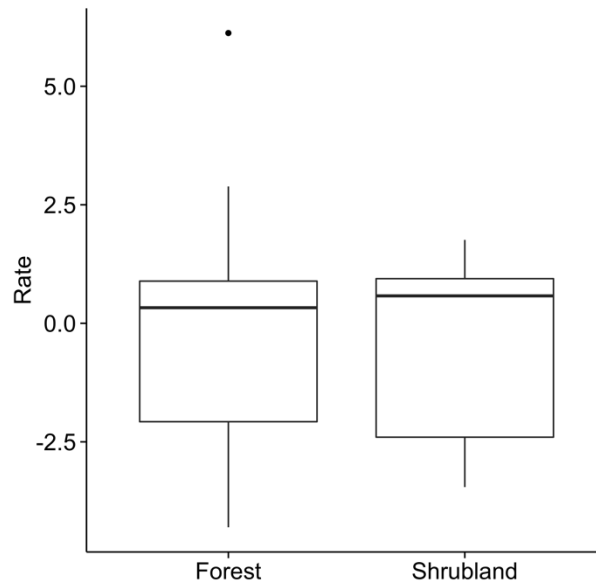


Figure S4. Rates of forest and shrubland expansion across scenarios and simulation repetitions, excluding baseline scenarios. Rates of forest expansion (RFE) towards higher elevations were not different from those of shrublands (RSE) (medians of RFE and RSE across scenarios were approximately 0.33 and 0.58, respectively, and their distributions were not significantly different: Mann-Whitney $U = 34464$, $n_{RFE} = n_{RSE} = 270$, $P = 0.27$). Boxes indicate inter-quantile ranges (IQR; distance between the first and third quantiles), with the median indicated by horizontal line. Upper and lower whiskers extend until the maximum and minimum values within $1.5 \times$ IQR and outliers are shown as points.

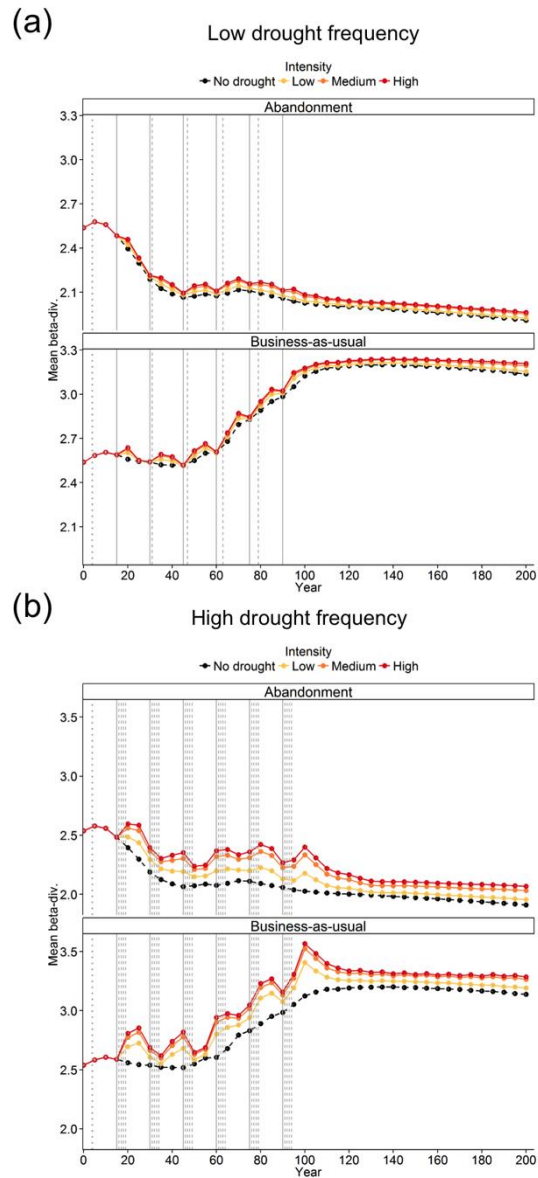


Figure S5. Effects of drought intensity (colour coded) and land-use practices on spatial β -diversity are shown for scenarios of a) low drought frequency (droughts at every 16 years) and b) high frequency (droughts every two years). Spatial β -diversity was calculated every five years, across all pixels within forest-grassland ecotone boundaries defined at year 0 in each scenario, and averaged across simulation repetitions. Vertical grey lines indicate climate changes (full lines) and drought events (dashed lines); land-use changes (abandonment) were implemented at year 4. Standard error bars are also shown in grey for each point.

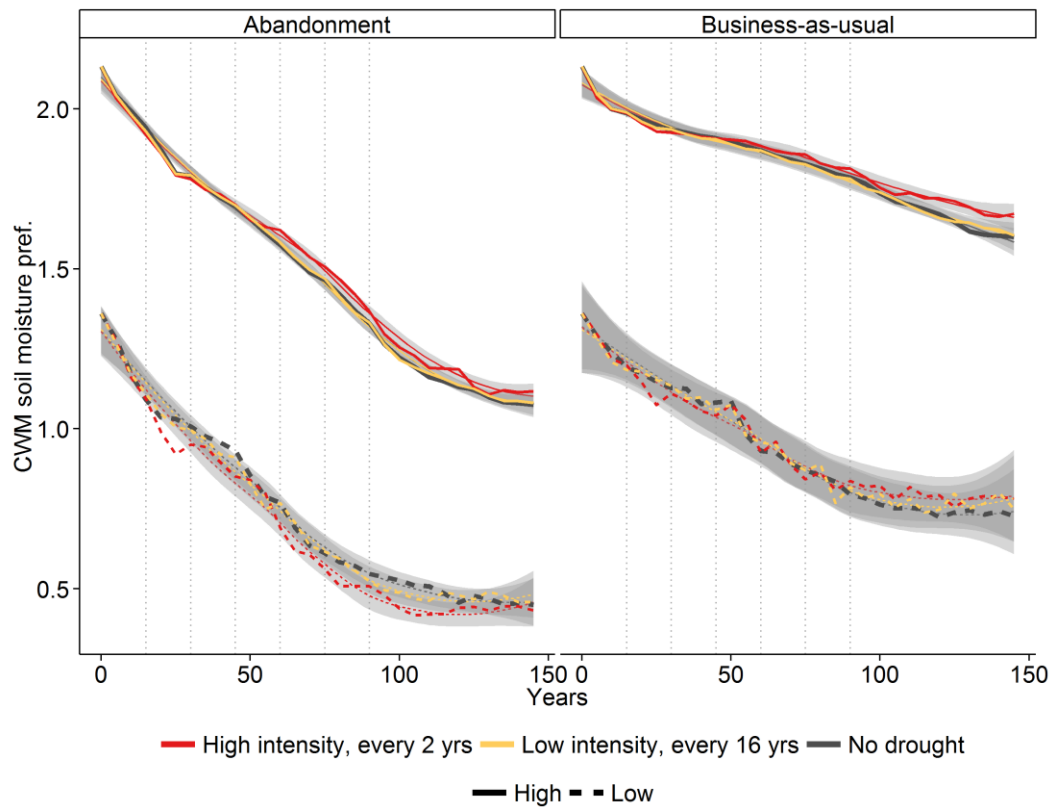


Figure S6. Temporal evolution of community-weighted mean (CWM) soil moisture preference. Effects of drought intensity and frequency (colour coded) and land-use practices on the temporal trends of CWM soil moisture preference are shown for two elevation bands within the forest-grassland ecotone. Elevation bands were defined as ecotone pixels below 1500m (low elevation – dashed lines) and ecotone pixels above 2000m (high elevation – full lines), which corresponded to the first and third quantiles of elevation values in the ecotone (rounded to the nearest hundred). In the figure, we show CWM values averaged across 10 pixels that were sampled for each elevation band. The same pixels were used across scenarios, years and simulation repetitions (results being averaged across repetitions). For each case, we fitted a loess smooth function, for which confidence intervals (95%) are shown as semi-transparent grey areas. Vertical dashed lines indicate climate changes; land-use abandonment was implemented from year 4 onward.

APPENDIX 3: SUPPLEMENTARY MATERIALS TO CHAPTER II

Bandwidth selection for hypervolume calculation

The calculation of hypervolumes requires choosing a kernel bandwidth and quantile threshold that allow avoiding disjunctions, or ‘holes’. Briefly, the calculation of a hypervolume for a set of points involves the sum of axis-aligned density kernels estimated for each point, in each dimension (Blonder *et al.* 2014); for small kernel bandwidths, or large threshold quantiles, the density kernels will include fewer of the adjacent points leading to a small hypervolume, with points appearing disjunct from the others (Blonder *et al.* 2014). Therefore, a large enough bandwidth (or small enough quantile threshold) must be chosen to avoid disjunctions. Since the choice of bandwidth will affect hypervolume size, we chose the same bandwidth to calculate all hypervolumes for a given component (raw and relative plant functional group, PFG, abundances or CWM trait values), so that hypervolumes could be directly compared. As for the quantile threshold we kept it at 0% following Blonder *et al.* (2014).

Optimal bandwidths were obtained by first calculating all hypervolumes (within a set of components) using a “free bandwidth” option⁸. This option allows an optimisation of the bandwidth value in function of the *disjunct factor*.

Given a starting value of bandwidth, hypervolumes are calculated and their disjunct factor is checked. The disjunct factor is the ratio between the size of the calculated hypervolume and the size of a hypervolume constructed from the same data with disjunct data points (Blonder *et al.* 2014). Values > 0.9 indicate that the hypervolume has ‘holes’ and should be avoided by increasing the bandwidth value. When this occurs, the bandwidth value is increased by 0.05 and the hypervolumes are re-calculated. The disjunct factor of the new hypervolumes is checked and bandwidth is further increased, if necessary.

We ran this process for all hypervolumes in all sets of components, with starting bandwidth values of 0.1, which were increased in steps of 0.05, when necessary, until the disjunct factor was ≤ 0.9 . The maximum bandwidth value obtained across communities (i.e. combinations of scenario, habitat-land-use and repetitions) was then used as the fixed bandwidth value to re-calculate all hypervolumes. This ensured that all hypervolumes of a set of components were built with the same bandwidth value and that this value guaranteed a disjunct factor ≤ 0.9 . For a) the analysis of differences between ‘stable’ states, bandwidths were 0.4 raw PFG abundances and 0.1 for relative PFG abundances and trait values. For b)

⁸ See R scripts in Appendix S5 of the electronic supplementary materials published in Barros *et al.* (2016c).

the analysis of temporal stability, bandwidths were 0.75 for raw PFG abundances and 0.1 for relative PFG abundances.

Bandwidth sensitivity analysis

We assessed the effect of changing bandwidths by running a sensitivity analysis on a habitat under two types of land-use management. Thicket and scrubland areas had very consistent results across our analysis and provided two opposite extremes when under a scenario of land-use intensification: when areas grazed at low intensity ('grazed areas 1') were intensified hypervolumes did not intersect, whereas mown areas (which did not suffer land-use changes) always intersected. For each case, we built 10 pre- and 10 post-perturbation hypervolumes for different bandwidths, ranging from 0.1 to 1.0, in steps of 0.5. This one done for both raw PFG abundances and CWM trait values.

As expected, larger in bandwidths resulted in larger overlaps. For intensified grazed areas, results were qualitatively stable (i.e. overlap = 0) across the range of bandwidths tested in the case of raw PFG abundances, and up to 0.55 in the case of trait values (see Fig. S11 in this appendix). Whereas in mown areas, intersections (overlap > 0) were present across all bandwidth sizes, except for one repetition of the smallest bandwidth (note that values of overlap were very small for this bandwidth value; Fig. S11 in this appendix). This meant that in neither case did our optimal bandwidths significantly affect the probability of an intersection (tested using a Generalised Linear Model with a *logit* link function to estimate the effect of bandwidth and land-use type on the probability of intersection; neither had a significant effect, p -value > 0.05). Also, increases in overlap size due to a larger bandwidth do not influence our results qualitatively, since they occur across all scenarios and habitat-land-use combinations.

FATE-HD model description and simulation workflow

Model description

FATE-HD has been validated for the different plant communities present in the Ecrins National Park (ENP), situated in the southeast of France in the French Alps and covering an area of 178 400 ha. The ENP is characterized by mountainous to alpine ecosystems, its elevation ranging from 669m to 4102m a.s.l. Although large areas of the park are managed and used for different activities (around 68% of the total area), the park is a very diverse area with c. 2000 plant species. Grazing is the most important economic activity (occupying 48%

of the total area), followed by forestry (10.5%) and agriculture (9.8%) (Esterni *et al.* 2006). Vegetation states are mostly maintained by abiotic conditions or land-use activities and can thus be expected to shift under climate and land use changes.

FATE-HD currently simulates 24 plant functional groups (PFGs) and five different height strata (0-1.5m; 1.5-4m; 4-10m; 10-20m; taller than 20m). They are divided into 6 chamaephyte groups (only present in the first height stratum, except for one which reaches the second one), 10 herbaceous groups (mostly hemicryptophytes and only present in the first height stratum) and 8 phanerophyte groups (all reaching at least the third height stratum, 6 reaching the fourth stratum and two reaching the fifth). Population dynamics, dispersal and competition for light resources are all explicitly included in the model for each PFG, being simulated across time and space. Population dynamics partially depend on habitat suitability, which is calculated from bioclimatic variables (Thuiller *et al.* 2009) and includes a stochastic component in order to simulate yearly oscillations of habitat quality. Climate changes, when introduced, affect habitat suitability by changing bioclimatic variables used to calculate it. Dispersal of PFGs is modelled for both long and short distances, which depend on the PFG in question. Competition for light resources is also modelled according to PFG type and stratum, as both differ in relation to their shade tolerance. The amount of shade is calculated per cell in function of the abundance of PFGs abundances per stratum. Disturbances are included in the model under two forms: grazing and mowing. Both grazing and mowing affect vegetation once a year, and grazing has three levels of intensity, low (1), medium (2) and high (3). They affect juvenile and mature plants abundances differently, depending on PFG responses to these disturbances and on an annual basis (see Boulangeat *et al.* 2014b for further information).

Land-use and climate changes

Climate changes were simulated according to IPCC previsions of the A1B scenario for years 2020, 2050 and 2080 and fed into future habitat suitability (HS) maps. These maps were then interpolated between time steps 2020, 2050 and 2080 to obtain a more gradual change at every 15 years for 90 years and later fed into FATE-HD simulations (Boulangeat *et al.* 2014a).

Land-use changes followed one of three types: continuation of present management practices (business-as-usual), abandonment of all grazing and mowing activities and intensification of grazing in already grazed areas (to high intensity) with creation of new grazed and mown areas (Boulangeat *et al.* 2014a).

Community/habitat types

Stability analysis fell unto communities, which were defined per habitat type following the present DELPHINE habitat classification of the ENP (Esterni *et al.* 2006). According to the DELPHINE classification there are 13 broad habitat categories present in the Ecrins (Table S4 in this appendix). Non-colonized rocky habitats and rocky habitats in colonization were grouped due to their similarity. Habitats where no PFGs are present (glaciers, eternal snows and lakes), very specific habitats that FATE-HD cannot reproduce (ravines and wetlands) and highly artificial areas were excluded from the analysis (Table S4 in this appendix). Habitat areas were then subset according to land-use type: non-disturbed areas, grazed areas of three intensities, mown areas and future grazed, mown and non-disturbed areas in the LU intensification scenarios.

Simulation workflow

Simulations started with an initialisation phase, ran over 1650 years, to achieve the current vegetation state of the ENP. It started with the seeding of all PFGs across the whole landscape for 300 years every year, followed by 300 years without any sort of LU management. Past deforestation was then simulated by cutting all PFGs in the second stratum or above (taller than 1.5m) from areas that are currently managed (years 600 and 800). Current management practices (grazing, with three levels of intensity and mowing) were only implemented afterwards (year 801) and the initialisation simulations were run until year 1650.

Using outputs from the last initialisation year (1650), we simulated 6 scenarios of LU and, or, CC changes. Land-use changes were the abandonment of all grazing and mowing activities (scenario 2), business-as-usual (control scenario) and intensification of grazing and creation of new grazed and mown areas (scenario 3; Fig. 10) and then were repeated with presence of climate changes (scenarios 4-6 in Fig. 10). Land-use abandonment or intensification were applied 4 years after starting the simulation from initialisation outputs, whereas climate changes were applied from years 15 to 90, at every 15 years. Scenario outputs were saved on a yearly basis during 500 years.

An additional simulation of 100 years with no LU changes and no CC was run from the outputs from the last initialisation year (1650), to be used for proof-of-concept ('POC') comparisons to the control scenario.

All simulations were replicated 3 times and used corresponding 3 replicates from initialisation outputs as starting points.

Results obtained using relative PFG abundances

Another set of hypervolumes based on plant functional groups' (PFGs) abundances were built using relative abundances. These were calculated on a yearly basis and, as with other hypervolumes, the last 100 years of the scenarios of change were compared against the full 500 years of the control scenario. Proof-of-concept simulations were also compared against the control.

Hypervolume comparisons based on relative abundances mostly reflect changes in the evenness/dominance structure of communities. This means that communities must undergo quite large changes in their structure and, or, composition to result in new, post-perturbation, hypervolumes that do not intersect with their pre-perturbation counterparts. Results were in agreement with this, as intersections between hypervolumes were more frequent than those obtained with raw abundances, mean overlaps were generally larger, centroid distances were smaller and changes in hypervolume size (Δ size) were extremely small (see Figs. S12a, S13a and S14a in this appendix). In accordance with results from raw abundances, climate change (CC) led to larger overall differences between pre- and post-perturbation communities. The combination of CC and land-use abandonment led to generally larger departures from initial community states, which was not always evident from raw PFG abundances. All of these three metrics were mostly affected by CC and land-use-changes (LUC) (Table S5 in this appendix). Despite habitat-land-use combinations having a lower importance, some have shown to be more or less stable. For instance, low intensity grazing areas that suffered intensification showed consistently large departures from their pre-perturbed states across habitat types (see scenario 3 in 'grazed areas1' panel, Figs. S12b and S13b in this appendix), whereas those that only suffered CC remained generally similar after perturbations (see scenario 5 in 'grazed areas1' panel, Figs. S12b and S13b in this appendix). As with raw PFG abundances, mown areas (particularly in lowlands and thickets/scrublands) showed the largest changes in hypervolume size, mostly towards lower values (see 'mown areas' panel in Fig. S14b in this appendix).

Finally, results for the analysis of the stability of overlap in time are in accordance with the patterns just observed. Like when comparing two states, tracking stability in time using relative abundances resulted in slower decreases in overlap in the communities under focus (Fig. S15 in this appendix), than when using raw abundances. However, the patterns obtained were different (note that in Fig. S15 of this appendix overlap was scaled using a square-root, but this does not change the qualitative interpretation of results). For instance, intensively

grazed areas ('grazed areas 3') were the least stable communities in both habitat types (instead of mown areas, as seen with raw PFG abundances) and thickets and scrublands appear to be more stable than grasslands (with lower rates of decrease in overlap). This indicates that, although raw PFG abundances were quickly and strongly affected by changes in climate in both habitats and across land uses, thicket and scrubland community structure and composition were generally more stable, while grassland community structure and composition were stabilised under low intensity grazing, or no disturbances.

All in all, these results highlight that community structure remained more stable than PFG abundances in general, although being affected by both climate and land-use changes, the effects of which changed depending on the type of habitat and land-use management regime. Moreover, these results highlight the importance of taking care when choosing the community components that will constitute hypervolumes. As with choosing which taxonomic or functional diversity indices to use when studying perturbation effects, choosing to consider raw or relative abundances depends on the type of community changes one is interested in investigating.

Choice and analysis of complementary metrics

In this appendix, we present the rationale behind our selection of complementary metrics, as well as two additional functional diversity (FD) indices that were not presented in the main text, their statistical analyses and associated results. Results presented here are focused on these additional FD indices and we briefly discuss why they have not been included in the final manuscript.

Full set of complementary metrics

In the main text, we have presented 4 different complementary metrics that reflected changes in taxonomic (inverse Simpson concentration) and functional diversity (functional evenness and functional dispersion), and productivity (total plant functional group, PFG, abundances). However, in respect to FD, we have additionally calculated functional richness (FRic) and functional divergence (FDiv; Villéger *et al.* 2008) that were later excluded from the main text (see below).

Indices of taxonomic and functional diversity were chosen because they complemented the information given by hypervolumes built from raw PFG abundances or from community weighted mean (CWM) trait values. The inverse Simpson concentration reflects changes in PFG richness and evenness, which may not be reflected by hypervolumes based on raw

abundances. Functional richness, evenness and divergence are three complementary, but independent, indices that reflect the occupied volume in the trait space, the regularity of abundances in trait space and how they diverge from each other (respectively; Villéger *et al.* 2008; Pavoine & Bonsall 2011; Tucker *et al.* 2016). Functional dispersion, is similar to FDiv, but accounts for the total volume occupied by PFGs in the trait space (Laliberté & Legendre 2010). These indices decompose the information accounted for in hypervolumes and offer a more detailed analysis of functional changes in the community. Lastly, productivity was included as a measure ecosystem functioning, following biodiversity and ecosystem functioning (BEF) studies.

Statistical analyses

Responses of diversity indices and productivity were fit with linear models using generalised least squares, with errors allowed to have an autoregressive structure at time lag-1 (the value of the correlation varying between each case). In parallel to what was done for hypervolume calculations, these analyses were done on the last 100 years of data; however, replicates were averaged. Time series of the control scenario (rather than proof-of-concept, ‘POC’, comparisons) were used as “no change” data that corresponded to no climate and no land-use changes. Because the experimental design was not balanced (i.e. disturbances like future grazing and mowing were only applied on scenarios 3 and 6) two sets of models were calculated. The first, ‘set 1’, aimed at analysing the effect of LUC, CC on habitats under current land-use practices (note that under scenarios of LU intensification – scenarios 3 and 6 – present grazing areas become grazed at high intensity). The second, ‘set 2’, aimed at analysing the effect of CC and habitat-land-use combinations on scenarios of LU intensification. For all models, future non-disturbed areas were grouped with non-disturbed areas, as they corresponded to the same treatment. Model selection followed AIC scores from more complex to simpler models. Model results were analysed in terms of the importance of main effects and interaction effects, and the differences between factor levels were analysed graphically.

No temporal autocorrelation was found when modelling the response of functional evenness (FEve) and functional dispersion (FDis) to CC and habitat-land-use combinations under the intensification scenario (set 2). Hence, their responses were analysed using analyses of variance (ANOVAs).

Results – FD indices

Since results concerning taxonomic diversity and productivity are presented in the main text, we focus here on results obtained for FD indices.

The importance of climate change (CC), land-use changes (LUC) and habitat-land-use combinations varied depending on the FD index (Table S3 in this appendix). For instance, habitat-land-use combinations had a comparatively strong effect on functional richness (FRic), but a weak effect on FEve and FDiv (set 1 models, Table S3 in this appendix). A graphical analysis of model fitted values showed that FRic and FDiv were the least responsive to the effects of predictor variables (Figs. S8a,d in this appendix). Functional richness was equally low among scenarios for non-disturbed habitats and those under low and medium intensity grazing. Particular habitats, such as forests, thickets and scrublands and woodland mosaics showed higher FRic when under CC and high intensity grazing (Figs. S8a and S9a in this appendix). This can be a reflection of increasing abundances of woody species, which benefit from climate warming in Alpine ecosystems (Tasser & Tappeiner 2002; Asner *et al.* 2004). In mown areas FRic was generally highest in lowlands under land-use intensification and, for other habitats, it seemed to also benefit from CC (Figs. S8a and S9a in this appendix). As for FDiv, increases were mostly linked to land-use intensification and climate change (Figs. S8d and S9d in this appendix). Contrarily to FRic, FDiv was generally lower in mown areas, but being increased under land-use intensification.

Functional evenness and FDis were more responsive to CC, LUC and habitat-land-use combinations (Figs. S8b,c and S9b,c in this appendix). Their patterns were generally similar, with larger increases when land-use was abandoned and there was no CC. In some cases, however, FEve and FDis did not match. For instance, areas grazed at high intensity benefitted from CC in terms of FDis, but not so much in terms of FEve ('grazed areas3' in scenarios 5 and 6, Figs. S8b,c in this appendix). In mown lowland habitats FDis also increased, whereas it decreased for FEve. These results indicate that in these communities functional variance increased as PFGs became less equally spread in trait space (Figs. S8b,c and S9b,c in this appendix).

Selecting relevant functional diversity indices

As a rule of thumb, we propose choosing functional indices that, like hypervolume metrics, can reflect changes in a community's functional characteristics. Following Pavoine & Bonsall (2011) and Tucker *et al.* (2016), the indices we measured can be organised into three classes of measures of multivariate distances. Each class groups several indices together (Pavoine & Bonsall 2011; Tucker *et al.* 2016), but here we use only the most common ones.

- Richness. We use FRic (measured as the volume of the minimum convex hull occupied by all species, or in our case PFGs, in the trait space; Villéger *et al.* 2008) that indicates changes in the number of functionally unique identities in the community;
- Regularity (or evenness). We use FEve (Villéger *et al.* 2008) that indicates changes in the regularity of the distribution of species and their abundances in the functional trait space, and can be related to the variance in functional distances among PFGs (low variance = high regularity);
- Divergence. We use both FDis and FDiv that indicate changes in the mean abundance-weighted distances of species in functional space to the centroid of the functional space occupied by the community (which is also abundance-weighted for FDis, but not for FDiv; Villéger *et al.* 2008; Laliberté & Legendre 2010; Mouillot *et al.* 2013), thus providing a measure of the average functional distances between PFGs (Pavoine & Bonsall 2009, 2011; Laliberté & Legendre 2010).

In our case, measures of FRic and FDiv had very similar results across scenarios of CC and LUC. Since FRic does not take PFG abundances into account, unless habitats gain or lose functionally distinct PFGs, FRic is expected to remain stable. Similarly, because in FDiv the functional centroid solely based on the PFGs at the vertices of the occupied functional space and is not abundance-weighted (functionally extreme PFGs; Villéger *et al.* 2008), FDiv values will remain fairly constant if changes in PFG abundances do not occur at the extremes of the functional trait space occupied by the community. Thus, FRic and FDiv are more affected by changes occurring at the extremes of the trait gradients. Hence, in our case, FEve and FDis provided a finer indication of changes in the functional structure of a community than FRic and FDiv, respectively.

We nevertheless believe that calculating a full set of FD indices that are uncorrelated (like FRic, FEve and FDis, or FDiv) from which some can later be selected, is not of bad practise. Since these indices provide information on different aspects of FD, unless there are clear expectations or convictions regarding changes of a particular aspect, their analysis can only be of interest to the understanding of functional changes that might have occurred in a community.

Supplementary results and discussion

Supplementary results

We present here the results obtained with raw PFG abundances and community weighted mean (CWM) trait values hypervolumes in more detail, especially in relation to habitat-land-use combinations.

Hypervolume intersections and overlap

The overlap between pre- and post-perturbation hypervolumes was mostly affected by climate change (CC) and land-use changes (LUC) (Table S3 in this appendix); yet, results also varied between habitats. Overlaps between raw PFG abundances were uncommon across most habitat-land-use combinations subjected to scenarios of change. However, comparisons between trait hypervolumes showed that areas kept undisturbed from both LUC and CC (non-disturbed areas in scenario 2 and future non-disturbed areas in scenario 3) were predicted to remain functionally more similar to their control scenario counterparts, as well as areas grazed at high intensity that suffered no changes ('grazed areas 3' in scenario 3) and thickets under mowing regimes (Fig. S3b in this appendix). Similar results were obtained for relative PFG abundance hypervolumes (see *Results obtained using relative PFG abundances* in this appendix).

Distances between hypervolumes and changes in size

Habitat-land-use combinations also had a weaker effect on mean PFG abundances and trait values than CC and LUC (Table S3 in this appendix). Nevertheless, changes in mean trait values seemed to depend on habitat type in intensively managed areas (see between-habitat differences in 'grazed areas3', mown areas and future grazed and mown areas; Fig. S5b in this appendix). Also, undisturbed rock and scree vegetation showed consistently larger functional changes than other undisturbed habitats, but changes in PFG abundances were not as large, comparatively (see purple bars in present and future 'non-disturbed' areas, Fig. S5 in this appendix).

Changes in the variance of PFG abundances and trait values, however, were more affected by habitat-land-use combinations (Table S3 in this appendix). Areas grazed at high intensities and mown areas showed larger Δ size values across several habitats and scenarios of CC and LUC (see 'grazed areas3' and mown and future mown areas panels Fig. S6 in this appendix).

Finally, and in accordance with intersection results, the majority of unmanaged habitats seemed to suffer larger changes in mean PFG abundances than in CWM trait values, even

when suffering no CC (see non-disturbed and future non-disturbed areas in scenarios 2 and 3, respectively, in comparison to POC; Fig. S5 in this appendix), but this did not result in large changes in variance (Fig. S6 in this appendix).

Supplementary discussion

Taxonomic and functional changes in non-disturbed rock and scrub vegetation

Unlike other undisturbed habitats, rock and scree vegetation showed larger functional changes (relatively to taxonomic deviations) than other habitats, even under no climate change (non-disturbed areas in scenario 2 and future non-disturbed areas in scenario 3, Figs. S3b and S5b in this appendix). Rocky habitats can be found at relatively high elevations at the core of the Ecrins (Fig. S1 in this appendix), where environmental filtering is likely to lead to relatively low functional α -diversity (de Bello *et al.* 2013). Colonisations resulting from spill over effects could cause functional changes in these communities, even if not causing large changes on overall taxonomic and functional α -diversity (Figs. S7a and S8b,c in this appendix). Under climate change, rocky habitats have also shown larger changes in mean plant functional group (PFG) abundances and increases in PFG α -diversity, in opposition to other habitats (scenarios 4-6, Figs. S5a and S7 in this appendix). Although FATE-HD has a tendency to over-predict tree cover in rocky habitats (Boulangeat *et al.* 2014b), our results agree with observations of range expansions of alpine species towards higher elevations, accompanied by range contractions of sub-nival and nival species (Pauli *et al.* 2007; Gottfried *et al.* 2012).

Potential applications in terms of ecosystem resilience

Our approach does not yet provide a parallel with the quantification of resilience in terms of rates of return to stability after perturbations – engineering resilience – or the magnitude of perturbation a community can withstand before shifting states – ecological resilience (*sensu* Holling 1996; Gunderson 2000). Instead, considering multiple community components links different facets of biodiversity and ecosystem stability, a key aspect of ecosystem resilience (Norberg 2004; Cadotte *et al.* 2012; Mori *et al.* 2013). Nevertheless, we can foresee how the framework we provide can be related with the two aspects of resilience defined by Holling (1996). Understanding if the overlap between hypervolumes depends on the magnitude of the applied perturbation can provide clues as to the amount of change at community can suffer before shifting to another state, indicating the width of the basin of attraction and the

community's ecological resilience. On the other hand, the time it takes for hypervolumes to return to their original state after a perturbation can be related to engineering resilience. Also, time series of hypervolume metrics, such as hypervolume size, calculated in the vicinity of a state shift could be used to detect phenomena like critical slowing down and flickering (Scheffer *et al.* 2009; Dakos *et al.* 2012), which would be reflected in changes of statistical properties of the hypervolume metrics' time series. The limitations being that 1) very large and complete time series would be necessary to calculate enough hypervolumes and statistical analyses on their metrics, and 2) that early warning signals do not occur under several cases, such as systems under push-perturbations (non-gradual changes in external variables), or for systems with chaotic behaviour (Sharma *et al.* 2014; Dakos *et al.* 2015).

Importantly, our framework allows an analysis of ecosystem stability under different perspectives. Not only can it provide a measure of departures from equilibrium within a same basin of attraction (see Fig. 9e in Chapter II), but it can also be used to study alternative stable states (Fig. 9f in Chapter II) or shifts in the stable state *per se* after changes in the system's parameters (Beisner *et al.* 2003; Horan *et al.* 2011).

Supplementary Tables

Table S1. Plant functional groups and their trait values. Trait values were averaged across species for continuous traits and the majority class was taken for ordinal traits (Boulangeat et al. 2012). Life form classes are chamaephytes (C), herbaceous (H) and phanerophytes (P). We selected four traits, three reflecting the leaf-height-seed (LHS) plant ecology strategy by Westoby (1998) – average specific leaf area (SLA), log height, log seed mass – and one reflecting plant responses to grazing – palatability. Traits with an asterisk were log-transformed for all analysis to approach a normal distribution; however, in this table we present only the non-transformed values. SLA values for species of PFGs H10 and P8 obtained from Kattge et al. (2011). Table partially adapted from Boulangeat et al. (2012).

PFG	PFG description	Average SLA (mm ² /mg)	Height* (cm)	Seed mass* (mg)	Palatability (class)
C1	Thermophilous chamaephytes with long dispersal distances	19.21	27	23.91	3
C2	Alpine and subalpine chamaephyte species	18.02	13	0.38	3
C3	Chamaephytes with short dispersal distances	14.39	7	0.51	0
C4	Tall shrubs	16.83	209	192.99	2
C5	Dry climate mountainous to subalpine heath	8.28	76	75.01	0
C6	Wet climate mountainous to subalpine heath	13.40	18	39.50	2
H1	Alpine species (with no shade tolerance and with short dispersal distances)	17.22	17	0.86	3
H2	Mountainous species tolerant of nitrophilous soils and with long dispersal distances	22.11	42	4.04	3
H3	Mountainous to lowland species found in wet niches and with long dispersal distances	24.43	50	2.37	3
H4	Undergrowth and shadow-tolerant species, but that do not tolerate full light	29.76	76	0.36	0
H5	Mountainous to subalpine species, tolerant of dry soils and with short dispersal distances	20.71	40	1.94	3
H6	Tall plants typical of ‘mégaphorbiaies’, which can form undergrowth	28.21	73	2.31	3
H7	Species found in rocky habitats and undergrowth at all elevations	19.25	19	0.40	0
H8	Subalpine to alpine species not usually grazed and with short dispersal distances	23.11	19	0.89	0
H9	Short subalpine to alpine species with long dispersal distances	21.09	19	0.38	3
H10	Mountainous species, shade tolerant and with long dispersal distances	21.14	100	6.20	3
P1	Thermophilous pioneer trees (deciduous trees and pines)	12.03	1175	177.93	2
P2	Small deciduous pioneer trees (e.g. colonising riversides)	17.17	750	0.13	2
P3	Tall forest edge trees	15.30	1667	86.41	2
P4	Tall pioneer (larch)	10.06	2500	6.82	0
P5	Wet climate late succession trees	11.86	2500	114.06	2
P6	Dry climate intermediate succession trees	19.24	1650	6.10	2

Appendices - Appendix 3: Supplementary materials to Chapter II

P7	Small forest edge trees	15.65	600	78.27	2
P8	Small pioneer found in cold climates (white birch)	14.60	800	0.17	2

Table S2. Effects of climate change (CC), land-use changes (LUC), habitat-land-use combinations and management type on hypervolume metrics. Hypervolumes were compared using three metrics: proportion of overlap (overlap), distance between centroids and changes in hypervolume size (Δ size). Overlap was calculated as the ratio between the volume of intersection and the volume of the union. Δ size were calculated as the difference between the size post-perturbation hypervolume size and the control hypervolume size, after scaling all sizes in respect to the largest hypervolume obtained for a set of components. The response of each metric to climate changes, land-use changes and habitat-land-use combinations was modelled using analyses of variance (ANOVAs). To comply with linear models' assumptions (normality and homoscedasticity of residuals), we used a square-root transformation on overlap values (for both PFG and trait hypervolumes) and removed three extreme outliers from the trait hypervolumes Δ size data. In all cases, the full model provided the best AICc score. Effects of main factors and interaction terms are shown in decreasing order of F-statistic. 'Df' stands for degrees of freedom, 'Sum Sq' for sums of squares, 'Mean Sq.' for mean squares and 'F value' is the F-statistic.

		Df	Sum Sq	Mean Sq	F value	
PFG hypervolumes overlap						
$\sqrt{\text{Overlap}} \sim (\text{Habitat-land-use} + \text{CC} + \text{LUC})^{3\dagger}$	LUC	2	18.79	9.39	42945.73	*
	CC:LUC	2	18.72	9.36	42793.66	*
	CC	1	9.11	9.11	41649.23	*
	CC:Habitat-land-use	55	2.51	0.05	208.32	*
	Habitat-land-use	55	2.50	0.05	207.73	*
	CC:LUC:Habitat-land-use	61	0.41	0.01	30.58	*
	LUC:Habitat-land-use	61	0.38	0.01	28.76	*
	Residuals	476	0.10	0.00		
PFG hypervolumes centroid distances						
Centroid dist. $\sim (\text{Habitat-land-use} + \text{CC} + \text{LUC})^{3\dagger}$	LUC	2	3721.00	1860.50	130243.50	*
	CC	1	517.00	516.90	36184.44	*
	CC:LUC	2	316.00	157.90	11050.73	*
	LUC:Habitat-land-use	61	776.00	12.70	890.09	*
	Habitat-land-use	55	547.00	10.00	696.72	*
	CC:Habitat-land-use	55	200.00	3.60	254.09	*
	CC:LUC:Habitat-land-use	61	70.00	1.10	79.91	*
	Residuals	476	7.00	0.00		
PFG hypervolumes size change						

Appendices - Appendix 3: Supplementary materials to Chapter II

$\Delta\text{size} \sim (\text{Habitat-land-use} + \text{CC} + \text{LUC})^{3\ddagger}$	LUC	2	1.34	0.67	901.17	*
	Habitat-land-use	55	17.00	0.31	414.59	*
	LUC:Habitat-land-use	61	4.71	0.08	103.52	*
	CC	1	0.03	0.03	37.54	*
	CC:LUC	2	0.03	0.02	20.73	*
	CC:Habitat-land-use	55	0.79	0.01	19.24	*
	CC:LUC:Habitat-land-use	61	0.67	0.01	14.76	*
	Residuals	476	0.36	0.00		
Trait hypervolumes overlap						
$\sqrt{\text{Overlap}} \sim (\text{Habitat-land-use} + \text{CC} + \text{LUC})^{3\ddagger}$	CC	1	21.75	21.75	169764.50	*
	LUC	2	18.46	9.23	72055.50	*
	CC:LUC	2	16.93	8.46	66078.50	*
	Habitat-land-use	55	11.76	0.21	1668.80	*
	CC:Habitat-land-use	55	9.36	0.17	1328.60	*
	LUC:Habitat-land-use	61	5.33	0.09	682.40	*
	CC:LUC:Habitat-land-use	61	4.61	0.08	589.50	*
	Residuals	476	0.06	0.00		
Trait hypervolumes centroid distances						
Centroid dist. $\sim (\text{Habitat-land-use} + \text{CC} + \text{LUC})^{3\ddagger}$	LUC	2	155.14	77.57	290381.00	*
	CC	1	44.21	44.21	165496.00	*
	CC:LUC	2	19.44	9.72	36385.00	*
	Habitat-land-use	55	213.38	3.88	14523.00	*
	LUC:Habitat-land-use	61	120.54	1.98	7397.00	*
	CC:Habitat-land-use	55	64.81	1.18	4411.00	*
	CC:LUC:Habitat-land-use	61	41.16	0.67	2526.00	*
	Residuals	476	0.13	0.00		

Trait hypervolumes size change

$\Delta\text{size} \sim (\text{Habitat-land-use} + \text{CC} + \text{LUC})^{3\dagger}$	CC	1	0.04	0.04	1799.07	*
	CC:LUC	2	0.01	0.01	244.74	*
	CC:Habitat-land-use	55	0.22	0.00	190.56	*
	LUC	2	0.01	0.00	125.60	*
	Habitat-land-use	55	0.12	0.00	103.51	*
	CC:LUC:Habitat-land-use	60	0.12	0.00	98.05	*
	LUC:Habitat-land-use	61	0.08	0.00	59.62	*
	Residuals	474	0.01	0.00		

*Significant at p-value < 0.01.

†Superscript “3” indicates the inclusion of all main factors and their two-way and three-way interactions in the model.

‡Three extreme outliers were removed from this model in order follow linear models’ assumptions.

Appendices - Appendix 3: Supplementary materials to Chapter II

Table S3. Effects of climate change (CC), land-use changes (LUC), habitat-land-use combinations and management type on complementary metrics. Responses of taxonomic (PFG α -diversity) and functional diversity (FRic, FEve, FDis, FDiv), as well as productivity to effects of climate change, land-use change and habitat-land-use combinations were modelled for the last 100 years of the scenario and control simulations. To account for temporal autoregressive structures models were separated in two sets to have a balanced design. Models in 'set 1' investigated the effects of CC and LUC on "current" habitat-land-use combinations and models in 'set 2' investigated the effects of CC and all habitat-land-use combinations on scenarios of LU intensification. Model selection was based on AIC scores. The response of each metric to climate changes, land-use changes and habitat-land-use combinations was modelled accounting for an autoregressive structure at time lag-1. Not temporal autocorrelations were found for set 2 models of FEve and FDis, which were modelled using analyses of variance (ANOVAs). Best models were selected on the basis of AIC scores. Effects of main factors and interaction terms are shown in decreasing order of F-statistic. 'Df' stands for degrees of freedom, 'Sum Sq' for sums of squares, 'Mean Sq.' for mean squares and 'F value' is the F-statistic.

			Df	F-value	
SET 1	PFG α -diversity				
	AlphaDiv ~ (Habitat-land-use + CC + LUC) ^{3†}	(Intercept)	1.00	61.85	*
		CC	1.00	2.52	
		LUC	2.00	1.62	
		CC:LUC	2.00	0.87	
		Habitat-land-use	34.00	0.26	
		CC:Habitat-land-use	34.00	0.05	
		LUC:Habitat-land-use	68.00	0.04	
		CC:LUC:Habitat-land-use	68.00	0.01	
SET 2	PFG α -diversity				
	AlphaDiv ~ (Habitat-land-use + CC) ^{2†}	(Intercept)	1.00	22.48	*
		Habitat-land-use	48.00	0.21	
		CC	1.00	0.09	
		CC:Habitat-land-use	48.00	0.02	
SET 1	Trait α -diversity (FRic)				
	FRic ~ (Habitat-land-use + CC + LUC) ^{3†}	(Intercept)	1	518347.70	*
		Habitat-land-use	34	52210.80	*
		CC	1	26802.10	*
		LUC	2	13961.50	*
		LUC:Habitat-land-use	68	4160.20	*

Studying ecosystem stability to global change across spatial and trophic scales

	CC:LUC:Habitat-land-use	68	4124.60	*
	CC:LUC	2	3329.10	*
	CC:Habitat-land-use	34	3013.60	*
Trait α -diversity (FEve)				
FEve ~ (Habitat-land-use + CC + LUC) ^{3†}	(Intercept)	1	2852167.70	*
	LUC	2	22672.20	*
	CC	1	15177.60	*
	CC:LUC	2	10066.50	*
	Habitat-land-use	34	5504.80	*
	CC:Habitat-land-use	34	1249.60	*
	LUC:Habitat-land-use	68	1079.40	*
	CC:LUC:Habitat-land-use	68	588.60	*
Trait α -diversity (FDis)				
FDis ~ (Habitat-land-use + CC + LUC) ^{3†}	(Intercept)	1	19677794	*
	CC:LUC	2	86539	*
	Habitat-land-use	34	15511	*
	LUC	2	12258	*
	CC:Habitat-land-use	34	6257	*
	CC	1	5005	*
	LUC:Habitat-land-use	68	4541	*
	CC:LUC:Habitat-land-use	68	1757	*
Trait α -diversity (FDiv)				
FDiv ~ (Habitat-land-use + CC + LUC) ^{3†}	(Intercept)	1	62536563	*
	LUC	2	63151	*
	CC	1	6930	*
	Habitat-land-use	34	6524	*
	CC:LUC	2	4040	*
	LUC:Habitat-land-use	68	2234	*

Appendices - Appendix 3: Supplementary materials to Chapter II

	CC:Habitat-land-use	34	613	*
	CC:LUC:Habitat-land-use	68	292	*
SET 2	Trait α -diversity (FRic)			
	FRic ~ (Habitat-land-use + CC) ^{2†}	(Intercept)	1	251698.56 *
		Habitat-land-use	48	19933.83 *
		CC	1	7138.96 *
		CC:Habitat-land-use	48	3160.08 *
	Trait α -diversity (FEve)			
	FEve ~ (Habitat-land-use + CC) ^{2†}	Habitat-land-use	48	2024.01 *
	(ANOVA)	CC:Habitat-land-use	48	222.51 *
		CC	1	1.49
		Residuals	9698	
	Trait α -diversity (FDis)			
	FDis ~ (Habitat-land-use + CC) ^{2†}	CC	1	262057.00 *
	(ANOVA)	Habitat-land-use	48	64531.00 *
		CC:Habitat-land-use	48	17040 *
		Residuals	9800	
	Trait α -diversity (FDiv)			
	FDiv ~ (Habitat-land-use + CC) ^{2†}	(Intercept)	1	9080792 *
		Habitat-land-use	48	1198 *
		CC:Habitat-land-use	48	180 *
		CC	1	8 *
SET 1	Productivity			
	Productivity ~ (Habitat-land-use + CC + LUC) ^{3†}	(Intercept)	1	1501126403 *
		Habitat-land-use	34	130709416 *
		LUC	2	54725448 *
		CC	1	8782855 *
		CC:Habitat-land-use	34	2608206 *

Studying ecosystem stability to global change across spatial and trophic scales

	LUC:Habitat-land-use	68	2170306	*
	CC:LUC	2	136463	*
	CC:LUC:Habitat-land-use	68	41973	*
SET 2	Productivity			
	Productivity ~ (Habitat-land-use + CC) ^{2†}			
	(Intercept)	1	572526574	*
	Habitat-land-use	48	55372872	*
	CC	1	6101056	*
	CC:Habitat-land-use	48	1138545	*

*Significant at p-value < 0.01

†Superscripts “2” and “3” indicate the inclusion of all main factors, their two-way and three-way interactions (in case of “3”) in the model.

Appendices - Appendix 3: Supplementary materials to Chapter II

Table S4. Habitats used to define communities. Habitat classification followed the DELPHINE habitat classification of the Ecrins National Park (Esterni et al. 2006). Dashes indicate habitats removed from the analysis. Non-colonized and colonized rocky habitats were grouped under the “rocks” habitat type. FATE-HD output (yearly PFG abundances) was subset by habitat type and, within each habitat, by land-use type (grazed areas of intensities 1 to 3, mown areas, and non-disturbed areas and future grazed, mown and non-disturbed areas) resulting in 56 habitat-land-use combinations.

DELPHINE habitat code and designation	Details	Habitat
0. Glaciers and eternal snows		-
11. Lakes		-
14. Ravines	Water courses in deeply carved ravines	-
20. Wetlands	Swamps and stagnant water bodies	-
31. Non colonized rocks	10% or less vegetation cover	Rocks
36. Rocks in colonization	Scree and rocky areas with sparse vegetation	Rocks
40. Grasslands	Natural or artificial (includes cereal fields)	Grasslands
50. Lowlands	Alpine lowlands and lowlands with short woody vegetation (30-60cm) and some trees	Lowlands
60. Open habitats	Areas that can easily be invaded by shrubs and, or, trees; from hedged farmlands, to scrublands and grasslands and even scree and rocky cliffs	Open habitats
70. Semi-closed habitats	Generally mosaics of small woodlands and non-forested habitats that rapidly evolve to thickets or forests; composed of tall or short woody species, with 40-60% closure	Woodland mosaics
81. Closed habitats	Impenetrable scrublands or thickets, that may have resulted from woody encroachment from past agricultural abandonment	Thickets/Scrubs
83. Forests	Dense forests with understory communities of grasses and shrubs	Forests
90. Artificial areas	Highly artificial environments, from roads and buildings, to gardens, vineyards and poplar/aspen production fields	-

Studying ecosystem stability to global change across spatial and trophic scales

Table S5. Effects of climate change (CC), land-use changes (LUC), habitat-land-use combinations and management type on hypervolume metrics based on relative PFG abundances. Hypervolumes were compared using three metrics: proportion of overlap (overlap), distance between centroids and changes in hypervolume size (Δ size). Overlap was calculated as the ratio between the volume of intersection and the volume of the union. Size changes, or Δ size, were calculated as the difference between the size post-perturbation hypervolume size and the control hypervolume size. The response of each metric to climate changes, land-use changes and habitat-land-use combinations was modelled using analyses of variance (ANOVAs). To comply with linear model assumptions (normality and homoscedasticity of residuals), overlap values were modelled using a variant of the logit transformation, $\log[(y+c)/(1-y+c)]$ (where c is the absolute of the minimum non-zero observed value) and two extreme outliers were removed from the Δ size data. In all cases, the full model provided the best AICc score. Effects of main factors and interaction terms are shown in decreasing order of F -statistic. 'Df' stands for degrees of freedom, 'Sum Sq' for sums of squares, 'Mean Sq.' for mean squares and 'F value' is the F -statistic.

		Df	Sum Sq	Mean Sq	F value	
Overlap						
$\sqrt{\text{Overlap}} \sim (\text{Habitat-land-use} + \text{CC} + \text{LUC})^{3\dagger}$	CC	1	27.57	27.57	623862.00	*
	LUC	2	22.14	11.07	250489.00	*
	CC:LUC	2	7.83	3.92	88605.00	*
	Habitat-land-use	55	15.73	0.29	6472.00	*
	CC:Habitat-land-use	55	11.61	0.21	4777.00	*
	LUC:Habitat-land-use	61	11.68	0.19	4331.00	*
	CC:LUC:Habitat-land-use	61	6.49	0.11	2407.00	*
	Residuals	476	0.02	0.00		
Centroid distances						
Centroid dist. $\sim (\text{Habitat-land-use} + \text{CC} + \text{LUC})^{3\dagger}$	CC	1	5.84	5.84	536916.00	*
	LUC	2	11.21	5.61	515694.00	*
	LUC:Habitat-land-use	61	8.82	0.15	13305.00	*
	CC:LUC	2	0.23	0.11	10422.00	*
	Habitat-land-use	55	6.08	0.11	10171.00	*
	CC:Habitat-land-use	55	1.56	0.03	2606.00	*
	CC:LUC:Habitat-land-use	61	0.86	0.01	1296.00	*
	Residuals	476	0.01	0.00		
Size changes						

Appendices - Appendix 3: Supplementary materials to Chapter II

$\Delta\text{size} \sim (\text{Habitat-land-use} + \text{CC} + \text{LUC})^{3\dagger\ddagger}$					
CC	1	0.13	0.13	1196.30	*
Habitat-land-use	55	1.04	0.02	169.26	*
CC:Habitat-land-use	55	0.39	0.01	63.11	*
CC:LUC:Habitat-land-use	61	0.23	0.00	33.01	*
LUC:Habitat-land-use	61	0.22	0.00	32.90	*
CC:LUC	2	0.00	0.00	16.25	*
LUC	2	0.00	0.00	14.66	*
Residuals	474	0.05	0.00		

*Significant at p-value < 0.01.

†Superscript “3” indicates the inclusion of all main factors and their two-way and three-way interactions in the model.

‡Two extreme outliers were removed from this model in order follow linear model assumptions.

Supplementary Figures

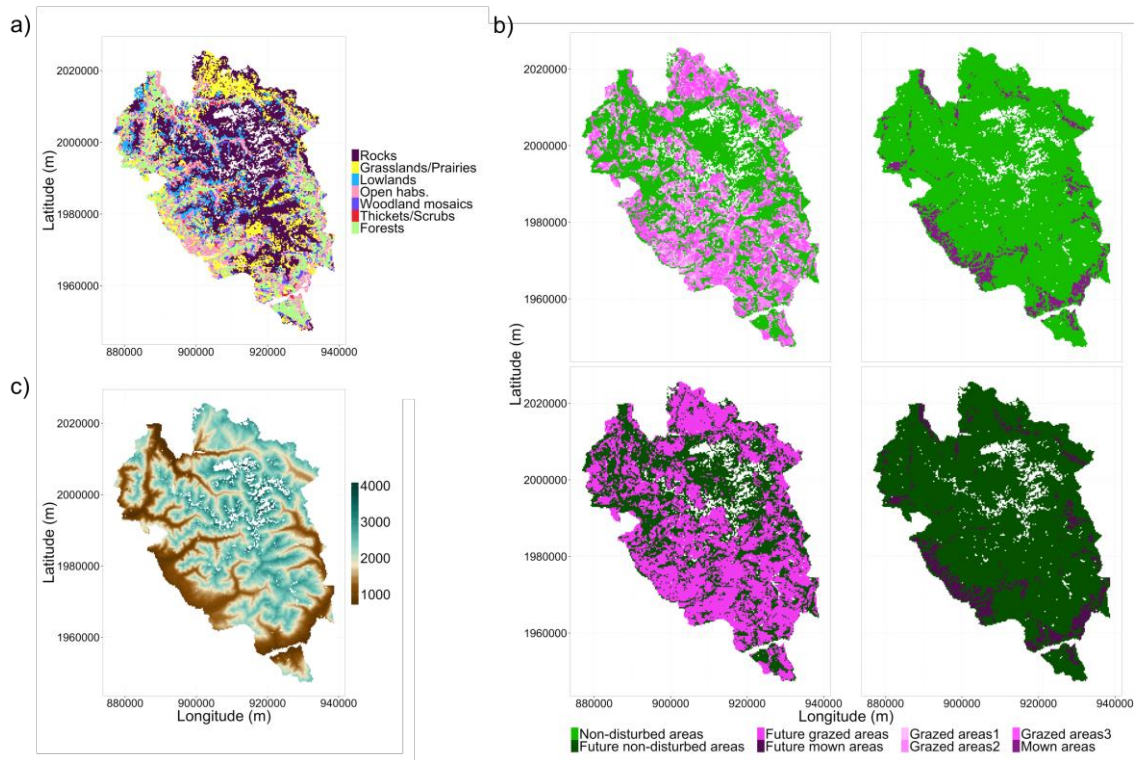


Figure S1. Maps of a) current habitat types and b) current and potential land-use regimes in the Ecrins National Park and c) elevation in meters a.s.l. Habitats were classified following the DELPHINE habitat classification of the park (Esterni et al. 2006) and land-use regimes followed (Boulangeat et al. 2014a). Presently grazed areas (with intensities ‘low’, ‘medium’ and ‘high’ numbered sequentially) and mown areas are shown in the top-left and top-right panels in b), respectively. Future grazed areas (grazed at the highest grazing intensity) and future mown areas are shown in the bottom-left and bottom-right panels, respectively. Non-disturbed areas correspond to all areas that are not currently grazed or mown (light green); future non-disturbed areas are areas that will not be grazed or mown under land-use intensification scenarios (dark green).

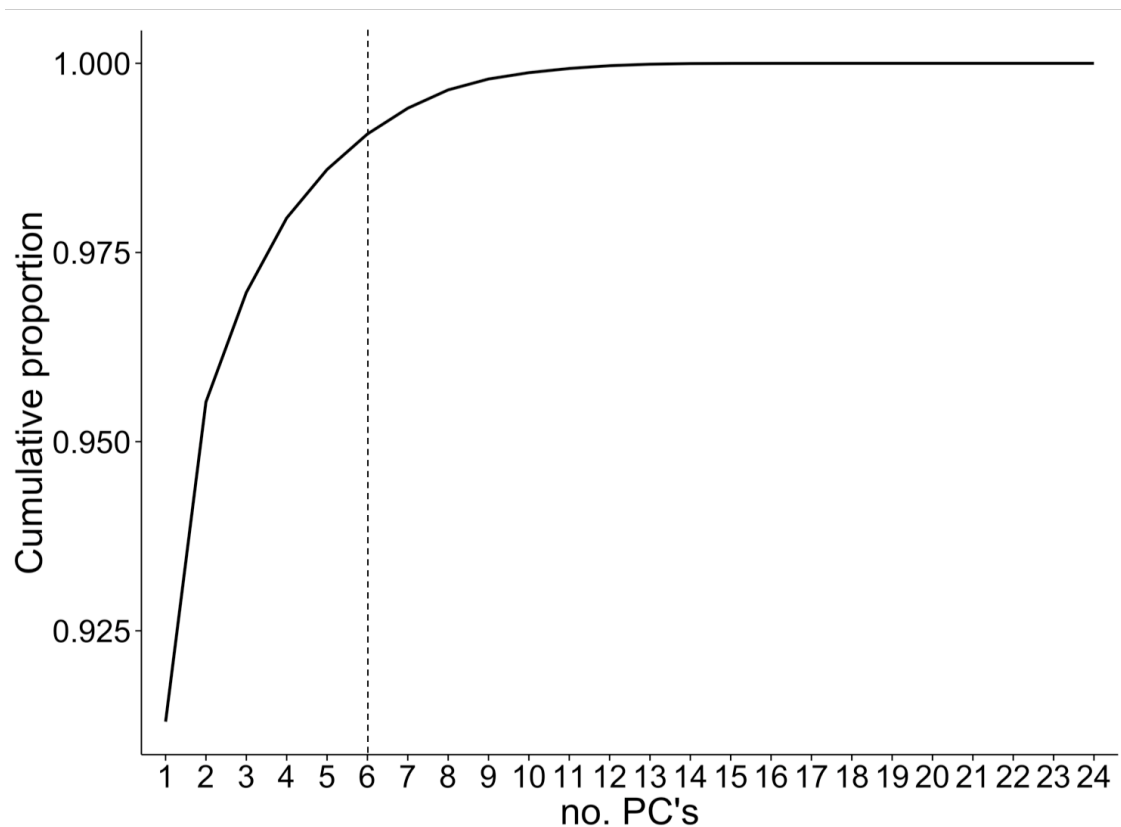


Figure S2. Overall cumulative curve of the proportion of variance explained by principal components (PCs). The mean cumulative of explained variance is shown in function of dimensionality, across all Principal Components Analyses (PCAs) calculated on raw plant functional groups' (PFG) abundances. Cumulative explained variances were averaged at each number of PCs across scenario and habitat-land-use combinations. The inflexion point of the curve was taken to be at the 6th PC (shown as the vertical dashed line), which meant that building hypervolumes using 6 PCs explained over 95% of the total variance.

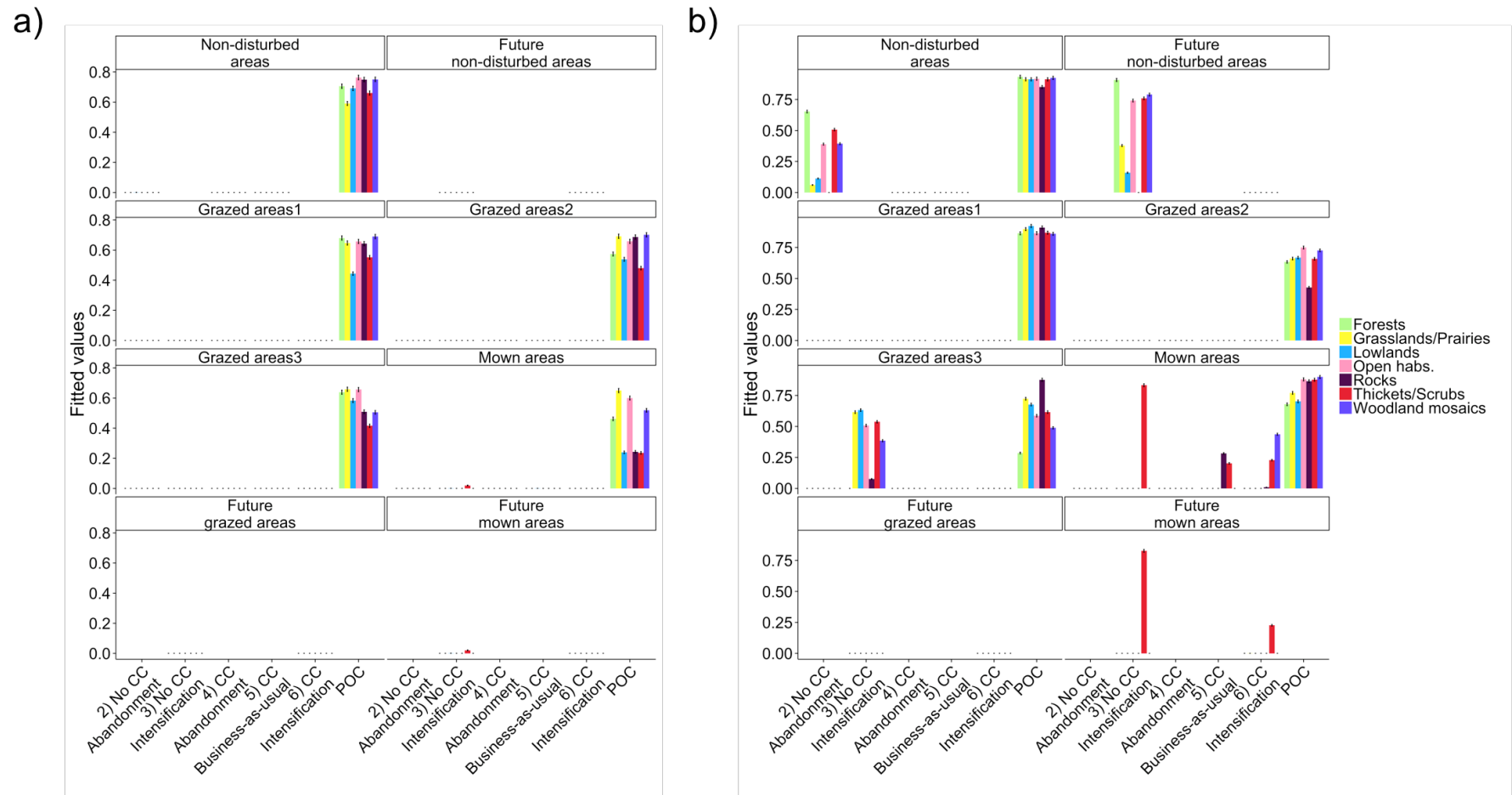


Figure S3. Fitted proportion of overlap by scenario and habitat-land-use combination. Fitted values of proportion of overlap (overlap) between control and post-perturbation hypervolumes built are shown for a) raw PFG abundances and b) CWM trait values. Fitted values were calculated from the best models relating the square-root proportion of overlap with climate change, land-use changes, habitat-land-use combinations and their interactions (see Table S2 in this appendix) and are shown by habitat-land-use combination in each scenario, after being back-transformed. Standard errors of the observed means and of fitted values are shown as error bars. Grazing intensities low, medium and high are coded 'grazed areas1', 'grazed areas2' and 'grazed areas3', respectively. Comparisons between proof-of-concept ('POC') and control scenario hypervolumes are also included.

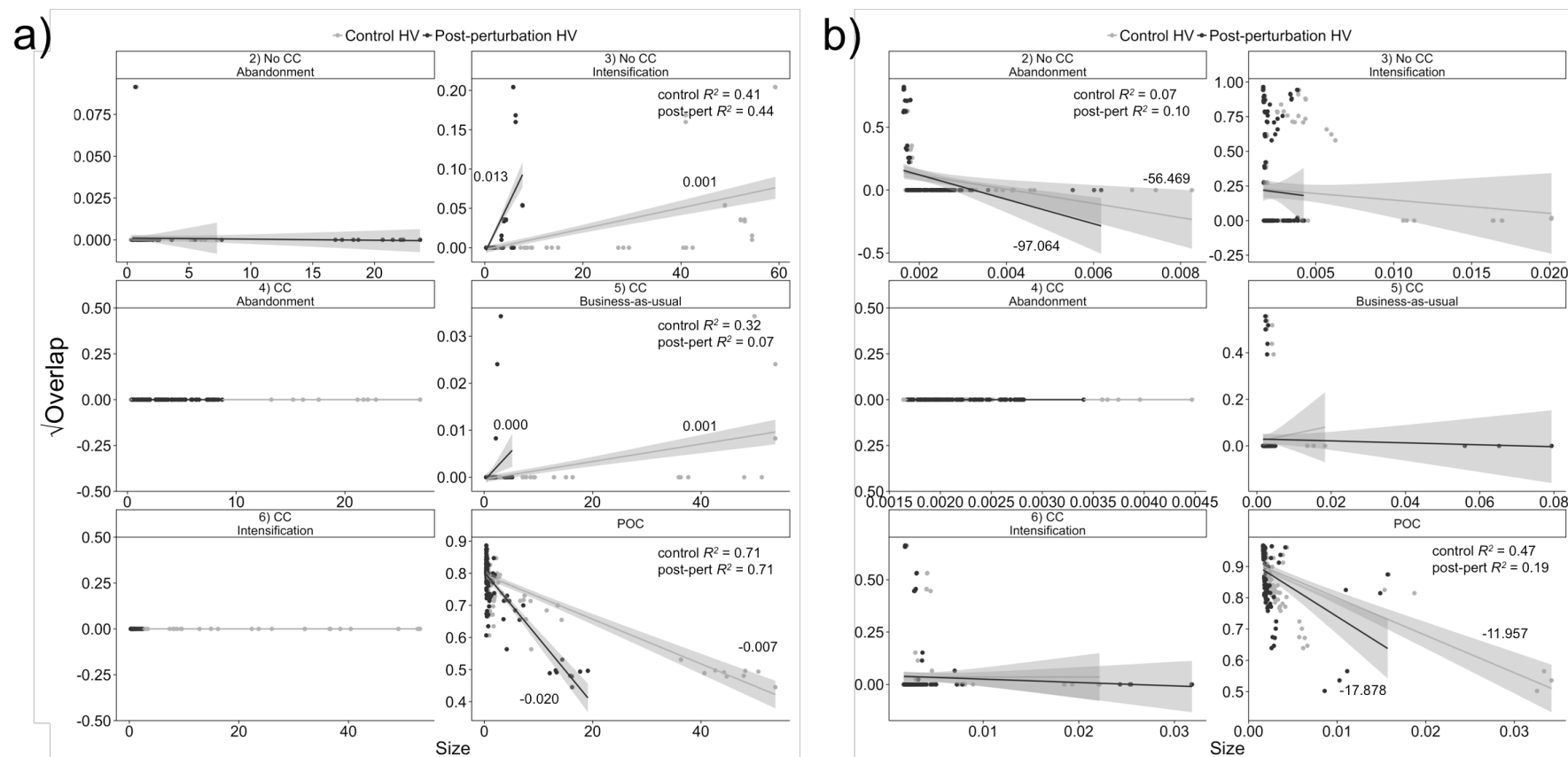


Figure S4. Relationship between hypervolume size and the proportion of overlap. Relationships between the proportion of overlap (overlap) between control and post-perturbation hypervolumes ('HV') and their sizes are shown for each scenario, for a) hypervolumes based on raw PFG abundances and on b) community weighted mean (CWM) trait values. Proof-of-concept ('POC') comparisons for each set of components are also shown. Overlap values were square-rooted to follow linear model assumptions and improve model fit. Each point represents a habitat-land-use combination for a given repetition (sample size varying between 105 and 147 depending on scenarios). Information on adjusted R^2 and coefficient values (next to each line) is shown for significant relationships only. Shaded areas denote confidence intervals at 95%.

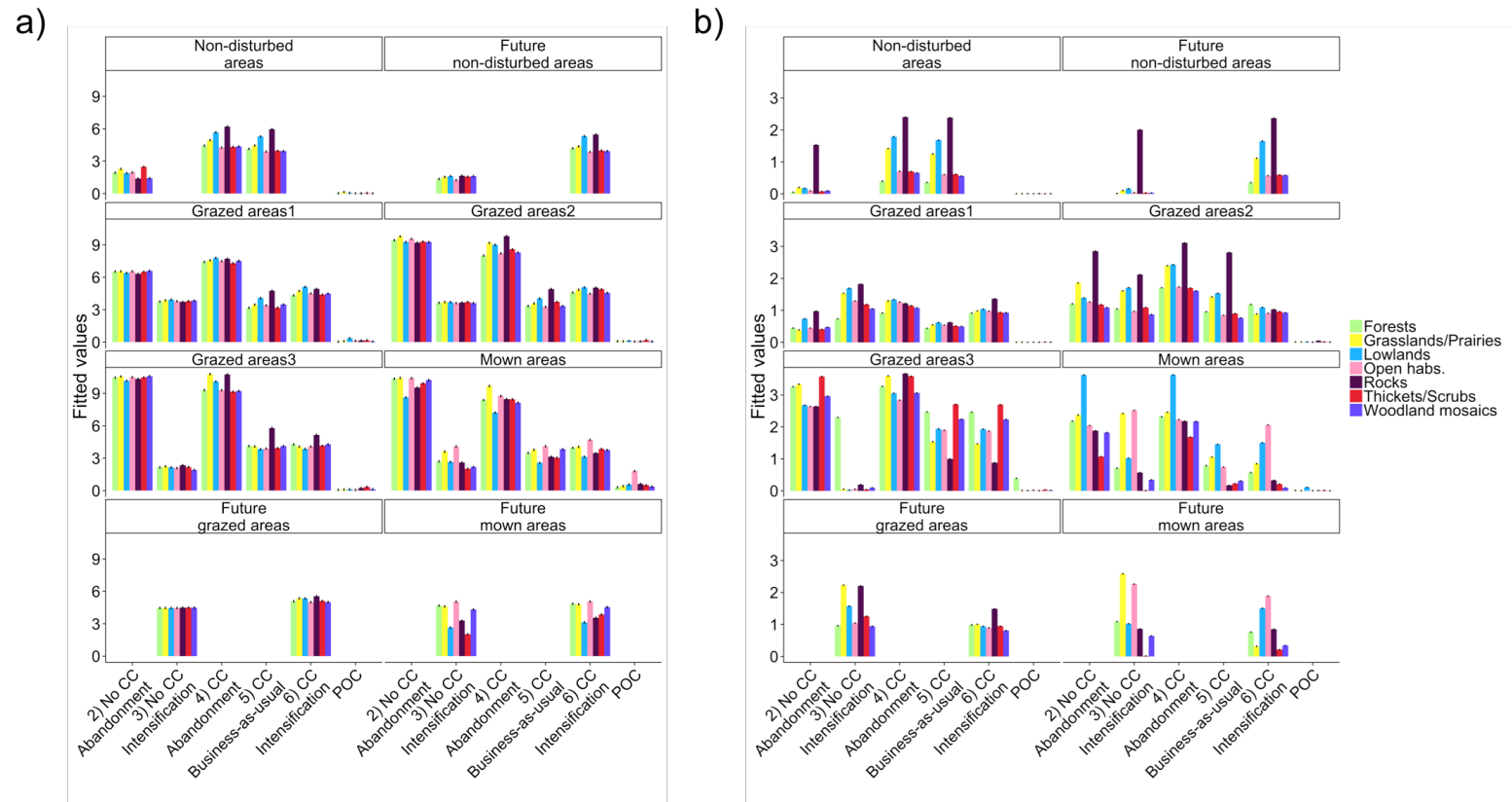


Figure S5. Fitted hypervolume centroid distances by scenario and habitat-land-use combination. Fitted distances between control and post-perturbation hypervolume centroids built are shown for a) raw PFG abundances and b) CWM trait values. Fitted values were calculated from the best models relating the centroid distances with climate change, land-use changes, habitat-land-use combinations and their interactions (see Table S2 in this appendix) and are shown by habitat-land-use combination in each scenario. Standard errors of the observed means and of fitted values are shown as error bars. Grazing intensities low, medium and high are coded ‘grazed areas1’, ‘grazed areas2’ and ‘grazed areas3’, respectively. Comparisons between proof-of-concept (‘POC’) and control scenario hypervolumes are also included.

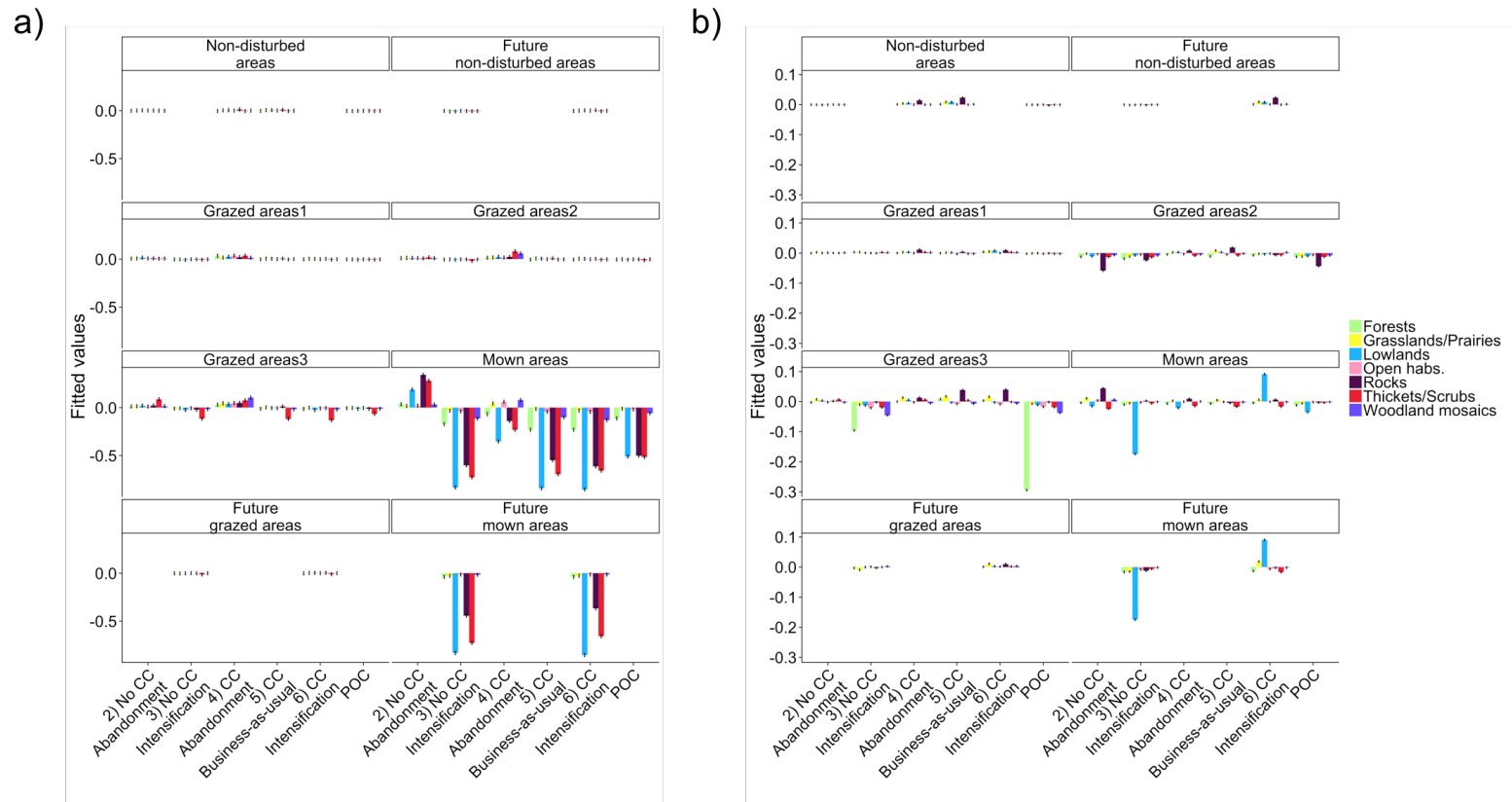


Figure S6. Fitted hypervolume size changes by scenario and habitat-land-use combination. Hypervolume size changes (Δ size) were calculated as the difference between post-perturbation and control hypervolumes (negative values indicating size reductions and positive values indicating size increases). Fitted size changes are shown for hypervolumes built from a) raw PFG abundances and b) CWM trait values. Fitted values were calculated from the best models relating the centroid distances with climate change, land-use changes, habitat-land-use combinations and their interactions (see Table S2 in this appendix) and are shown by habitat-land-use combination in each scenario. Standard errors of the observed means and of fitted values are shown as error bars. Grazing intensities low, medium and high are coded 'grazed areas1', 'grazed areas2' and 'grazed areas3', respectively. Comparisons between proof-of-concept ('POC') and control scenario hypervolumes are also included.

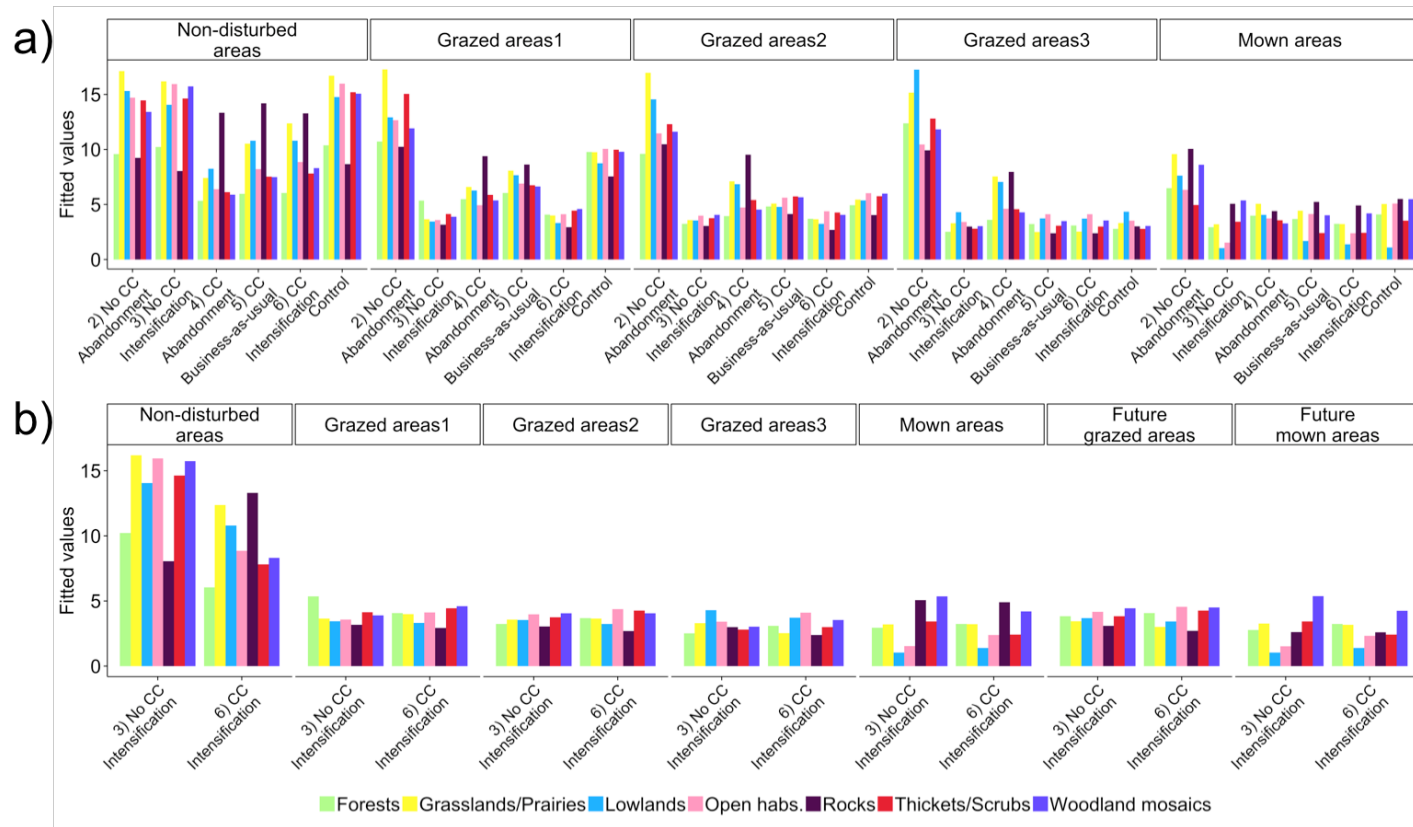


Figure S7. Taxonomic diversity by scenario and habitat-land-use combination. Taxonomic diversity was calculated yearly as the inverse Simpson concentration (Leinster & Cobbold 2012), based on PFG abundances of the last 100 years of the control and scenario simulations. Calculations were done per scenario and habitat-land-use combination and averaged across repetitions. Fitted values were calculated from the best models explaining the variation of PFG diversity in function of climate change, land-use changes and habitat-land-use combinations. To guarantee a balanced design, models were broken in two sets. The first set investigating the effects of CC and LUC on “current” habitat-land-use combinations (‘set 1’ shown in panel a) and the second to investigate the effects of CC and all habitat-land-use combinations on scenarios of LU intensification (‘set 2’, shown in panel b); see Table S3 in this appendix). Grazing intensities low, medium and high are coded ‘grazed areas1’, ‘grazed areas2’ and ‘grazed areas3’, respectively.

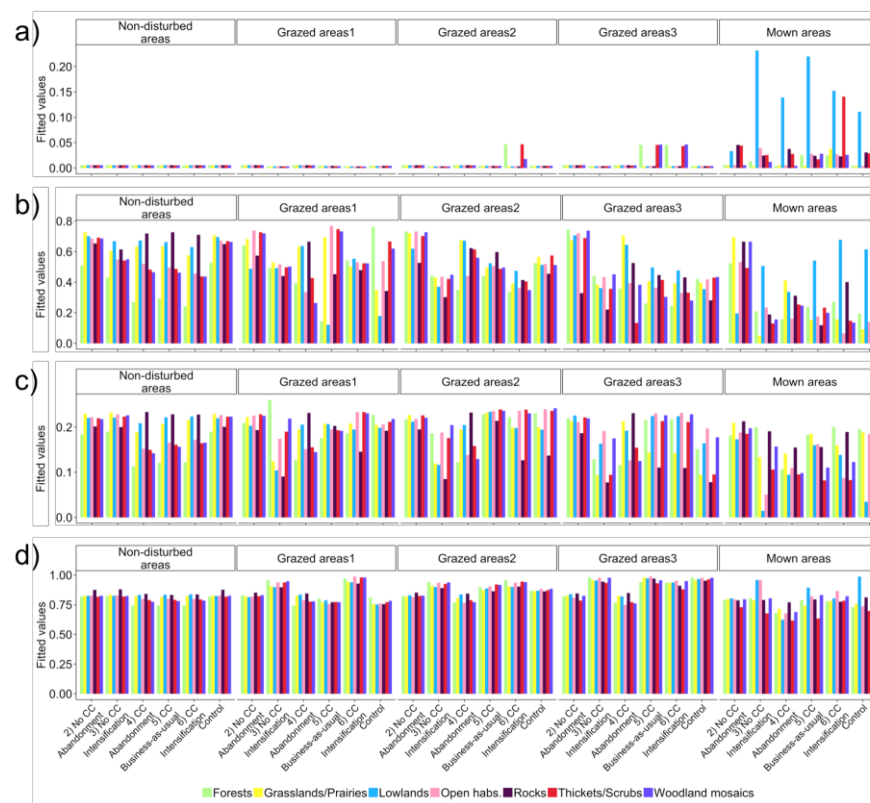


Figure S8. Functional diversity by scenario and habitat-land-use combination, first set of models. Functional diversity was estimated using four functional diversity indices: functional richness (FRic), functional evenness (FEve), functional divergence (FDiv; Villéger et al. 2008) and functional dispersion (FDis; Laliberté & Legendre 2010), calculated for the traits used to build trait hypervolumes (specific leaf area, log height, log seed mass and palatability). All indices were calculated yearly for the last 100 years of the control and scenario simulations. Fitted values shown in the figure were calculated from the best models explaining the variation of functional diversity indices in function of climate change, land-use changes and habitat-land-use combinations. Details on statistical analyses and a presentation of results obtained for FRic and FDiv are available above in Choice and analysis of complementary metrics. Only the first set of models ('set 1'; see Table S3 in this appendix) is shown here for a) FRic, b) FEve, c) FDis and d) FDiv. The first set of models investigates the effects of CC and LUC on "current" habitat-land-use combinations. Grazing intensities low, medium and high are coded 'grazed areas1', 'grazed areas2' and 'grazed areas3', respectively.

Studying ecosystem stability to global change across spatial and trophic scales

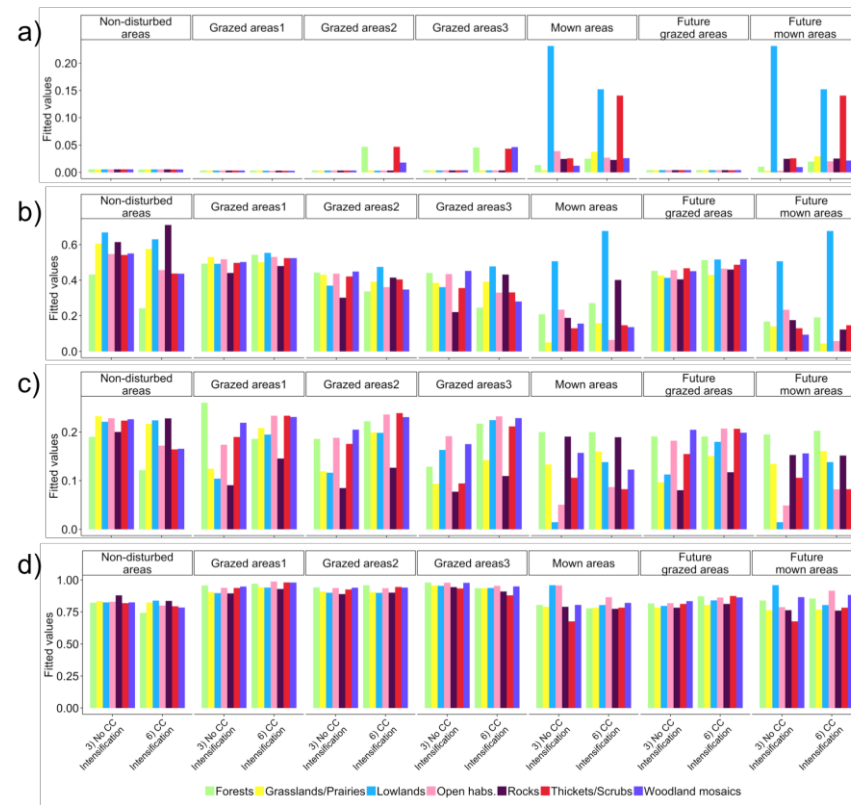


Figure S9. Functional diversity by scenario and habitat-land-use combination, second set of models. Functional diversity was estimated using four functional diversity indices: functional richness (FRic), functional evenness (FEve), functional divergence (FDiv; Villéger et al. 2008) and functional dispersion (FDis; Laliberté & Legendre 2010), calculated for the traits used to build trait hypervolumes (specific leaf area, log height, log seed mass and palatability). All indices were calculated yearly for the last 100 years of the control and scenario simulations. Fitted values shown in the figure were calculated from the best models explaining the variation of functional diversity indices in function of climate change, land-use changes and habitat-land-use combinations. Details on statistical analyses and a presentation of results obtained for FRic and FDiv are available above in Choice and analysis of complementary metrics. The second set of models ('set 2'; see Table S3) is shown here for a) FRic, b) FEve, c) FDis and d) FDiv. This set of models investigates the effects of CC and all habitat-land-use combinations on scenarios of LU intensification. Grazing intensities low, medium and high are coded 'grazed areas1', 'grazed areas2' and 'grazed areas3', respectively.

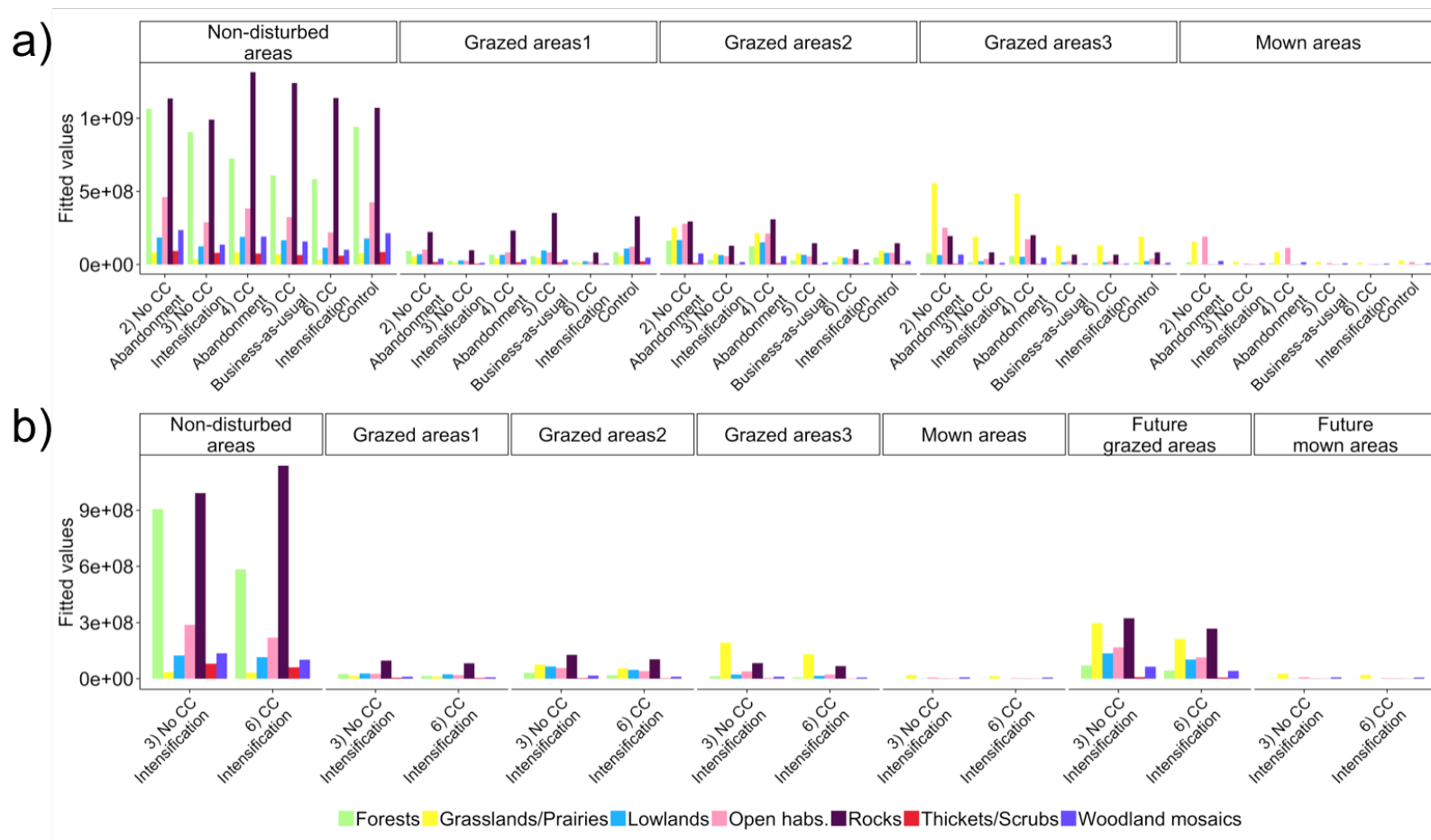


Figure S10. Productivity by scenario and habitat-land-use combination. Productivity was calculated yearly as the sum of PFG raw abundances, for the last 100 years of the control and scenario simulations. Fitted values were calculated from the best models explaining the variation of productivity in function of climate change, land-use changes and habitat-land-use combinations. To guarantee a balanced design, models were broken in two sets. The first set investigating the effects of CC and LUC on “current” habitat-land-use combinations (‘set 1’ shown in panel a) and the second to investigate the effects of CC and all habitat-land-use combinations on scenarios of LU intensification (‘set 2’, shown in panel b); see Table S3 in this appendix). Grazing intensities low, medium and high are coded ‘grazed areas1’, ‘grazed areas2’ and ‘grazed areas3’, respectively.

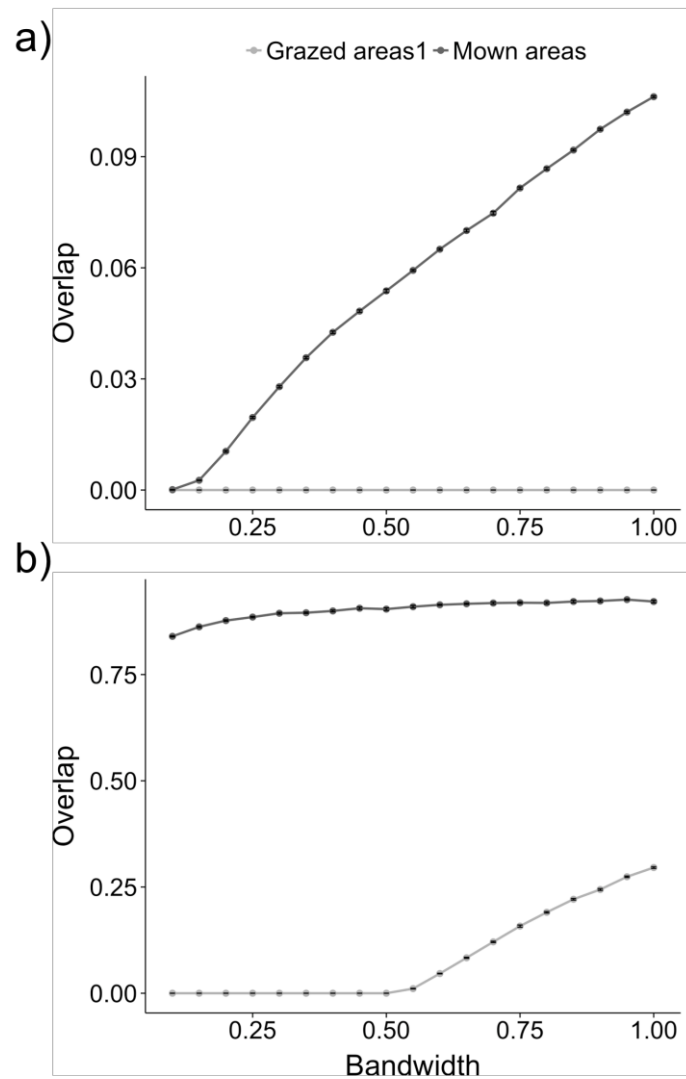


Figure S11. Evolution of proportion of overlap in function of bandwidth size. We chose thickets and scrubland habitats to assess the effect of increasing bandwidths on the proportion of overlap between control and post-perturbation hypervolumes of a) raw PFG abundances and b) community weighted mean trait values. This was done under a scenario of land-use intensification (scenario 3) and for areas presently grazed at low intensities, ‘grazed areas 1’ (which become grazed at high intensities) and presently mown areas (that suffer no land-use changes). Zero overlaps indicate an absence of intersection. Each point is the mean overlap between 10 pairs of hypervolumes and standard errors are shown as error bars.

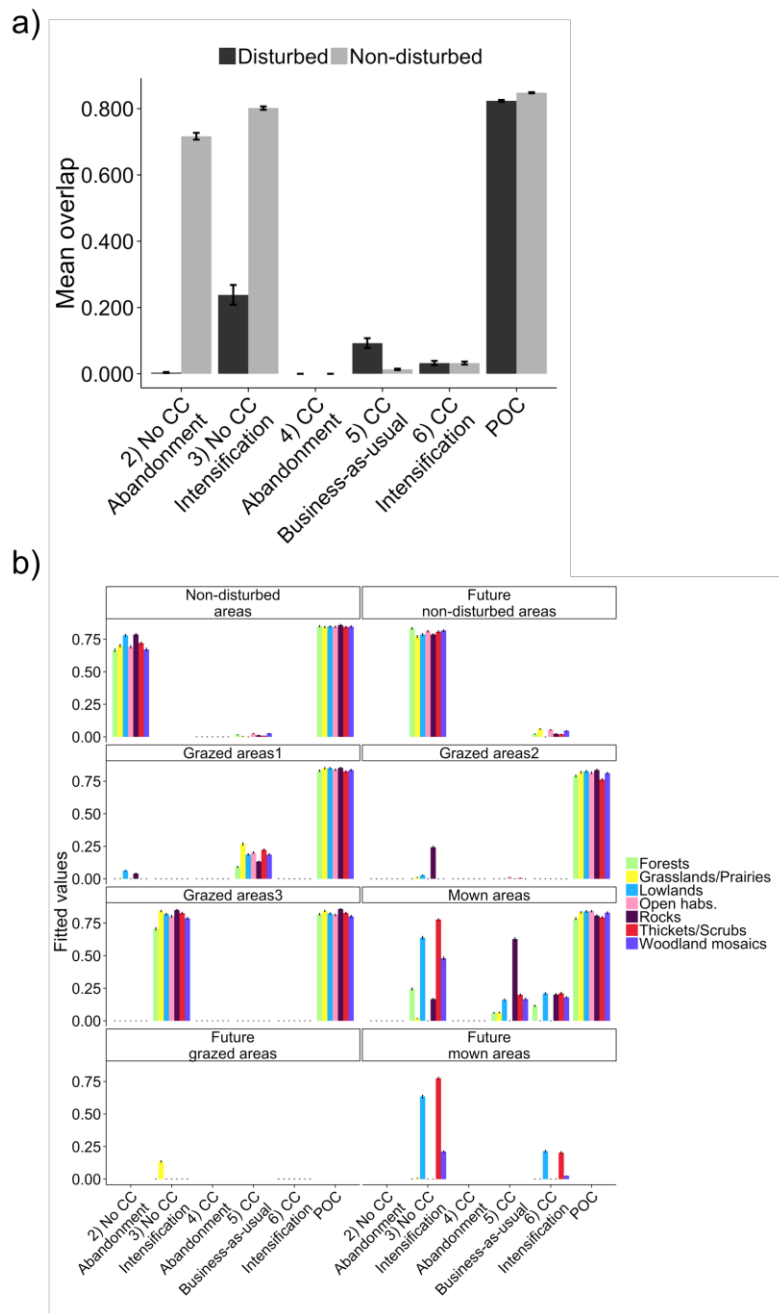


Figure S12. Proportion of overlap between hypervolumes based on relative PFG abundances. The a) observed mean proportion of overlap between control and post-perturbation hypervolumes are shown for each scenario, across all habitat types and grouped by disturbed areas (areas under present grazing or mowing regimes and areas that will become grazed on mown under scenarios of land-use intensification) and non-disturbed areas (all areas that are not currently grazed or mown and those that will remain so, under land-use intensification scenarios). Fitted overlap values in b) are shown for each scenario and habitat-land-use combination, and were obtained from analyses of variance detailed in Table S2 in this appendix. Fitted values were back-transformed to be shown on the original scale. Standard errors of the observed means and of fitted values are shown as error bars. Comparisons between proof-of-concept ('POC') and control scenario hypervolumes are also shown.

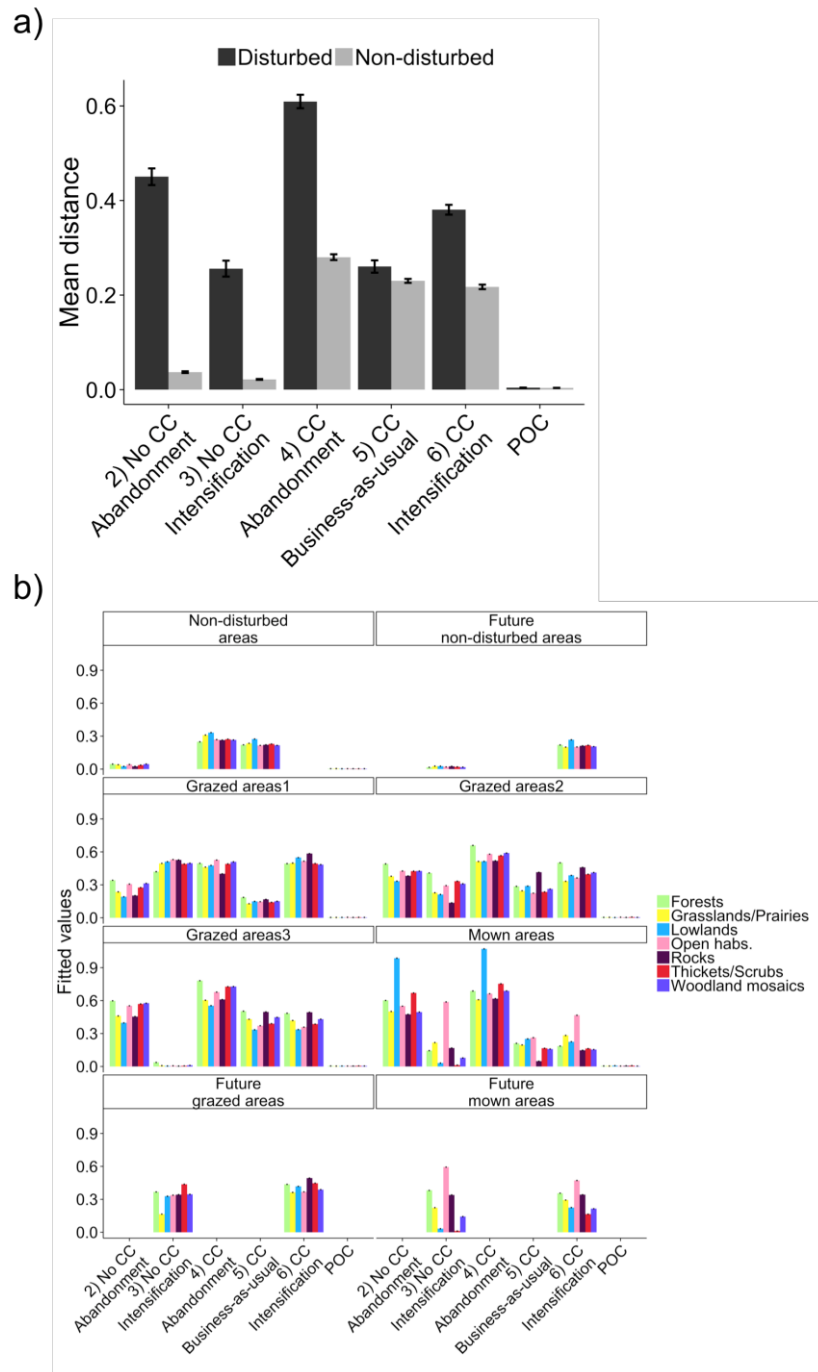


Figure S13. Centroid distances between hypervolumes based on relative PFG abundances. The a) observed centroid distances between control and post-perturbation hypervolumes are shown for each scenario, across all habitat types and grouped by disturbed areas (areas under present grazing or mowing regimes and areas that will become grazed on mown under scenarios of land-use intensification) and non-disturbed areas (all areas that are not currently grazed or mown and those that will remain so, under land-use intensification scenarios). Fitted centroid distances in b) are shown for each scenario and habitat-land-use combination and were obtained from analyses of variance detailed in Table S2 in this appendix. Standard errors of the observed means and of fitted values are shown as error bars. Comparisons between proof-of-concept ('POC') and control scenario hypervolumes are also shown.

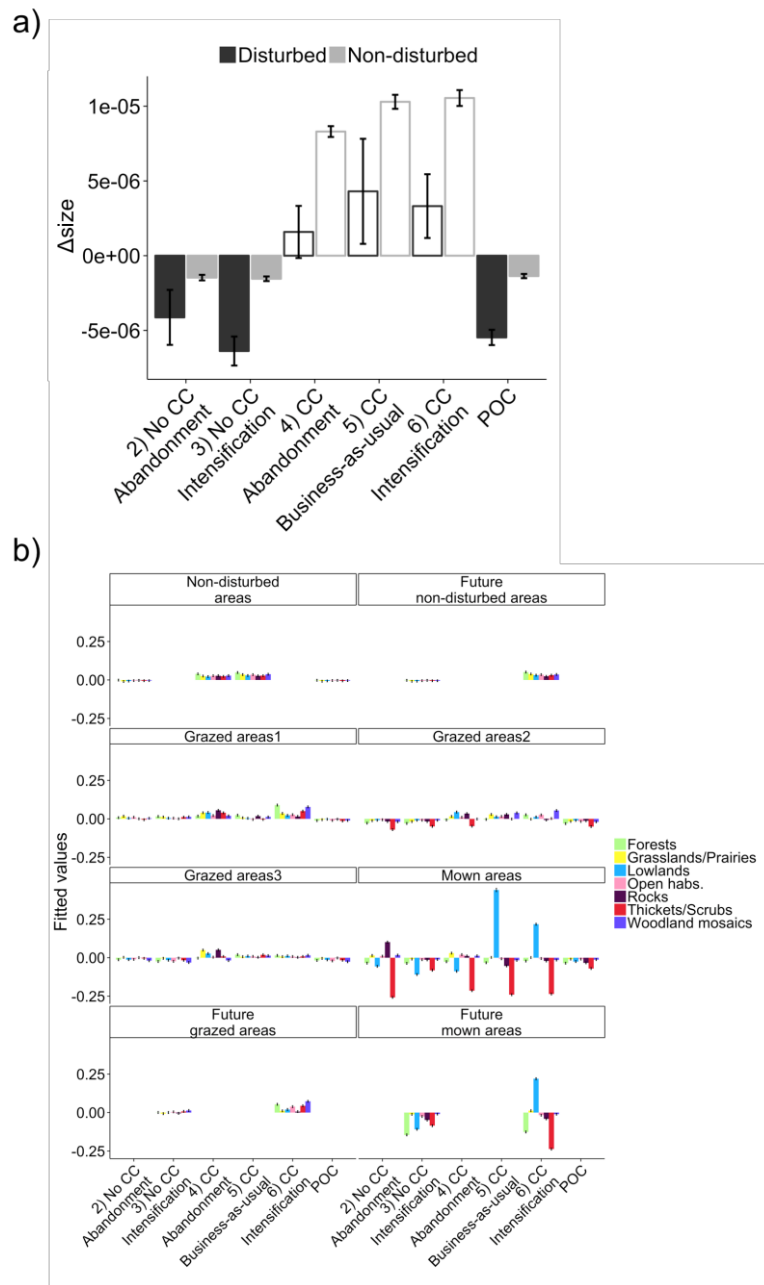


Figure S14. Size differences between hypervolumes based on relative PFG abundances. The a) observed size changes ($\Delta size$) from control to post-perturbation hypervolumes are shown for each scenario, across all habitat types and grouped by disturbed areas (areas under present grazing or mowing regimes and areas that will become grazed on mown under scenarios of land-use intensification) and non-disturbed areas (all areas that are not currently grazed or mown and those that will remain so, under land-use intensification scenarios). Negative $\Delta size$ values indicate that the post-perturbation hypervolume was smaller than its pre-perturbation counterpart, and vice-versa for positive $\Delta size$ values. Fitted $\Delta size$ in b) are shown for each scenario and habitat-land-use combination and were obtained from analyses of variance detailed in Table S2 in this appendix. Standard errors of the observed means and of fitted values are shown as error bars. Comparisons between proof-of-concept ('POC') and control scenario hypervolumes are also shown.

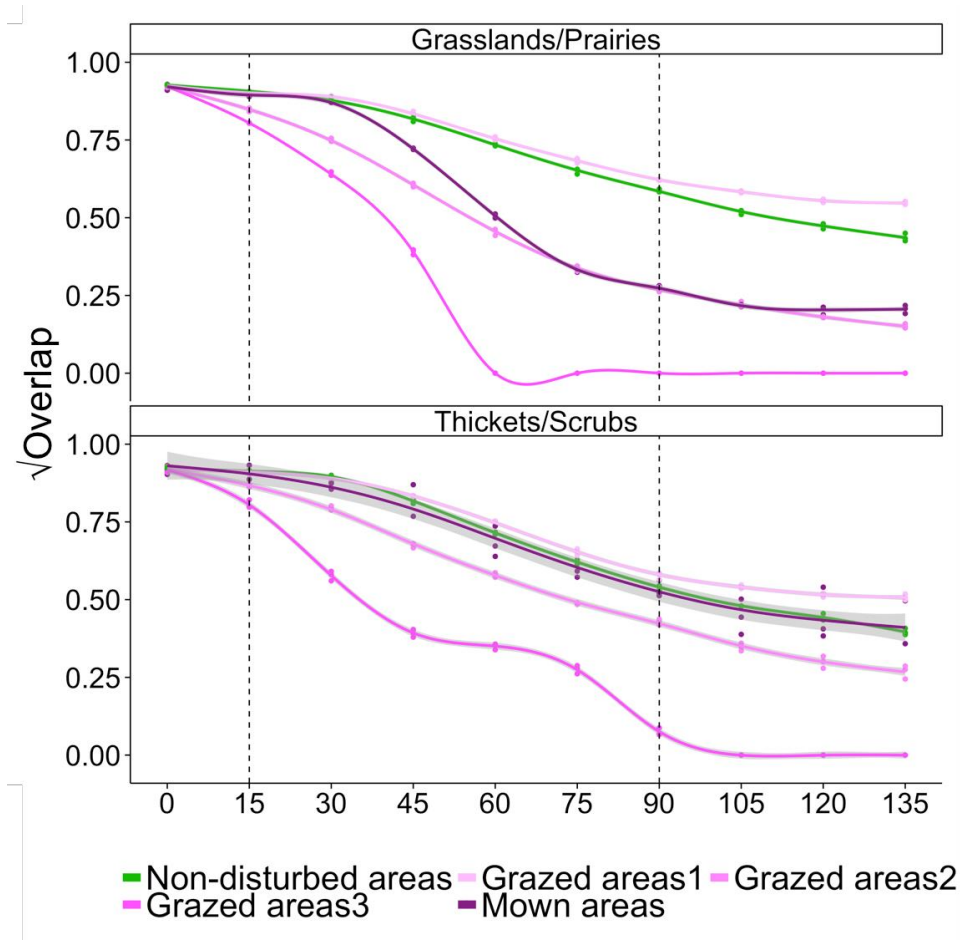


Figure S15. Temporal stability measured by hypervolume overlap, based on relative PFG abundances. Temporal stability was analysed by modelling the temporal response of the square-root of proportion of overlap (overlap) under different habitat-land-use combinations, using generalised additive models (GAMs) with a Gaussian smoother fitted for each habitat-land-use combination. Each coloured point corresponds to the comparison between a hypervolume at a given time slice and the first hypervolume, with colours referring to land-use (the first year of each 15-year time slice is indicated in the x-axis). Dashed vertical lines indicate the start and end of simulated climate changes.

APPENDIX 4: SUPPLEMENTARY MATERIALS TO CHAPTER III

The FATE-HD simulation platform and drought simulation experiment

FATE-HD basics

FATE-HD is a dynamical vegetation model that allows reproducing vegetation dynamics, by simulating plant functional groups' (PFGs) spatio-temporal dynamics. The model was parameterised to reproduce the vegetation of the Ecrins National Park (NP), situated in the French Alps (Boulangeat *et al.* 2014b). Thanks to its large elevation gradient (from 669 to 4102 m a.s.l.) and its diverse flora, the park hosts a variety of plant communities, from lowland forests to nival communities, passing through wetlands, as well as sclerophyllous vegetation. Around 68% of the park's surface is currently managed, mainly for agriculture (grazing, 48%; crop fields and mown grasslands, 9.8%; and forest management, 14%), and land use has been accurately mapped (Esterni *et al.* 2006). Like many other mountainous regions, the ecosystems of the Ecrins NP are threatened by climate and land-use changes. Hence, the assessment of potential impacts and synergies between climate and land-use drivers is crucial for adequate ecosystem conservation and management.

To reproduce the vegetation present in the Ecrins NP, FATE-HD explicitly simulates the population dynamics, dispersal, biotic interactions via light, and responses to disturbances of 24 PFGs that represent the dominant species of the park (Boulangeat *et al.* 2014b). Each PFG can reach one to 6 vertical strata, depending on its maximum height value (averaged across species within the group). Six chamaephyte groups, C1-6, and ten herbaceous groups, H1-10 (mostly hemicryptophytes), are only present in the first height stratum (0-1.5 m), except for C4 that can reach the second stratum (1.5-4 m). The remaining 8 phanerophyte groups, P1-8, reach at least the third height stratum (4-10 m), with six reaching the fourth stratum (10-20 m) and two reaching the fifth (> 20 m; for details on PFG building see Boulangeat *et al.* 2012; for PFG species list and modelling parameters see Tables S1 and S2 in this appendix).

Population dynamics depend not only on the demographic parameters of each PFG, but also on habitat suitability. Habitat suitability (HS) was calculated for each PFG using a species distribution modelling approach (*R* package *biomod2*; Thuiller *et al.*, 2009) as a function of slope, percentage of calcareous soil and five bioclimatic variables (isothermality, temperature seasonality, temperature annual range, mean temperature of coldest quarter and annual precipitation) averaged across 1961-1990 to reproduce 'current' climate conditions, and including a stochastic component to simulate interannual climate variability. Final PFG

distributions were calculated from the weighted sum predictions of a set of different models (Boulangeat *et al.* 2014b) and constituted PFGs' HS maps.

Short and long-distance dispersal and competition for light resources were parameterised according to PFGs functional traits and modelled explicitly. As for disturbances, FATE-HD simulates the responses of each PFG to grazing and mowing. Binary maps of mown areas and areas grazed at low, medium and high intensities are fed into the model to simulate the presence/absence of each disturbance per pixel. Grazing affects PFGs by either increasing mortality, decreasing fertility or causing them to resprout (depending on the PFGs' palatability and age classes). Mowing also increased PFG mortality and affected PFG reproduction, depending on PFGs age classes and caused the removal of all trees taller than 1.5m (second height stratum). For the present study, grazing and mowing activities were kept constant and mimicked the current land use in the park.

The for the full list of parameters used for population dynamics and responses to disturbances see Boulangeat *et al.* (2014b).

Modelling gradual climate warming and drought regimes in FATE-HD

Gradual changes in climate were simulated in FATE-HD as changes in HS. Hence, for each PFG future HS maps were calculated following a similar procedure as the one used to calculate the current HS maps. The PFG distributions were calculated using the same seven environmental variables, but following IPCC forecasts from the A1B scenario for years 2020, 2050 and 2080. Bioclimatic variables were projected using the regional climate model (RCM) RCA3 (Samuelsson *et al.* 2011), fed by the global circulation model (GCM) CCSM3 (derived from the ENSEMBLES EU project outputs NCAR community 2004). Outputs from the RCM were downscaled to 100 x 100 m resolution using the change factor method (Diaz-Nieto & Wilby 2005) before being used to calculate future HS maps for years 2020, 2050 and 2080. Interpolations were calculated between the current (1961-1990 period) and 2020 values, and between 2020-2050 and 2050-2080 to obtain a more gradual change in climate at every 15 years during 90 years (Boulangeat *et al.* 2014b).

Drought regimes were simulated mechanistically in two phases: 1) identification of drought effects and 2) modelling drought responses (Barros *et al.* 2017). Drought effects were identified in a similar way to gradual changes in climate. This is, FATE-HD was fed drought intensity (*Din*) maps at particular annual frequencies, which contained pixel-based information on drought intensity. Then 1) drought effects were 'identified' for the PFGs present in a given pixel after comparing *Din* pixel values against the PFGs' 'past drought

exposure', and 2) PFG responses to drought (increases in mortality and, or, lower fertility) were modelled in function of their tolerance to drought.

Two types of *Din* maps were used: 'current' *Din* maps and 'future' *Din* maps. Current *Din* maps were calculated as the average *Din* per pixel across years 1961-1990. Future *Din* maps were based on climate predictions for 2080 (following the A1B scenario; see above). Future 'moderate' *Din* maps corresponded to a 20% increase of *Din* values relatively to projections for 2080, while future 'severe' *Din* maps corresponded to 20% decrease of the projected values (note that lower *Din* values cause more intense droughts; see Barros *et al.* 2017 for details on the calculation of *Din* values and Fig. S1 in this appendix for *Din* maps).

Drought effects on PFGs and their parameterisation have been detailed elsewhere (Barros *et al.* 2017) and will only be briefly explained here. Each PFG's past drought exposure (used to both trigger drought effects and determine their magnitude for a given a PFG) was based on the distribution of historical moisture index values "experienced" by the PFG between 1961-1990 ($MI_{1961-1990}$ distributions). Each year, FATE-HD compared the *Din* values in a given pixel to the past drought exposures of PFGs present in that pixel. If the *Din* value was below a certain threshold, drought effects would be triggered. Drought effects always lowered PFG recruitment and fertility to 0 and increased mortality depending on drought intensity, on the accumulation of successive drought events and on PFG sensitivity. Also, very severe drought events had post-drought effects (on the following year) that also negatively affected PFG recruitment, fertility and survival. Finally, PFGs' sensitivities to drought were determined based on their soil moisture preference classes, which were calculated based on PFGs' $MI_{1961-1990}$ distributions (see Barros *et al.* 2017 for details and full drought-related parameter lists).

Simulation experiment

For the present study, we focused on climate-related effects and assumed a constant land use based on the current grazing and mowing regimes in the park. We ran simulations for three scenarios of climate change: *no drought*, *sporadic/moderate drought* and *frequent/severe drought* (see Fig. S2 in this appendix for simulation scheme). Simulations started with an initialisation phase of 850 years to achieve the 'current' state of the Ecrins NP vegetation (Boulangeat *et al.* 2014b). Scenario simulations started from the final year of the initialisation phase, lasting for 150 years (scenario phase). Gradual climate warming was simulated in all scenarios by changing HS maps (see above) between years 15-90 of the scenario phases, with the last HS map being kept until the end of the simulations. Scenarios differed in respect to drought regimes, which were simulated by feeding *Din* maps to FATE-HD. The current *Din*

map was used in no-drought years (every year in the no drought scenario). The sporadic/moderate drought scenario was simulated by feeding the moderate *Din* map to FATE-HD every 16 years. The frequent/severe drought scenario was simulated by feeding the severe *Din* map to FATE-HD every year. To simulate post-drought recovery, 10 no-drought years were implemented after each sequence of 5 drought events. Drought events started at the same time as climate warming (year 15) and were stopped between years 90 and 105 (Barros *et al.* 2017). After each scenario phase, the model ran for an additional 50 years to achieve quasi-equilibrium (stabilisation phase). All simulations lasted a total of 200 years and were repeated 3 times.

Additional simulations without climate warming or drought were also run for null comparisons. Null comparison simulations lasted 50 years started from a single repetition of an initialisation phase and were repeated 100 times.

Across all simulations, outputs were saved every 5 years starting at year 800 of the initialisation phase, in the form of yearly PFG abundances per pixel.

Treatment of model outputs

We explored the effects of gradual climate warming and different drought regimes on the stability of forest and grassland communities situated on the forest-grassland ecotone belt. The ecotone belt was spatially delimited using the first year of the one *no drought* scenario simulation, as this year was similar across all simulations, and fixed across all years to follow the temporal dynamics of the same ecotone communities (i.e. pixels). The ecotone was delineated as buffer drawn 500 m below and 1000 m above the upper tree line. The upper tree line was defined at the third quartile of elevation values of pixels with > 60% tree cover (i.e. phanerophyte plant functional groups with > 1.5 m; Esterni *et al.* 2006). To subset forest and grassland communities inside the ecotone belt, we used the accurate habitat maps available for the Ecrins NP (Esterni *et al.* 2006) combined with the grazing and mowing maps that were used in the model. We subset pixels from three types of plant communities and management: unmanaged forests, unmanaged grasslands and managed grasslands (grasslands grazed at medium intensity; see *The FATE-HD simulation platform and drought simulation experiment* above for grazing intensities). Raw PFG abundances were averaged across all pixels of the same category, per year, before calculating relative yearly PFG abundances. In cases where average raw PFG abundances were zero across a whole period of analysis (pre- or post-disturbance), we avoided suppressing PFGs (and thus changes in dimensionality) by adding 0.000001 to the missing groups before calculating the relative abundances.

Applying the hypervolumes framework and statistical analysis

Applying the hypervolumes framework

Hypervolumes were used to represent the pre- and post-disturbance states of the simulated forest and grassland communities, using plant functional groups (PFGs) yearly relative abundances (see *Treatment of model outputs* above). The pre-disturbance state was defined from the last 45 years of the initialisation phase ($n = 10$), a period during which communities were relatively stable, while the post-disturbance state was defined as the 50 years of the stabilisation phase ($n = 11$). Each post-disturbance state was compared against the pre-disturbance state. The pre-disturbance state was also compared against each of the 100 states corresponding to the null comparison simulations ($n = 11$ for each state; see *The FATE-HD simulation platform and drought simulation experiment* above).

Two steps were necessary before calculating and comparing the hypervolumes: 1) reducing the number of dimensions, and 2) choosing the ideal bandwidth size (Barros *et al.* 2016c).

1) Dimensionality reduction. It is recommended that hypervolumes are built from a maximum of 5-8 dimensions to avoid having highly disjunct hypervolumes (Blonder *et al.* 2014). Since we chose to explore changes in community structure using PFG abundances the initial 24 dimensions needed to be reduced. Following the approach detailed in (Barros *et al.* 2016c), we calculated Principal Components Analyses (PCAs) for each pair of compared states, i.e. on the joint datasets of yearly relative PFGs abundances from the pre- and post-disturbance periods. This approach also ensured that the axes used to calculate hypervolumes were orthogonal. We chose to use the factor scores on the first 3 principal components (PC's), at which the cumulative explained variance had saturated close to 1.0 (Fig. S3 in this appendix).

2) Bandwidth selection. Bandwidth sizes should be large enough to avoid disjunct hypervolumes (Blonder *et al.* 2014). Bandwidth sizes were estimated using a sensitivity analysis, where we observed how the disjunct factor (Blonder *et al.* 2014) and qualitative results varied with changing bandwidth. The interval at which we varied bandwidths was based on initial bandwidth estimates calculated on the factor scores of the chosen PCs of each drought scenario PCA. We used the Silverman bandwidth estimator and standard deviations to calculate initial bandwidths; maximum obtained value across all PCAs determined the magnitude of the bandwidth gradient for the sensitivity analysis. Having obtained a maximum bandwidth of ≈ 0.08 , we started the sensitivity analysis using bandwidth values between 0.01

and 0.16, in steps of 0.01. Pre- and post-disturbance hypervolume pairs (all 27 pairs), together with null comparison hypervolume pairs (only 3 pairs) were tested for the entire range of bandwidths. For the purpose of the sensitivity analysis, hypervolume calculations and comparisons were repeated 10 times for each bandwidth value. Since no overlaps were found between pre- and post-disturbance hypervolumes at very small bandwidths (< 0.12) and disjunct factor values were always below the recommended threshold of 0.9 (Fig. S4a in this appendix), we extended the sensitivity analyses to bandwidth values between 0.2 and 0.5, in steps of 0.05.

Disjunct factor values seemed to stabilise close to 0.1, around bandwidths of 0.15 (Fig. S4a in this appendix). Hypervolumes did not intersect (overlap = 0) for bandwidths smaller than 0.12 and, as expected, the proportion of overlap increased with increasing bandwidth. Mean distances between hypervolume centroids were approximately stable across bandwidth sizes, while size changes, albeit quite small, were negatively related with bandwidth size (Fig. S4b in this appendix). However, the relative effects of the different drought scenarios on mean distance, size changes and overlap were similar across bandwidth values. Null comparisons always resulted in smaller mean distances and larger overlaps relatively to drought scenarios, and frequent/severe droughts also led to smaller mean distances and larger overlaps relatively to other drought scenarios (Fig. S4b in this appendix). Hence, we chose a final bandwidth value of 0.15, which was close to the inflection point of disjunct factor values and to the minimum bandwidth value that allowed overlaps between the pre-disturbance and post-disturbance hypervolumes.

Final hypervolume calculations and comparisons were thus obtained as follows. For each comparison between a post-disturbance state (drought scenario) and the pre-disturbed state, we 1) calculated a PCA on the combined PFG relative abundances of each state; 2) extracted the factor scores on the first 3 PCs corresponding to each state; 3) used the extracted factor scores to calculate the pre- and post-disturbance hypervolumes; and 4) compared the hypervolumes using three metrics: mean distance, size changes and overlap (see main text and Barros *et al.* 2016c).

Hypervolume calculations rely on random sampling techniques (Blonder *et al.* 2014), whose results can be influenced by small sample sizes. To account for this, steps 3 and 4 were repeated 100 times. In addition, the pre-disturbance state was compared to 100 additional hypervolumes built from 50-year-long simulations without climate warming or drought regimes – null comparison simulations. In this case, each pair of hypervolumes was only

calculated and compared once. This provided a set of ‘null comparisons’ to which results from drought scenarios could be compared to.

Statistical analysis

As shown in the scheme of the simulation experiment (Fig. S2 in this appendix), the experimental design was not balanced as grasslands were subjected to two management regimes and forests were always unmanaged. Hence, the statistical analysis of results was divided into two main questions: 1) do different drought regimes affect forests and grasslands differently? 2) Do the effects of different drought regimes on grasslands depend on management regime?

To address the first question managed grasslands were excluded from the analysis, and we tested the effects and interactions of different drought scenarios and of different community types (‘scenario*community’) on the overlap, mean distance and sizes changes between pre- and post-disturbance hypervolumes. To address the second question, forests were excluded from the analyses, and we tested the effects and interactions of different drought scenarios and of different management regimes (‘scenario*management’) on the overlap, mean distance and sizes changes between pre- and post-disturbance hypervolumes. Separate analyses of variance (ANOVAs) were calculated to assess the effects of scenario and community/management on each hypervolume metric (mean distance, size changes and overlap). A first round of ANOVAs was calculated to compare drought scenarios’ effects against null comparisons results (as a control treatment scenario). Since sample sizes were different between null comparisons ($n = 100$ for a given community and management type) and drought scenarios ($n = 100$ for a given community and management type \times 3 repetitions, hence $n = 300$), Type III ANOVA’s were used at this instance (Table S3 in this appendix). Another set of ANOVAs was calculated without null comparisons (using Type I ANOVAs; Table S4 in this appendix) to assess significant differences between drought scenarios. Parametric conditions (normality and homoskedasticity) were verified before calculating ANOVAs and response variables (overlap, mean distance, size changes) were log-transformed when necessary to ensure that these conditions were met.

Lastly, we analysed functional changes in communities by fitting yearly community weighted mean values of 12 functional traits (Table S2 in this appendix) to the PCAs, using the function *envfit* in the *vegan R* package. This function “*finds directions in the ordination space towards which the [trait] vectors change most rapidly and to which they have maximal*

correlations with the ordination configuration" (vegan R documentation). Although this is a passive *post-hoc* approach, it allows finding the trait vectors best correlated with axis of the calculated PCAs, without constraining the hypervolumes to changes in functional diversity. Trait vector coordinates were scaled by the corresponding trait vectors' correlations with ordination axes. Only the traits with absolute coordinate values ≥ 0.8 on the first PC (thus the highest correlations) were selected for plotting and further analysis.

Additional results and discussion

Additional results

Changes in community structure were driven by different plant functional groups (PFGs) depending on the type of community/management considered, but were relatively consistent across drought scenarios (for a given community-management type; Figs. S5, S6 and S7 in this appendix). For instance, across all drought scenarios changes in managed grasslands were mostly driven by non-palatable and light-loving PFGs that are relatively abundant in these communities (see Table S2 in this appendix). Herbaceous groups H7 and H8 were replaced by chamaephytes C3 and C5 (woody) and the tree group P6, leading to reductions in average specific leaf area and increased overall longevity (see Fig. 15 in Chapter III and Fig. S5 in this appendix). Woody encroachment was even more evident in unmanaged grasslands, where almost all herbaceous and non-woody PFGs (except for C1 and C3) were replaced by woody chamaephyte and tree groups. Exceptions were P2 and P8, which were outcompeted due to their high soil moisture and light requirements (see Table S2 in this appendix), and the highly palatable and drought-tolerant C1 and H1 groups, whose relative abundances increased in the absence of grazing. These changes led to decreases in SLA and soil moisture requirements, and increases in leaf dry matter content (LDMC) and seed mass. Forests also showed a relative increase in woody groups, relatively to non-woody groups. Riparian pioneer trees (P2), late successional deciduous trees (P3) and undergrowth groups (H4, H6 and H7) were replaced by thermophilous pioneers (P1) late successional trees (P5, P7), shrubs and woody chamaephytes (C4 and C5, respectively). Interestingly, the relative abundance of P1 was more positively affected than that of P5 when drought was absent or sporadic/moderate, but the opposite happened when drought was frequent/severe. As in grasslands, these changes also led to a general decrease in SLA and soil moisture requirements, and increases in seed mass. Additionally, average longevity, maturity and dispersal capacity also increased in forests subjected to drought and climate warming.

Additional discussion

While past studies focused on how drought destabilised particular ecosystem functions (Wardle *et al.* 2000; Bloor & Bardgett 2012; Isbell *et al.* 2015), we followed the stability of community structure, assuming that a stable community structure ensures similar levels of functional diversity and, thus, ecosystem services. Indeed, changes in forest and grassland community structure (via changes in relative abundances of the simulated PFGs) impacted the communities' functional diversity, which can ultimately affect ecosystem functioning and the provisioning of ecosystem services. Particularly, reductions in average SLA in managed grasslands are linked to shifts towards less productive communities, which may implicate lower quantity and quality of fodder in grazing pastures (Lavorel & Grigulis 2012). On the other hand, increases in the woody-non-woody ratio in unmanaged grasslands indicate the encroachment of open habitats associated with climate change (Theurillat & Guisan 2001), and can lead to the loss of biodiversity and protected species (Andrello *et al.* 2012). Our results also concur that changes in forest composition will probably occur both at the undergrowth and canopy levels (Allen *et al.* 2010). Moreover, frequent/severe drought facilitated different groups, relatively to climate warming alone and sporadic/moderate drought. For instance, while under climate warming alone and sporadic/mild drought the group P1 (containing *Pinus sylvestris*) was more positively affected than P5 (containing *Picea abies*), this pattern was reversed when drought was frequent/severe. The shade-tolerant *P. abies* has already been shown to be facilitated by drought, in Valais, Switzerland, where it invaded *P. sylvestris* stands outcompeting the later species on the long-term (Bigler *et al.* 2006).

As in any other model, our results are evidently linked to how climate warming and drought events were parameterised. The fact that gradual climate warming drove the long-term dynamics of community structure is linked to climate warming effects being kept until the end of the simulation, while drought events ended before the stabilisation phase. Nevertheless, the agreement between our results and field observations indicates that the results of our simulations are not unrealistic. Also, the parameterisation of PFG responses to drought events was done in conjunction with botanists working within the study area, whose knowledge is highly valuable. Finally, other drivers, such as changes in carbon, nutrient and water cycles, and pest outbreaks are known to interact with drought in affecting vegetation dynamics (Wang *et al.* 2012; Reichstein *et al.* 2013). We expect that drought effects would have been stronger if we had included these factors in our model. However, we do not currently have the data that would enable us to simulate these processes at large spatial scales

Studying ecosystem stability to global change across spatial and trophic scales

and across multiple plant groups. Yet, we advocate that modelling approaches are crucial to assess large-scale consequences of global change drivers despite their limitations, and should be used while field studies gather data that will aid in the parameterisation of more complex and realistic models.

Supplementary Tables

Table S1. List of dominant species in the Ecrins National Park constituting each of the simulated plant functional groups (PFGs). Groups were built based on species' abiotic requirements and functional traits (Boulangeat et al. 2012). Table adapted from Boulangeat et al. (2014b).

Group	Species list
H1	<i>Oxyria digyna</i> , <i>Polygonum viviparum</i> , <i>Ranunculus glacialis</i> , <i>Ranunculus kuepferi</i> , <i>Ranunculus montanus</i> , <i>Geum montanum</i> , <i>Geum reptans</i> , <i>Potentilla aurea</i> , <i>Potentilla erecta</i> , <i>Potentilla grandiflora</i> , <i>Saxifraga stellaris robusta</i> , <i>Linaria alpina alpina</i> , <i>Carex capillaris</i> , <i>Carex curvula</i> , <i>Carex foetida</i> , <i>Carex frigida</i> , <i>Carex nigra</i> , <i>Carex panicea</i> , <i>Carex rupestris</i> , <i>Eriophorum latifolium</i> , <i>Eriophorum polystachion</i> , <i>Eriophorum scheuchzeri</i> , <i>Kobresia myosuroides</i> , <i>Trichophorum cespitosum</i> , <i>Juncus alpinoarticulatus alpinoarticulatus</i> , <i>Juncus trifidus</i> , <i>Luzula alpinopilosa</i> , <i>Agrostis alpina</i> , <i>Agrostis rupestris</i> , <i>Alopecurus alpinus</i> , <i>Avenula versicolor versicolor</i> , <i>Festuca halleri halleri</i> , <i>Festuca quadriflora</i> , <i>Phleum alpinum</i> , <i>Poa alpina</i> , <i>Poa cenisia</i> , <i>Poa laxa</i> , <i>Doronicum grandiflorum</i> , <i>Trisetum distichophyllum</i> , <i>Athamanta cretensis</i> , <i>Hieracium glaciale</i> , <i>Leontodon montanus</i> , <i>Leontodon pyrenaicus helveticus</i> , <i>Taraxacum alpinum</i> , <i>Campanula cochleariifolia</i> , <i>Astragalus alpinus</i> , <i>Lotus alpinus</i> , <i>Trifolium alpinum</i> , <i>Trifolium pallescens</i> , <i>Achillea nana</i> , <i>Gentiana punctata</i> , <i>Arnica montana</i> , <i>Epilobium anagallidifolium</i> , <i>Plantago alpina</i> .
H2	<i>Rumex acetosa</i> , <i>Rumex pseudalpinus</i> , <i>Fragaria vesca</i> , <i>Galium aparine</i> , <i>Galium verum</i> , <i>Carex caryophyllea</i> , <i>Carex sempervirens</i> , <i>Agrostis capillaris</i> , <i>Agrostis stolonifera</i> , <i>Festuca nigrescens</i> , <i>Sesleria caerulea</i> , <i>Astrantia major</i> , <i>Leucanthemum vulgare</i> , <i>Carum carvi</i> , <i>Meum athamanticum</i> , <i>Chenopodium bonus-henricus</i> , <i>Lathyrus pratensis</i> , <i>Lotus corniculatus</i> , <i>Onobrychis montana</i> , <i>Trifolium montanum</i> , <i>Trifolium pratense</i> , <i>Geranium sylvaticum</i> , <i>Plantago media</i> .
H3	<i>Ranunculus acris</i> , <i>Trollius europaeus</i> , <i>Urtica dioica</i> , <i>Aegopodium podagraria</i> , <i>Anthoxanthum odoratum</i> , <i>Arrhenatherum elatius elatius</i> , <i>Dactylis glomerata</i> , <i>Deschampsia cespitosa</i> , <i>Festuca rubra</i> , <i>Crepis pyrenaica</i> , <i>Poa pratensis</i> , <i>Taraxacum officinale</i> , <i>Heracleum sphondylium</i> , <i>Pimpinella major</i> , <i>Trifolium repens</i> , <i>Vicia cracca</i> , <i>Plantago lanceolata</i> .
H4	<i>Aconitum lycoctonum vulparia</i> , <i>Aruncus dioicus</i> , <i>Dryopteris dilatata</i> , <i>Dryopteris filix-mas</i> , <i>Athyrium filix-femina</i> , <i>Prenanthes purpurea</i> .
H5	<i>Pulsatilla alpina</i> , <i>Ranunculus bulbosus</i> , <i>Anthericum liliago</i> , <i>Luzula sieberi</i> , <i>Achnatherum calamagrostis</i> , <i>Agrostis agrostiflora</i> , <i>Briza media</i> , <i>Bromus erectus</i> , <i>Deschampsia flexuosa</i> , <i>Festuca acuminata</i> , <i>Festuca flavescens</i> , <i>Festuca laevigata</i> , <i>Festuca marginata gallica</i> , <i>Koeleria vallesiana</i> , <i>Phleum alpinum rhaeticum</i> , <i>Stipa eriocaulis eriocaulis</i> , <i>Trisetum flavescens</i> , <i>Leontodon autumnalis</i> , <i>Leontodon hispidus</i> , <i>Tolpis staticifolia</i> , <i>Festuca melanopsis</i> , <i>Hugueninia tanacetifolia</i> , <i>Laserpitium halleri</i> , <i>Laserpitium siler</i> , <i>Silene flos-jovis</i> , <i>Hypericum maculatum</i> , <i>Salvia pratensis</i> , <i>Epilobium dodonaei fleischeri</i> .
H6	<i>Ranunculus aduncus</i> , <i>Cacalia alliariae</i> , <i>Saxifraga rotundifolia</i> , <i>Valeriana officinalis</i> , <i>Carex flacca</i> , <i>Cicerbita alpina</i> , <i>Luzula nivea</i> , <i>Avenula pubescens</i> , <i>Brachypodium rupestre</i> , <i>Calamagrostis varia</i> , <i>Festuca altissima</i> , <i>Melica nutans</i> , <i>Milium effusum</i> , <i>Molinia caerulea arundinacea</i> , <i>Poa nemoralis</i> , <i>Hieracium murorum</i> , <i>Hieracium prenanthoides</i> , <i>Senecio ovatus ovatus</i> , <i>Chaerophyllum aureum</i> , <i>Chaerophyllum villarsii</i> , <i>Cardamine pentaphyllos</i> , <i>Laserpitium latifolium</i> , <i>Knautia dipsacifolia</i> , <i>Mercurialis perennis</i> , <i>Gentiana lutea</i> , <i>Epilobium angustifolium</i> .
H7	<i>Cacalia alpina</i> , <i>Cryptogramma crispa</i> , <i>Asplenium ramosum</i> , <i>Asplenium septentrionale septentrionale</i> , <i>Asplenium trichomanes quadrivalens</i> , <i>Equisetum arvense</i> , <i>Cystopteris fragilis</i> , <i>Gymnocarpium robertianum</i> , <i>Woodsia alpina</i> , <i>Hieracium pilosella</i> , <i>Homogyne alpina</i> , <i>Petasites albus</i> , <i>Tussilago farfara</i> .
H8	<i>Cacalia leucophylla</i> , <i>Cirsium spinosissimum</i> , <i>Omalotheca supina</i> , <i>Murbeckiella pinnatifida pinnatifida</i> , <i>Gentiana alpina</i> .
H9	<i>Anthoxanthum odoratum nipponicum</i> , <i>Nardus stricta</i> , <i>Poa supina</i> , <i>Silene vulgaris prostrata</i> .
H10	<i>Heracleum sphondylium elegans</i> .
C1	<i>Rumex acetosella</i> , <i>Cotoneaster integerrimus</i> , <i>Potentilla neumanniana</i> , <i>Rubus idaeus</i> , <i>Rubus saxatilis</i> , <i>Valeriana montana</i> , <i>Lonicera caerulea</i> , <i>Helianthemum grandiflorum</i> , <i>Helianthemum nummularium</i> ,

Studying ecosystem stability to global change across spatial and trophic scales

	<i>Anthyllis montana, Hippocrepis comosa, Achillea millefolium, Stachys recta, Teucrium chamaedrys, Thymus pulegioides.</i>
C2	<i>Rumex scutatus, Salix hastata, Saxifraga aizoides, Saxifraga oppositifolia, Helictotrichon sedenense sedenense, Leucanthemopsis alpina, Cerastium alpinum, Cerastium cerastoides, Cerastium latifolium, Cerastium pedunculatum, Cerastium uniflorum, Sempervivum arachnoideum, Vaccinium uliginosum microphyllum, Antennaria dioica, Thymus polytrichus, Artemisia umbelliformis eriantha, Artemisia umbelliformis umbelliformis.</i>
C3	<i>Androsace pubescens, Androsace vitaliana, Primula hirsuta, Primula latifolia, Dryas octopetala, Salix herbacea, Salix reticulata, Salix retusa, Saxifraga bryoides, Saxifraga exarata, Eritrichium nanum nanum, Noccaea rotundifolia, Pritzelago alpina alpina, Gypsophila repens, Sagina glabra, Sagina saginoides, Silene acaulis, Silene acaulis bryoides, Sedum album, Sedum alpestre, Sedum dasypyllum, Empetrum nigrum hermaphroditum, Rhododendron ferrugineum, Globularia cordifolia.</i>
C4	<i>Amelanchier ovalis, Crataegus monogyna, Rosa pendulina, Salix laggeri, Juniperus communis, Alnus alnobetula, Lonicera xylosteum, Cornus sanguinea, Corylus avellana, Ribes petraeum.</i>
C5	<i>Arctostaphylos uva-ursi crassifolius, Calluna vulgaris, Hippocrepis emerus.</i>
C6	<i>Vaccinium myrtillus, Vaccinium vitis-idaea vitis-idaea.</i>
P1	<i>Prunus avium, Sorbus aria, Sorbus aucuparia, Sorbus mougeotii, Pinus cembra, Pinus sylvestris.</i>
P2	<i>Populus tremula, Salix daphnoides.</i>
P3	<i>Tilia platyphyllos, Acer pseudoplatanus, Fraxinus excelsior.</i>
P4	<i>Larix decidua.</i>
P5	<i>Picea abies, Fagus sylvatica.</i>
P6	<i>Pinus uncinata, Betula pendula.</i>
P7	<i>Acer opalus, Acer campestre campestre.</i>
P8	<i>Betula pubescens.</i>

Appendices - Appendix 4: Supplementary materials to Chapter III

Table S2. Trait values of the simulated plant functional groups' (PFGs). Groups belong to one of three life form classes: chamaephytes (C1-6), herbaceous (H1-10), or phanerophytes (P1-8). PFGs with larger values of 'light', 'dispersal' and 'palatability' are, respectively, light-loving, long-distance dispersers and more palatable. 'No. strata' indicates the maximum stratum that a PFG can reach. 'SLA' and 'LDMC' stand for average specific leaf area and average leaf dry matter content, respectively. SLA values for species of PFGs H10 and P8 were obtained from Kattge et al. (2011). Table partially adapted from Boulangeat et al. (2012) and Boulangeat et al. (2014b) and identical to the table in Barros et al. (2017).

PFG	No. strata	Dispersal	Light	Height (cm)	Palatability	Longevity (years)	Maturity (years)	Seed mass (g)	SLA (mm ² mg ⁻¹)	LDMC (mg g ⁻¹)	Leaf area (mm ²)	Soil moisture
C1	1	6	7	27	3	27	5	23.91	19.21	262.74	12.95	0
C2	1	4	8	13	3	19	4	0.38	18.02	196.03	1.05	2
C3	1	1	8	7	0	45	6	0.51	14.39	221.21	0.66	2
C4	2	6	6	209	2	158	10	192.99	16.83	330.52	16.97	1
C5	1	6	6	76	0	39	8	75.01	8.28	390.18	0.94	0
C6	1	7	6	18	2	92	8	39.50	13.40	354.97	0.86	2
H1	1	3	8	17	3	11	4	0.86	17.22	260.65	5.00	2
H2	1	6	7	42	3	10	3	4.04	22.11	250.74	18.76	2
H3	1	7	7	50	3	9	3	2.37	24.43	238.24	79.05	2
H4	1	3	5	76	0	7	4	0.36	29.76	228.53	541.13	2
H5	1	3	7	40	3	7	4	1.94	20.71	243.02	31.34	1
H6	1	3	6	73	3	8	4	2.31	28.21	227.85	76.68	2
H7	1	5	6	19	0	7	4	0.40	19.25	195.45	97.07	2
H8	1	3	8	19	0	8	4	0.89	23.11	274.24	0.18	3
H9	1	7	8	19	3	9	4	0.38	21.09	417.58	1.40	3
H10	1	7	6	100	3	9	4	6.20	21.14	0.22	353.31	2
P1	3	6	6	1175	2	193	15	177.93	12.03	346.77	34.01	0
P2	3	5	6	750	2	177	15	0.13	17.17	350.81	14.43	2
P3	4	4	5	1667	2	351	18	86.41	15.30	265.26	65.52	2
P4	5	6	7	2500	0	600	15	6.82	10.06	279.75	0.20	3
P5	5	6	4	2500	2	450	25	114.06	11.86	309.25	20.28	1
P6	4	4	8	1650	2	160	20	6.10	19.24	282.18	12.36	1
P7	3	4	5	600	2	310	15	78.27	15.65	360.50	47.42	0

Studying ecosystem stability to global change across spatial and trophic scales

P8	3	4	7	800	2	100	15	0.17	14.62	0.36	8.26	2
-----------	---	---	---	-----	---	-----	----	------	-------	------	------	---

Appendices - Appendix 4: Supplementary materials to Chapter III

Table S3. Results of the analyses of variance (ANOVAs) including null comparisons as control treatment. Type III ANOVAs were used to assess whether the effects of drought scenarios and their interaction with community/management types on hypervolume metrics significantly differed from a no-changes scenario (null comparisons). Response variables (overlap, mean distance and size changes) were transformed when necessary to obey linear model assumptions. In model formulas '*' denotes the inclusion of main effects and their interaction in the model. For instance, $\text{overlap} \sim \text{scenario} * \text{community}$ is to be understood as $\text{overlap} \sim \text{scenario} + \text{community} + \text{scenario}:\text{community}$, with ':' denoting the interaction between two factors. Asterisks indicate the level of significance of F-test statistics (** for p-values < 0.05, *** for p-values < 0.001). 'df' stands for degrees of freedom and 'Sum sq.' for sums of squares.

		df	Sum sq.	F value	
overlap ~ scenario*community	scenario	3	117.80	838500.0	***
	community	1	0.01	133.3	***
	scenario:community	3	0.01	70.2	***
	residuals	1992	0.09		
log-overlap ~ scenario*management	management	1	10148.40	342212.2	***
	scenario	3	6279.70	70586.2	***
	scenario:management	3	736.20	8275.1	***
	residuals	1992	59.10		
mean distance ~ scenario*community	scenario:community	3	0.00	121.1	***
	community	1	0.00	358.9	***
	scenario	3	10.03	344568.8	***
	residuals	1992	0.02		
mean distance ~ scenario*management	management	1	14.40	1313232.3	***
	scenario	3	8.19	248771.0	***
	scenario:management	3	0.12	3684.2	***
	residuals	1992	0.02		
size changes ~ scenario*community	scenario	3	2.79	19256.0	***
	community	1	0.38	7903.0	***

Studying ecosystem stability to global change across spatial and trophic scales

	scenario:community	3	0.12	822.5	***
	residuals	1992	0.10		
size changes ~ scenario*management	management	1	73.42	1237080.3	***
	scenario:management	3	5.42	30427.4	***
	scenario	3	0.71	3970.3	***
	residuals	1992	0.12		

Appendices - Appendix 4: Supplementary materials to Chapter III

Table S4. Results of the analyses of variance (ANOVAs) when null comparisons are excluded. Type I ANOVAs were used to assess the significant differences between drought scenarios and community/management types (and their interactions) on hypervolume metrics. Response variables (overlap, mean distance and size changes) were transformed when necessary to obey linear model assumptions. In model formulas '*' denotes the inclusion of main effects and their interaction in the model. For instance, $overlap \sim scenario * community$ is to be understood as $overlap \sim scenario + community + scenario:community$, with ':' denoting the interaction between two factors. Asterisks indicate the level of significance of F-test statistics (** for p-values < 0.05, *** for p-values < 0.001). 'df' stands for degrees of freedom and 'Sum sq.' for sums of squares.

		df	Sum sq.	F value	
overlap ~ scenario*community	community	1	0.03	605.6	***
	scenario:community	2	0.00	11.5	***
	scenario	2	0.00	0.2	
	residuals	1794	0.07		
log-overlap ~ scenario*management	management	1	14210.30	450193.4	***
	scenario	2	504.30	7988.7	***
	scenario:management	2	491.90	7791.7	***
	residuals	1794	56.60		
mean distance ~ scenario*community	community	1	0.01	1002.3	***
	scenario:community	2	0.00	66.8	***
	scenario	2	0.00	7.4	***
	residuals	1794	0.02		
mean distance ~ scenario*management	management	1	14.52	1329380.3	***
	scenario	2	0.07	3232.8	***
	scenario:management	2	0.05	2163.1	***
	residuals	1794	0.02		
size changes ~ scenario*community	community	1	0.59	11428.0	***
	scenario:community	2	0.10	941.3	***
	scenario	2	0.01	78.0	***

Studying ecosystem stability to global change across spatial and trophic scales

	residuals	1794	0.09		
size changes ~ scenario*management	management	1	119.42	1941000.0	***
	scenario	2	0.06	473.5	***
	scenario:management	2	0.00	3.2	**
	residuals	1794	0.11		

Supplementary Figures

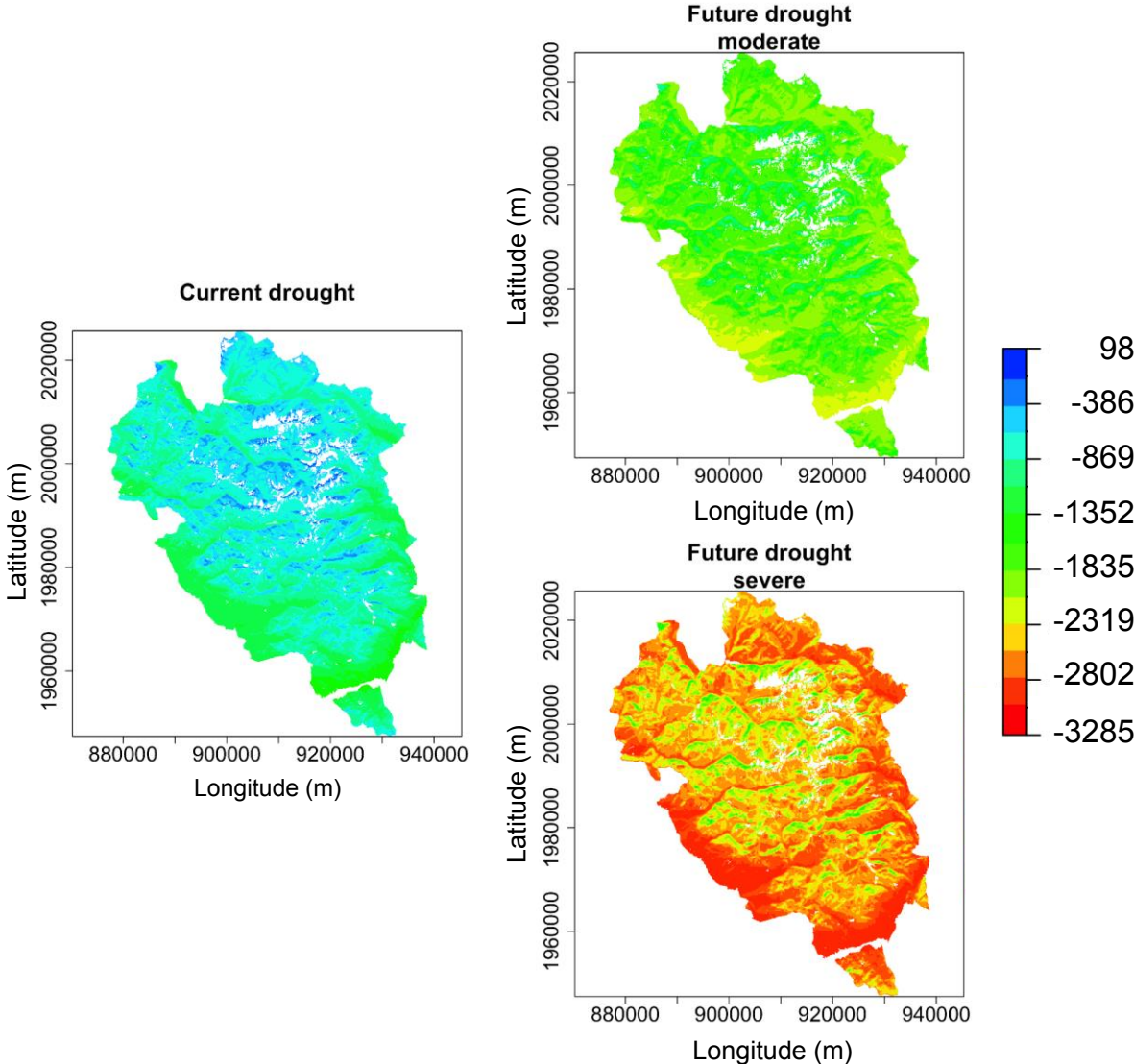


Figure S1. Current and future drought intensity (Din) maps. Figure adapted from Barros et al. (2017).

Studying ecosystem stability to global change across spatial and trophic scales

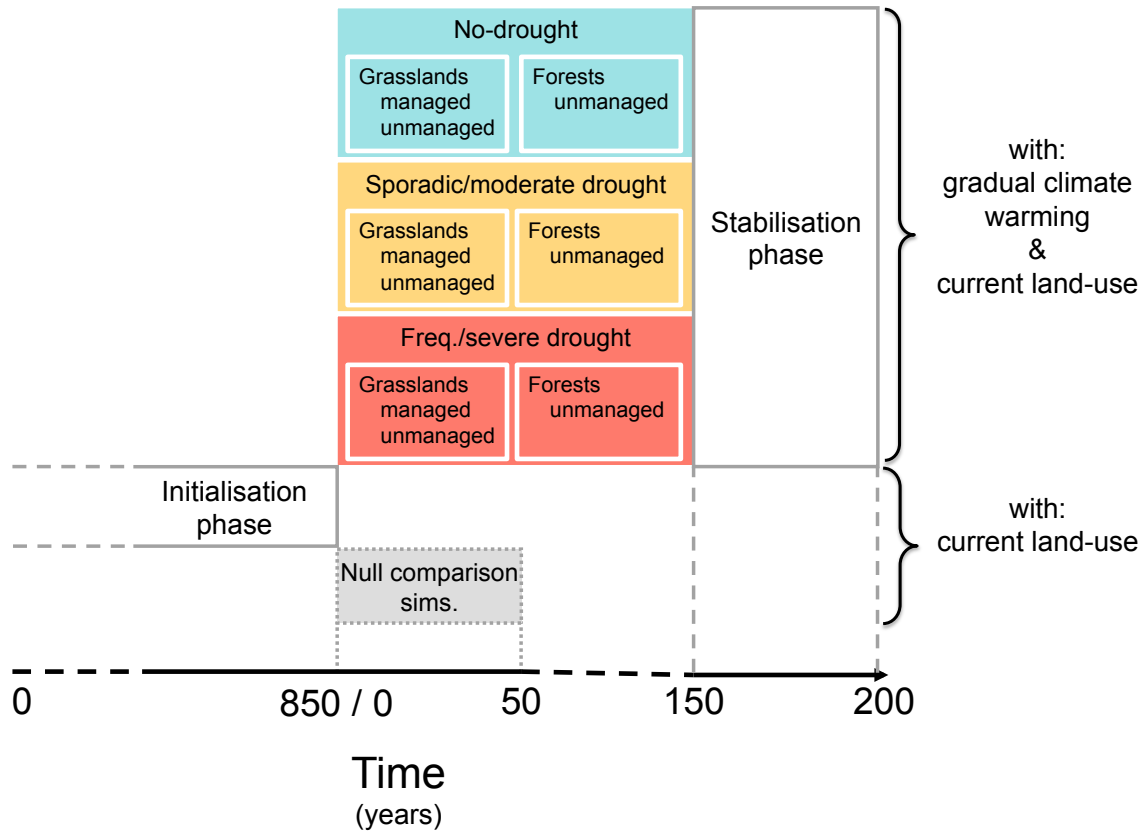


Figure S2. Simulation experiment. Scheme of the simulation experiment used to understand the effects of climate warming and drought regimes on departures from stability of grassland and forest communities. Note that in the case of grasslands effects of different management regimes were also assessed, leading to an unbalanced design. Simulations – initialisation phase + scenario phases (blue, yellow and red boxes) + stabilisation phase – were repeated 3 times. Null comparison simulations were repeated 100 times, each repetition starting from the first repetition of the initialisation phase.

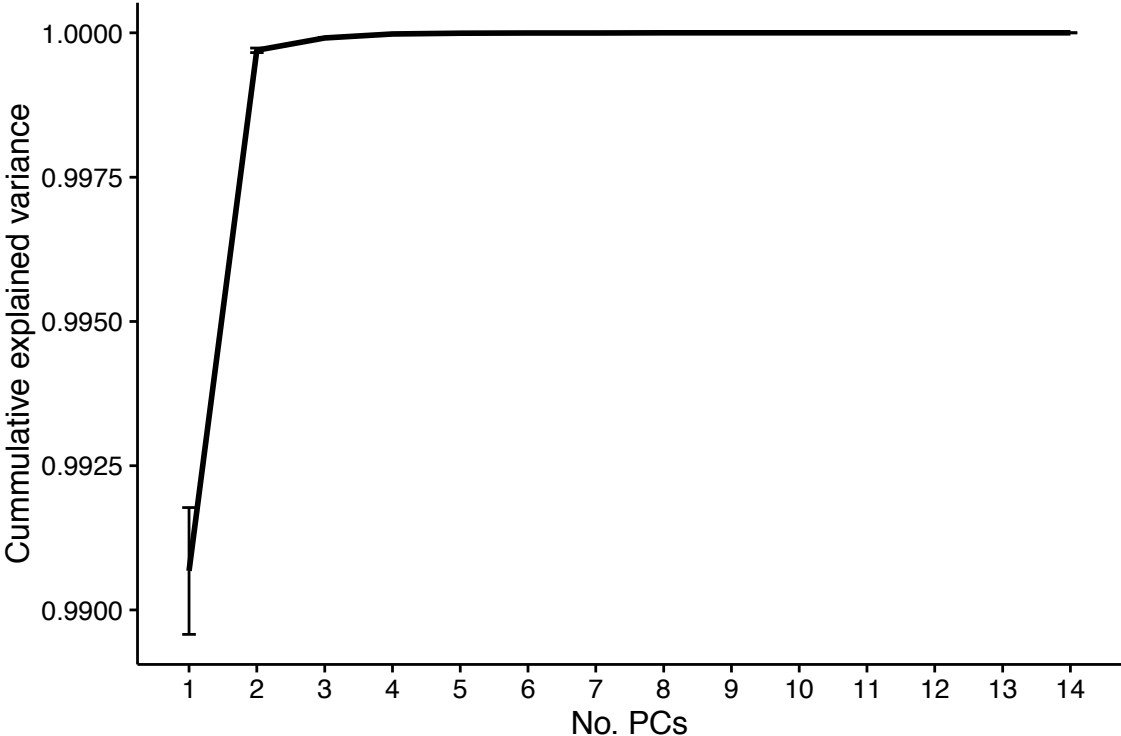


Figure S3. Average proportion of explained variance accumulated across principal components (PCs). We show here the cumulative explained variance for an increasing number of PCs, averaged across all the calculated Principal Components Analyses (one per pair of pre- and post-disturbance hypervolumes), except for those from null comparisons. Error bars represent standard errors.

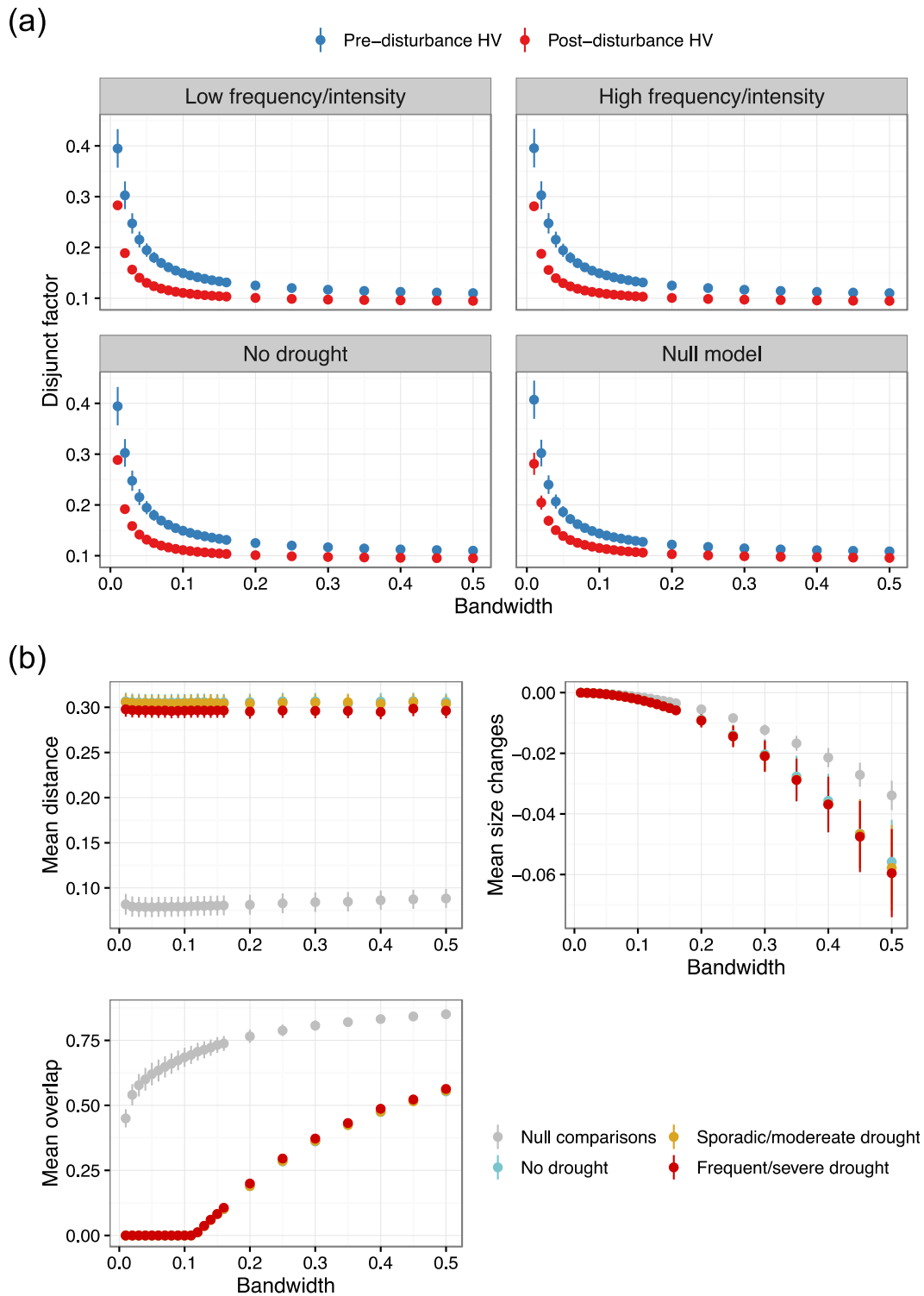
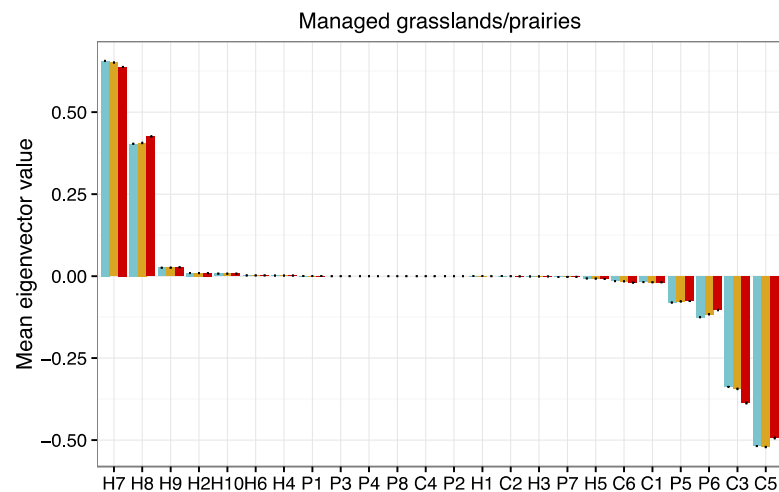
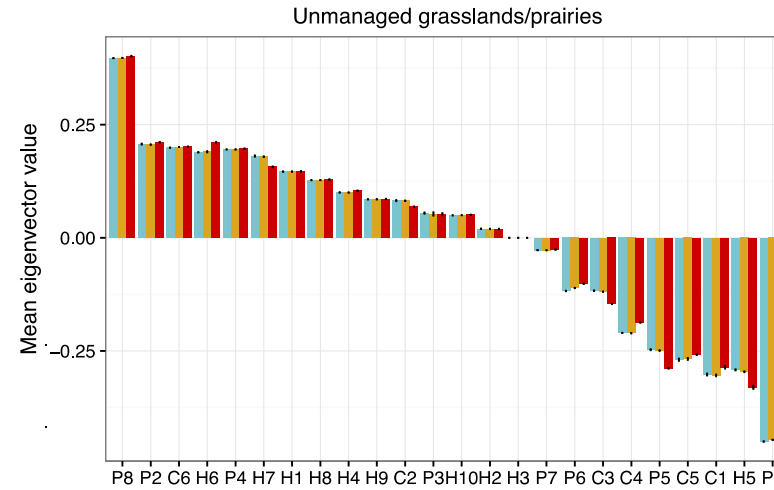


Figure S4. Bandwidth sensitivity analysis. Effect of bandwidth values on (a) hypervolumes' disjunct factor values and (b) hypervolume comparison metrics. Results of the bandwidth sensitivity analyses shown here are averaged across plant community and management combinations, and across repetitions. Vertical bars indicate standard errors. Only the first 3 repetitions of null comparison simulations were used.



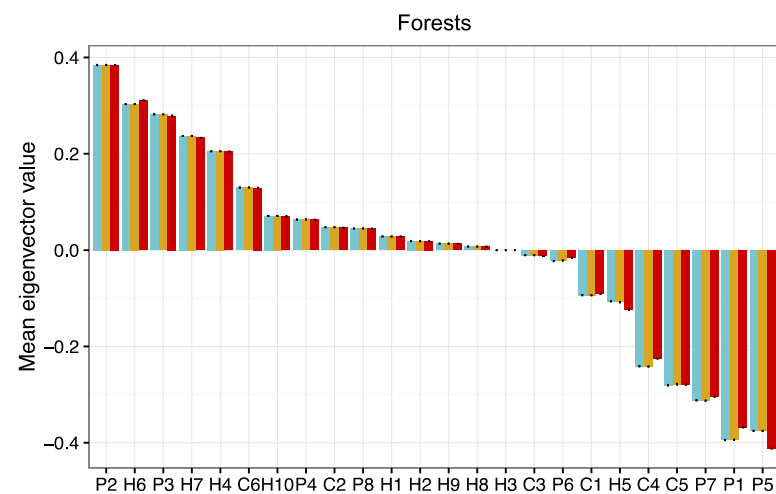
	H7	H8	H9	H2	H10	H6	H4	P1	P3	P4	P8	C4	P2	H1	C2	H3	P7	H5	C6	C1	P5	P6	C3	C5
Longevity	7	8	9	10	9	8	7	193	351	600	100	158	177	11	19	9	310	7	92	27	450	160	45	39
SLA	19.2	23.1	21.1	22.1	21.1	28.2	29.8	12	15.3	10.1	14.6	16.8	17.2	17.2	18	24.4	15.7	20.7	13.4	19.2	11.9	19.2	14.4	8.3

Figure S5. PFGs eigenvalues on the first principal component of managed grasslands PCAs. One PCA was calculated per drought scenario (no drought in blue, sporadic/moderate drought in yellow and frequent/severe drought in red), including the last 50 years of the initialisation phase from which the pre-disturbance state was defined. Corresponding PFG trait values are shown in the same order as the figure. Only the traits with highest correlations with the first principal component, across all scenarios, are shown (see Applying the hypervolumes framework and statistical analysis above for details). Other trait values are listed in Table S2 in this appendix.



	P8	P2	C6	H6	P4	H7	H1	H8	H4	H9	C2	P3	H10	H2	H3	P7	P6	C3	C4	P5	C5	C1	H5	P1
LDMC	0.4	350.8	355.0	227.8	279.8	195.4	260.7	274.2	228.5	417.6	196.0	265.3	0.2	250.7	238.2	360.5	282.2	221.2	330.5	309.3	390.2	262.7	243.0	346.8
Seed mass	0.2	0.1	39.5	2.3	6.8	0.4	0.9	0.9	0.4	0.4	0.4	86.4	6.2	4.0	2.4	78.3	6.1	0.5	193.0	114.1	75.0	23.9	1.9	177.9
SLA	14.6	17.2	13.4	28.2	10.1	19.2	17.2	23.1	29.8	21.1	18.0	15.3	21.1	22.1	24.4	15.7	19.2	14.4	16.8	11.9	8.3	19.2	20.7	12.0
Soil moisture	2	2	2	2	3	2	2	3	2	3	2	2	2	2	2	0	1	2	1	1	0	0	1	0

Figure S6. PFGs eigenvalues on the first principal component of unmanaged grasslands PCAs. One PCA was calculated per drought scenario (no drought in blue, sporadic/moderate drought in yellow and frequent/severe drought in red), including the last 50 years of the initialisation phase from which the pre-disturbance state was defined. Corresponding PFG trait values are shown in the same order as the figure. Only the traits with highest correlations with the first principal component, across all scenarios, are shown (see Applying the hypervolumes framework and statistical analysis above for details). Other trait values are listed in Table S2 in this appendix.



	P2	H6	P3	H7	H4	C6	H10	P4	C2	P8	H1	H2	H9	H8	H3	C3	P6	C1	H5	C4	C5	P7	P1	P5
Dispersal	5	3	4	5	3	7	7	6	4	4	3	6	7	3	7	1	4	6	3	6	6	4	6	6
Longevity	177	8	351	7	7	92	9	600	19	100	11	10	9	8	9	45	160	27	7	158	39	310	193	450
Maturity	15	4	18	4	4	8	4	15	4	15	4	3	4	4	3	6	20	5	4	10	8	15	15	25
Seed mass	0.1	2.3	86.4	0.4	0.4	39.5	6.2	6.8	0.4	0.2	0.9	4.0	0.4	0.9	2.4	0.5	6.1	23.9	1.9	193.0	75.0	78.3	177.9	114.1
SLA	17.2	28.2	15.3	19.2	29.8	13.4	21.1	10.1	18.0	14.6	17.2	22.1	21.1	23.1	24.4	14.4	19.2	19.2	20.7	16.8	8.3	15.7	12.0	11.9
Soil moisture	2	2	2	2	2	2	2	3	2	2	2	2	3	3	2	2	1	0	1	1	0	0	0	1

Figure S7. PFGs eigenvalues on the first principal component of forest PCAs. One PCA was calculated per drought scenario (no drought in blue, sporadic/moderate drought in yellow and frequent/severe drought in red), including the last 50 years of the initialisation phase from which the pre-disturbance state was defined. Corresponding PFG trait values are shown in the same order as the figure. Only the traits with highest correlations with the first principal component, across all scenarios, are shown (see Applying the hypervolumes framework and statistical analysis above for details). Other trait values are listed in Table S2 in this appendix.

APPENDIX 5: SUPPLEMENTARY MATERIALS TO CHAPTER IV

Extended methods

Our study was focused on all terrestrial tetrapods present in EU countries for which we had information on potential prey, habitat preferences and geographical distribution (a final total of 840 species – 83 amphibians, 435 birds, 201 mammals and 121 reptiles). This information was summarised into four different matrices (the metaweb, species x habitat, pixel x habitats and pixel x species matrices), which we detail separately before explaining how local networks were calculated across Europe, the scenarios of land-use and climate changes, and the workflow of our simulation experiment. All analyses were done at 10 Km resolution.

The metaweb – potential trophic interactions between all pan-European vertebrates

The metaweb is a species x species square matrix containing all potential binary trophic interactions between n rows of prey and n columns of predators, n being the number of vertebrate species plus 11 diet categories (DC; Algae, Mosses/Lichens, Mushrooms, Fruits, Grains/Nuts/Seeds, Other Plant Parts, Insects, Fish, Domestic Animals, Coprofagous and Detritus). Information on potential pairwise species interactions was obtained per life stage (juvenile, adult and carrion, with carrion life stages only being prey) using available literature and expert knowledge on species' feeding ecology. Links between juvenile reptiles and DC were ignored if not present in the adult diet; for birds and mammals, links with diet categories were removed if the species' diet was composed of <50% of non-vertebrate items and fish (with reference to EltonTraits 1.0 diet categories; Wilman *et al.* 2014). This resulted in a total of 111 species being considered exclusively as carnivores (0 amphibians, 50 birds, 26 mammals and 35 reptiles). Links with carrion life stages were removed for all amphibian and reptile species, under the assumption that these species either rely on DC items or actively hunt. For birds and mammals, links with carrion life stages were kept for species that relied on scavenging for $\geq 50\%$ of their diet (with reference to EltonTraits 1.0), resulting in a total of 7 scavengers. All life stages were later collapsed by species into a binary matrix, and 0s were assigned to all columns of DC.

We are aware that the thresholds we used to filter species dietary requirements are arbitrary. Unfortunately, it was not possible to obtain information on the proportion of tetrapod vertebrate items required to ensure the survival of the >800 species in our metaweb. Hence, we opted to use a neutral threshold of 50% that does not assume a species to be more or less dependent on terrestrial vertebrates than on other dietary items.

Species x habitat matrix – species' habitat preferences

Species' habitat preferences were obtained from Maiorano *et al.* (2013), who assigned a value of habitat suitability to each of the 46 land-use classes from GlobCover V2.2, following expert-based knowledge and available literature. Maiorano *et al.* (2013) classified land-use classes as 2 if they were optimal habitats for a species (i.e. where the species is able to persist), 1 if they constituted secondary habitat for the species (i.e. where the species can be present, but will not persist in the absence of optimal habitat), and 0 if they were unsuitable habitat for the species. For the purpose of the present study, we considered secondary and optimal habitats equally, in order to maintain a maximum degree of potentiality in our analyses. We also converted GlobCover classes into the Dyna-CLUE model classes (Stürck *et al.* 2015; see further details below) to obtain a correspondence with the classes present in the present and future land-use maps used to build local networks (see Table S2 in this appendix).

Pixel x habitats matrix – habitat maps

Habitat maps were obtained from land-use projections by Stürck *et al.* (2015) using the land-use model Dyna-CLUE. Dyna-CLUE projects the cover of different land-use classes by combining projections from urban, agricultural and forest models with different future land change trajectories (Stürck *et al.* 2015). Land-use maps used to build baseline networks and in scenarios with no land-use change (LUC) corresponded to model projections for year 2000. Future land-use maps, used for LUC scenarios, came from simulated projections for year 2040 under an A2 IPCC-equivalent scenario (Fig. S3 in this appendix). Maps were at 1Km resolution and since 2040 projections only covered European Union (EU) countries, our simulations were limited to these territories. We chose a scenario equivalent to the A2 IPCC climate change scenario in order to simulate a worst-case situation. The A2 scenario is a high-greenhouse-gas emission scenario coupled with a governmentally heterogeneous Europe, where governance is made at the local scale and aiming at the preservation of local identities. Human population is predicted to increase, but economic growth and technological change happen slowly and are spatially fragmented (Nakicenovic *et al.* 2000). In terms of land-use changes, this means an overall cropland intensification across EU countries and lower expansion of wild areas than in other scenarios (Stürck *et al.* 2015).

The final pixel x habitat matrix was built at 10 Km, by extracting the proportion of each land-use class present in each 10 Km grid-cell and converting proportions to binary values

(presences/absences). The extraction of land-use proportions was achieved in ArcGIS v10.4 (ESRI 2011) by intersecting all 1 Km land-use pixels with a 10 Km grid. A land-use type was assumed present if it had at least one 1 Km pixel inside a 10 Km grid pixel.

Baseline and future pixel x species matrices – species' geographical distributions

Species' geographical distributions came from species distribution models' (SDMs) projections. The model aims to establish the statistical link between species' presences (and absences) and climate. Species presence/absence information was obtained from Maiorano *et al.* (2013) and rescaled from 300 m resolution to 10 Km resolution using a potential presence perspective. A species was considered present in a 10 Km² pixel if it was detected in at least one 300 m² pixel of secondary or optimal habitat. After rescaling, species whose distributions were smaller than twenty 10 Km² pixels were excluded from further analyses, since low sample size would result in poor SDM projections accuracy. Baseline and future species' distributions were then obtained by projecting species presences/absences in function of four bioclimatic variables (annual mean temperature, temperature seasonality, annual precipitation and precipitation seasonality 'BIOCLIM' variables from WorldClim at 10' resolution – available at <http://www.worldclim.org/bioclim>) chosen to represent dominant N-S and E-W climatic gradients in Europe. Baseline distributions were based on climate values averaged between 1960-1990 and future distributions were based on climate change projections for years 2021-2050 also following the A2 IPCC scenario. Climate change was simulated using the regional climate model (RCM) RCA3 (Samuelsson *et al.* 2011) fed by the global circulation model (GCM) ECHam5, which was in turn derived from the ENSEMBLES EU project output.

Species distributions were projected using a Random Forest SDM within the *biomod2 R* package (Thuiller *et al.* 2009). The model was run separately for baseline and future distributions and repeated 5 times for each species. Each replicate was calibrated using 80% of the total presence/absence dataset and evaluated on the remaining 20% (using random data splitting). Each replicate was evaluated by calculating the TSS (true skill statistics) and the area under the curve (AUC) of the receiver operating characteristic (ROC) algorithms available in *biomod2*. TSS reflects how well the model predicts presences and absences, being calculated as the difference between the sensitivity (the ratio between true presences and predicted presences) and specificity (the ratio of true absences and predicted absences) of the model minus 1. TSS values range from -1, no agreement, to +1, perfect agreement, with 0

meaning a random fit. AUC summarises model accuracy by evaluating the rate of true presences vs. false absences. AUC values range from 0, all predictions are false, to 1, all predictions are true, with 0.5 indicating a random fit. Final projections were obtained using a weighted average ensemble forecasting method. This is, the final distribution of each species was built by averaging individual model replicates weighted proportionally to their TSS score. Only model replicates for which $TSS > 0.4$ were used for ensemble forecasting. A second set of ensemble projections was calculated using committee averaging (please see Araújo & New 2007 for details), but later discarded as model performance (measured by TSS and AUC scores) was worse than when using weighted averaging. Final distributions were later converted to binary values using a threshold maximizing the TSS statistics. The weighted average ensemble model fit was overall very good, with mean TSS and AUC scores across species being $0.991 (\pm 0.010)$ and $0.998 (\pm 0.003)$ respectively. Lastly, the obtained species baseline and future binary distributions were summarised into baseline and future pixel x species binary matrices.

Building local networks

Building the local trophic networks (i.e. trophic networks present in each 10 Km pixel) involved four major steps (Fig. S4 in this appendix):

1. Listing the species and habitats present in the pixel – using the pixel x species and pixel x habitats matrices described above;
2. Subset the complete species x habitats matrix and metaweb by the species present in the pixel;
3. Building a local trophic network based on species habitat co-occurrences multiplying the filtered species x habitat matrix by its transpose, which automatically removed forbidden links (i.e. links that could not occur between two locally present species because they did not share any habitat preference). For instance, if species A prefers forest and grassland habitats and species B prefers grassland and wetland habitats, but in pixel i there are only forest and marsh habitats, the two species are locally present, but will not interact.
4. Links with DC were added and links that were not present in the metaweb were removed. Also, species that lost too many prey items (according to the threshold of extinction – see main text) after step 3 were removed iteratively, since removing one

prey-less species can cause another to become prey-less as well. Note that diet categories were ubiquitously present across the landscape.

Sensitivity analysis

In order to choose an adequate threshold of extinction, we assessed the consequences of changing this threshold for baseline network properties. After having calculated all baseline networks assuming a completely conservative approach (i.e. a species was present in a network if it had at least one prey item) and extracted the distributions of the number of prey items across pixels for each species ('species prey distributions'), we calculated the minimum, median and different quantile values (10%, 25%, 75% and 90%) of number of prey items per species. We then re-built all baseline network pixels using these values as species-specific thresholds of extinction. Although it can be argued that generalist species would survive with a smaller proportion of potential prey items than specialist species, we did not wish to vary thresholds of extinction in function of the degree of generalism to avoid large impacts on network topology (i.e. preferentially removing specialist species).

Using a threshold equal to the minimum number of prey per species did not cause baseline networks to change, as would be expected. Increasing this threshold to the 10% quantile value caused relatively small changes in the distribution of network properties, and thresholds equal to or larger than the 25% quantile values caused large changes in to baseline network properties (Fig. S5 in this appendix). Notably, higher thresholds increased the number of pixels with negative modularity values (Fig. S6 in this appendix), as the loss of intermediate and top species caused more and more networks to become disconnected (Fig. S7 in this appendix). Because network properties based on species links are meaningless in disconnected networks, pixels whose baseline networks had negative modularity values needed to be excluded from further analyses. Hence, we chose to use the 10% quantile for our simulations, since it provided a more realistic representation of species abilities to survive in a given pixel, relatively to assuming that all species survive with at least one prey item, without significantly disrupting baseline networks.

Statistical analyses

To assess which network properties drove network robustness in PAs we focused our statistical analyses on pixels that suffered at least one secondary extinction (note that robustness is 'infinite' when no secondary extinctions occur). Although we expected

robustness to be driven mostly by the species richness, omnivory and connectance of the baseline networks (Gilbert 2009; Saint-Béat *et al.* 2015), we still investigated whether other network properties would be better predictors of network robustness (see Table S3 in this appendix for the list of properties measured). A small percentage of pixels ($\approx 0.5\%$; Fig. S3 in this appendix) had negative baseline modularity scores and were excluded from all statistical analyses.

To select the baseline network properties to include as predictors of robustness in our statistical models, we calculated correlations between robustness and each property, using Spearman rank correlations to account for potential non-linear relationships (Table S4 in this appendix). Highest positive correlations were obtained for species richness, S , number of links, L , and mean trophic level, $mean.TL$. Highest negative correlations were obtained for the proportion of basal species, $propB$, generality, $normGen$, and its standard deviation, $SDnormGen$. Because these network properties were highly correlated with each other (Table S4 in this appendix), only S was selected to enter the initial models. This is not surprising, as the number of species is known to be an important driver of trophic network structure (Vermaat *et al.* 2009; Baiser *et al.* 2012).

We used a linear mixed effects analysis to account for the effect of the number of secondary extinctions ($Sext$) on the relationships between robustness, network properties and scenarios of extinction. Despite that baseline connectance had a low correlation with robustness, we tested whether its inclusion as a predictor would improve the model. Connectance provides information on network complexity that is not directly reflected by network size (i.e. species richness), and is usually more dissociated from the number of nodes than other metrics (Vermaat *et al.* 2009; Baiser *et al.* 2012). Since this was also the case for our baseline networks (note the lower correlation values between S and C , relatively to other properties; Table S4 in this appendix) we believe that including C in our model provides valuable additional information. Moreover, including C improved model fit considerably (see Table S1 in this appendix). For the final model we included S , C and their interactions with scenario as fixed effects, with S and C being centred (by subtracting the mean from each value) and scaled (by dividing centred values by their standard deviation). As random effects, we included intercepts for $Sext$, as well as by-scenario random slopes for the effects of S and C (see Table S1 in this appendix for an analysis of variance of the model terms and Fig. S2 for effect sizes). Visual analysis of residual assumptions did not show significant deviations from homoscedasticity or normality. Intercepts and slopes fitted according to the random

Studying ecosystem stability to global change across spatial and trophic scales

effect of *Sext* had variances of, respectively, ≈ 93.23 and ≈ 8.23 for *S*, and ≈ 0.19 and ≈ 0.17 for *C* (residual variance ≈ 2.91).

All statistical analyses were done in *R* (R Core Team 2016). Linear mixed effects models were performed within the *lme4* *R* package (Bates *et al.* 2015).

Supplementary Tables

Table S1. Drivers of network robustness. *F* statistics of the main effects of initial species richness (*S*), initial connectance (*C*) and scenarios of land-use and climate changes on network robustness. The model was fitted using restricted maximum likelihood (REML) and effects are ordered by decreasing value of *F*. The asterisk, ‘*’, denotes the inclusion of main effects and their interaction (‘:’); random effect groupings (number of secondary extinctions, *Sext*) are indicated after the vertical bars. ‘*df*’, ‘*Sum Sq*’ and ‘*Mean Sq*’ stand for degrees of freedom, sum of squares and mean squares, respectively.

		df	Sum Sq	Mean Sq	F value
<i>Robustness</i> ~ (<i>S</i> + <i>C</i>) * <i>Scenario</i> +	<i>S</i> : <i>Scenario</i>	4	2217.15	554.29	190.202
(<i>S</i> <i>Sext</i>) + (<i>C</i> <i>Sext</i>)^{1,2}	<i>Scenario</i>	4	473.29	118.32	40.602
	<i>S</i>	1	63.61	63.61	21.828
	<i>C</i>	1	48.39	48.39	16.604
	<i>C</i> : <i>Scenario</i>	4	160.36	40.09	13.757

¹Likelihood ratio test against null model (*Robustness* ~ *Scenario* + (*S*|*Sext*) + (*C*|*Sext*)): χ^2 (10) = 678.24, p-value < 0.05

²Likelihood ratio test against model without *C* (*Robustness* ~ *S***Scenario* + (*S*|*Sext*)): χ^2 (8) = 4639.6, p-value < 0.0

Table S2. Correspondence between Dyna-CLUE land-cover model classes and GlobCover V2.2 classes and their description.

Dyna-CLUE		GlobCover V2.2	
0	Built-up area	190	Artificial surfaces and associated areas (urban areas >50%)
1	Arable land (non-irrigated)	14	Rainfed croplands
		20	Mosaic cropland (50-70%) / vegetation (grassland/shrubland/forest) (20-50%)
2	Pasture	30	Mosaic vegetation (grassland/shrubland/forest) (50-70%) / cropland (20-50%)
		120	Mosaic grassland (50-70%) and forest or shrubland (20-50%)
3	(semi-) Natural vegetation (including natural grasslands, scrublands, regenerating forest below 2 m, and small forest patches within agricultural landscapes)	131	Closed to open (>15%) broad-leaved or needle-leaved evergreen shrubland (<5m)
		132	Closed to open (>15%) broad-leaved evergreen shrubland (<5m)
		133	Closed to open (>15%) needle-leaved evergreen shrubland (<5m)
		134	Closed to open (>15%) broad-leaved deciduous shrubland (<5m)
		136	Open (15-40%) broad-leaved deciduous shrubland (<5m)
		140	Closed to open (>15%) herbaceous vegetation (grassland)
		141	Closed (>40%) grassland
4	Inland wetlands	144	Open (15-40%) grassland with sparse (<15%) trees or shrubs
		180	Closed to open (>15%) grassland or woody vegetation on regularly flooded or waterlogged soil
		185	Closed to open (>15%) grassland on regularly flooded or waterlogged soil
5	Glaciers and snow	220	Permanent snow and ice
6	Irrigated arable land	11	Post-flooding or irrigated croplands (or aquatic)
		13	Post-flooding or irrigated herbaceous crops
8	Permanent crops	10	Cultivated and managed areas
		15	Rainfed herbaceous crops
		16	Rainfed shrub or tree crops (cash crops)
		21	Mosaic cropland (50-70%) / grassland or shrubland (20-50%)
		32	Mosaic forest (50-70%) / cropland (20-50%)
10	Forest	40	Closed to open (>15%) broad-leaved evergreen or semi-deciduous forest (> 5m)
		41	Closed (>40%) broad-leaved evergreen and/or semi-deciduous forest
		50	Closed (>40%) broad-leaved deciduous forest (>5m)
		60	Open (15-40%) broad-leaved deciduous forest/woodland (>5m)
		70	Closed (>40%) needle-leaved evergreen forest (>5m)
		90	Open (15-40%) needle-leaved deciduous or evergreen forest (>5m)

Appendices - Appendix 5: Supplementary materials to Chapter IV

		91	Open (15-40%) needle-leaved deciduous forest (>5m)
		92	Open (15-40%) needle-leaved evergreen forest (>5m)
		100	Closed to open (>15%) mixed broad-leaved and needle-leaved forest
		101	Closed (>40%) mixed broad-leaved and needle-leaved forest
		110	Mosaic forest or shrubland (50-70%) and grassland (20-50%)
11	Sparsely vegetated areas	150	Sparse (<15%) vegetation
		151	Sparse (<15%) grassland
		152	Sparse (<15%) shrubland
		201	Consolidated bare areas (hardpans)
		202	Non-consolidated bare areas (sandy desert)
12	Beaches, dunes and sands	200	Bare areas
13	Salines	203	Salt hardpans
14	Water and coastal flats	210	Water bodies
15	Heather and moorlands	130	Closed to open (>15%) (broad-leaved or needle-leaved)

Table S3. List of baseline network properties measured, their abbreviations and, where pertinent, formulas for their calculation. Modularity scores were calculated after defining network clusters using the walk trap algorithm, using the *igraph* R package. Omnivory was calculated as the proportion of omnivore species, with omnivore species being those whose prey differed in trophic level. Trophic levels were calculated based on prey-averaged trophic levels, using the *PreyAveragedTrophicLevel* function available in the *cheddar* R package.

Network property	Abbreviation
Species richness (= number of nodes)	<i>S</i>
Number of links	<i>L</i>
Connectance (L/S^2)	<i>C</i>
Modularity	<i>Q</i>
Generality (normalised by <i>S</i>)	<i>normGen</i>
Vulnerability (normalised by <i>S</i>)	<i>normVul</i>
Standard deviation of generality	<i>SDnormGen</i>
Standard deviation of vulnerability	<i>SDnormVul</i>
Proportion of basal species (species with no vertebrate prey)	<i>propB</i>
Proportion of intermediate species	<i>propI</i>
Proportion of top species (species with no predators)	<i>propT</i>
Omnivory	<i>propOmn</i>
Mean trophic level	<i>mean.TL</i>
Maximum trophic level	<i>max.TL</i>
Standard deviation of trophic level	<i>sd.TL</i>

Appendices - Appendix 5: Supplementary materials to Chapter IV

Table S4. Spearman's rank pairwise correlations amongst robustness and baseline network properties. Correlations $\geq |0.5|$ are in bold. All correlations were significant at p -value < 0.05 . See Table S3 in the appendix for the list of network properties and their abbreviations

	S	L	C	Q	normGen	normVul	SDnormGen	SDnormVul	propB	propI	propT	propOmn	mean.TL	max.TL
Robustness	0.20	0.19	0.06	-0.07	-0.12	-0.08	-0.12	-0.08	-0.12	0.13	-0.07	0.13	0.15	0.11
L	0.95													
C	0.35	0.56												
Q	-0.56	-0.55	-0.38											
normGen	-0.73	-0.79	-0.59	0.46										
normVul	-0.46	-0.57	-0.64	0.43	0.45									
SDnormGen	-0.73	-0.79	-0.59	0.46	1.00	0.45								
SDnormVul	-0.46	-0.57	-0.64	0.43	0.45	1.00	0.45							
propB	-0.73	-0.79	-0.59	0.46	1.00	0.45	1.00	0.45						
propI	0.72	0.81	0.68	-0.48	-0.94	-0.70	-0.94	-0.70	-0.94					
propT	-0.36	-0.48	-0.56	0.35	0.36	0.93	0.36	0.93	0.36	-0.63				
propOmn	0.76	0.79	0.52	-0.51	-0.98	-0.42	-0.98	-0.42	-0.98	0.91	-0.36			
mean.TL	0.80	0.89	0.66	-0.49	-0.91	-0.55	-0.91	-0.55	-0.91	0.92	-0.48	0.89		
max.TL	0.64	0.74	0.73	-0.42	-0.75	-0.61	-0.75	-0.61	-0.75	0.80	-0.55	0.69	0.86	
sd.TL	0.59	0.73	0.80	-0.39	-0.78	-0.59	-0.78	-0.59	-0.78	0.82	-0.55	0.72	0.91	0.90

Supplementary Figures

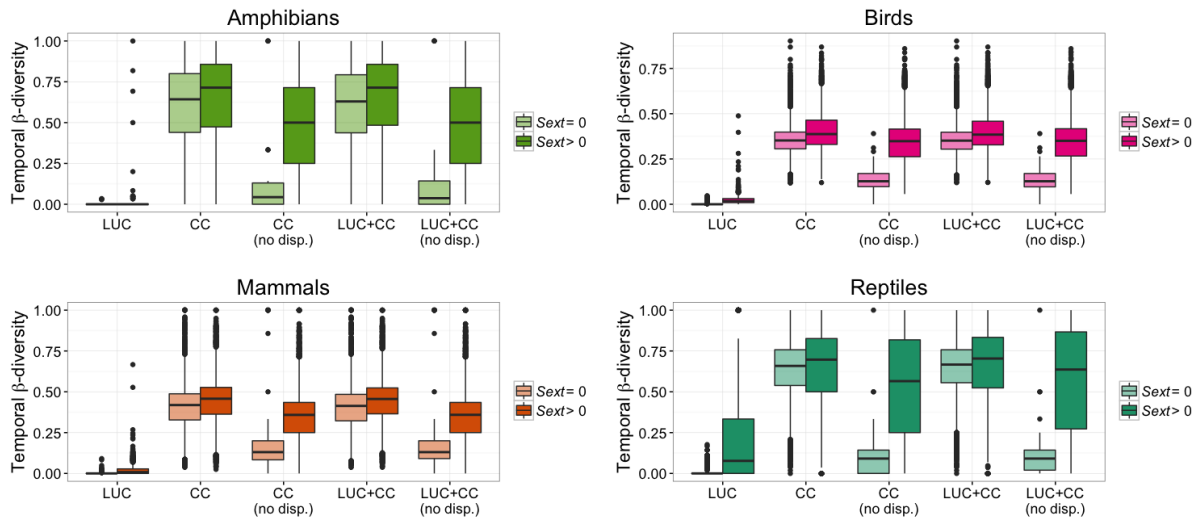


Figure S1. Temporal taxonomic turnover (β -diversity) of amphibians, birds, mammal and reptile species in PAs pixels, by land-use and climate change scenario. Light boxes correspond to PA pixels where no secondary extinctions (S_{ext}) occurred, while dark boxes correspond to pixels that had at least one S_{ext} . See Extended methods above for details on the calculation of temporal β -diversity.

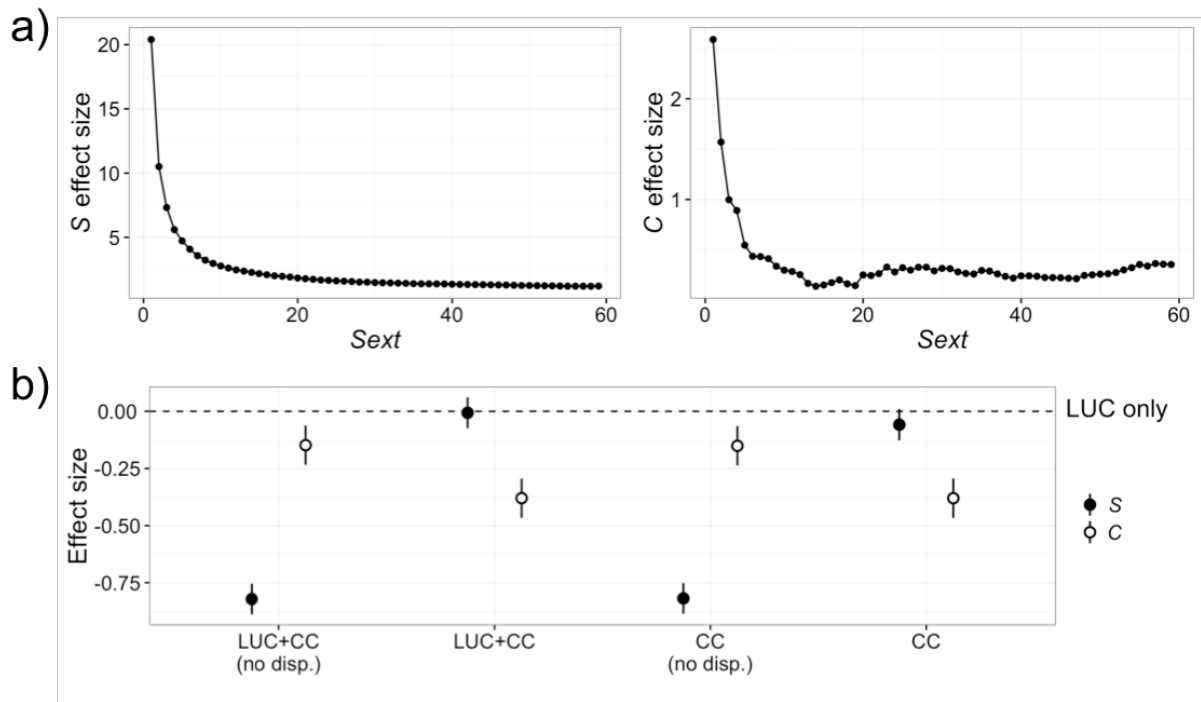


Figure S2. Species richness (*S*) and connectance (*C*) effect sizes by a) the number of secondary extinctions (*Sext*) and b) under the effect of the different scenarios. Note that effects sizes per scenario are shown relatively to the reference scenario of land-use changes alone ('LUC only'). Scenario acronyms 'CC' and 'LUC' stand for climate change and land-use changes, respectively, and 'no disp.' for no dispersal. See Table S1 and Extended methods in this appendix for model details and further results.

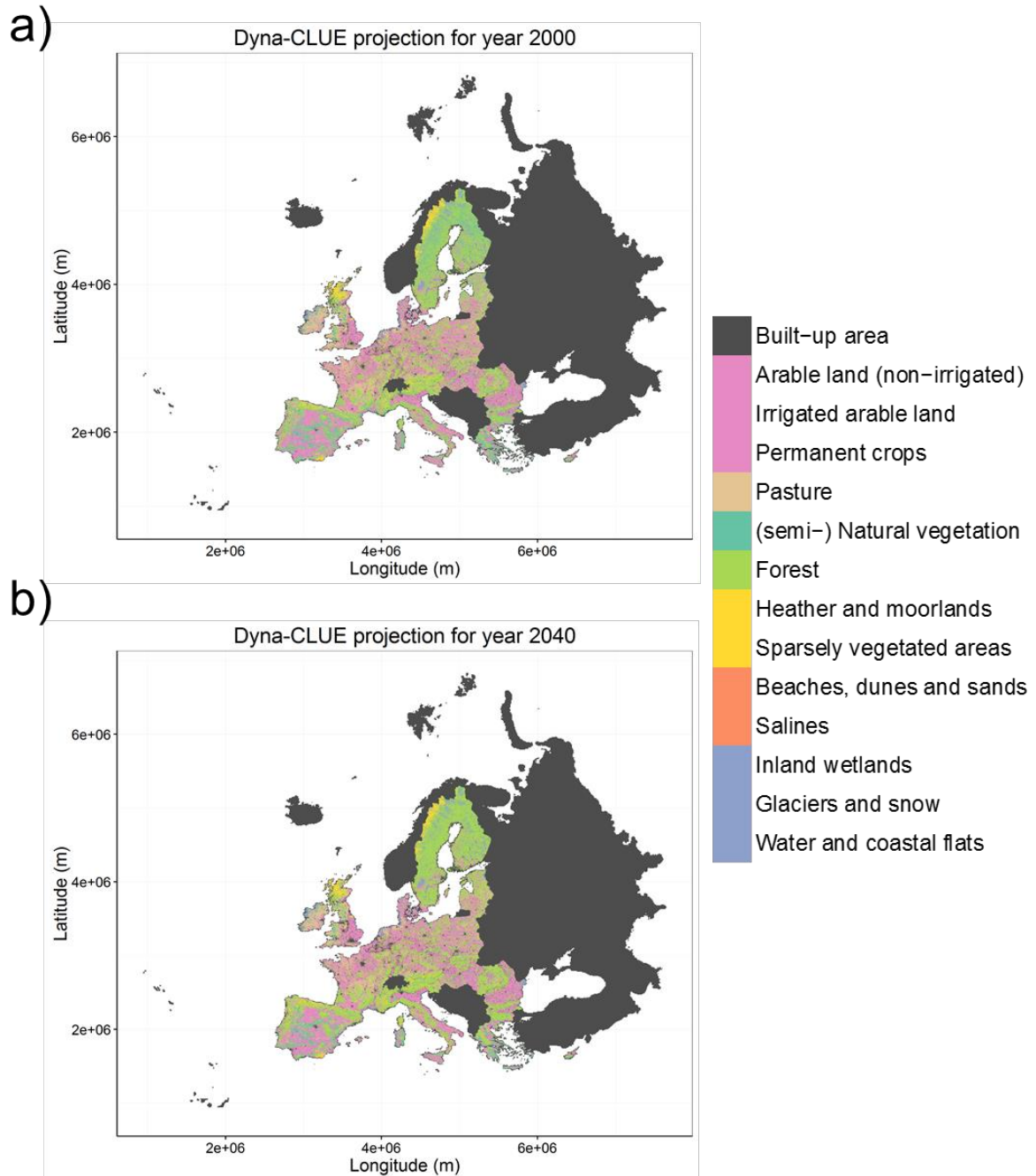


Figure S3. 'Present' and future land-use projections. Land-use maps were obtained from Dyna-CLUE land-use projections for years a) 2000 (baseline, or no land-use changes) and b) 2040 (future land-use changes). Projections for year 2040 followed an IPCC A2-equivalent scenario. See the Extended methods above for details.

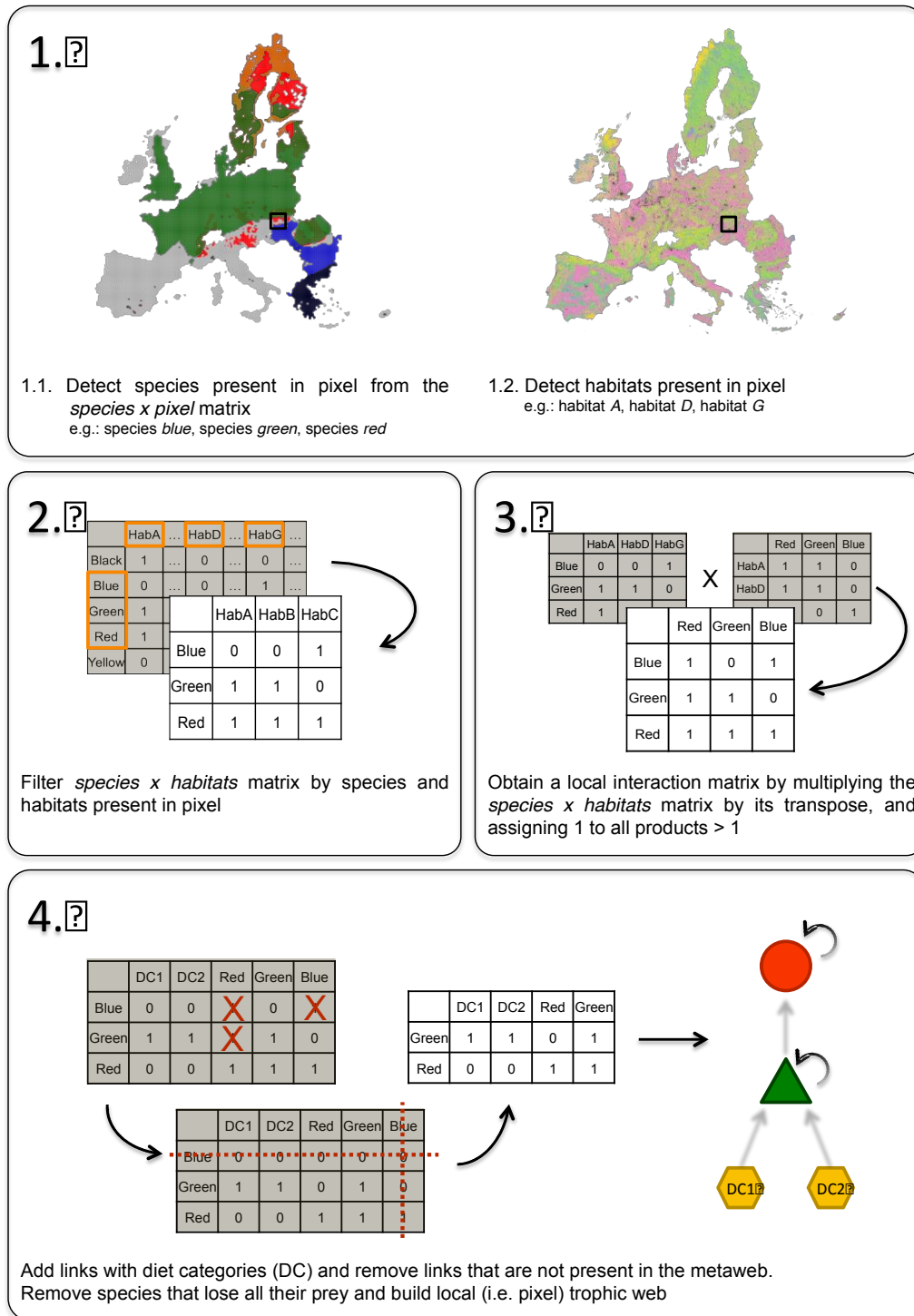


Figure S4. Building local trophic networks. Schematic representation of the four steps involved in building local trophic networks at 10 Km scale, based on species distributions, habitats and the metaweb. Note that the pixel representation is not to scale and that white areas in maps represent areas excluded from the analyses (countries outside EU, as well as large lakes in species distribution maps).

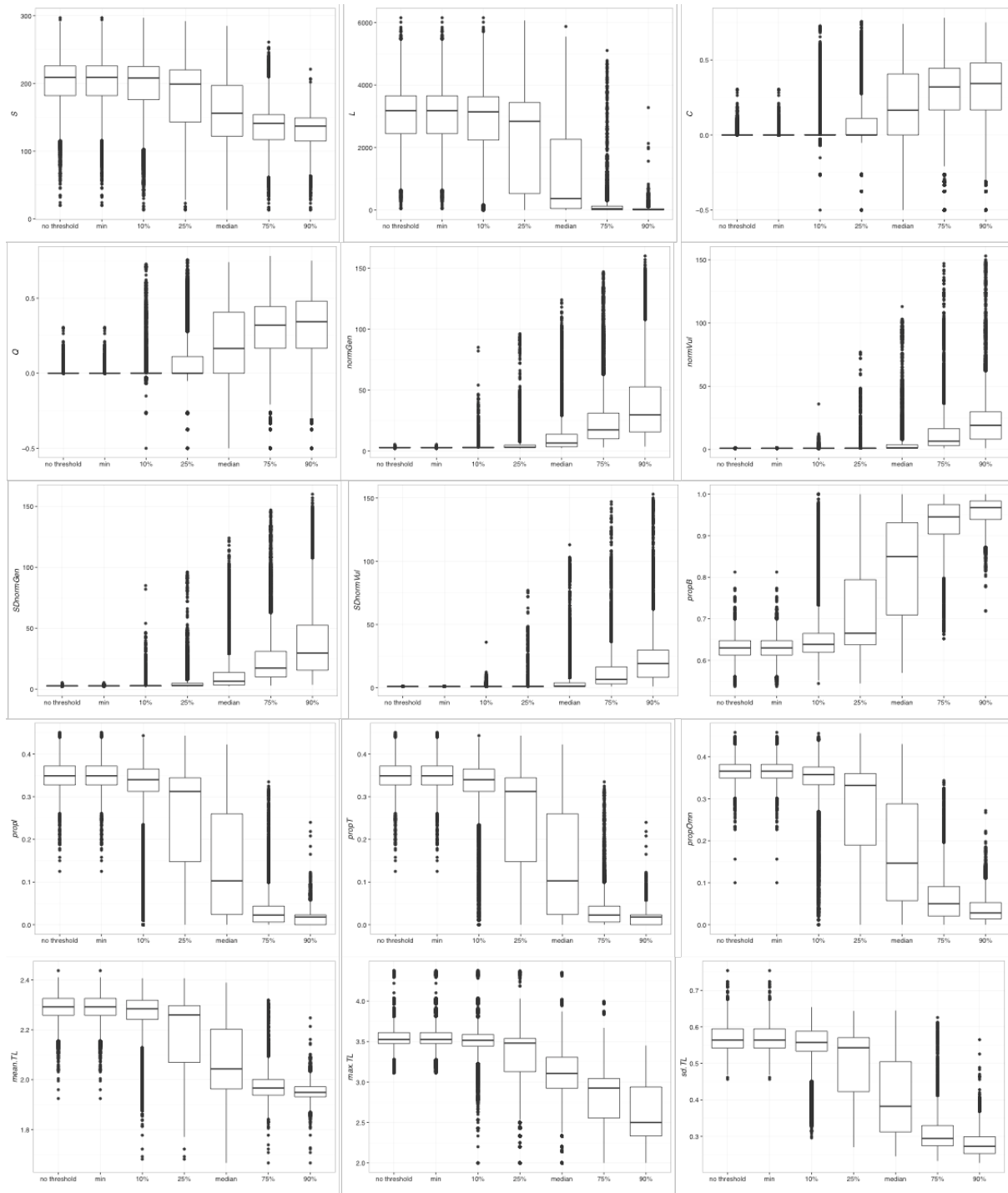


Figure S5. Sensitivity analysis of baseline network properties to changing species quantile thresholds. Thresholds were calculated per species as the min, median and quantile values (10%, 25%, 75% and 90%) from the distribution of number of prey items of a given species across all baseline networks built using a conservative approach (i.e. species only required one prey item – ‘no threshold’). See Table S3 for the list of network properties abbreviations.

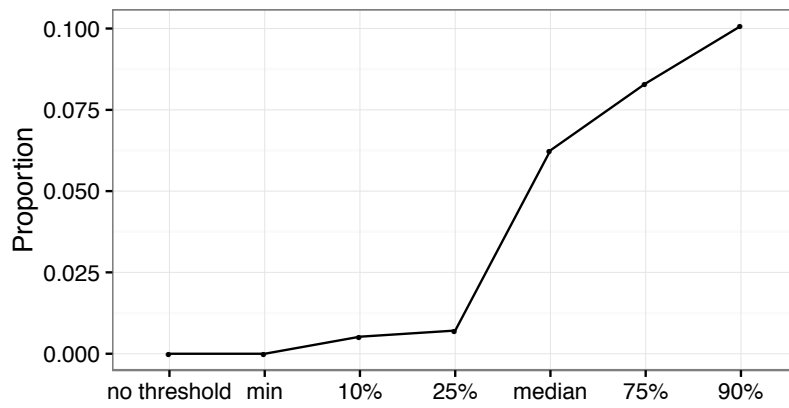


Figure S6. Proportion of pixels with negative modularity values in function of extinction thresholds used. Thresholds were calculated per species as the min, median and quantile values (10%, 25%, 75% and 90%) from the distribution of number of prey items of a given species across all baseline networks built using a conservative approach (i.e. species only required one prey item – ‘no threshold’).

Studying ecosystem stability to global change across spatial and trophic scales

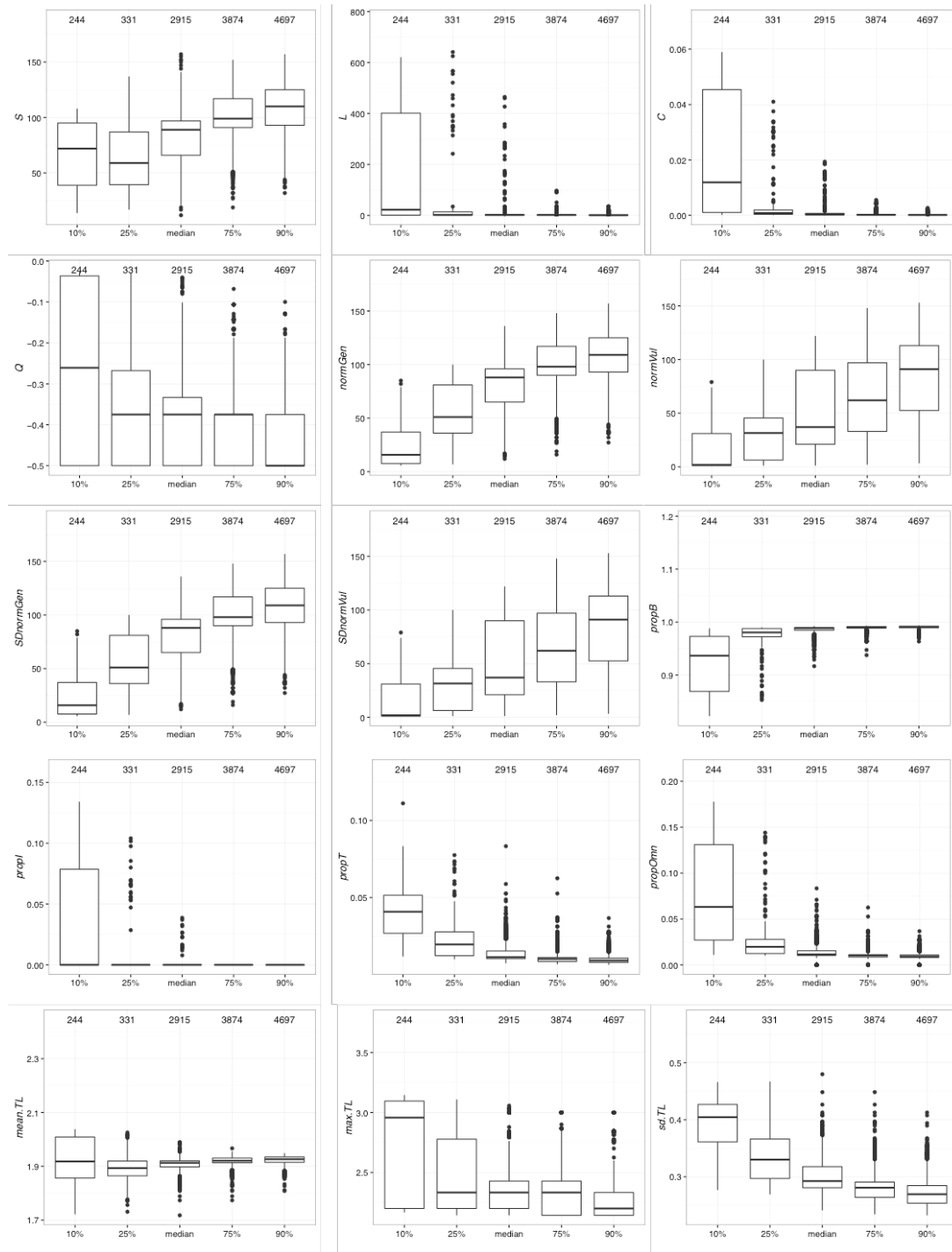


Figure S7. Baseline network properties in pixels with negative modularity values, in function of the extinction threshold used. Thresholds were calculated per species as the min, median and quantile values (10%, 25%, 75% and 90%) from the distribution of number of prey items of a given species across all baseline networks built using a conservative approach (i.e. species only required one prey item – ‘no threshold’). See Table S3 in this appendix for the list of network properties abbreviations.

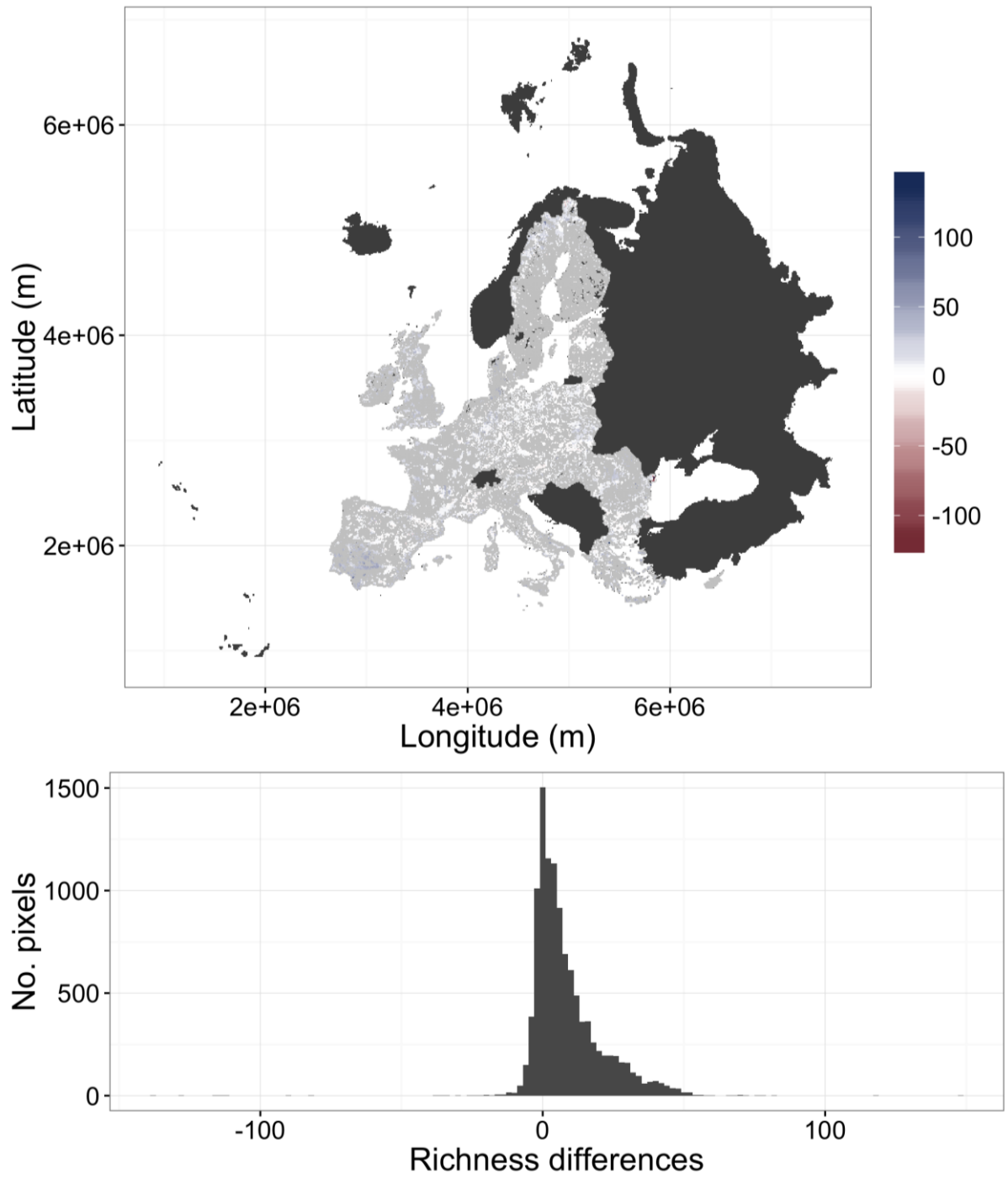


Figure S8. Impact of trophic interactions on vertebrate diversity projections under climate change. The map shows the difference between vertebrate species richness obtained by stacking species distribution model (SDM) projections and species richness in trophic networks, under a scenario of climate change only and full dispersal. Negative values indicate SDM underpredictions (in red) and positive values indicate SDM overpredictions (in blue), relatively to trophic network diversity. The histogram shows the frequency of difference values in number of pixels.

APPENDIX 6: SIMULATING PLANT INVASION DYNAMICS IN MOUNTAIN ECOSYSTEMS UNDER GLOBAL CHANGE SCENARIOS

Submitted.

Marta Carboni^{1*}, Maya Guéguen¹, Ceres Barros¹, Damien Georges^{1,2}, Isabelle Boulangeat³, Rolland Douzet⁴, Stefan Dullinger⁵, Guenther Klöner⁵, Mark van Kleunen⁶, Franz Essl⁵, Oliver Bossdorf⁷, Emily Haeuser⁶, Matthew V. Talluto¹, Dietmar Moser⁵, Svenja Block⁷, Iwona Dullinger^{5,8}, Tamara Münkemüller¹, Wilfried Thuiller¹

¹ Univ. Grenoble Alpes, CNRS, LECA, Laboratoire d'Écologie Alpine, F-38000 Grenoble, France

² International Agency for Research on Cancer, Lyon, France

³ Section for Ecoinformatics and Biodiversity, Department of Bioscience, Ny Munkegade 114, DK-8000 Aarhus C, Denmark

⁴ Station Alpine Joseph Fourier, UMS 3370 UJF-CNRS

⁵ Division of Conservation Biology, Vegetation and Landscape Ecology, Department of Botany and Biodiversity Research, Faculty of Life Sciences, University of Vienna, Rennweg 14, 1030 Vienna, Austria

⁶ Department of Biology, University of Konstanz, Universitätsstrasse 10, 78457 Konstanz, Germany

⁷ Institute of Evolution & Ecology, University of Tübingen, Auf der Morgenstelle 5, 72076 Tübingen, Germany

⁸ Institute of Social Ecology, Faculty for Interdisciplinary Studies, Alps Adria University, Schottenfeldgasse 29, 1070 Vienna, Austria

*Corresponding author: marta.carboni@gmx.net

Keywords: alien species, biotic interactions, dynamic vegetation model, global change scenarios, mountain ecosystems, ornamental species, propagule pressure

Abstract

Across the globe, invasive alien species cause severe environmental changes, altering species composition and ecosystem functions. So far, mountain areas have largely been spared from large-scale invasions. However, we hypothesize that climate change, land-use abandonment, development of tourism and the increasing ornamental trade will weaken the barriers to invasions in these systems. Here, we used a spatially and temporally explicit simulation model to forecast invasion risks in a protected mountain area in the French Alps under future conditions. We combined scenarios of climate change, land-use abandonment and tourism-linked increases in propagule pressure to test if the spread of alien species in the region will increase in the future. We modelled already naturalized aliens and new ornamental plants, accounting for interactions among global change components but also competition with the native vegetation. Our results show that propagule pressure and climate change will interact to increase overall species richness, maximum elevation reached and regional range-sizes of both naturalized aliens and new ornamentals. Under climate change, woody aliens are

predicted to more than double in range-size and herbaceous species occupy up to 20% of the park area. In contrast, land-use abandonment will open new invasion opportunities for woody aliens, but decrease invasion probability for naturalized and ornamental herbs as a consequence of colonization by native trees. This emphasises the importance of interactions with the natives either for facilitating or potentially for curbing invasions. Overall, our work highlights an additional and previously underestimated threat for the fragile mountain flora of the Alps already facing climate changes, land-use transformations and overexploitation by tourism in the near future.

Introduction

Despite the recognized and growing problem of invasive species damaging native diversity and ecosystem function (Mack *et al.*, 2000; Sax & Gaines, 2008), it is clear that not all habitats are equally susceptible to invasion by introduced aliens (Chytrý *et al.*, 2008). Mountain ecosystems, for example, have largely been spared from invasions, mostly because of harsh climatic conditions and comparatively low human population densities (Pauchard *et al.*, 2009; Kueffer *et al.*, 2013). However, the diversity and abundance of alien plants in mountain ranges has been increasing over the last few years (Johnston & Pickering, 2001; Becker *et al.*, 2005; Pickering *et al.*, 2008; Pauchard *et al.*, 2009), suggesting that the potential already exists for increasing invasion impacts in the future.

Alpine environments in Europe (and elsewhere) are increasingly threatened by climate change (Engler *et al.*, 2011), abandonment of traditional agro-pastoral practices leading to shrub and tree encroachment (Gehrig-Fasel *et al.*, 2007) and the development of mountain areas for recreational use (Godde *et al.*, 2000). In the future, these three aspects of environmental change are likely to interact with biological invasions and with the potential for native vegetation to resist such invasions. A warming climate is likely to weaken some of the barriers currently constraining aliens to lower elevations (Petitpierre *et al.*, 2016). The effects of land-use abandonment on the future spread of alien species are more difficult to predict as it could either open new opportunities for the invasion of alien trees and shrubs or, in contrast, lead to greater biotic resistance of the resident vegetation following woody encroachment. Increased tourism and growing human populations will inevitably lead to higher colonization and propagule pressures of alien species, which is known to enhance their spread (Colautti *et al.*, 2007; Kalwij *et al.*, 2008; Lockwood *et al.*, 2009). Finally, given that ornamental horticulture is the major introduction pathway for invasive plants (Weber, 2005),

new alien invasions in mountains could be fostered through the introduction of pre-adapted ornamental species for revegetation of disturbed sites or as amenity plantings in resorts (McDougall *et al.*, 2005; Kueffer *et al.*, 2013).

Preventing biological invasions is much more time- and cost-efficient for conservation management than control and eradication efforts following introduction (Leung *et al.* 2002). However, although researchers are increasingly acknowledging the growing importance of biological invasions as a threat in mountain areas (Pauchard *et al.*, 2009; Kueffer *et al.*, 2013; Pauchard *et al.*, 2016), scenario-based assessments of plant invasion risks, and particularly those that account for the effects of different drivers of invasion, are largely missing (but see Petitpierre *et al.* 2016). Modelling alien species spread does pose several challenges (Gallien *et al.*, 2010). For example, given that alien species interact with natives, it is critical to account for native vegetation changes under global change (Pauchard *et al.*, 2016). Further, because invading alien species are typically not at equilibrium, the dynamics of dispersal and spread must be taken into account (Theoharides & Dukes, 2007; Gallien *et al.*, 2010). Finally, since different global change components such as climate, land-use and propagule pressure have so far been mostly studied in isolation, we still poorly understand their interactive effects (Nobis *et al.*, 2009; Bradley *et al.*, 2010). Hybrid dynamic vegetation models integrate the advantages of phenomenological environmental suitability models and of process-based models, and can therefore address all of the challenges described above. They thus represent an excellent tool for investigating alien species expansion in mountain regions under global change (Bradley *et al.*, 2010; Gallien *et al.*, 2010; Boulangeat *et al.*, 2014a).

In this paper, we use the hybrid simulation model FATE-HD to predict invasion risks (i.e. the likelihood of invasion) in a protected mountain area in the French Alps under different scenarios of future climate, land-use and propagule pressure. More specifically, we ask (1) whether increased propagule pressure, climate change, land-use abandonment and their interactions will lead to greater plant invasion risks in mountain ecosystems, and (2) whether the escape and spread of pre-adapted alien plants introduced through ornamental trade will also present an additional risk under these scenarios.

Methods

Study area

We focused on a protected mountain area in the French Alps (Ecrins National Park - ENP), which covers 270 000 ha and is characterized by large environmental and altitudinal gradients

Appendices - Appendix 6: Simulating plant invasion dynamics in mountain ecosystems under global change scenarios

(650 to 4100 m a.s.l.). The ENP is located at the crossroads of temperate and Mediterranean climates and harbours ca. 2000 vascular plant species, with so far only very few occurrences of alien species. Currently, two-thirds of the park consist of open habitats, managed mostly through traditional agro-pastoral practices such as extensive grazing (80%) and/or mowing (25%), while forests cover ca. 25% of the area. The department Hautes-Alpes (where the ENP is located) is currently the third least populated in France, but since 2006 its population has increased by ca. 1.2% each year, more than twice the national average (INSEE 2014), supporting more than 360000 tourist beds. The national park is in itself a tourist destination, supported by a network of 740 km of mountain trails and more than 30 mountain huts.

Hybrid simulation model

We used the spatially explicit hybrid model FATE-HD to simulate spatio-temporal dynamics of resident vegetation and plant invasions under different global change scenarios (Boulangéat *et al.*, 2014b; Boulangéat *et al.*, 2014a). FATE-HD combines species distribution models (SDMs) with process-based modelling to simulate population dynamics (dispersal, germination, recruitment, survival and seed production) of species or plant functional groups as a function of environmental suitability (with temporal stochasticity), competition for light and species traits. A disturbance sub-model allows the simulation of management practices by including spatially explicit and species-specific mortality in relation to grazing and mowing.

The FATE-HD model was recently parameterized for the ENP and used for simulating the dynamics of 24 plant functional groups (PFGs) at 100 m resolution (Boulangéat *et al.* 2014a; Appendix S1). Using PFGs, i.e. clustering species with similar characteristics that respond to biotic and abiotic constraints in a similar way, was required to increase computing speed. The PFGs for the dominant native species in the park were constructed using a clustering approach (Boulangéat *et al.*, 2012) based on environmental preferences and five functional traits related to the processes implemented in FATE-HD (tolerance to shading, vegetative height, dispersal distance class, tolerance to grazing, and life form). Environmental suitability maps for each PFG were created through species distribution models (SDMs) with the ensemble platform biomod2 (Thuiller *et al.*, 2009), by pooling occurrences of the representative species in the French Alps and relating them to seven topo-climatic variables (slope, percentage of calcareous soil, and five bioclimatic variables). Mowing and three intensities of grazing were simulated annually based on a map of the currently managed areas in the ENP (Esterni *et al.*, 2006). Through this approach, Boulangéat *et al.* (2014a) were able

to successfully reconstruct and validate the current distribution and structure of the native vegetation in the park. Here, we used this model and its output as a baseline for simulating introductions of non-native species. For a more detailed description of the base model, parameterization and databases used see Appendix S1, and for a full description see Boulangeat *et al.* (2014a).

Alien and ornamental species

In order to simulate potential invasions, in addition to the 24 PFGs of native species already parameterised and simulated in the ENP, we built a set of PFGs of alien species. We focused on two groups of potential future plant invaders for the park: 1) the most abundant alien species currently naturalized in the surrounding French Alps, and 2) a set of mountain-adapted species from a pool of candidate ornamental species that have been shown to harbour potential for future invasions in Europe (Dullinger *et al.*, 2016). First, we identified the alien species already naturalized in the region, using a vegetation-plot database provided by the National Alpine Botanical Conservatory (CBNA) for the French Alps. We selected alien species recorded in at least 100 plots in the French Alps and occurring at least once within the ENP. This left us with a set of 40 current alien invaders in the region (“naturalized aliens” hereafter). Second, for the set of ornamental species we based our selection on the species identified by Dullinger *et al.* (2016) as potential future ornamental escapes in Europe. These are all non-native ornamental plants currently cultivated or commercially available in Europe, known to have already naturalized in the wild outside Europe, and predicted to be favoured under climate change in Europe. We narrowed this candidate species group based on availability of trait data, and by identifying, through a search on efloras.org, those species reported to occur in alpine environments in their native or naturalized ranges. As a result, we ended up with 10 herbaceous candidate ornamental species not yet naturalized in Europe but with high potential of escaping in the ENP (“ornamentals” hereafter).

We used the same approach previously adopted for the native species (outlined in detail in Boulangeat *et al.* 2012) to build and parameterize functional groups of naturalized alien and ornamental species (Appendix S2); here, however, we opted for creating groups of relatively few species as the starting species pool was more functionally diverse. Demographic factors for parameterization (longevity and age at maturity) and most functional trait values (tolerance to shade, vegetative height, dispersal distance class, tolerance to grazing) were derived from the literature (Landolt *et al.*, 2010; Kattge *et al.*, 2011) and/or

Appendices - Appendix 6: Simulating plant invasion dynamics in mountain ecosystems under global change scenarios

from expert assessment (see Appendices S1-2). For the ornamental species (for which many trait values were not available through databases or expert knowledge), we used data from experiments with the same set of ornamental species: a shading experiment to judge species tolerance to shade (Haeuser, Dawson & van Kleunen, unpublished data) and a competition experiment across different watering treatments to measure height (Conti *et al.* submitted). In the end, the functional group classification identified 18 functionally homogenous alien species groups (Table 2, Appendix S2): 13 PFGs for the naturalized aliens (four phanerophytes, ‘P’, one chamaephyte, ‘C’, eight herbaceous, ‘H’) and five PFGs for the ornamentals (one chamaephyte and four herbaceous).

Table 1. Alien plant functional groups (PFGs) with examples of species for naturalized aliens (aH1-8, aC1 and aP1-4) and ornamentals (oH1-4, oC1). Life form classes are herbaceous (aH1-8, oH1-4), chamaephytes (aC1, oC1) and phanerophytes (aP1-4).

PFG	Species
Naturalized Aliens	
aC1	<i>Senecio inaequidens</i>
aH1	<i>Amaranthus albus</i> , <i>Amaranthus hybridus</i> , <i>Amaranthus retroflexus</i> , <i>Panicum capillare</i>
aH2	<i>Ambrosia artemisiifolia</i> , <i>Bunias orientalis</i> , <i>Euphorbia lathyris</i> , <i>Juncus tenuis</i>
aH3	<i>Artemisia annua</i> , <i>Euphorbia maculata</i> , <i>Datura stramonium</i> , <i>Tragus racemosus</i>
aH4	<i>Bidens frondosa</i> , <i>Conyza sumatrensis</i> , <i>Arundo donax</i> , <i>Sorghum halepense</i>
aH5	<i>Conyza canadensis</i> , <i>Solidago canadensis</i> , <i>Solidago gigantea</i> , <i>Oenothera biennis</i> , <i>Oenothera glazioviana</i>
aH6	<i>Erigeron annuus</i> , <i>Impatiens balfourii</i> , <i>Impatiens glandulifera</i> , <i>Galega officinalis</i> , <i>Oxalis fontana</i> , <i>Bromus catharticus</i> , <i>Panicum dichotomiflorum</i>
aH7	<i>Phytolacca americana</i> , <i>Reynoutria japonica</i> , <i>Reynoutria sachalinensis</i>
aH8	<i>Sporobolus vaginiflorus</i>
aP1	<i>Buddleja davidii</i> , <i>Robinia pseudoacacia</i> , <i>Syringa vulgaris</i>
aP2	<i>Pyracantha coccinea</i> , <i>Parthenocissus inserta</i>
aP3	<i>Ailanthus altissima</i>
aP4	<i>Cedrus atlantica</i>
Ornamentals	
oC1	<i>Potentilla argyrophylla</i>
oH1	<i>Centaurea americana</i> , <i>Centaurea macrocephala</i> , <i>Zinnia peruviana</i>
oH2	<i>Eritrichium canum</i> , <i>Iris domestica</i>
oH3	<i>Helenium bigelovii</i>
oH4	<i>Heliotropium arborescens</i> , <i>Nepeta racemosa</i> , <i>Persicaria capitata</i>

For each alien PFG, we produced environmental suitability maps through the ensemble platform biomod2 (Thuiller *et al.*, 2009), by pooling occurrences of the associated species. For the “naturalized alien” group, we used exactly the same approach as for the natives and based the SDMs on environmental and occurrence data (presence and absence) from the CBNA in the entire French Alps (using the same variable set as for the natives), in order to account for the realized niche in the adventive range in the study region. This approach has

been shown to provide equal performance for predicting potential presences of alien species in the French Alps as models that contemporarily account for global occurrences (Gallien *et al.*, 2012). For the “ornamental” group this approach was not possible since these species have not yet naturalized in the region. We therefore used the world-wide occurrence data available through GBIF (within 10' x 10' grid cells) as the best available approximation. We acknowledge that this likely represents an overestimation of the realized environmental niche for these species in the region (as shown by Gallien *et al.* 2012 for the French Alps), but in our approach the environmental suitability only represents the fundamental climatic constraints. The limits imposed by dispersal and biotic interactions are explicitly modelled in FATE-HD and should reduce this bias. We used a bioclimatic variable set to span a range of influential temperature and precipitation conditions with negligible multicollinearity effects, obtained from WorldClim (Hijmans *et al.*, 2005): BIO2 – mean diurnal temperature range, BIO6 – minimum temperature of coldest month, BIO10 – mean temperature of warmest quarter, BIO12 – annual precipitation, BIO14 – precipitation of driest month, and BIO15 – precipitation seasonality. For model details and evaluation see Appendix S3.

Simulation workflow and scenarios

As a starting point for our simulation workflow, we used the validated simulations of the equilibrium vegetation of the ENP under current climate and land-use management (Boulangeat *et al.* 2014). We then simulated the introduction of the alien PFGs through annual seeding. The sites of simulated introduction were based on a map of the Human Footprint in the ENP. The Human Footprint (Sanderson *et al.*, 2002) is an index combining information on land-use, population density and transportation network (including mountain footpaths). As such it represents an excellent proxy of potential local propagule pressure for introduced species (Lockwood *et al.*, 2005). Simulations were run for 800 time-steps after starting alien introductions, in order to allow reaching quasi-equilibrium and stabilization of the long-lived alien PFGs, as well as for comparability with the natives. Note that there is considerable uncertainty about the temporal scale and resolution of the transient dynamics and we have insufficient data for a precise temporal validation. For this reason, we focus mostly on equilibrium conditions (as done previously, e.g. Boulangeat *et al.* 2014a,b), though we also examine mid-term responses and interpret temporal dynamics in relative terms. Further, to assess the naturalization potential of the alien PFGs in the ENP independently of propagule pressure, in a separate set of simulations the yearly introductions were stopped after 300 years. This set of simulations, though unrealistic, also allowed evaluation of potential effects

Appendices - Appendix 6: Simulating plant invasion dynamics in mountain ecosystems under global change scenarios

of bans on alien species from park managers. Although alien abundance dropped considerably when stopping introductions, and the effect to each PFG differed in strength, the overall response of the alien species to future global change scenarios was qualitatively very similar in simulations with and without continued introductions (see Appendix S4). In the following, we thus focus on simulations in which introductions were continued throughout.

We simulated two scenarios of propagule pressure (current or increased) derived from tourism development, combined with two scenarios of future climate (current climate or climate change) and two land-use scenarios (current land-use or land-use abandonment). In the current propagule pressure scenario, introductions were a proportion of a set maximum number of seeds depending on the human footprint value in each pixel (i.e. highest introduction intensity in the most densely populated centres, and lowest introduction intensity along mountain footpaths; see Appendix S2 for maps and for details). In the increased propagule pressure scenario, the maximum introduction level was applied in all areas that had a non-zero human footprint (simulating a maximum exploitation of all areas suitable to humans). Climate change was simulated by changing habitat suitability maps at 15 year intervals for the first 90 years of simulation, based on climatic projections for the intermediate emissions scenario A1B, and then held constant for the remaining simulation years to allow vegetation to reach quasi-equilibrium under the target future climate conditions (Appendix S1,3, Boulangeat *et al.* 2014). Land-use abandonment was simulated by stopping all grazing and mowing activities everywhere in the park at year 4 and until the end of the simulation (Boulangeat *et al.* 2014). We thus had one baseline scenario in which we simulated the persistence of the current conditions in the ENP (current climate, current management and current human footprint), and several scenarios with combinations of changing conditions. Each alien PFG was introduced in separate simulation runs in order to focus only on biotic interactions with the natives, and each simulation scenario was repeated three times for a total of 432 runs for the set of simulations with continuous introductions (2 PPs * 2 Climate * 2 Land-use * 18 PFGs (13 naturalized aliens + 5 ornamentals) * 3 repetitions).

Analyses

To answer our first question focusing on naturalized alien PFGs, we analysed different features of alien ranges and abundance that characterize invasion risk under different global change scenarios: (1) the final potential range of each naturalized alien PFG in the ENP at equilibrium, (2) the aggregated richness of naturalized aliens in each grid cell (100 x 100 m),

and (3) the upward shift of the upper altitudinal invasion limit. To assess the final potential range of each naturalized alien PFG in the ENP at equilibrium, we calculated the final area of occupancy per PFG as the proportion of grid cells occupied at the end of each simulation run (year 800). To disentangle the effects of land-use we also calculated PFG occupancy in undisturbed and managed grid cells (mown or grazed) separately. We then fit a generalized linear mixed effects model (GLMM) to analyse the response of alien spread (i.e. final occupancy) to different propagule pressures, land use regimes and climate scenarios, and all their two-way interactions (package ‘nlme’ in R). Life form (‘P’, ‘C’ and ‘H’) was included as a fixed factor, while PFG identity was included as a random factor. This model allowed us to assess the average invasion risk in the ENP (i.e. the proportion of the park at risk for being invaded) at equilibrium across PFGs and scenarios. Second, we assessed the aggregated richness of alien species spatially by summing the numbers of alien PFGs predicted to occur in each grid cell. This allowed us to quantify a cumulative invasion risk for each area of the park (but note that this likely represents an upper-bound as interactions among alien species are not accounted for). Finally, we quantified the upper altitudinal invasion limit by calculating the 75th quantile of elevation reached by the alien PFGs. We then assessed the overall dynamics of average aliens’ upward spread in time (annual shift of the 75th quantile of elevation) and space (final average number of PFGs at each elevation) across the different scenarios. This allowed us to evaluate invasion risks at higher elevations.

To answer our second question and to test how invasion risk increases as a consequence of the escape and spread of ornamental plants we followed the same approach outlined above (for the naturalized aliens). We assessed the final area of occurrence of each ornamental PFG in the ENP and the aggregated richness of ornamentals in each grid cell at the end of the simulation period. Then, we fit a GLMM relating final occupancy of ornamentals to propagule pressure, land-use, climate, life form and their interactions as fixed factors, including PFG identity as random factor.

Results

Effects of global change on naturalized aliens

In the baseline scenario, alien species already naturalized in the French Alps (‘naturalized aliens’) tended to be relatively uncommon (occupying well below 10% of the park surface) and mostly limited to lower elevations at the margins of the ENP (Figs. 1-6). The relatively tall and shade intolerant herbaceous PFGs aH4 and aH5 (including e.g. *Coryza* and

Appendices - Appendix 6: Simulating plant invasion dynamics in mountain ecosystems under global change scenarios

Oenothera spp.) as well as aH6 (including *Impatiens spp.* and *Erigeron annuus*) were the most widespread among the herbs, while the shrub group aP2 (e.g. *Pyracantha coccinea*) characterized by long distance bird-mediated dispersal was the most widespread phanerophyte. However, propagule pressure, climate change, land-use abandonment and their interactions all affected invasion success, resulting in significant changes in occupancy within the ENP across PFGs (Fig. 1). The strength of the effects of these global change factors depended on the life form and functional group of the invaders (interaction terms in Fig. 1). Increased human-mediated propagule pressure led to greater occupancy for almost all functional groups across scenarios (Fig. 2), but certain aliens were particularly affected. Specifically, the long-lived herbaceous (aH7, e.g. *Reynoutria japonica*) and woody (aP4, *Cedrus atlantica*) PFGs more than doubled in occupancy in the high propagule pressure scenarios (Fig. 2). In accordance with its high dependence on propagule pressure, the occupancy of the *R. japonica* group (aH7) dropped drastically below 1% of the park area if introductions were stopped after an establishment period (Appendix S4). This was not the case for the phanerophyte *C. atlantica*, which once established was independent of further introductions and persisted in the study area with similar area of occupancy even in the long term (Appendix S4).

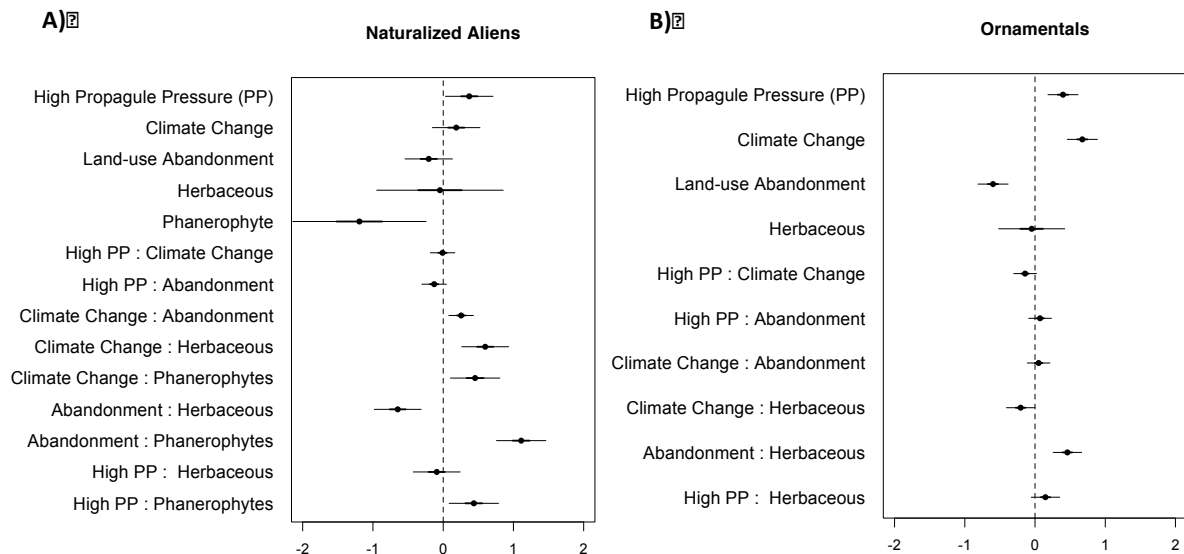


Figure 1. Generalized linear mixed effects models (GLMMs) of the response of alien species spread (i.e. final area of occupancy) to different propagule pressure, land-uses and climate change scenarios, and their two-way interactions for “naturalized aliens” (A) and “ornamentals” (B). Life Form (‘Phanerophyte’, ‘Chamaephyte’ and ‘Herbaceous’) was included as a fixed factor, while plant functional group identity was included as a random factor. Shown are effect sizes plus and minus 2 SDs.

Across propagule pressure scenarios, simulated climate change resulted in significantly greater spread for all life forms, with herbaceous PFGs occupying up to 20% of the park area and woody PFGs more than doubling in range at the end of the simulation time (Fig. 3).

Herbaceous aliens migrated rapidly upslope following the on-going climate changes and the upper margin of their ranges stabilized on average 100-150 m higher than in the baseline scenario (Fig. 5c). The upward shift of alien trees was more modest, not as long-lasting (Fig. 5d), and also less pronounced compared to the native trees (Boulangeat *et al.* 2014, Fig. S8-9). This pattern was driven mostly by *Ailanthus altissima* (aP3), which initially migrated upslope but was then likely outcompeted by forest-edge and late-successional native trees (such as nP7 and nP5; Appendix S1, Fig. S9). Overall, this resulted in an increase in the average number of potentially occurring alien species at all elevations (Fig. 5a) and in the interior of the park (Fig. 6), and in an upward shift of the invasion front (from ca. 2000 to 2500 m a.s.l., Fig. 5a).

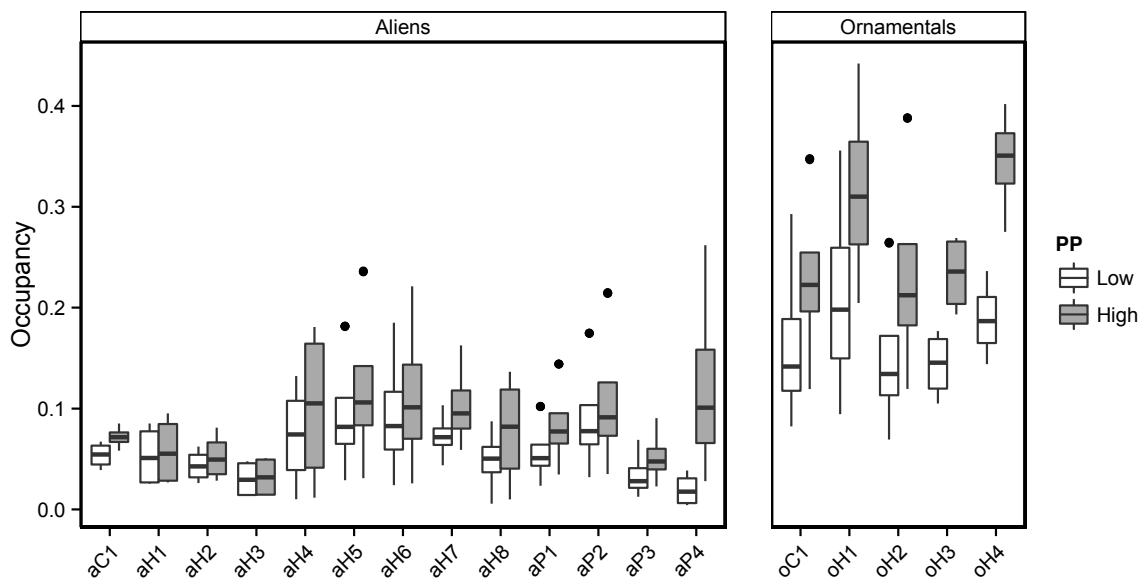


Figure 2. Effects of propagule pressure (PP) scenarios on area of occupancy of the alien plant functional groups (PFGs) in the Ecrins National Park at the end of the simulations after reaching quasi-equilibrium. Shown separately are results for already naturalized alien PFGs (a) and for ornamental PFGs (b). See [Table 1](#) for the PFG codes and the species included in each group and [Table S5](#) for their parameter values.

Land-use abandonment had contrasting effects on herbaceous and woody aliens. On the one hand, abandonment led to a strong decrease in the area occupied by herbaceous aliens (Fig. 3) as these were quickly outshaded by native shrubs and trees colonizing the abandoned grasslands (Fig. 4). Alien herbs therefore attained much lower elevations in general (Fig. 5c), resulting in lower potential alien richness at all elevations other than in the lowlands below 1000 m a.s.l. (Fig. 5a) and in the periphery of the park (Fig. 6). On the other hand, woody aliens profited, just like native shrubs and trees, from abandonment, invading the previously managed areas and expanding their ranges more than under climate change (Fig. 3 and 4). This resulted also in an upward shift in the invasion front of woody aliens driven again mostly

Appendices - Appendix 6: Simulating plant invasion dynamics in mountain ecosystems under global change scenarios

by *A. altissima* gradually replacing the native pioneer groups after an initial time lag (e.g. the native *Larix decidua*, nP4; Fig. S8,9). As expected, invasion of unmanaged areas was not strongly affected by abandonment (for neither herbs nor trees, Fig. 4).

Overall, climate change and land-use abandonment had mostly additive effects on final alien range (Fig. 3). These were antagonistic for the herbs and synergistic for the trees. Thus, on the one hand, the occupancy of alien herbs under land-use abandonment combined with climate change was intermediate compared to the scenario with land-use abandonment under current climate and the scenario with climate change under current management (Fig. 3). On the other hand, the combined effects of climate change and land-use abandonment resulted in a four-fold increase in the average range of the woody PFGs at the end of the simulation (Fig. 3). In the scenario in which both climate change and land-use abandonment took place, aliens (including trees such as *A. altissima* in aP3 and *Robinia pseudoacacia* in aP1) initially colonized higher elevations following climate change, but were later gradually replaced at the upper limits of their elevation range as native tree cover fully developed after ca. 200-300 years (Fig. S8, 9). At the end of the simulation, this resulted in higher potential local richness of aliens mostly below 1500 m and at the borders of the park, but lower average richness than under current management at higher altitudes (Figs. 5, 6).

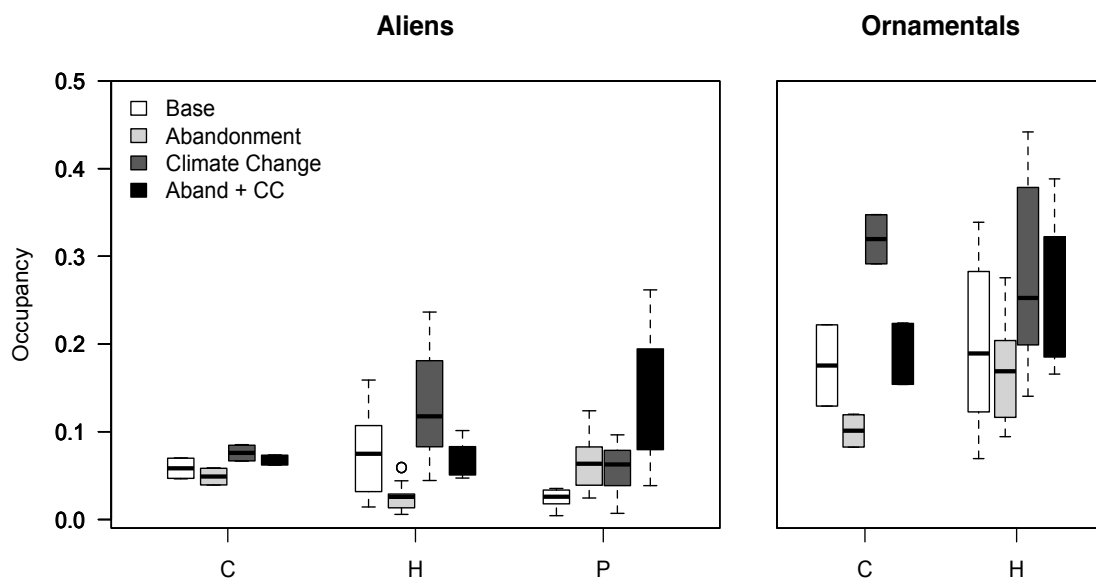


Figure 3. Effects of climate change and land-use abandonment scenarios on area of occupancy of alien plant functional groups (PFGs) of different life forms (C for chamaephytes, H for herbaceous and P for phanerophytes) in the Ecrins National Park at the end of the simulations. The baseline scenario (“Base”) represents the persistence of the current conditions in the ENP (current climate and current land-use). Results are shown separately for already naturalized alien PFGs (a) and for ornamental PFGs (b).

Ornamental species

Simulations for ornamental PFGs generally resulted in greater occupancy than for naturalized aliens across simulations, with on average ca. 20% of the park area being suitable for ornamental establishment in the baseline scenario. In general, all ornamental PFGs were also strongly affected by propagule pressure (Fig. 1), with the group oH4 of *Heliotropium arborescens* (characterized by limited dispersal ability but high shade tolerance) roughly doubling in abundance in the high propagule pressure scenario (Fig. 2). Overall, ornamentals responded to other global change components in a qualitatively similar way as the herbaceous naturalized aliens. Climate change led to a strong increase, while land abandonment resulted in a net decrease in the area occupied by ornamentals (Fig. 3). In combination, climate change and land abandonment had antagonistic effects, with grid cells becoming suitable for a larger number of ornamentals mostly located in the peripheral lower altitudes of the park (Figs. 3, 6). Interestingly, in the land-use abandonment scenarios ornamental plants were less affected by colonizing native trees within abandoned grasslands compared to herbaceous naturalized aliens (Fig. 4).

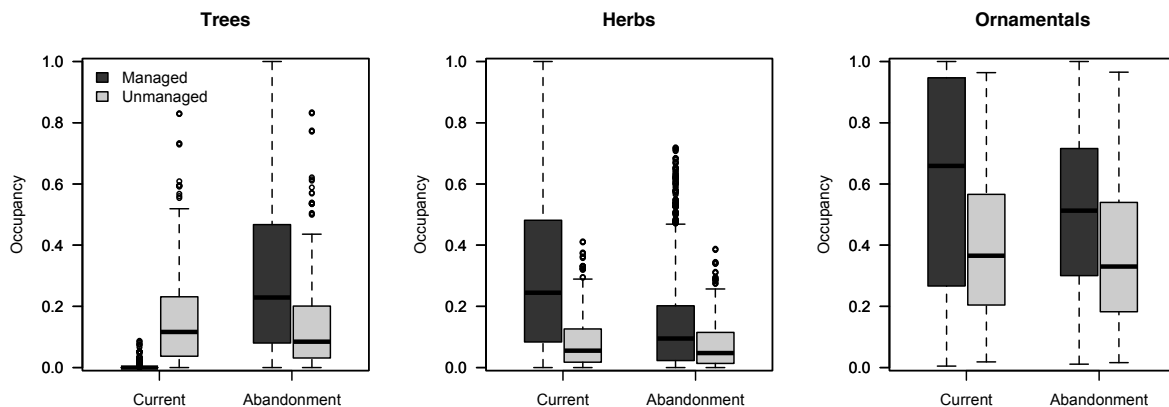


Figure 4. Effects of land-use abandonment on area of occupancy of alien plant species of different plant functional groups in the Ecrins National Park at the end of the simulations after reaching quasi-equilibrium. Results are shown separately for managed (grazed or mown) and unmanaged habitats for the naturalized alien trees (a), for the naturalized alien herbs (b) and for the ornamental functional groups (c).

Discussion

Mountain ecosystems typically host few alien species, but this situation is rapidly changing with increasing global environmental change (Alexander *et al.*, 2016). Here, we assessed the future potential distribution of a selection of alien plant species in a protected mountainous area in the European Alps, and showed that predicted future global and local changes are likely to relax many of the constraints that currently limit plant invasions to lower altitudes.

Appendices - Appendix 6: Simulating plant invasion dynamics in mountain ecosystems under global change scenarios

Our spatially and temporally explicit vegetation model predicts a range expansion and often a shift of the upper elevational distribution limit for most modelled alien plant species under different climate and land-use scenarios. These results highlight an additional and previously underestimated threat for the fragile mountain flora of the Alps, already facing climate changes, land-use transformations and increased tourism in the near future.

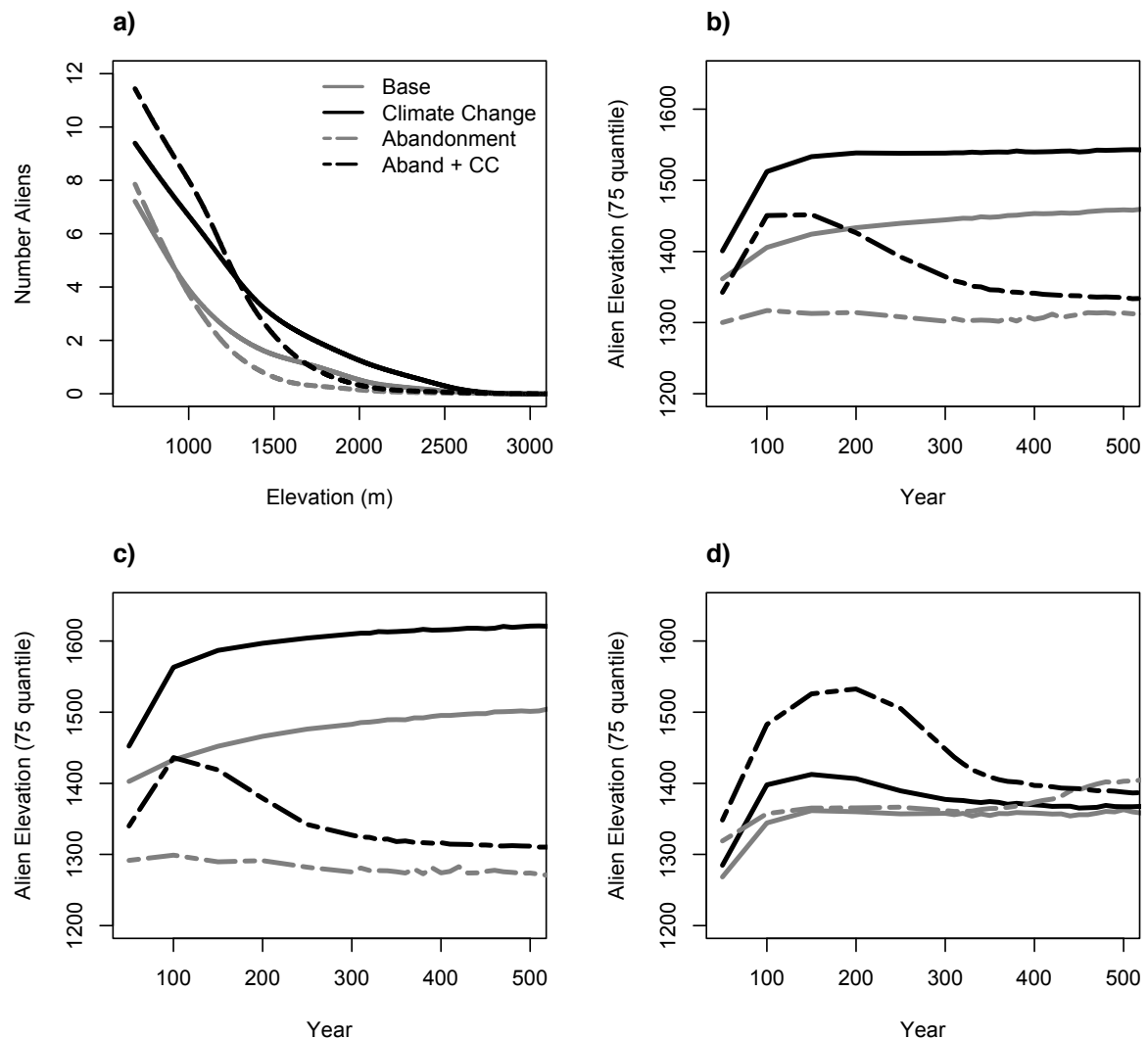


Figure 5. Changes in the upper altitudinal invasion limit under different climate and land-use scenarios and under constant (current) propagule pressure. Shown are the average numbers of naturalized alien functional groups across elevation at the end of the simulation after reaching quasi-equilibrium (a) and the change of the upper quartile of PFG's elevation occurrence for the naturalized aliens (averaged across PFGs) over time for the first 500 years of simulation (b). In panels (c) and (d), the simulation dynamics of herbaceous and woody alien PFGs, respectively, are shown. Grey lines represent current climate and black lines climate change scenarios; solid lines represent current land management and dashed lines represent land abandonment scenarios.

Mountain invasions under global change scenarios

Our baseline scenario confirmed that mountain ecosystems in the French Alps are currently characterized by limited suitability for alien species, which are largely restricted to lower

altitudes in valleys. Indeed, most previous studies from different biomes around the world show a consistent pattern of declining alien plant richness from a maximum at the lowest or lower third of the elevation gradient (Pauchard *et al.*, 2009; Alexander *et al.*, 2011; Seipel *et al.*, 2012). Interestingly, in our simulated baseline scenario, we found declining richness patterns that mirror very closely those observed by Becker *et al.* (2005) along a similar altitudinal gradient in Switzerland (500-2500 m a.s.l.), although in our case we recorded numbers of distinct PFGs rather than species. Compared to previous phenomenological modelling work we obtained more realistic elevational ranges for our modelled aliens (cfr. Petitpierre *et al.*, 2016). Indeed, FATE-HD allows for the modelling of the two critical processes of species spread, i.e. the demography of metapopulations and the dispersal rate of species, both of which are considered key for expanding invasive species (Hastings *et al.*, 2005; Theoharides & Dukes, 2007; Wilson *et al.*, 2009). We note also that several of the top-ten of the most frequently-recorded alien species by Becker *et al.* (2005) in the Swiss Alps matched the functional groups occupying larger ranges in our baseline simulations (*Conyza sp.* and *Solidago canadensis* in aH5, *Erigeron annuus* and *Oxalis fontana* in aH6). These congruencies between our baseline simulations and observed patterns in similar environments offer support for our approach. However, in accordance with trends already under way in the European Alps and other mountain ranges (Johnston & Pickering, 2001; Becker *et al.*, 2005; Pickering *et al.*, 2008; Pauchard *et al.*, 2009), we found an increase in the spread potential of alien species under most future scenarios.

We found strong effects of climate change on invasion risk in the ENP, leading to greater alien occupancy in valleys in the interior of the protected area. A recent study already showed that under a warmer and drier climate, most plant invaders currently naturalized in the surrounding lowlands will strongly gain climatically suitable area in the European Alps (Petitpierre *et al.*, 2016). However, shifts in the native vegetation driven by climate change may potentially limit alien species spread, or alternatively these shifts could further facilitate alien spread (Pauchard *et al.*, 2009). Here, we improve on previous work by accounting for light-mediated interactions with the concurrently shifting native vegetation. While, to a large degree, we corroborate previous results by finding that herbaceous alien species track their climatic niche upslope, we also found evidence that biotic resistance can partially mitigate the upward spread of alien trees such as *A. altissima* or *R. pseudoacacia* as a consequence of native woody species encroachment and vegetation succession. These results highlight the importance of accounting for changing biotic interactions.

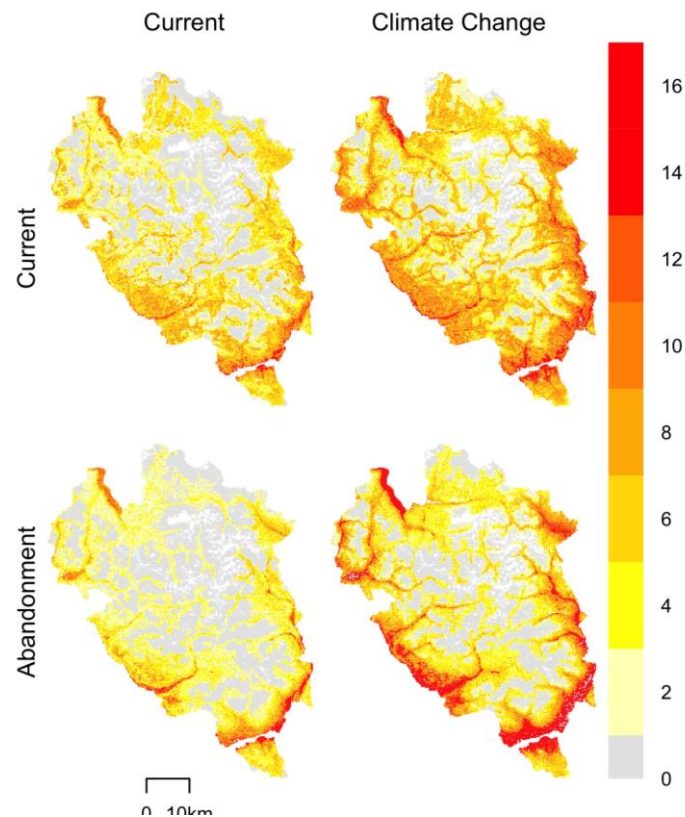


Figure 6. Number of alien plant functional groups (naturalized aliens and ornamentals combined) predicted to occur across the Ecrins National Park at the end of the simulation after reaching quasi-equilibrium under different combinations of climate (current or climate change) and land-use scenarios (current or abandonment). The baseline scenario represents the persistence of the current conditions in the ENP (current climate and current land-use). See Fig. S10 for patterns at intermediate time-frames.

In addition to climate change, we simulated the two main trends in the future anthropogenic development of European mountain landscapes: abandonment of pastoral activities vs. the development of tourism. Both significantly affected the future risk of plant invasions in the ENP. Higher propagule pressure, associated with the development of tourism in mountains, increased the area potentially invaded by alien species, a pattern reinforced under climate change in accordance with previous results (Nobis *et al.*, 2009). While propagule pressure increased the risk of invasion across all modelled functional groups, the abandonment of grazing and mowing had more complex effects. Abandonment opened new invasion opportunities only for woody alien groups, leading to increases comparable to those associated with climate change in terms of final occupancy and upslope shift, though after a considerable time-lag (ca. 300 years). Indeed, lagged spreads of certain trees such as *Robinia pseudoacacia* and *A. altissima* into natural environments after more than a century of planting into public parks are known from Central Europe, potentially also in response to warming climates and the availability of more suitable sites (Kowarik, 1995). In contrast, we found opposite patterns for herbs. Herbaceous alien species are known to profit from anthropogenic

disturbances, particularly in cold climates such as high elevation habitats (Vavra *et al.*, 2007; Eskelinen *et al.*, 2017). When such grazing and mowing disturbances were eliminated in our simulations, we observed strong declines in the spread of alien herbs, as a consequence of colonization by native trees that outshaded them. Such declines after abandonment were consistent among all herbaceous aliens groups, while herbaceous natives had more mixed responses depending on their shade tolerance (Boulangéat *et al.* 2014).

Climate changes and land-use abandonment also interacted in a complex fashion by influencing the transient dynamics of alien species spread in the ENP. Aliens profited from the slow growth, long life cycles and consequently slow recolonization of native plants (Dullinger *et al.*, 2004; Pauchard *et al.*, 2009) and thus temporarily spread upslope, tracking the gradually more suitable climate in the first 200 years of simulation. These results suggest that even if the responding native vegetation may eventually exclude aliens at higher altitudes, interacting climate and land-use changes may offer a window of temporary invasion in the short to mid-term. Indeed at year 100, which represents a mid-term time-frame which is relevant for conservation, invasion risk and richness of aliens across the park was higher for almost all scenarios (Fig. S10, year 100). We note that the later exclusion of aliens depends on our parameterization assumption that allows germination and recruitment in shady conditions for woody native species (Boulangéat *et al.* 2014). Lastly, in the long run, the interaction of land-use abandonment with climate change at equilibrium also shifted the areas of highest invasion risk spatially, restricting the areas suitable for the maximum number of aliens to lower altitudes at the periphery of the ENP.

Overall, we showed that interacting agents of global change in combination with the responses of the native vegetation can have unforeseen effects on both the temporal dynamics and final distributions of alien plants in mountains. By accounting jointly for several main agents of anthropogenic environmental change, we illustrate invasion opportunities driven by the interactions between climate change and other human-caused changes (i.e. land-use abandonment and increased propagule pressure). Our results also highlight the importance of accounting for often-neglected biotic interactions with the resident vegetation, including the potential facilitating effects of range-expanding natives and the relaxation of biotic resistance from declining alpine species.

Finally, pre-adaptation to severe abiotic conditions might promote future invasions of newly introduced ornamental plants into touristically-developing mountains (McDougall *et al.*, 2005; Pauchard *et al.*, 2009; Kueffer *et al.*, 2013). We tested this idea in the ENP for a set

Appendices - Appendix 6: Simulating plant invasion dynamics in mountain ecosystems under global change scenarios

of functional groups of ornamental plants that already have a naturalization history in high altitudes of other mountain ranges. Our simulations showed that, if introduced, large areas of the ENP would be suitable for the establishment of these alien ornamentals under different future scenarios. Though we cannot quantitatively compare the final area of occupancy of these ornamental species to that of the already naturalized aliens, because of differences in the underlying environmental suitability models, the qualitative response to global change agents was informative. For example, we found that pre-adapted ornamental species were very strongly favoured by increased propagule pressure at higher elevations (strong propagule pressure effect, Fig. 1, Fig. 2). This effect was on average less strong for the already naturalized aliens (Fig. 2). Because most alien species to date have been initially introduced into lowland habitats, there may be selection against taxa adapted to higher elevations (Becker *et al.*, 2005; Marini *et al.*, 2013). In our future scenario in which pre-adapted aliens were introduced directly into higher elevations because of increased propagule pressure, this “lowland filter” was reduced and invasion risks became much higher than under current introduction scenarios (e.g. oH4, *Heliotropium arborescens*). Further, while ornamental plants and already naturalized herbaceous aliens responded to climate and management change in a similar way, the ornamentals were less affected by developing forest cover in abandoned pastures. This was because they were on average more tolerant to shade and to competition (i.e. had higher survival rates and recruitment in competitive environments). This result suggests that traits that might typically be selected for in the horticultural trade for alpine gardens (e.g. fast growth under limited resources, winter hardiness) might provide a competitive advantage for ornamental plants escaping into mountain landscapes under future land use transformations (Van Kleunen & Johnson, 2007; Marco *et al.*, 2010; Maurel *et al.*, 2016). Overall, by relying on both functional traits and climatic envelopes from global ranges, we could provide first estimates of suitability of a European mountain region for alien ornamental plants that have not yet escaped cultivation, as well as their responses to future global change agents. Although these insights are certainly still approximations, they provide a basis for putting in place proactive alien species management in mountain environments.

Threat to native mountain flora and management responses

Mountainous environments are assumed to be threatened by a suite of ongoing environmental changes, but biological invasions are considered to be of less relevance (Sala *et al.*, 2000). We have shown that global change factors will reduce the potential of native

vegetation in mountains to resist invasion, and that it is a matter of time before alien species will spread to higher elevations. Given that the flora of mountains is particularly vulnerable to rapid environmental changes due to dispersal-limiting rugged mountain morphology and the presence of many range-restricted species (Engler *et al.*, 2011; Thuiller *et al.*, 2014), the additional pressure caused by increased biological invasions may have serious long-term consequences for mountain biota.

Contrary to many already highly invaded ecosystems, science and management still have the opportunity to act precautionarily in mountain environments. First, limiting the spread of existing alien species populations along elevational gradients is an important first management goal (Lembrechts *et al.*, 2017). We have shown that if introductions are limited or completely stopped, e.g. through appropriate regulations drastically curbing propagule pressure, some alien functional groups, such as *Ambrosia artemisiifolia* or *Reynoutria japonica*, which are highly invasive in other settings, would very quickly be excluded in these harsh environments under most future scenarios. However, this was not the case for many other groups (e.g. *Cedrus atlantica*), highlighting the importance of cost-effective early management response. One essential tool for precluding future invasions is the close control and regulation of pre-adapted ornamental plants in new ski or mountain resorts for amenity plantings or revegetation (McDougall *et al.* 2005). Examples of available policy instruments that tackle invasions at different stages of the horticulture supply-chain include pre-border import restrictions at a national level for the species most at risk of spreading, post-border bans at a local level within the park, voluntary codes of conduct for mountain nurseries and those of the surrounding areas, and consumer education towards non-invasive functional groups of ornamental plants for mountain gardens and resorts (Hulme *et al.* submitted).

In conclusion, using the hybrid dynamic model FATE-HD to simulate plant invasions, we predict range expansions for most modelled alien plant species and a shift of the invasion front to higher elevations under most future scenarios in the ENP. Climate change and higher propagule pressures will be the most significant drivers of increasing invasion risk across species. Land-use abandonment in interaction with climate change will open invasion opportunities for alien trees at intermediate time-frames. The introduction of well-adapted ornamental plants will further increase invasion risks in these environments. However, the native vegetation responding to global change can partially mitigate more widespread invasions. Our spatially and temporally explicit approach addresses many of the limitations of previous works, highlighting the promise of hybrid models for studying alien species and

Appendices - Appendix 6: Simulating plant invasion dynamics in mountain ecosystems under global change scenarios

critically assessing the risk of future invasions into mountain environments. It also opens many perspectives for future developments, including accounting for species-specific introduction pathways of aliens (Wilson *et al.*, 2009) and mutualisms such as animal-mediated dispersal (Traveset & Richardson, 2014), or modelling additional mechanisms for biotic interactions such as competition for nutrient uptake and multi-trophic partners.

References

- Alexander, J.M., Kueffer, C., Daehler, C.C., Edwards, P.J., Pauchard, A., Seipel, T., Arévalo, J., Cavieres, L., Dietz, H. & Jakobs, G. (2011) Assembly of nonnative floras along elevational gradients explained by directional ecological filtering. *Proceedings of the National Academy of Sciences*, 108, 656-661.
- Alexander, J.M., Lembrechts, J.J., Cavieres, L.A., Daehler, C., Haider, S., Kueffer, C., Liu, G., McDougall, K., Milbau, A. & Pauchard, A. (2016) Plant invasions into mountains and alpine ecosystems: current status and future challenges. *Alpine Botany*, 126, 89-103.
- Becker, T., Dietz, H., Billeter, R., Buschmann, H. & Edwards, P.J. (2005) Altitudinal distribution of alien plant species in the Swiss Alps. *Perspectives in Plant Ecology, Evolution and Systematics*, 7, 173-183.
- Boulangeat, I., Georges, D. & Thuiller, W. (2014a) FATE - HD: a spatially and temporally explicit integrated model for predicting vegetation structure and diversity at regional scale. *Global change biology*, 20, 2368-2378.
- Boulangeat, I., Georges, D., Dentant, C., Bonet, R., Van Es, J., Abdulhak, S., Zimmermann, N.E. & Thuiller, W. (2014b) Anticipating the spatio - temporal response of plant diversity and vegetation structure to climate and land use change in a protected area. *Ecography*, 37, 1230-1239.
- Boulangeat, I., Philippe, P., Abdulhak, S., Douzet, R., Garraud, L., Lavergne, S., Lavorel, S., Van Es, J., Vittoz, P. & Thuiller, W. (2012) Improving plant functional groups for dynamic models of biodiversity: at the crossroads between functional and community ecology. *Global change biology*, 18, 3464-3475.
- Bradley, B.A., Blumenthal, D.M., Wilcove, D.S. & Ziska, L.H. (2010) Predicting plant invasions in an era of global change. *Trends in Ecology & Evolution*, 25, 310-318.
- Chytrý, M., Maskell, L.C., Pino, J., Pyšek, P., Vilà, M., Font, X. & Smart, S.M. (2008) Habitat invasions by alien plants: a quantitative comparison among Mediterranean, subcontinental and oceanic regions of Europe. *Journal of Applied Ecology*, 45, 448-458.
- Colautti, R.I., Grigorovich, I.A. & MacIsaac, H.J. (2007) Propagule pressure: a null model for biological invasions. *Biological Invasions*, 9, 885-885.
- Dullinger, I., Wessely, J., Bossdorf, O., Dawson, W., Essl, F., Gattringer, A., Klöner, G., Kreft, H., Kuttner, M., Moser, D., Pergl, J., Pyšek, P., Thuiller, W., van Kleunen, M., Weigelt, P., Winter, M. & Dullinger, S. (2016) Climate change will increase the naturalization risk from garden plants in Europe. *Global Ecology and Biogeography*, 1466-8238.
- Dullinger, S., Dirnböck, T. & Grabherr, G. (2004) Modelling climate change-driven treeline shifts: relative effects of temperature increase, dispersal and invasibility. *Journal of Ecology*, 92, 241-252.
- Engler, R., Randin, C.F., Thuiller, W., Dullinger, S., Zimmermann, N.E., Araujo, M.B., Pearman, P.B., Le Lay, G., Piedallu, C., Albert, C.H., Choler, P., Coldea, G., De Lamo, X., Dirnböck, T., Gegout, J.-C., Gomez-Garcia, D., Grytnes, J.-A., Heegaard, E.,

- Hoistad, F., Nogues-Bravo, D., Normand, S., Puscas, M., Sebastia, M.-T., Stanisci, A., Theurillat, J.-P., Trivedi, M.R., Vittoz, P. & Guisan, A. (2011) 21st century climate change threatens mountain flora unequally across Europe. *Global Change Biology*, 17, 2330-2341.
- Eskelinen, A., Kaarlejärvi, E. & Olofsson, J. (2017) Herbivory and nutrient limitation protect warming tundra from lowland species' invasion and diversity loss. *Global Change Biology*, 23, 245-255.
- Esterni, M., Rovera, G., Bonet, R., Salomez, P., Cortot, H. & Guilloux, J. (2006) DELPHINE - Découpage de l'Espace en Liaison avec les Potentialités Humaines et en Interrelation avec la Nature. Parc National des Ecrins.
- Gallien, L., Münkemüller, T., Albert, C.H., Boulangeat, I. & Thuiller, W. (2010) Predicting potential distributions of invasive species: where to go from here? *Diversity and Distributions*, 16, 331-342.
- Gallien, L., Douzet, R., Pratte, S., Zimmermann, N.E. & Thuiller, W. (2012) Invasive species distribution models – how violating the equilibrium assumption can create new insights. *Global Ecology and Biogeography*,
- Gehrig-Fasel, J., Guisan, A. & Zimmermann, N.E. (2007) Tree line shifts in the Swiss Alps: Climate change or land abandonment? *Journal of Vegetation Science*, 18, 571-582.
- Godde, P., Price, M.F. & Zimmerman, F.M. (2000) *Tourism and development in mountain regions*. CABI, New York.
- Hastings, A., Cuddington, K., Davies, K.F., Dugaw, C.J., Elmendorf, S., Freestone, A., Harrison, S., Holland, M., Lambrinos, J., Malvadkar, U., Melbourne, B.A., Moore, K., Taylor, C. & Thomson, D. (2005) The spatial spread of invasions: new developments in theory and evidence. *Ecology Letters*, 8, 91-101.
- Hijmans, R.J., Cameron, S.E., Parra, J.L., Jones, P.G. & Jarvis, A. (2005) Very high resolution interpolated climate surfaces for global land areas. *International Journal of Climatology*, 25, 1965-1978.
- Johnston, F.M. & Pickering, C.M. (2001) Alien plants in the Australian Alps. *Mountain Research and Development*, 21, 284-291.
- Kalwij, J.M., Robertson, M.P. & van Rensburg, B.J. (2008) Human activity facilitates altitudinal expansion of exotic plants along a road in montane grassland, South Africa. *Applied Vegetation Science*, 11, 491-498.
- Kattge, J., Diaz, S., Lavorel, S., Prentice, C., Leadley, P., Bonisch, G., Garnier, E., Westoby, M., Reich, P.B., Wright, I.J., Cornelissen, J.H.C., Violle, C., Harrison, S.P., van Bodegom, P.M., Reichstein, M., Enquist, B.J., Soudzilovskaia, N.A., Ackerly, D.D., Anand, M., Atkin, O., Bahn, M., Baker, T.R., Baldocchi, D., Bekker, R., Blanco, C.C., Blonder, B., Bond, W.J., Bradstock, R., Bunker, D.E., Casanoves, F., Cavender-Bares, J., Chambers, J.Q., Chapin, F.S., Chave, J., Coomes, D., Cornwell, W.K., Craine, J.M., Dobrin, B.H., Duarte, L., Durka, W., Elser, J., Esser, G., Estiarte, M., Fagan, W.F., Fang, J., Fernandez-Mendez, F., Fidelis, A., Finegan, B., Flores, O., Ford, H., Frank, D., Freschet, G.T., Fyllas, N.M., Gallagher, R.V., Green, W.A., Gutierrez, A.G., Hickler, T., Higgins, S.I., Hodgson, J.G., Jalili, A., Jansen, S., Joly, C.A., Kerkhoff, A.J., Kirkup, D., Kitajima, K., Kleyer, M., Klotz, S., Knops, J.M.H., Kramer, K., Kuhn, I., Kurokawa, H., Laughlin, D., Lee, T.D., Leishman, M., Lens, F., Lenz, T., Lewis, S.L., Lloyd, J., Llusia, J., Louault, F., Ma, S., Mahecha, M.D., Manning, P., Massad, T., Medlyn, B.E., Messier, J., Moles, A.T., Muller, S.C., Nadrowski, K., Naeem, S., Niinemets, U., Nollert, S., Nuske, A., Ogaya, R., Oleksyn, J., Onipchenko, V.G., Onoda, Y., Ordóñez, J., Overbeck, G., Ozinga, W.A., Patino, S., Paula, S., Pausas, J.G., Penuelas, J., Phillips, O.L., Pillar, V., Poorter, H., Poorter, L., Poschlod, P., Prinzing, A., Proulx, R., Rammig, A., Reinsch, S., Reu, B., Sack, L., Salgado-Negre, B., Sardans,

Appendices - Appendix 6: Simulating plant invasion dynamics in mountain ecosystems under global change scenarios

- J., Shiodera, S., Shipley, B., Siefert, A., Sosinski, E., Soussana, J.F., Swaine, E., Swenson, N., Thompson, K., Thornton, P., Waldram, M., Weiher, E., White, M., White, S., Wright, S.J., Yguel, B., Zaehle, S., Zanne, A.E. & Wirth, C. (2011) TRY - a global database of plant traits. *Global Change Biology*, 17, 2905-2935.
- Kowarik, I. (1995) Time lags in biological invasions with regard to the success and failure of alien species. *Plant Invasions: General Aspects and Special Problems* (ed. by P. Pyšek, K. Prach, M. Rejmánek and M. Wade), pp. 15-38. SPB academic publishing, Amsterdam, The Netherlands.
- Kueffer, C., McDougall, K., Alexander, J., Daehler, C., Edwards, P., Haider, S., Milbau, A., Parks, C., Pauchard, A. & Reshi, Z.A. (2013) Plant invasions into mountain protected areas: assessment, prevention and control at multiple spatial scales. *Plant Invasions in Protected Areas*, pp. 89-113. Springer.
- Landolt, E., Bäuml, B., Erhardt, A., Hegg, O., Klötzli, F., Lämmler, W., Nobis, M., Rudmann-Maurer, K., Schweingruber, F.H., Theurillat, J.-P., Urmi, E., Vust, M. & Wohlgemuth, T. (2010) *Flora indicativa*. Haupt Verlag, Bern - Stuttgart - Wien.
- Lembrechts, J.J., Alexander, J.M., Cavieres, L.A., Haider, S., Lenoir, J., Kueffer, C., McDougall, K., Naylor, B.J., Nuñez, M.A. & Pauchard, A. (2017) Mountain roads shift native and non - native plant species' ranges. *Ecography*, 40, 353-364.
- Lockwood, J.L., Cassey, P. & Blackburn, T. (2005) The role of propagule pressure in explaining species invasions. *Trends in Ecology & Evolution*, 20, 223-228.
- Lockwood, J.L., Cassey, P. & Blackburn, T.M. (2009) The more you introduce the more you get: the role of colonization pressure and propagule pressure in invasion ecology. *Diversity and Distributions*, 15, 904-910.
- Mack, R.N., Simberloff, D., Lonsdale, W.M., Evans, H., Clout, M. & Bazzaz, F.A. (2000) Biotic invasions: Causes, epidemiology, global consequences, and control. *Ecological Applications*, 10, 689-710.
- Marco, A., Lavergne, S., Dutoit, T. & Bertaudiere-Montes, V. (2010) From the backyard to the backcountry: how ecological and biological traits explain the escape of garden plants into Mediterranean old fields. *Biological Invasions*, 12, 761-779.
- Marini, L., Bertolli, A., Bona, E., Federici, G., Martini, F., Prosser, F. & Bommarco, R. (2013) Beta - diversity patterns elucidate mechanisms of alien plant invasion in mountains. *Global Ecology and Biogeography*, 22, 450-460.
- Maurel, N., Hanspach, J., Kühn, I., Pyšek, P. & van Kleunen, M. (2016) Introduction bias affects relationships between the characteristics of ornamental alien plants and their naturalization success. *Global Ecology and Biogeography*, 25, 1500-1509.
- McDougall, K.L., Morgan, J.W., Walsh, N.G. & Williams, R.J. (2005) Plant invasions in treeless vegetation of the Australian Alps. *Perspectives in Plant Ecology, Evolution and Systematics*, 7, 159-171.
- Nobis, M.P., Jaeger, J.A.G. & Zimmermann, N.E. (2009) Neophyte species richness at the landscape scale under urban sprawl and climate warming. *Diversity and Distributions*, 15, 928-939.
- Pauchard, A., Milbau, A., Albiñ, A., Alexander, J., Burgess, T., Daehler, C., Englund, G., Essl, F., Evengård, B. & Greenwood, G.B. (2016) Non-native and native organisms moving into high elevation and high latitude ecosystems in an era of climate change: new challenges for ecology and conservation. *Biological Invasions*, 18, 345-353.
- Pauchard, A., Kueffer, C., Dietz, H., Daehler, C.C., Alexander, J., Edwards, P.J., Arevalo, J.R., Cavieres, L.A., Guisan, A., Haider, S., Jakobs, G., McDougall, K., Millar, C.I., Naylor, B.J., Parks, C.G., Rew, L.J. & Seipel, T. (2009) Ain't no mountain high enough: plant invasions reaching new elevations. *Frontiers in Ecology and the Environment*, 7, 479-486.

- Petitpierre, B., McDougall, K., Seipel, T., Broennimann, O., Guisan, A. & Kueffer, C. (2016) Will climate change increase the risk of plant invasions into mountains? *Ecological Applications*, 26, 530-544.
- Pickering, C., Hill, W. & Green, K. (2008) Vascular plant diversity and climate change in the alpine zone of the Snowy Mountains, Australia. *Biodiversity and Conservation*, 17, 1627-1644.
- Sala, O.E., Chapin, F.S., Armesto, J.J., Berlow, E., Bloomfield, J., Dirzo, R., Huber-Sanwald, E., Huenneke, L.F., Jackson, R.B., Kinzig, A., Leemans, R., Lodge, D.M., Mooney, H.A., Oesterheld, M., Poff, N.L., Sykes, M.T., Walker, B.H., Walker, M. & Wall, D.H. (2000) Biodiversity - Global biodiversity scenarios for the year 2100. *Science*, 287, 1770-1774.
- Sanderson, E.W., Jaiteh, M., Levy, M.A., Redford, K.H., Wannebo, A.V. & Woolmer, G. (2002) The Human Footprint and the Last of the Wild: The human footprint is a global map of human influence on the land surface, which suggests that human beings are stewards of nature, whether we like it or not. *BioScience*, 52, 891-904.
- Sax, D.F. & Gaines, S.D. (2008) Species invasions and extinction: The future of native biodiversity on islands. *Proceedings of the National Academy of Sciences of the United States of America*, 105, 11490-11497.
- Seipel, T., Kueffer, C., Rew, L.J., Daehler, C.C., Pauchard, A., Naylor, B.J., Alexander, J.M., Edwards, P.J., Parks, C.G. & Arevalo, J.R. (2012) Processes at multiple scales affect richness and similarity of non - native plant species in mountains around the world. *Global Ecology and Biogeography*, 21, 236-246.
- Theoharides, K.A. & Dukes, J.S. (2007) Plant invasion across space and time: factors affecting nonindigenous species success during four stages of invasion. *New Phytologist*, 176, 256-273.
- Thuiller, W., Lafourcade, B., Engler, R. & Araujo, M.B. (2009) BIOMOD - a platform for ensemble forecasting of species distributions. *Ecography*, 32, 369-373.
- Thuiller, W., Guéguen, M., Georges, D., Bonet, R., Chalmandrier, L., Garraud, L., Renaud, J., Roquet, C., Van Es, J. & Zimmermann, N.E. (2014) Are different facets of plant diversity well protected against climate and land cover changes? A test study in the French Alps. *Ecography*, 37, 1254-1266.
- Traveset, A. & Richardson, D.M. (2014) Mutualistic Interactions and Biological Invasions. *Annual Review of Ecology, Evolution, and Systematics*, Vol 45, 45, 89-+.
- Van Kleunen, M. & Johnson, S.D. (2007) South African Iridaceae with rapid and profuse seedling emergence are more likely to become naturalized in other regions. *Journal of Ecology*, 95, 674-681.
- Vavra, M., Parks, C.G. & Wisdom, M.J. (2007) Biodiversity, exotic plant species, and herbivory: the good, the bad, and the ungulate. *Forest Ecology and Management*, 246, 66-72.
- Weber, E. (2005) *Invasive plant species of the world*. CABI Publishing, UK.
- Wilson, J.R.U., Dormontt, E.E., Prentis, P.J., Lowe, A.J. & Richardson, D.M. (2009) Something in the way you move: dispersal pathways affect invasion success. *Trends in Ecology & Evolution*, 24, 136-144.

CURRICULUM VITAE

I was born in Lisbon, Portugal, on May 1st, 1989. I attended the Colégio Marista de Carcavelos from primary school until 2007, when I graduated from high school. At this time, I passed my national exams and was granted entrance in the Biology Licence degree of the Faculty of Sciences, University of Lisbon, from which I graduated in 2011 with a terrestrial ecology specialisation. During my last two years in Lisbon, from 2009 to 2011, I was awarded two undergraduate research grants that allowed me to take my first steps into academic research, under the supervision of Dr Cristina Branquinho. Both consisted in investigating the use of lichens as biomonitors of atmospheric sulphur pollution in the south-west coast of Portugal. I then moved to Aberdeen, Scotland, to pursue my master's studies in ecology, having graduated from the Ecology and Environmental Sustainability MSc of the University of Aberdeen in 2012. I developed my master's thesis around the study of the stability and resilience of animal behaviour from a theoretical perspective, with the supervision of Dr David Lusseau. After graduating from my MSc, I was employed by the University of Aberdeen on three instances. From October to December 2012 I was employed as a tutor to teach undergraduate student's semi-practical lessons. From November 2012 to January 2013 I worked for Dr Lusseau as a research assistant, under a project that aimed to study the effects of caloric restriction on mice behavioural patterns. After spending two months in a scientific expedition in Oman (from January to March 2013), I was reemployed by the University of Aberdeen in August as a research assistant within Dr Justin Travis's research group to investigate the synergistic effects of species' life history traits, dispersal traits and habitat quality on virtual species' spread rates through fragmented landscapes. In January 2014 I moved to Grenoble, France, to start my PhD under the supervision of Drs Wilfried Thuiller and Tamara Münkemüller, where I have focused my research on the study of ecosystem stability at large spatial scales, and from single to multitrophic perspectives. During my years as a PhD candidate, I collaborated both with team members and with international teams. I kept my professional links with Dr Branquinho's and Dr Travis's research teams, but also formed new collaborations by visiting Dr Niklaus Zimmermann in Zürich, Switzerland, and Dr José Montoya in Moulis, France.

Being passionate about my work, I wish to pursue a research career focusing on ecosystem stability and resilience, and on bridging the gap between theoretical developments and applied science.

PUBLICATIONS

- Barros, C.**, Braga, J., Galiana, N., Montoya, J., Münkemüller, T., Thuiller, W. Are trophic networks in European protected areas robust to global change? A spatially explicit analysis. *In prep.*
- Münkemüller, T., Gallien, L., **Barros, C.**, ..., Thuiller, W. Do's and don'ts when inferring assembly rules from diversity patterns. *In prep.*
- Carboni, M., Guéguen, M., **Barros, C.**, ..., Thuiller, W. Simulating plant invasion dynamics in alpine ecosystems under climate change and land-use scenarios. *Submitted.*
- Durão, R., **Barros, C.**, Pinho, P., Augusto, S., Máguas, C., Pereira, M. J., Branquinho, C. Tracking atmospheric S temporal dynamics using lichens as biomonitors. *In prep.*
- Barros, C.**, Lusseau, D. Motivational feedback rates influence behavioural resilience and stability. *In prep.*
- Barros, C.**, Thuiller, W., Münkemüller, T. Drought changes the effects of climate warming on forest-grassland ecotone stability. *In prep.*
- Pinho, P., **Barros, C.**, Augusto, S., Pereira, M. J., Máguas, C., Branquinho, C. Using nitrogen concentration and isotopic composition in lichens to spatially assess atmospheric nitrogen sources in mixed landscapes. *Environmental Pollution. Accepted.*
- Barros, C.**, Palmer, S., Bocedi, G., Travis, J. (2016). Spread rates on fragmented landscapes: the interacting roles of demography, dispersal and habitat availability. *Diversity and Distributions*. doi: 10.1111/ddi.12487
- Barros, C.**, Guéguen, M., Douzet, R., Carboni, M., Boulangeat, I., Zimmermann, N., Münkemüller, T., Thuiller, W. (2016). Extreme climate events counteract the effects of climate and land-use changes in Alpine treelines. *Journal of Applied Ecology*. doi: 10.1111/1365-2664.12742
- Barros, C.**, Thuiller, W., Georges, D., Boulangeat, I., Münkemüller, T. (2016). *N*-dimensional hypervolumes to study stability of complex ecosystems. *Ecology Letters*. 19(7), 729-742.
- Barros, C.**, Pinho, P., Durão, R., Augusto, S., Máguas, C., Pereira, M. J., & Branquinho, C. (2015). Disentangling natural and anthropogenic sources of atmospheric sulfur in an industrial region using biomonitors. *Environmental Science & Technology*, 49(4), 2222-2229.
- Lusseau, D., Mitchell, S. E., **Barros, C.**, ..., Speakman, J. R.. (2015). The effects of graded levels of calorie restriction: IV. Non-linear change in behavioural phenotype of mice in response to short-term calorie restriction. *Scientific Reports*, 5.

GLOSSARY

- anisohydric species, 13
- connectance, 18
- diversity
 - functional, 10
 - phylogenetic, 10
- early warning signals
 - critical slowing down, 126
 - flickering, 126
- early warning signals, 126
- functional redundancy, 125
- isohydric species, 13
- metaweb, 20
- network robustness, 17
- press-perturbations, 126
- push-perturbations, 126
- resilience, 121
- slow changing variables, 126
- stability, 121
 - global stability, 121
 - local stability, 121
- woody encroachment, 14